

**A protein in search of a function:  
The c-di-AMP-binding protein  
DarA of *Bacillus subtilis***

**Dissertation**

**for the award of the degree**

**“*Doctor rerum naturalium*”**

of the Georg-August-University Göttingen

within the doctoral program

“Microbiology and Biochemistry”

of the Georg-August University School of Science (GAUSS)

submitted by

**Martin Weiß**

from Erlangen

Göttingen 2018



## **Thesis committee**

Prof. Dr. Jörg Stülke (Supervisor and 1<sup>st</sup> Reviewer)

Institute for Microbiology and Genetics, Department of General Microbiology

PD Dr. Fabian Commichau (2<sup>nd</sup> Reviewer)

Institute for Microbiology and Genetics, Department of General Microbiology

Prof. Dr. Ralf Ficner

Institute for Microbiology and Genetics, Department of Molecular Structural Biology

## **Further members of the examination board**

Prof. Dr. Stefan Klumpp

Institute for Nonlinear Dynamics, Theoretical Biophysics Group

Prof. Dr. Rolf Daniel

Institute for Microbiology and Genetics, Department of Genomic and Applied Microbiology and G2L

Prof. Dr. Carsten Lüder

University Medical Center Göttingen, Department for Medical Microbiology

Date of oral examination: 17<sup>th</sup> January 2019





I hereby declare that this doctoral thesis entitled “A protein in search of a function: The c-di-AMP-binding protein DarA of *Bacillus subtilis*” has been written independently and with no other sources and aids than quoted.

Martin Weiß



# Danksagung

Als Erstes möchte ich Prof. Dr. Jörg Stülke für die fachliche Betreuung und Unterstützung während der letzten drei Jahre danken. Ich habe mich ab dem ersten Tag beim Vorstellungsgespräch wohl gefühlt. Danke für die kurze Stadtführung. Dir liegen deine Doktoranden und Studenten wirklich am Herzen. Ich hoffe meine jährlichen Nürnberger Lebkuchen haben dir immer geschmeckt.

PD Dr. Fabian Commichau möchte ich für die Übernahme des Korreferats danken. Du standest mir immer mit äußerst hilfreichen Ideen zur Seite. Auch dein Sektsflöten-Einsatz war stets exzellent. Ich hoffe deine HIF läuft auch in Zukunft immer auf Hochtouren.

Desweiteren danke ich Prof. Dr. Ralf Ficner für die Teilnahme am Thesis Committee und der Prüfungskommission. Ebenso möchte ich Prof. Dr. Stefan Klumpp, Prof. Dr. Rolf Daniel und Prof. Dr. Carsten Lüder für die Teilnahme an der Prüfungskommission danken.

Laborarbeit benötigt immer Unterstützung. Ein riesen Dank gebührt Silvia Carrillo-Castellón für die immer heitere Art und Späße. Ohne deine Arbeit im Hintergrund würden wir alle alt aussehen. Meinen Praktikanten, Bachelor- und Masterstudenten Oguz Bolgi, Tobias Krammer, Patrick Faßhauer, Björn Richts und Julis Fülleborn danke ich für die hervorragende Arbeit die zu meiner beigetragen hat. Danke auch an die zahlreichen Kooperationspartner und ihre Forschungsgruppen die eine Vielzahl unterschiedlicher Messungen ermöglicht haben: Prof. Dr. Volkhardt Kaefer (Hannover), Dr. Hannes Link (Marburg), Dr. Elke Hammer (Greifswald), Dr. Dietrich Hertel (Göttingen) und das G2L (Göttingen).

Liebe Christina, ich danke dir außerordentlich für deine herzliche Art, die auch frustrierende Ergebnisse vergessen macht. Du hast deinen Nachnamen nicht ohne Grund. Dein Engagement, Mitgefühl und Ideenreichtum sucht seinesgleichen. Vielen Dank an die zwei Jans, G. und K.. Ihr habt mir mit eurer lockeren Art während der ersten Monate geholfen Fuß zu fassen. Jan G., danke für viele interessante Unterhaltungen und Ideen. Larissa, deine lustige, positive Art sowie deine Ideen waren ein Zugewinn für die Laborarbeit. Cedric, du standest mir immer für Aufreinigungs-Fragen zur Verfügung und hast dich wie kein anderer in gefühlt tausend Bereichen engagiert. Danke dir. Danke an die Nerd-Office Bewohner Raphael, Bingyao und Nora für die gute Zeit. Ein herzlicher Dank geht an die gesamte AGS/AGC für drei wirklich tolle Jahre. Ihr habt alle zu einer spitzen Atmosphäre beigetragen, auch außerhalb der Arbeit. Danke Martin für die tolle Geschenke-Auswahl aus Prag.

Franzi, ich danke dir für all deine Unterstützung und Bestärkung in den schwierigen Phasen und für die wirklich wunderschönen vergangenen Jahre. Danke für die Leichtigkeit und gute Laune Jerry. Danke Nikola und Johannes für die legendären Essens-Entdeckungen und B2 Zeiten. Das pendeln hat sich ausgezahlt und ich hoffe wir bleiben immer in so gutem Kontakt. Danke an alle (ehemaligen) Erlanger für die Aufrechterhaltung der traditionellen Treffen in der "Fränkischen" und die gute Zeit im Studium, die bis hierher geführt hat. Dank geht auch an meinen Bruder Markus für die Unterstützung. Liebe Eltern, ohne eure immerwährende Unterstützung wäre all dies nicht möglich gewesen. Danke, dass ihr immer für mich da wart.



# Table of Contents

Summary	IX
<b>1 Introduction</b>	<b>1</b>
1.1 Signal transduction by second messengers . . . . .	1
1.2 A unique second messenger – cyclic di-AMP . . . . .	3
1.2.1 Synthesis and degradation of cyclic di-AMP . . . . .	3
1.2.2 Targets of cyclic di-AMP . . . . .	6
1.2.3 Elucidation of cyclic di-AMP essentiality . . . . .	9
1.3 Regulation of potassium homeostasis in <i>Bacillus subtilis</i> . . . . .	11
1.4 Glutamate biosynthesis in <i>Bacillus subtilis</i> . . . . .	12
1.5 P <sub>II</sub> proteins as cellular signal integrators . . . . .	13
1.6 DarA – a c-di-AMP receptor of unknown function . . . . .	14
1.7 Aim of this work . . . . .	16
<b>2 Materials and Methods</b>	<b>17</b>
2.1 Materials . . . . .	17
2.1.1 Bacterial strains and plasmids . . . . .	17
2.1.2 Media, buffers and solutions . . . . .	17
2.1.3 Antibiotics . . . . .	22
2.2 Methods . . . . .	23
2.2.1 Cultivation of bacteria . . . . .	23
2.2.2 Storage of bacteria . . . . .	24
2.2.3 Genetic modification of <i>Escherichia coli</i> . . . . .	24
2.2.4 Genetic modification of <i>Bacillus subtilis</i> . . . . .	25
2.2.5 Growth analysis of <i>Bacillus subtilis</i> . . . . .	26
2.2.6 Preparation and detection of DNA . . . . .	27
2.2.7 Preparation and analysis of proteins . . . . .	31
2.2.8 Bacterial adenylate cyclase-based two-hybrid (BACTH) system . . . . .	40
2.2.9 Determination of intracellular metabolite amounts . . . . .	40
2.2.10 Determination of intracellular c-di-AMP amounts . . . . .	41
2.2.11 Determination of intracellular potassium amounts . . . . .	42
2.2.12 Phenotype screening . . . . .	42
2.2.13 Rational bioinformatic search of interaction partners . . . . .	44
<b>3 Results</b>	<b>45</b>
3.1 The genomic context of <i>darA</i> and its possible implications . . . . .	45
3.2 Unbiased screening for <i>darA</i> mutant phenotypes . . . . .	46
3.3 Construction of a c-di-AMP insensitive DarA variant . . . . .	47

3.4	DarA – a link to glutamate and potassium homeostasis? . . . . .	49
3.4.1	DarA can inhibit growth at low potassium availability . . . . .	49
3.4.2	The ligand-bound DarA impairs growth in liquid medium . . . . .	51
3.4.3	DarA is solely located in the cytosol . . . . .	53
3.4.4	The cytosolic interaction partner of DarA . . . . .	55
3.4.4.1	A search of DarA interaction partners by SPINE . . . . .	55
3.4.4.2	Suppressor evolution to elucidate the function of DarA . . . . .	56
3.4.4.3	Metabolite pools in a <i>darA</i> mutant . . . . .	58
3.4.4.4	Potassium and c-di-AMP amounts in a <i>darA</i> mutant . . . . .	60
3.5	Rational bioinformatic search of interaction partners . . . . .	61
3.6	DarA and extreme potassium limitation . . . . .	63
3.6.1	DarA is needed during extreme potassium limitation . . . . .	63
3.6.2	Suppressor mutations that compensate the <i>darA</i> deletion . . . . .	65
3.7	Interaction studies of DarA and the glutamate synthase . . . . .	67
3.8	Implications for DarA’s function in a <i>DAC</i> mutant . . . . .	71
3.9	Elevated potassium amounts stabilize a <i>DAC</i> mutant . . . . .	74
<b>4</b>	<b>Discussion</b>	<b>77</b>
4.1	No apparent functional link within the <i>darA</i> operon . . . . .	77
4.2	DarA interacts with a cytosolic target . . . . .	78
4.3	DarA allows to cope with extreme potassium limitation . . . . .	80
4.3.1	Does DarA interact with the glutamate synthase? . . . . .	81
4.3.2	Cyclic di-AMP – does it stimulate or inhibit DarA? . . . . .	84
4.3.3	Are there additional putative targets? . . . . .	88
4.4	Too much potassium is not enough without c-di-AMP . . . . .	91
4.5	Outlook . . . . .	92
<b>5</b>	<b>Bibliography</b>	<b>95</b>
<b>6</b>	<b>Appendix</b>	<b>119</b>
6.1	Supplementary data . . . . .	119
6.2	Bacterial strains . . . . .	129
6.3	Oligodeoxynucleotides . . . . .	134
6.4	Plasmids . . . . .	142
6.5	Materials . . . . .	145
	<i>Curriculum vitae</i>	<b>153</b>

## Publications

Gundlach, J., Herzberg, C., Kaefer, V., Gunka, K., Hoffmann, T., **Weiß, M.**, Gibhardt, J., Thürmer, A., Hertel, D., Daniel, R., Bremer, E., Commichau, F.M. and Stülke, J. (2017b) Control of potassium homeostasis is an essential function of the second messenger cyclic di-AMP in *Bacillus subtilis*. *Sci Signal* **10**: eaal3011.





# Abbreviations, units and nomenclatures

## General

% (v/v)	% (volume/volume)
% (w/v)	% (weight/volume)
$\alpha$ -KG	$\alpha$ -ketoglutarate
<i>A.</i>	<i>Arabidopsis</i>
$A_x$	absorbance, measured at wavelength $\lambda = x$ in nm
ABC	ATP binding cassette (transporter)
<i>ad</i>	to (latin)
ADP	adenosine diphosphate
AMP	adenosine monophosphate
AP	alkaline phosphatase
APS	ammonium peroxydisulfate
ATP	adenosine-5'-triphosphate
ATPase	adenosine triphosphatase
<i>B.</i>	<i>Bacillus</i>
BACTH	bacterial adenylate cyclase-based two-hybrid system
BHI	brain heart infusion (medium)
BSA	bovine serum albumin
<i>c</i>	concentration
cAMP	cyclic 3',5'-adenosine monophosphate
CBS	cystathionine- $\beta$ -synthase
CCR	carbon catabolite repression
CCR-PCR	combined chain reaction PCR
CE	cell extract
c-di-AMP	3',5'-cyclic di-adenosine monophosphate
c-di-GMP	3',5'-cyclic di-guanosine monophosphate
CFP	cyan fluorescent protein
cGAMP	2'/3',3'-cyclic GMP-AMP
cGMP	cyclic 3',5'-guanosine phosphate
CHAPS	3-[(3-Cholamidopropyl)dimethylammonio]-1-propanesulfonate hydrate
CRP	cyclic AMP receptor protein
GTP	guanosine-5'-triphosphate
CoA	coenzyme A
CY	cytosolic fraction
DAC	diadenylate cyclase
$\Delta DAC$	<i>cdaA disA cdaS</i> triple deletion mutant
$\Delta K$	<i>ktrAB kimA</i> double deletion mutant
DGC	diguanylate cyclase
dH <sub>2</sub> O	deionized water
DMSO	dimethylsulfoxid
DNA	deoxyribonucleic acid
DNase	deoxyribonuclease
dNTPs	deoxy nucleotide triphosphates
E	elution fraction
<i>E.</i>	<i>Escherichia</i>
EDTA	ethylenediamineacetic acid
<i>et al.</i>	latin: <i>et alii</i> (and others)
FA	formaldehyde

FBI-GS	feedback inhibited GS
Fc	fragment crystallizable (antibody region)
Fd	ferredoxin
5'-pApA	5'-phosphoadenylyl-(3'-5')-adenosine
5'-pGpG	5'-phosphoguanlylyl-(3'-5')-guanosine
5'-UMP	5'-uridine monophosphate
FRET	Förster resonance energy transfer
FT	flow-through
fwd	forward
GC	gas chromatography
GDH	glutamate dehydrogenase
GFP	green fluorescent protein
GMP	guanosine monophosphate
GOGAT	glutamine oxoglutarate aminotransferase
<i>goi</i>	gene of interest
GS	glutamine synthetase
HPLC	high performance liquid chromatography
ICP-OES	inductively coupled plasma optical emission spectrometry
IF	inoculation fluid
IgG	immunoglobulin G
IPTG	isopropyl- $\beta$ -D-thio-galactopyranoside
ITC	isothermal titration calorimetry
L	protein ladder
<i>L.</i>	part of: <i>Listeria monocytogenes</i> or <i>Lactococcus lactis</i>
LB	lysogeny broth (medium)
LC	liquid chromatography
LD	lysozyme-DNase I (mix)
LFH	long-flanking homology
<i>M.</i>	<i>Mycobacterium</i>
ME	membrane fraction
mRNA	messenger RNA
MS	mass spectrometry
MS $x$	modified sodium ( $x$ = medium or base type)
MSSM	modified sodium Spizizen's minimal (medium/base)
M $_w$	molecular weight
$n$	sample size
NAD $^+$ /H	nicotinamide adenine dinucleotide (oxidized/reduced)
NADP $^+$ /H	nicotinamide adenine dinucleotide phosphate (oxidized/reduced)
NAGK	<i>N</i> -acetyl-L-glutamate kinase
NG	new group
NTA	nitrilotriacetic acid
OD $_x$	optical density, measured at wavelength $\lambda = x$ in nm
ODH	2-oxoglutarate dehydrogenase complex
oligo	oligodeoxynucleotide
ONPG	<i>o</i> -nitrophenyl- $\beta$ -D-galactopyranoside
<i>p</i>	promoter
<i>p.a.</i>	latin: <i>pro analysi</i> (for analysis)
PAA	polyacrylamide
PAGE	polyacrylamide gel electrophoresis

PAS	Per-Arnt-Sim (domain)
PBS	phosphate buffered saline
PCR	polymerase chain reaction
PDB	protein data bank
PDE	phosphodiesterase
PDH	pyruvate dehydrogenase complex
pH	power of hydrogen
PIPES	1,4-piperazinediethanesulfonic acid
(p)ppGpp	guanosine tetra/pentaphosphate
PM	Phenotype MicroArray
PVDF	polyvinylidene fluoride
RCK	regulator of conductance K <sup>+</sup> (domain)
rev	reverse
RNA	ribonucleic acid
<i>RS</i>	riboswitch
<i>S.</i>	part of: <i>Staphylococcus aureus</i> , <i>Streptococcus pneumoniae</i> or <i>Synechococcus elongatus</i>
SD	Shine Dalgarno sequence
SDS	sodium dodecyl sulfate
SEC	size exclusion chromatography
SOB	super optimal broth (medium)
SP	sporulation (medium)
SPINE	Strep-protein interaction experiment
START	start codon (ATG in DNA)
STOP	stop codon (TAG, TGA or TAA in DNA)
<i>t</i>	time
<i>T.</i>	<i>Thermotoga</i>
TAE	Tris-acetate-EDTA (buffer)
TB	transformation buffer
TBS	Tris buffered saline
TCA	tricarboxylic acid
TE	Tris-EDTA (buffer)
TEMED	<i>N,N,N',N'</i> -tetramethylethylenediamine
T <sub>m</sub>	melting temperature
TMR	transmembrane helix
Tris	Tris(hydroxymethyl)aminomethane
UV	ultraviolet
vol.-%	volume percent
<i>V</i>	volume
W	washing fraction
w/o	without
WT	wildtype
X-Gal	5-bromo-4-chloro-3-indolyl-β-D-galactopyranoside
YFP	yellow fluorescent protein
ZAP	german: <i>Zellaufschlusspuffer</i> (cell disruption buffer)
WGS	whole genome sequencing

**Units and constants**

%	percent
°C	degree Celsius
A	ampere
Å	ångström
Au	absorption units
bar	bar
bp	base pair
Da	dalton
<i>g</i>	earth's gravitational acceleration
g	gram
h	hour
l	liter
m	meter
M	molar
min	minute
mol	mol
psi	pound-force per square inch
rpm	rounds per minute
s	second
U	enzyme unit
V	volt

**Prefixes**

M	mega
k	kilo
m	milli
μ	micro
n	nano
p	pico

**Amino acid nomenclature**

A	Ala	alanine
C	Cys	cysteine
D	Asp	aspartate
E	Glu	glutamate
F	Phe	phenylalanine
G	Gly	glycine
H	His	histidine
I	Ile	isoleucine
K	Lys	lysine
L	Leu	leucine
M	Met	methionine
N	Asn	asparagine
P	Pro	proline
Q	Gln	glutamine
R	Arg	arginine
S	Ser	serine
T	Thr	threonine
Y	Tyr	tyrosine
V	Val	valine
W	Trp	tryptophan

**Nucleosides**

A	adenine
C	cytosine
G	guanine
T	thymine
U	uracil

## Summary

Adaptation to changing environmental conditions is crucial for any organism to thrive in nature. Bacteria like the Gram-positive model organism *Bacillus subtilis* have evolved so-called second messengers to facilitate signal transduction processes. An important and unique second messenger is cyclic di-AMP (c-di-AMP) which has been discovered ten years ago. This small molecule has attracted much attention as it is essential for many bacteria that produce it but also can become toxic upon accumulation. Accordingly, it has been coined “essential poison”. In *B. subtilis* an essential function of c-di-AMP is the regulation of potassium homeostasis and the second messenger is nonessential when the cation is scarce. More advances in the last years refined the essential role of c-di-AMP as it becomes dispensable in several different bacteria under very specific growth conditions or by accumulation of suppressor mutations. It seems that the superordinate function of the small molecule is the adjustment of the cellular turgor by interaction with a plethora of targets. One major target is the P<sub>II</sub>-like protein DarA. P<sub>II</sub> proteins form one of the largest families of signal transduction proteins and are nearly ubiquitous in bacteria. These proteins bind low-molecular weight effectors and interact with a variety of targets to control nitrogen metabolism. DarA structurally resembles these classical P<sub>II</sub> proteins but binds c-di-AMP instead of ATP, ADP or 2-oxoglutarate. DarA is conserved in almost all c-di-AMP-producing firmicutes. Despite extensive efforts prior to this work the function of DarA has remained enigmatic. In this work, we conducted a large unbiased phenotype screening, but this did not reveal the function of DarA to us. However, we could show that DarA is interacting with a cytosolic target. Furthermore, we provide and discuss evidence that DarA is involved in glutamate metabolism and that apo-DarA is toxic for a c-di-AMP-free strain on rich medium. Apo-DarA most likely promotes a metabolic flux towards glutamate and arginine synthesis which is revealed in *B. subtilis* cells experiencing extreme potassium limitation. These cells accumulate positively charged amino acids derived from glutamate like ornithine, citrulline or arginine to compensate the lack of sufficient intracellular K<sup>+</sup> amounts. Surprisingly, DarA is needed for this compensatory mechanism. Our results show that DarA has to act on a target that feeds into the arginine biosynthesis. Structurally and rationally the glutamate synthase GltAB is the most promising interaction partner of DarA. Although unambiguous evidence for an interaction with GltAB is still pending, the established connection of DarA to glutamate metabolism will be crucial for further investigation. The results are especially interesting since the homeostases of c-di-AMP, K<sup>+</sup> and glutamate are somehow intricately intertwined but no target of c-di-AMP has been reported to be involved in the homeostasis of glutamate until this thesis. In addition, we show that c-di-AMP is not only dispensable at low K<sup>+</sup> concentrations, as reported before, but also when the cation is highly abundant. This contributes to a model of cellular turgor regulation by c-di-AMP. Although the interaction partner of DarA has escaped detection, we have linked DarA to glutamate metabolism which might aid the elucidation of c-di-AMP and glutamate homeostasis interconnections in the future.



# 1 Introduction

## 1.1 Signal transduction by second messengers

Bacteria, as all living cells, are frequently exposed to changing environments. Adaptation to altered conditions like temperature, nutrient supply, osmotic pressure and a multitude of other factors is consequently crucial for any organism to thrive in nature. Typically, this adaptation includes initial signal sensing, subsequent integration and amplification as well as the final response(s). For this signal transduction process, bacteria have evolved many different types of small nucleotides, termed second messengers. These small molecules diffuse within or even between cells and thus transduce the perceived signal. Common output responses of diverse signaling pathways include the alteration of gene expression or the regulation of protein activities (Commichau *et al.*, 2015a; Parkinson, 1993).

The first second messenger cyclic 3',5'-adenosine monophosphate (cAMP) however, was not identified in bacteria but in eukaryotic cells and first described to transduce intracellular hormone responses (Rall and Sutherland, 1958; Sutherland and Rall, 1958). After a few years, the prime example cAMP was also reported for the Gram-negative model organism *Escherichia coli* and linked to carbon catabolite repression (CCR) (Makman and Sutherland, 1965; Ullmann and Monod, 1968). CCR is a regulatory process which favors the utilization of a preferred carbon source like glucose and represses the utilization of less preferred, secondary carbon sources. Stunningly, 5 to 10 percent of genes are subjected to CCR in bacteria (Görke and Stülke, 2008; Magasanik, 1961). In glucose starved *E. coli* cells, cAMP is synthesized by an adenylate cyclase from adenosine-5'-triphosphate (ATP) and bound by the so-called cyclic AMP receptor protein (CRP). The cAMP-CRP complex activates the expression of several catabolic genes and operons by binding to the respective promoter regions, which alone are usually weak and thus rely on activation (Görke and Stülke, 2008; Stülke and Hillen, 1999). This is different for the Gram-positive model organism *Bacillus subtilis*. There is only little evidence for the presence of cAMP in sporulating or oxygen limited *B. subtilis* cells and cyclic AMP receptor proteins seem to be missing (Biville and Guiso, 1989; Diethmaier *et al.*, 2014; Mach *et al.*, 1984). CCR in *B. subtilis* is governed by the pleiotropic transcription factor CcpA, the histidine-carrier protein HPr of the phosphotransferase system, the HPr kinase/phosphorylase HPrK as well as glycolytic intermediates. Availability of a preferred carbon source like glucose triggers glycolytic processes and leads to the phosphorylation of HPr by HPrK. CcpA binds the phosphorylated HPr and represses the expression of catabolic genes by binding of the complex to catabolite responsive elements within the respective promoter regions (Görke and Stülke, 2008; Stülke and Hillen, 1999).

Another second messenger is cyclic 3',5'-guanosine monophosphate (cGMP) which is synthesized by guanylate cyclases from guanosine-5'-triphosphate (GTP). For a long time, cGMP was solely attributed to eukaryotes and reports about bacterial cGMP were contradictory or incomplete (Gomelsky, 2011; Linder, 2010). A few years ago unambiguous evidence was

provided for a guanylyl cyclase in *Rhodospirillum centenum* and involvement of cGMP in cyst formation (Marden *et al.*, 2011). Similar to cAMP, there is no robust evidence for cGMP signaling in *B. subtilis* (Diethmaier *et al.*, 2014; Gomelsky, 2011).

The “alarmones” guanosine tetra- (ppGpp) and pentaphosphate (pppGpp), collectively (p)ppGpp, are widely distributed in bacteria. They are synthesized and degraded by bifunctional RelA/SpoT homologue proteins during the so-called stringent response. Diverse stresses such as starvation for amino acids, phosphates, fatty acids, carbon and iron induce (p)ppGpp synthesis. As a response, a variety of cellular processes are negatively regulated both on gene and on protein level (Hauryliuk *et al.*, 2015; Liu *et al.*, 2015).

Structurally different to the aforementioned are the cyclic dinucleotide second messengers, the best studied being 3',5'-cyclic di-GMP (c-di-GMP). Synthesis of c-di-GMP out of two molecules of GTP is achieved by diguanylate cyclases (DGCs) containing a catalytic GGDEF domain. Degradation is carried out by c-di-GMP-specific phosphodiesterases (PDEs) which contain either an EAL or an HD-GYP domain and hydrolyze the second messenger to 5'-phosphoguanylyl-(3'-5')-guanosine (5'-pGpG) or 5'-GMP, respectively. DGCs and PDEs are widely distributed and present in almost all bacteria. In correlation to the abundance of DGCs and PDEs, numerous targets binding c-di-GMP have been identified, among them proteins containing PilZ domains or degenerate GGDEF and EAL domains, transcriptional regulators and even mRNA (messenger ribonucleic acid) riboswitches. Consequently, c-di-GMP is involved or implicated in a multitude of different cellular processes, such as flagellar motility, switching between motile and sessile lifestyles, formation of biofilms and virulence (Hengge *et al.*, 2016; Jenal *et al.*, 2017; Römling *et al.*, 2013). *B. subtilis* encodes three DGCs (DgcK, DgcP and DgcW). However, c-di-GMP seems to be of minor importance. Intracellular amounts are low, physiological triggers for c-di-GMP synthesis remain elusive and biofilm formation is governed by the phosphodiesterase YmdB and not by c-di-GMP. Recently, a model was proposed that c-di-GMP might act during stresses and govern exclusivity of motility and extra cellular polysaccharide production (Bedrunka and Graumann, 2017; Diethmaier *et al.*, 2014; Kampf and Stülke, 2017). Another cyclic dinucleotide that gained more and more attention over the last ten years is 3',5'-cyclic di-AMP (c-di-AMP), which will be discussed later in detail (see Section 1.2).

In addition to c-di-GMP and c-di-AMP, synthesis of a cyclic hybrid molecule has also been reported in *Vibrio cholerae* (Davies *et al.*, 2012). The identified 3',3'-cyclic GMP-AMP (3',3'-cGAMP) was implicated in chemotaxis and intestinal colonization of the human pathogen and demonstrated to bind and activate the serine hydrolase/phospholipase CapV. Activated CapV degrades phospholipids of the cell membrane and leads to the release of fatty acids, which might favor the adaptation of the pathogen to membrane stresses (Davies *et al.*, 2012; Severin *et al.*, 2018). Shortly thereafter, 2'-3'-cGAMP was reported as the first cyclic dinucleotide in metazoa and shown to act in the innate immune response. The mammalian deoxyribonucleic acid (DNA) sensor cGAS synthesizes 2'-3'-cGAMP, which binds and activates the STING adaptor protein, leading to type-I interferon production (Sun *et al.*, 2012; Wu *et al.*, 2013).



## 1.2 A unique second messenger – cyclic di-AMP

### 1.2.1 Synthesis and degradation of cyclic di-AMP

Cyclic di-AMP was described only ten years ago as a surprising discovery on the side. The nucleotide was identified within the crystal structure of the DNA integrity scanning protein DisA from *Thermotoga maritima* and *B. subtilis*, and catalytic diadenylate cyclase (DAC) activity was shown (Witte *et al.*, 2008). So far, c-di-AMP has been reported for many different bacteria like firmicutes, actinobacteria, cyanobacteria, deltaproteobacteria, and even for some archaea (Commichau *et al.*, 2018b).

DACs synthesize c-di-AMP in a condensation reaction from two molecules of ATP. All enzymes harbor the catalytically active DAC domain, which is joined by other domains of different functionality. So far, five classes of DACs have been identified which are referred to as CdaA- (DacA), DisA-, CdaS-, CdaM- and CdaZ-type (see Figure 1.1). Most bacteria produce either only CdaA or DisA. The latter is found in spore-forming firmicutes, *T. maritima* and is the only DAC in actinobacteria. The CdaA-type is probably the most widespread class and can be found in most firmicutes, cyanobacteria, spirochaetes and other bacteria. CdaA is also the only DAC in pathogenic firmicutes like the model organisms *Staphylococcus aureus*, *Listeria monocytogenes* and *Streptococcus pneumoniae*. The novel cyclases CdaM and CdaZ have just been discovered recently in *Mycoplasma pneumoniae* and in *Methanocaldococcus jannaschii*, respectively (Blötz *et al.*, 2017; Commichau *et al.*, 2018b; Kellenberger *et al.*, 2015).

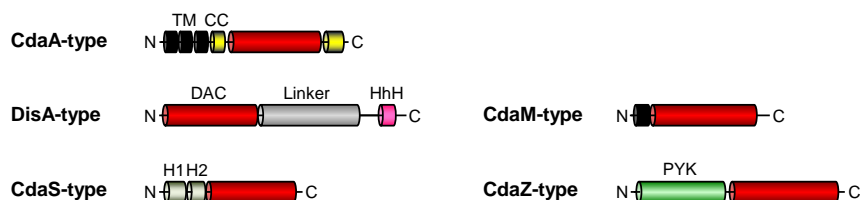


**Figure 1.1: Domain organization of the five known diadenylate cyclase types.** (adapted from Commichau *et al.*, 2018b). Domains are indicated by color. Diadenylate cyclase domain (DAC), helix-hinge-helix domain (HhH), transmembrane helix (TM), coiled-coil domain (CC), autoinhibitory domain 1/2 (H1/2), pyruvate kinase-like domain (PYK).

In contrast to most bacteria, *B. subtilis* produces three DACs: CdaA, DisA and CdaS. The genes for CdaA and DisA are expressed constitutively, while CdaS is sporulation-specific (Commichau *et al.*, 2018b; Nicolas *et al.*, 2012). The three DACs are differentially localized within the cell. CdaA is localized at the membrane, while the other two are cytosolic with DisA being found in the nucleoid region. This led to the proposal of subcellular c-di-AMP pools to locally regulate different cellular processes (Commichau *et al.*, 2018b). Local pools and subcellular signaling have already been discussed frequently for the structurally similar c-di-GMP (Sarenko *et al.*, 2017). However, this model needs more extensive validation for c-di-AMP. Interestingly, *L. monocytogenes* CdaA has quite unusual co-factor requirements,

as it either utilizes  $Mn^{2+}$  or  $Co^{2+}$  (Rosenberg *et al.*, 2015). DisA of *T. maritima*, *B. subtilis*, *B. thuringiensis* and *Mycobacterium tuberculosis* however require  $Mg^{2+}$  or  $Mn^{2+}$ , which cannot be replaced effectively by  $Co^{2+}$  (Bai *et al.*, 2012; Witte *et al.*, 2008; Zheng *et al.*, 2013).

In *B. subtilis* *cdaA* is encoded in an operon together with genes encoding the regulatory membrane protein CdaR and the phosphoglucosamine mutase GlmM. CdaR interacts with CdaA and subsequent inhibition of catalytic CdaA activity was shown *in vivo* for *L. monocytogenes* and *S. aureus* (Bowman *et al.*, 2016; Gundlach *et al.*, 2015b; Mehne *et al.*, 2013; Rismondo *et al.*, 2016). Interactions of GlmM with CdaA have also been documented, and resulting repression of CdaA activity has been shown in *Lactococcus lactis* (Gundlach *et al.*, 2015b; Zhu *et al.*, 2016). This is particularly interesting, since GlmM is an essential enzyme that catalyzes the reaction from D-glucosamine-6-phosphate to D-glucosamine-1-phosphate, a precursor of cell wall building blocks (Mengin-Lecreux and van Heijenoort, 1996). However, GlmM is not an essential target of c-di-AMP (Gundlach *et al.*, 2015b).

The nucleoid associated DisA binds and moves along the chromosomal DNA and produces c-di-AMP. When DisA encounters DNA damages, like Holliday junctions or double strand breaks, movement is stalled and c-di-AMP synthesis is impaired (Gándara and Alonso, 2015; Witte *et al.*, 2008). Moreover, DisA activity is inhibited by binding of the 6-*O*-methylguanine-DNA methyltransferase RadA in *B. subtilis* and *M. tuberculosis* (Gándara *et al.*, 2017; Zhang and He, 2013). c-di-AMP synthesis by DisA was proposed to regulate sporulation in concert with potentially present DNA damages in *B. subtilis* (Gándara and Alonso, 2015). However, another model was proposed recently. Since c-di-AMP regulates potassium homeostasis (described in Section 1.3) and  $K^+$  is responsible for buffering the negatively charged phosphate backbone of the DNA, DisA might provide local c-di-AMP synthesis in response to a locally altered  $K^+$  concentration (Commichau *et al.*, 2018b; Gundlach *et al.*, 2018; 2017a; b).

As mentioned before, the third DAC in *B. subtilis*, CdaS, is sporulation specific and only found in sporulating bacilli and in few clostridia species (Commichau *et al.*, 2015a; Corrigan and Gründling, 2013). The physiological triggers affecting CdaS and why c-di-AMP is required for efficient sporulation is still unknown (Commichau *et al.*, 2018b; Mehne *et al.*, 2014).

Most interestingly, c-di-AMP is essential under most common laboratory conditions in almost all bacteria encoding the membrane-associated diadenylate cyclase CdaA. This is for example true for the well studied firmicutes *B. subtilis*, *L. monocytogenes* and *S. aureus* (Commichau *et al.*, 2018b). Intriguingly, essentiality in cyanobacteria is not entirely obvious since the *cdaA* gene is essential in *Synechocystis subspecies* PCC 6803 but not in *Synechococcus elongatus* PCC 7942 (Agostoni *et al.*, 2018; Rubin *et al.*, 2018). As mentioned before, *B. subtilis* encodes three distinct diadenylate cyclases. Under most common laboratory growth conditions either *cdaA* or *disA* has to be expressed to ensure viability. CdaS does not contribute to c-di-AMP essentiality since *cdaA cdaS* or *disA cdaS* double deletion mutants are both viable in contrast to *cdaA disA* or *cdaA disA cdaS* deletion mutants where c-di-AMP is essential (Luo and Helmann, 2012; Mehne *et al.*, 2013). Whereas the lack of the second messenger is lethal for many bacteria, accumulation of c-di-AMP can also become toxic. This is for example

observed in cells overexpressing the synthesizing enzymes or in a double deletion mutant for the c-di-AMP degrading phosphodiesterases GdpP and PgpH. Accordingly, c-di-AMP has also been coined “essential poison” (Gundlach *et al.*, 2015b; Mehne *et al.*, 2013).

To prevent toxic accumulation, the cyclic dinucleotide is degraded by phosphodiesterases (PDEs). So far, four classes of c-di-AMP degrading PDEs have been identified which are referred to as GdpP-, PgpH-, DhhP- and CdnP-type (see Figure 1.2). All PDEs are able to degrade c-di-AMP to 5'-phosphoadenylyl-(3'-5')-adenosine (5'-pApA) (Commichau *et al.*, 2018b). In the case of the DhhP-type PDE, 5'-pApA is even further hydrolyzed to 5'-AMP in a second step (Bai *et al.*, 2013; Manikandan *et al.*, 2014; Ye *et al.*, 2014). The model organism *B. subtilis* contains two PDEs: GdpP and PgpH (Commichau *et al.*, 2015a).

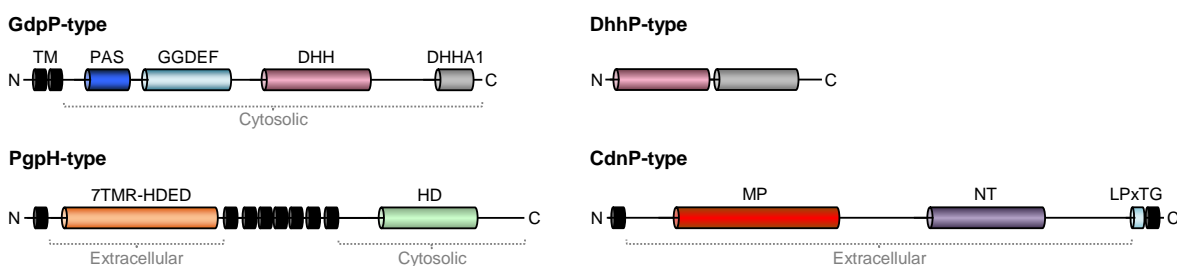


**Figure 1.2: Domain organization of the four known phosphodiesterase types.** (adapted from Commichau *et al.*, 2018b). Domains are indicated by color. Transmembrane helix (TM), Per-Arnt-Sim domain (PAS), degenerate GGDEF domain (GGDEF), DHH domain (DHH), DHHA1 domain (DHHA1), seven transmembrane helix-HDED domain (7TMR-HDED), HD domain (HD), metallophosphatase domain (MP), 5'-nucleotidase domain (NT), surface localization motif (LPxTG).

The GdpP- and DhhP-type PDEs contain the catalytically active DHH/DHHA1 domain which is essential for cleaving c-di-AMP to 5'-pApA. Interestingly, GdpP contains two N-terminal transmembrane helices which also seem to be essential for its function (Cho and Kang, 2013). The GdpP-type PDEs can be found in many c-di-AMP-producing bacteria such as firmicutes, actinobacteria, spirochaetes and cyanobacteria. The DhhP-type PDEs have been reported for several bacteria like mycobacteria, *Borrelia burgdorferi*, *M. pneumoniae*, *S. aureus* and *T. maritima*. In addition to the DHH/DHHA1 domain, the GdpP-type PDEs contain a Per-Arnt-Sim (PAS) and a degenerate GGDEF domain. The specific role of the degenerate GGDEF domain is currently still unknown (Commichau *et al.*, 2015a; Commichau *et al.*, 2018b). Inhibition of GGDEF ATPase and DHH/DHHA1 phosphodiesterase activity has been reported by binding of b-type heme to the PAS domain (Rao *et al.*, 2011). The stringent response alarmone (p)ppGpp is also a strong competitive inhibitor for the DHH/DHHA1 domain in some firmicutes, which is especially interesting since c-di-AMP and (p)ppGpp metabolism seem to be connected to each other (Corrigan *et al.*, 2015; Liu *et al.*, 2006; Rao *et al.*, 2010; Whiteley *et al.*, 2015). However, the interplay between the two messengers needs further elucidation. c-di-AMP is clearly the preferred substrate for GdpP, but cleavage of c-di-GMP to 5'-pGpG is also possible. This is also true for DhhP, which furthermore cleaves 5'-pApA and 5'-pGpG to 5'-AMP and 5'-GMP, respectively (Huynh and Woodward, 2016).

The PgpH-type is yet another class and contains a catalytically active HD domain for c-di-AMP degradation to 5'-pApA and an extracellular 7TMR-HDED domain. Attributed to their abundance among bacteria, especially firmicutes, PgpH-type PDEs are thought to be the major c-di-AMP degrading enzymes (Commichau *et al.*, 2018b). Similar to GdpP, PgpH is also inhibited by the alarmone (p)ppGpp. As already mentioned, (p)ppGpp and c-di-AMP metabolism seems to be linked. *L. monocytogenes* *pgpH* and *S. aureus* *gdpP* mutants contain higher levels of c-di-AMP and accumulated higher levels of (p)ppGpp during stress (Corrigan *et al.*, 2015; Liu *et al.*, 2006). Intriguingly, the opposite was reported for a *L. monocytogenes* c-di-AMP depletion strain, which lead to accumulation of (p)ppGpp and growth inhibition. It was suggested that low and high c-di-AMP amounts influence alarmone production by modulating central metabolism and amino acid biosynthesis (Whiteley *et al.*, 2015).

A novel fourth class of PDEs, the membrane-anchored, extracellular CdnP, has just been discovered recently in the human pathogen *Streptococcus agalactiae*. CdnP acts sequentially with the ectonucleotidase NudP and degrades extracellular c-di-AMP to 5'-AMP and further to adenosine and inorganic phosphate (Andrade *et al.*, 2016; Firon *et al.*, 2014). CdnP is composed of a 5'-nucleotidase domain and a metallophosphoesterase domain, containing a conserved NHE motif. The NHE motif is required for enzymatic activity. Interestingly, *B. subtilis* encodes the promiscuous nucleotide phosphoesterase YfkN which is similar to CdnP (46% amino acid identity), but involvement in c-di-AMP metabolism is not known so far (Chambert *et al.*, 2003; Commichau *et al.*, 2018b).

### 1.2.2 Targets of cyclic di-AMP

The essentiality of the second messenger c-di-AMP in many bacteria is a unique feature and has attracted much attention during the last decade (Commichau *et al.*, 2015a; Corrigan and Gründling, 2013). Consequently, many research groups tried to elucidate the essential role of the nucleotide in various bacteria. Several new methods were developed in the process to aid the elucidation, among them pull-down assays, high-throughput screenings and conditional generation and analyses of suppressor mutants (Corrigan *et al.*, 2013; Kampf *et al.*, 2017; Orr and Lee, 2017; Rubin *et al.*, 2018). Indeed, a plethora of c-di-AMP targets (see Figure 1.3) has been identified in a diverse set of bacteria, among them *B. subtilis*, the pathogenic firmicutes *L. monocytogenes*, *S. aureus* and *S. pneumoniae*, the genome-reduced *Mollicute* *M. pneumoniae* as well as lactic acid bacteria and actinobacteria (Blötz *et al.*, 2017; Corrigan *et al.*, 2013; Gundlach, 2017; Gundlach *et al.*, 2015a; Pham *et al.*, 2018; Sureka *et al.*, 2014; Zarrella *et al.*, 2018; Zhang *et al.*, 2013).

The first identified c-di-AMP receptor was the TetR-like transcription factor DarR in *Mycobacterium smegmatis*. DarR represses the expression of its own gene, of *cspA*, encoding a cold shock family protein, and of two genes associated with fatty acid metabolism (Zhang *et al.*, 2013). However, DarR homologues are only present in few actinobacteria suggesting a

minor, specialized role of DarR in c-di-AMP signal transduction (Corrigan and Gründling, 2013; Zhang *et al.*, 2013).

Interestingly, several c-di-AMP targets from different bacteria are involved in various ways in the regulation of the cellular potassium homeostasis (Commichau *et al.*, 2018b). One major target is the cytoplasmic gating component KtrA of the high-affinity K<sup>+</sup> importer KtrAB, which was first identified in *S. aureus* (Corrigan *et al.*, 2013). KtrA can also be found in *L. monocytogenes*, *B. subtilis* as well as in close relatives, and binding of c-di-AMP to *B. subtilis* KtrA was shown recently (Commichau *et al.*, 2015a; Gundlach, 2017). KtrA contains two highly conserved regulator of conductance K<sup>+</sup> (RCK) domains, RCK\_C and RCK\_N (Albright *et al.*, 2006). While the RCK\_N domain binds ADP/ATP and NAD<sup>+</sup>/NADH, the RCK\_C domain binds c-di-AMP (Albright *et al.*, 2006; Corrigan *et al.*, 2013). Another K<sup>+</sup> uptake system, highly similar to KtrAB, is the low-affinity K<sup>+</sup> importer KtrCD in *B. subtilis* (Holtmann *et al.*, 2003). KtrC also exhibits both RCK domains and binds c-di-AMP (Corrigan *et al.*, 2013; Gundlach, 2017). Yet another pair of orthologues are CabP (for KtrA/C) and TrkH (for KtrB/D) from *S. pneumoniae*. Both proteins are required for growth of the bacteria at low K<sup>+</sup> concentrations. It is assumed that direct binding of c-di-AMP to CabP, KtrA or KtrC leads to inhibition of K<sup>+</sup> uptake by CabP/TrkH, KtrAB or KtrCD, respectively (Bai *et al.*, 2014; Zarrella *et al.*, 2018). Interestingly, c-di-AMP levels in a *S. pneumoniae* *cabP* deletion mutant were significantly reduced, which was not the case for a *trkH* deletion mutant (Zarrella *et al.*, 2018).

Furthermore, the novel high-affinity K<sup>+</sup> importer *kimA* was just identified in *B. subtilis* and shown to be negatively regulated by c-di-AMP binding to the protein (Gundlach, 2017). Interestingly, c-di-AMP also binds to the *kimA* (*ydaO*) riboswitch that is located upstream of *kimA* and inhibits expression upon ligand-binding (genetic OFF-switch) (Gundlach *et al.*, 2017b; Nelson *et al.*, 2013). The *kimA* riboswitch is also found in front of the *ktrAB* operon, encoding a high-affinity K<sup>+</sup> transporter as described before. This again makes c-di-AMP a unique second messenger. The dinucleotide governs one physiological process (K<sup>+</sup> uptake) by regulating both the protein activity and gene expression through binding to the protein and the corresponding mRNA riboswitch (Gundlach *et al.*, 2017b; Nelson *et al.*, 2013).

Another target protein involved in K<sup>+</sup> homeostasis is the sensor histidine kinase KdpD in *S. aureus* (Commichau *et al.*, 2018b; Corrigan *et al.*, 2013). The membrane-bound KdpD together with the cytosolic response regulator KdpE constitute a classical two-component system. Under severe K<sup>+</sup> limitation KdpD is autophosphorylated and the phosphate group is transferred to KdpE which triggers expression of the high-affinity K<sup>+</sup> uptake system *kdpFABC* (Ballal *et al.*, 2007; Greie, 2011). The bacterial KdpDE/FABC system is widely distributed and also found in other c-di-AMP-producing bacteria such as *M. smegmatis* and the well studied *L. monocytogenes*, but not in *B. subtilis* (Ali *et al.*, 2017; Ballal *et al.*, 2007; Commichau *et al.*, 2015a; Commichau *et al.*, 2018a; Corrigan *et al.*, 2013). Binding of c-di-AMP to *S. aureus* KdpD occurs at the universal stress protein domain, which impairs the expression of KdpFABC and consequently inhibits K<sup>+</sup> import (Moscoso *et al.*, 2016).

Another protein containing both RCK domains and that binds c-di-AMP is the cation/H<sup>+</sup> antiporter CpaA from *S. aureus* (Corrigan *et al.*, 2013). Recently, c-di-AMP binding was also shown for the orthologue YjbQ from *B. subtilis* (Gundlach, 2017). Binding of c-di-AMP stimulates the activity of CpaA. However, CpaA has no specificity for K<sup>+</sup> over Na<sup>+</sup> ions (Chin *et al.*, 2015; Corrigan *et al.*, 2013). Consequently, it is not entirely conclusive whether the K<sup>+</sup>, Na<sup>+</sup> or H<sup>+</sup> gradient, or a combination, is the relevant function.

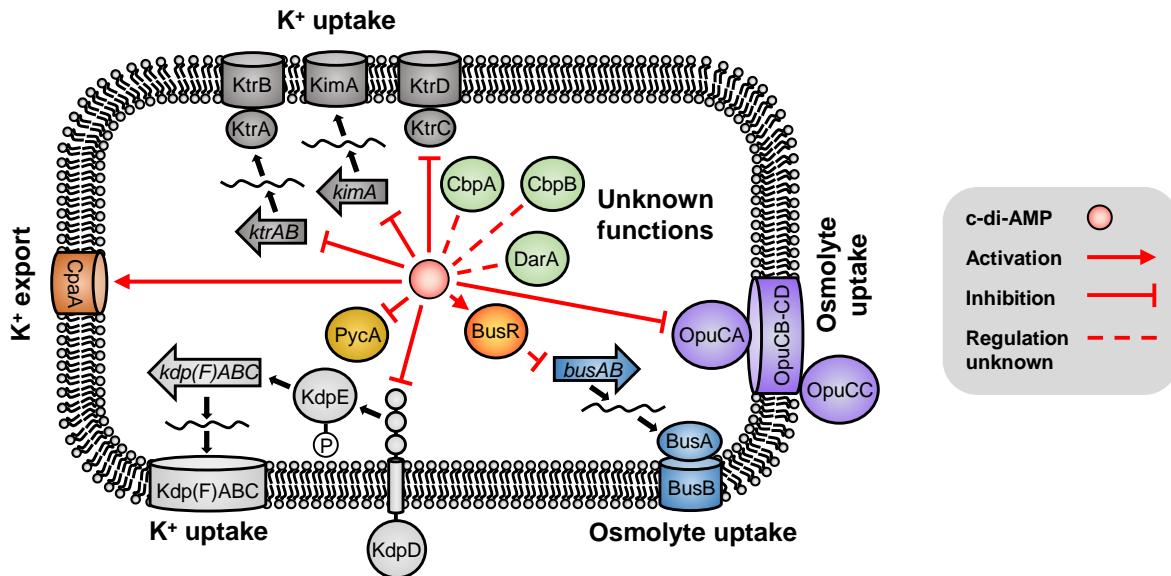


**Figure 1.3: Targets known to bind c-di-AMP.** (adapted from Commichau *et al.*, 2018b). Major targets of c-di-AMP are proteins and RNA molecules that are involved in K<sup>+</sup> or osmolyte homeostasis. Another target is the pyruvate carboxylase PycA in some bacteria. Several c-di-AMP-binding proteins are still of unknown function like CbpA, CbpB (YkuL) and DarA. More target proteins await characterization.

Other targets of c-di-AMP are involved in osmolyte uptake. c-di-AMP inhibits the OpuC osmolyte uptake system in *S. aureus* and *L. monocytogenes* (Huynh *et al.*, 2016; Schuster *et al.*, 2016). OpuC is an ATP binding cassette (ABC) osmoprotectant import system of the Opu family. OpuC consists of four different subunits, OpuCA, OpuCB, OpuCC and OpuCD (Hoffmann and Bremer, 2017). c-di-AMP binds to the cystathionine- $\beta$ -synthase (CBS) domain of the adenosine triphosphatase (ATPase) subunit OpuCA. Subsequently, import of the compatible solute carnitine is inhibited as shown for *S. aureus* and *L. monocytogenes* (Huynh *et al.*, 2016; Schuster *et al.*, 2016). Binding of c-di-AMP to OpuCA in *B. subtilis* was also shown recently (Gundlach, 2017).

Inhibition of osmolyte uptake by c-di-AMP is also found in lactic acid bacteria, however the mode of action is different (Devaux *et al.*, 2018; Pham *et al.*, 2018). Expression of *busAA-AB*, encoding a glycine betaine osmoprotectant transporter, is inhibited by the transcriptional repressor BusR (Romeo *et al.*, 2003). Binding of c-di-AMP to the TrkA\_C domain of BusR enhances the repression of *busAA-AB*, leading to the inhibition of glycine betaine uptake (Devaux *et al.*, 2018; Pham *et al.*, 2018).

In addition to targets involved in potassium and osmolyte homeostasis, c-di-AMP binding has also been reported for a variety of other proteins. c-di-AMP binds to the pyruvate carboxylase PycA in *Enterococcus faecalis*, *S. aureus*, *L. monocytogenes* and *L. lactis* and inhibits its activity (Choi *et al.*, 2017; Sureka *et al.*, 2014; Whiteley *et al.*, 2017). PycA acts in the tricarboxylic acid (TCA) cycle and catalyzes the ATP-dependent conversion of pyruvate to oxaloacetate (Jitrapakdee *et al.*, 2008). Interestingly, PycA is of special importance in *L. monocytogenes* and *L. lactis* since both bacteria only contain a truncated TCA cycle (Schär *et al.*, 2010; Wang *et al.*, 2000). c-di-AMP binding to *B. subtilis* PycA has not been addressed so far. Recently, the mycobacterial recombinase RecA was shown to bind both c-di-AMP and c-di-GMP. It was further demonstrated that c-di-AMP repressed the translation of *recA* mRNA and influenced homologous recombination and DNA damage repair (Manikandan *et al.*, 2018). In addition to the aforementioned OpuCA, the poorly characterized proteins CbpA and CbpB (YkuL in *B. subtilis*) from *L. monocytogenes* also contain CBS domains which bind c-di-AMP (Gundlach, 2017; Sureka *et al.*, 2014). However, their function remains to be elucidated (Commichau *et al.*, 2018b). Another c-di-AMP-binding protein of unknown function is the P<sub>II</sub>-like protein DarA (PstA in some organisms), which is highly conserved among Gram-positive, c-di-AMP-producing firmicutes (Gundlach *et al.*, 2015a). DarA itself is subject of this thesis and will be discussed later in detail. Even more c-di-AMP-binding proteins have been identified recently in *B. subtilis*, among them KhtT and MgtE (Gundlach, 2017). KhtT is part of the K<sup>+</sup>/H<sup>+</sup> antiporter KhtSTU and contains an RCK\_C domain, which is known to bind c-di-AMP. KhtT has no RCK\_N domain, in contrast to KtrA and KtrC (Albright *et al.*, 2006; Corrigan *et al.*, 2013; Fujisawa *et al.*, 2004). MgtE is the main Mg<sup>2+</sup> importer in *Bacillus* and contains a CBS domain, which is already known to bind c-di-AMP (Sureka *et al.*, 2014; Wakeman *et al.*, 2014). Interplay of the two proteins in the c-di-AMP signaling network still remains to be unraveled.

### 1.2.3 Elucidation of cyclic di-AMP essentiality

Under most common laboratory conditions, c-di-AMP is essential in almost all bacteria encoding diadenylate cyclases of the CdaA-type. For example in the pathogenic model organisms *S. aureus*, *L. monocytogenes* and *S. pneumoniae*, which encode only CdaA, and in *B. subtilis* which encodes CdaA, DisA and CdaS. c-di-AMP is also essential in *M. pneumoniae* encoding a CdaM-type DAC (Blötz *et al.*, 2017; Commichau *et al.*, 2018b). Interestingly, c-di-AMP is not essential in actinobacteria which only encode a DisA-type DAC. Essentiality of the CdaZ-type DAC is not known so far (Commichau *et al.*, 2018b).

Recent advances in the last years refined the essential role of c-di-AMP in bacteria, as more and more conditions were identified that allow for dispensability of the cyclic dinucleotide. In *L. monocytogenes*, c-di-AMP metabolism was linked to the alarmone (p)ppGpp and it was proposed that low and high c-di-AMP levels influence (p)ppGpp production by modulating

central metabolism and amino acid biosynthesis (Liu *et al.*, 2006; Whiteley *et al.*, 2015). Surprisingly, c-di-AMP is not essential anymore in a *L. monocytogenes* mutant lacking all three (p)ppGpp synthases. This was attributed to the inactivation of the pleiotropic transcriptional regulator CodY and indeed c-di-AMP was also dispensable when *L. monocytogenes* was grown in minimal medium that favored CodY inactivation (Whiteley *et al.*, 2015). c-di-AMP also modulates central metabolism at the pyruvate node of the TCA cycle, as observed by toxic accumulation of citrate in a *L. monocytogenes cdaA* null mutant. It should be noted that *L. monocytogenes* contains an incomplete TCA “cycle” (Whiteley *et al.*, 2015). In addition, suppressor mutations were identified in the operons of the oligopeptide permease system Opp, the putative glycine betaine transporter Gbu and in the c-di-AMP target proteins CbpB and DarA (PstA). Consequently, one hypothesis was that unregulated uptake of osmolytes and peptides in a *cdaA* null mutant might increase the turgor pressure of the cells and culminate in cell lysis (Whiteley *et al.*, 2017; 2015).

The situation is similar for *S. aureus* where c-di-AMP is dispensable in defined minimal medium when cells are osmotically stabilized by salt supplementation. Mutations inactivating the main glycine betaine uptake system OpuD or the putative amino acid transporter AlsT restored growth of the *S. aureus cdaA* mutant in rich medium again (Zeden *et al.*, 2018). Interestingly, c-di-AMP was also dispensable for *S. aureus* grown under anaerobic conditions, a condition where TCA cycle activity is reduced (Fuchs *et al.*, 2007; Zeden *et al.*, 2018).

All this is in excellent agreement with the essential function of c-di-AMP in *B. subtilis*. All three DACs, thus c-di-AMP, were recently shown to be dispensable for *B. subtilis* grown in defined minimal medium with low amounts of potassium when ammonium is used as nitrogen source (Gundlach *et al.*, 2017b). In *B. subtilis*, K<sup>+</sup> import is inhibited by c-di-AMP both on gene and protein level. Lack of c-di-AMP would consequently lead to uncontrolled import of K<sup>+</sup>, concomitant water influx and subsequent lysis of the cells due to increasing turgor pressure (Commichau *et al.*, 2018a; Gundlach *et al.*, 2017b). Mutations affecting the cation transporter NhaK restored growth of the *B. subtilis* c-di-AMP null mutant again when cells were subjected to higher amounts of the ion (Gundlach *et al.*, 2017b).

More and more recent reports in other bacteria highlight the role of c-di-AMP in osmoregulation. In Group B *Streptococcus* c-di-AMP also binds to osmolyte transporters and to the transcriptional regulator BusR. BusR represses the expression of *busAB*, encoding a glycine betaine transporter. In fact, a *cdaA* null mutant was viable in glycine betaine containing medium, when cells acquired loss-of-function mutations in *busAB* (Devaux *et al.*, 2018). It seems apparent that the essential function of c-di-AMP in various bacteria is the regulation of osmolyte homeostasis. This is also reflected by many identified c-di-AMP targets that contribute to maintaining the cellular turgor, as well as arising suppressor mutations provoked by perturbation of c-di-AMP levels (high and low). Surely, more examples of c-di-AMP dispensability for other bacteria and conditions are expected in the future (Commichau *et al.*, 2018a).



### 1.3 Regulation of potassium homeostasis in *Bacillus subtilis*

The potassium cation is the most abundant cation in bacterial and eukaryotic cells (Epstein, 2003). *B. subtilis* and other bacteria accumulate  $K^+$  to around 300 mM, which is stunning since most habitats only contain  $K^+$  concentrations as low as 0.1–10 mM (McLaggan *et al.*, 1994; Whatmore *et al.*, 1990). Potassium ions fulfill a plethora of vital functions in the cells. These include control of gene expression, pH regulation, maintaining ribosome function, enzyme activation and osmoregulation (Ballal *et al.*, 2007; Durand *et al.*, 2016; Ennis and Lubin, 1961; Epstein, 2003; Gralla and Vargas, 2006; H. and Wong, 1986; McLaggan *et al.*, 1994; Nissen *et al.*, 2000). Although  $K^+$  controls essential functions, excessive accumulation can also become toxic for the bacteria. Consequently,  $K^+$  transport has to be tightly controlled which is an essential function of the second messenger c-di-AMP in *B. subtilis* (Gundlach *et al.*, 2017b; Radchenko *et al.*, 2006a; b).

*B. subtilis* utilizes three  $K^+$  import systems in total: KtrAB, KtrCD and KimA which are all controlled by c-di-AMP (Gundlach *et al.*, 2017b; Holtmann *et al.*, 2003). The high-affinity  $K^+$  import systems KtrAB and KimA facilitate import at low external  $K^+$  concentrations. At high external  $K^+$  concentrations, c-di-AMP binds to the *kimA* riboswitch which is located upstream of the *ktrAB* and *kimA* gene and inhibits the expression. Import under this condition is then carried out by the low-affinity import system KtrCD (Gundlach *et al.*, 2017b; Holtmann *et al.*, 2003). Interestingly, c-di-AMP governs not only the expression of *ktrAB* but also binds to the KtrA protein and likely inhibits  $K^+$  import by KtrAB. Although no regulation of c-di-AMP for the expression of *ktrC* is known, import by KtrCD is also (likely negatively) regulated by binding of c-di-AMP to the KtrC subunit (Bai *et al.*, 2014; Corrigan *et al.*, 2013; Gundlach, 2017; Zarrella *et al.*, 2018). Recently, c-di-AMP binding to KimA was also shown which is likely inhibitory (Gundlach, 2017; Gundlach *et al.*, 2017b).

To prevent toxic accumulation the cation is also exported by *B. subtilis*. So far, only two systems are known to facilitate  $K^+$  export: KhtSTU and YugO (Hoffmann and Bremer, 2017). KhtS and KhtT modulate the activity of the  $K^+/H^+$  antiporter system KhtSTU. KhtU spans the membrane and binds KhtT which is located peripheral at the membrane (Fujisawa *et al.*, 2007; 2004). Interestingly, KhtT was just described to bind c-di-AMP, most likely via the contained RCK\_C domain which is also found in KtrA and KtrC (Gundlach, 2017). The RCK\_N domain however is missing. The second exporter, YugO, is a glutamate responsive  $K^+$  exporter and only contains an RCK\_N but no RCK\_C domain (Prindle *et al.*, 2015). YjbQ (CpaA in *S. aureus*) is another poorly characterized  $K^+$  exporter, contains both RCK domains and is likely stimulated by c-di-AMP binding (Chin *et al.*, 2015; Corrigan *et al.*, 2013; Gundlach, 2017). However, CpaA shows no specificity for  $K^+$  over  $Na^+$  ions (Chin *et al.*, 2015). Another potential  $K^+$  exporter is the still unknown YrvCD, since YrvC also contains the c-di-AMP-binding RCK\_C domain (Gundlach, 2017).

## 1.4 Glutamate biosynthesis in *Bacillus subtilis*

Glutamate is described as the major counterion for  $K^+$  (McLaggan *et al.*, 1994). *B. subtilis* and other bacteria accumulate glutamate to around 100 mM, which is  $\sim 40\%$  of the total *E. coli* metabolome (Bennett *et al.*, 2009; Whatmore *et al.*, 1990). Moreover, glutamate serves as the main amino group donor and  $\sim 88\%$  of the cellular nitrogen originates from glutamate (Bennett *et al.*, 2009; Wohlhueter *et al.*, 1973). Since the standard free energy of transamination reactions is almost zero, high intracellular levels of glutamate are required to drive the reactions (Bennett *et al.*, 2009). Glutamate is directly incorporated into proteins, or used for the biosynthesis of amino acids like glutamine, arginine or proline (Gunka and Commichau, 2012). Proline is demonstrated to function as the main compatible solute to protect *B. subtilis* against hyperosmotic conditions, which is also the case for glutamate in other bacteria (Brill *et al.*, 2011; Csonka *et al.*, 1994; Hoffmann and Bremer, 2017; Saum *et al.*, 2006). Furthermore, glutamate metabolism is of general importance as it links carbon (TCA cycle) and nitrogen metabolism. In *B. subtilis* glutamate is synthesized by the glutamate synthase (GOGAT) GltAB in a reductive, NADPH-dependent reaction out of glutamine and the TCA cycle intermediate 2-oxoglutarate. Necessary glutamine is provided by the ATP-dependent reaction of the glutamine synthetase (GS) which assimilates ammonium ( $NH_4^+$ ) and incorporates it into glutamate (Gunka and Commichau, 2012). Toxic accumulation of glutamate and downstream metabolites is prevented by the glutamate dehydrogenase (GDH) RocG, which catalyzes the  $NADP^+$ -dependent, oxidative deamination of glutamate to 2-oxoglutarate and  $NH_4^+$  (Gunka *et al.*, 2010; Gunka and Commichau, 2012). Although the GDH reaction is reversible *in vitro*, only deamination of glutamate is found *in vivo* because the *B. subtilis* GDH shows only low affinity towards  $NH_4^+$  and intracellular  $NH_4^+$  concentrations are low (Gunka *et al.*, 2010). In addition, *B. subtilis* encodes the GDH *gudB*. In the laboratory strain 168 however, a perfect direct repeat is inserted in the *gudB* gene and the enzyme is not functional (Belitsky and Sonenshein, 1998).  $NH_4^+$  assimilation in *B. subtilis* is consequently solely achieved by the GS/GOGAT system.  $NH_4^+$  can be taken up by the ammonium transporter NrgA (AmtB), which facilitates uptake at low external  $NH_4^+$  concentrations. Under excess  $NH_4^+$  supply however, the import activity of NrgA is inhibited by binding of the classical P<sub>II</sub> protein NrgB to NrgA. In this case, gaseous ammonia ( $NH_3$ ) enters the cells by passive diffusion (Coutts *et al.*, 2002; Detsch and Stülke, 2003; Heinrich *et al.*, 2006).

The GOGAT subunits GltA and GltB together form the dodecameric holoenzyme GltAB (Cotteville *et al.*, 2008). Expression of *gltAB* is elegantly regulated. Transcription of *gltAB* is activated by the LysR-type transcription factor GltC when glucose is present, ensuring sufficient amounts of the TCA cycle intermediate 2-oxoglutarate. Expression of *gltAB* is not activated when glucose is absent and glutamate is present in the medium. In case glutamine, the second substrate for GltAB, is lacking the expression of *gltAB* is inhibited by the global nitrogen regulator TnrA. Inhibition by TnrA is abolished under nitrogen excess. This is

achieved by binding of ThrA to the feedback inhibited GS, which under this condition is bound to glutamine (Gunka and Commichau, 2012).

Similar to potassium, glutamate is also implicated in c-di-AMP homeostasis and all three are intricately linked to each other. Synthesis of c-di-AMP is dependent on the nitrogen source as well as on the external  $K^+$  concentration. Low levels of  $K^+$  lead to reduced synthesis of c-di-AMP to abolish inhibition of  $K^+$  uptake by the high-affinity importers KtrAB and KimA. In addition, when  $NH_4^+$  is used as the nitrogen source c-di-AMP synthesis is also downregulated compared to glutamate-grown cells. Interestingly, expression of *kimA* at low  $K^+$  concentrations is dependent on the presence of glutamate in the medium (Gundlach, 2017; Gundlach *et al.*, 2018; 2017b; 2015b). Furthermore,  $K^+$  availability also governs glutamate homeostasis. Higher  $K^+$  levels result in elevated synthesis of glutamate and vice versa (Richts, 2018). Interestingly, glutamate synthesis is also highly dependent on  $K^+$  uptake during adaptation to hyperosmotic conditions in the c-di-AMP non-producer *E. coli* (McLaggan *et al.*, 1994). As mentioned, glutamate is a precursor for arginine. Surprisingly, arginine and similar positively charged amino acids can partially replace the role of potassium in *B. subtilis* cells that experience extreme limitation of the cation (Gundlach *et al.*, 2017a). The mechanisms how  $K^+$  and nitrogen signals are relayed to adjust c-di-AMP homeostasis are currently unknown.

## 1.5 P<sub>II</sub> proteins as cellular signal integrators

P<sub>II</sub> proteins form one of the largest families of signal transduction proteins. They are nearly ubiquitous in bacteria and found in nitrogen-fixating archaea and in the chloroplasts of red algae and green plants (Forchhammer and Lüddecke, 2016; Sant'Anna *et al.*, 2009). These proteins bind low-molecular weight effectors and interact with a large variety of targets such as transporters, enzymes and transcription factors. The typical P<sub>II</sub> proteins bind antagonistically ATP or ADP and synergistically 2-oxoglutarate and ATP and are pivotal players in nitrogen metabolism (Forchhammer and Lüddecke, 2016). The sequence, as well as the overall tertiary structure, is highly conserved among P<sub>II</sub> proteins. They usually are around 12–13 kDa in size and assemble to cylindrical homotrimers. Three long T-loops protrude from the compact, homotrimeric structure and govern the interaction with target proteins. Furthermore, smaller B- and C-loops at the interface between two monomers are important for constituting the nucleotide-binding cleft and sometimes are also involved in target-binding (Conroy *et al.*, 2007; Ll acer *et al.*, 2007; Merrick, 2015). Several P<sub>II</sub> proteins are covalently modified at their T-loop, for example by uridylation, adenylation or phosphorylation (Merrick, 2015). For *B. subtilis*, there are currently neither indications for post-translational modification(s) of the sole P<sub>II</sub> protein NrgB (GlnK) nor for the P<sub>II</sub>-like protein DarA (Detsch and St ulke, 2003; Gundlach *et al.*, 2015a).

The family of P<sub>II</sub> proteins can be divided into three subgroups: The closely related GlnB- and GlnK-type (sometimes termed GlnZ or GlnJ) and the NifI-type (Forchhammer

and Lüddecke, 2016). The founding member of the P<sub>II</sub> proteins, GlnB, was identified in *E. coli* and characterized shortly afterwards (Brown *et al.*, 1971; Huergo *et al.*, 2013; Shapiro, 1969). GlnB proteins are often genetically linked to the glutamine synthetase gene *glnA* or the NAD synthetase gene *nadE* and regulate nitrogen assimilation on a transcriptional and post-transcriptional level (Arcondéguy *et al.*, 2001; Forchhammer, 2008; Huergo *et al.*, 2013). The GlnK proteins control the activity of the ammonium importer AmtB. As already mentioned, in *B. subtilis* when NH<sub>4</sub><sup>+</sup> is abundant NrgA (AmtB) import activity is inhibited by binding of NrgB (GlnK) to NrgA (Coutts *et al.*, 2002; Detsch and Stülke, 2003; Heinrich *et al.*, 2006). Furthermore, NrgB is able to bind and sequester the global nitrogen regulator TnrA to the membrane when intracellular ATP levels are low (Heinrich *et al.*, 2006). Interestingly, even heterotrimers of *E. coli* GlnK and GlnB have been reported, when cells were grown in nitrogen-poor medium (van Heeswijk *et al.*, 2000). *B. subtilis* exhibits only one P<sub>II</sub> protein of the GlnK-type (NrgB), and the P<sub>II</sub>-like protein DarA, which will be discussed later in detail (Detsch and Stülke, 2003; Gundlach *et al.*, 2015a). The NifI proteins are almost invariably present as two related variants (NifI<sub>1</sub> and NifI<sub>2</sub>). As an exception to all other P<sub>II</sub> proteins NifI<sub>1,2</sub> do not form trimers but heteromultimers. The likely heterohexameric NifI<sub>1,2</sub> binds and inhibits dinitrogenase activity in response to low 2-oxoglutarate levels (Dodsworth and Leigh, 2006; Leigh and Dodsworth, 2007).

In addition, a phylogenetic analysis proposed another poorly described distinct clade termed P<sub>II</sub> new group (P<sub>II</sub>-NG) (Sant’Anna *et al.*, 2009). The P<sub>II</sub>-NG proteins show sequence homology to the classical P<sub>II</sub> but lack the typical PROSITE signature motifs and are genetically linked to heavy metal efflux pumps (Forchhammer and Lüddecke, 2016; Sant’Anna *et al.*, 2009). Interestingly, there is yet another diverse set of poorly characterized proteins within the large P<sub>II</sub> superfamily. The P<sub>II</sub>-like proteins display only rudimental sequence homology to the classical P<sub>II</sub> but show high similarity in size and structure. Although effector binding is not conserved, it has been argued that the trimeric, triangular structure suggests a similar mode of interaction (Forchhammer and Lüddecke, 2016; Sant’Anna *et al.*, 2009).

## 1.6 DarA – a c-di-AMP receptor of unknown function

The DarA (c-di-AMP receptor A) protein of *B. subtilis* is a DUF970 domain-containing P<sub>II</sub>-like protein of only 11.8 kDa and was shown to specifically bind c-di-AMP (Gundlach *et al.*, 2015a). However, c-di-AMP binding was first shown for the orthologue PstA from *S. aureus* and *L. monocytogenes*, which each show around 89 % sequence similarity and 65 % amino acid identity (Corrigan *et al.*, 2013; Gundlach *et al.*, 2015a; Sureka *et al.*, 2014).

DarA is highly conserved among Gram-positive, c-di-AMP-producing firmicutes and can be found in *Bacillus* and closely related genera like *Staphylococcus*, *Listeria*, *Lactobacillus*, *Enterococcus* and *Clostridium*. Notable exceptions are *Streptococcus*, *Lactococcus*, *Geobacillus* and the *Bacillus cereus* group (our unpublished research, Gundlach *et al.*, 2015a). In addition,

the genomic arrangement is also highly conserved. The essential gene *tmk* (coding for the thymidylate kinase) is located directly upstream of *darA* and is regulated by its own promoter, while the essential gene *holB* (coding for the  $\delta'$  subunit of the DNA polymerase III) is located downstream of *darA* and is under control of the same promoter as *darA* (Nicolas *et al.*, 2012). This arrangement is true for almost all bacteria expressing *darA* (our unpublished research) suggesting a functional linkage (Dandekar *et al.*, 1998). However, no unambiguous interaction of DarA with HolB or Tmk has been reported until now.

As mentioned before, DarA is structurally a P<sub>II</sub>-like protein. The monomers exhibit a double ferredoxin-like fold ( $\beta 1-\alpha 1-\beta 2-(\text{T-loop})-\beta 3/3'-\alpha 2-(\text{B-loop})-\beta 4$ ). The  $\beta$ -sheets of three monomers are assembled orthogonally and form the cylindrical core which is surrounded by the  $\alpha$ -helices (Forchhammer and Lüddecke, 2016; Gundlach *et al.*, 2015a). In contrast to the classical P<sub>II</sub> from *E. coli*, the length of the B- and T-loops is swapped. DarA exhibits an unusually long B-loop and a rather short T-loop (see Figure 1.4A). Furthermore, an N-terminal extension present in P<sub>II</sub> proteins is missing in DarA (Gundlach *et al.*, 2015a).

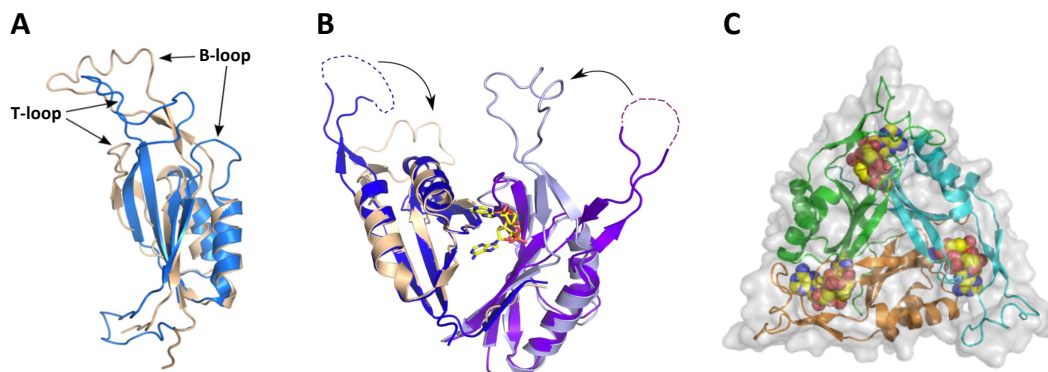


**Figure 1.4: Structural features of DarA.** (adapted from Gundlach *et al.*, 2015a; Commichau *et al.*, 2015a). (A) Superposition of *E. coli* P<sub>II</sub> (blue, PDB 2PII) and *B. subtilis* DarA (brown, PDB 4RLE) shows the high similarity. The B- and T-loop length is swapped and DarA lacks part of the N-terminal region. An N-terminal His<sub>6</sub>-tag attached to DarA is not shown for clarity. (B) c-di-AMP binding induces conformational changes. Superposition of *B. subtilis* DarA · c-di-AMP (beige and light blue) and the ligand-free *Pedococcus pentosaceus* orthologue (purple and dark blue, PDB 3M05). The B-loop moves towards the trimer core. Dotted lines are missing in the crystal structure. (C) DarA homotrimer bound to c-di-AMP.

In agreement with the low sequence conservation between DarA/PstA and P<sub>II</sub> the key residues for binding of ATP, Mg<sup>2+</sup> and 2-oxoglutarate are missing (Campeotto *et al.*, 2015; Forchhammer and Lüddecke, 2016). DarA/PstA specifically binds c-di-AMP in a deep pocket between two monomers of the trimer, but neither the mononucleotides ATP, ADP, AMP, nor the cyclic dinucleotides c-di-GMP or 2',3'-cGAMP (Campeotto *et al.*, 2015; Choi *et al.*, 2015; Gundlach *et al.*, 2015a; Müller *et al.*, 2015). Although, *in vitro* binding of 3',3'-cGAMP was observed for *B. subtilis* DarA, this is physiologically not relevant since the nucleotide is not present *in vivo* (Gundlach *et al.*, 2015a). Furthermore, 2-oxoglutarate binding is also absent (Müller *et al.*, 2015). Upon c-di-AMP binding, the B- and T-loops undergo major changes in orientation and flexibility (see Figure 1.4B). This will arguably influence the target

interaction and c-di-AMP binding was proposed to inhibit interactions since the accessibility of the B-loops is reduced upon ligand-binding (Campeotto *et al.*, 2015; Choi *et al.*, 2015; Gundlach *et al.*, 2015a).

As mentioned before, c-di-AMP,  $K^+$  and glutamate homeostasis are intricately linked to each other. However, not all specific mechanisms that link the three homeostases have been found yet. It is tempting to speculate that the c-di-AMP-binding, P<sub>II</sub>-like protein DarA provides a missing link that connects c-di-AMP with glutamate and/or  $K^+$  homeostasis (Gundlach, 2017; Gundlach *et al.*, 2018). Similar to other known c-di-AMP targets, DarA is not an essential target of the second messenger (Gundlach *et al.*, 2015a). Recently, it has been shown that loss-of-function mutations in *pstA* contribute to growth of a c-di-AMP-free *L. monocytogenes* strain in rich medium and suppress sensitivity of the  $\Delta dacA$  strain to the cell wall-targeting antibiotic cefuroxime. However, the underlying mechanisms have remained elusive (Whiteley *et al.*, 2017; 2015).

### 1.7 Aim of this work

The unique second messenger c-di-AMP is on the one hand essential for many Gram-positive bacteria that produce it, but on the other hand also toxic upon excessive accumulation. It only becomes dispensable under very specific growth conditions or by accumulation of suppressor mutations (Commichau *et al.*, 2018b). In *B. subtilis*  $K^+$  homeostasis has been shown to be an essential function of c-di-AMP (Gundlach *et al.*, 2017b). Furthermore, c-di-AMP,  $K^+$  and glutamate homeostasis are intricately linked to each other. However, not all specific mechanisms that link the three homeostases have been found yet (Gundlach, 2017; Gundlach *et al.*, 2018). DarA is a prominent c-di-AMP-binding receptor in *B. subtilis* that structurally resembles P<sub>II</sub> proteins (Gundlach *et al.*, 2015a). P<sub>II</sub> proteins are pivotal players of nitrogen metabolism in bacteria. Consequently, it is tempting to speculate that DarA provides a missing link that connects c-di-AMP with glutamate and/or  $K^+$  homeostasis (Gundlach, 2017; Gundlach *et al.*, 2018). In the past, our and several other groups tried to elucidate the function of DarA/PstA. Despite extensive research, the interaction partners and the function of DarA have remained enigmatic. The *B. subtilis darA* deletion mutant did not show significant or reproducible phenotypes in growth under various conditions. In addition, common methods like pull-down assays have been inconclusive and the conserved genomic context of *darA* did not aid the elucidation (our unpublished results; Gundlach, 2014; Hach, 2015; Jäger, 2015). This thesis aims to elucidate the function of the c-di-AMP-binding, P<sub>II</sub>-like protein DarA in *B. subtilis* and to unravel putative interaction partners. One goal was the detection of DarA related phenotypes which have not been detected so far. Several directed *in vivo* and *in vitro* interaction studies were conducted. Furthermore, unbiased *in silico* and *in vivo* screenings were carried out to broaden the knowledge about DarA and c-di-AMP signaling.

## 2 Materials and Methods

### 2.1 Materials

Materials including chemicals, enzymes, antibodies, oligodeoxynucleotides as well as commercial kits and equipment used in this work are listed in the Appendix.

#### 2.1.1 Bacterial strains and plasmids

Bacterial strains and plasmids generated and used in this work are listed in the Appendix.

#### 2.1.2 Media, buffers and solutions

Media, buffers and solutions were prepared with deionized water unless otherwise stated and sterilized by autoclaving for 20 min at 121 °C and 2 bar. Thermolabile substances were sterile filtrated (pore size: 0.22 µm). Concentrations of prepared solutions in percentage refer to weight/volume unless otherwise stated. For solidification, bacterial growth media were supplemented with 1.5 % agar-agar or 1.8 % Bacto agar in the case of complex or minimal media, respectively (Commichau *et al.*, 2015b).

**Table 2.1: Formulations of bacterial growth media, stock solutions and additives.**

Type	Name	Amount	Component/Procedure	
Complex media	LB medium	10 g	Tryptone	
		5 g	Yeast extract	
		10 g	NaCl	
				<i>ad</i> 1 l dH <sub>2</sub> O, autoclave
	SOB medium		20 g	Tryptone
			5 g	Yeast extract
			0.58 g	NaCl
			0.186 g	KCl
				<i>ad</i> 1 l dH <sub>2</sub> O, autoclave
			10 ml	MgCl <sub>2</sub> (1 M)
		10 ml	MgSO <sub>4</sub> (1 M)	
	SP medium		8 g	Nutrient broth
			0.25 g	MgSO <sub>4</sub> · 7 H <sub>2</sub> O
			1 g	KCl
				<i>ad</i> 1 l dH <sub>2</sub> O, autoclave
1 ml			CaCl <sub>2</sub> (0.5 M)	
1 ml			MnCl <sub>2</sub> (10 mM)	
1 ml			Ferric ammonium citrate (2.2 mg/ml)	

Table 2.1: Formulations of bacterial growth media, stock solutions and additives.

Type	Name	Amount	Component/Procedure	
Minimal media	MNGE medium	1 ml	MN base (10×)	
		400 µl	D-Glucose (50%)	
		50 µl	Potassium glutamate (40%)	
		50 µl	Ferric ammonium citrate (2.2 mg/ml)	
		100 µl	L-Tryptophan (5 mg/ml)	
		30 µl	MgSO <sub>4</sub> · 7 H <sub>2</sub> O (1 M)	
		8.37 ml	dH <sub>2</sub> O	
		+/- 100 µl	Casamino acids (10%)	
	MSMNGN medium	1 ml	MSMN base (10×)	
		400 µl	D-Glucose (50%)	
		100 µl	(NH <sub>4</sub> ) <sub>2</sub> SO <sub>4</sub> (20%)	
		50 µl	Ferric ammonium citrate (2.2 mg/ml)	
		100 µl	L-Tryptophan (5 mg/ml)	
		30 µl	MgSO <sub>4</sub> · 7 H <sub>2</sub> O (1 M)	
		1 µl	KCl (1 M)	
		8.37 ml	dH <sub>2</sub> O	
	+/- 100 µl	Casamino acids (10%)		
	MSSM medium	either or	100 ml	MSSM base (5×)
			10 ml	Trace elements (100×)
			10 ml	Iron citrate (100×)
			10 ml	D-Glucose (50%)
			10 ml	L-Tryptophan (5 mg/ml)
			10 ml	(NH <sub>4</sub> ) <sub>2</sub> SO <sub>4</sub> (20%) <sup>a</sup>
50 ml			Sodium glutamate (20%) <sup>a</sup>	
<i>x</i> ml			KCl (1 M), adjusted as indicated	
			<i>ad</i> 11 dH <sub>2</sub> O	
Stock solutions	100× Iron citrate	0.0135 g	FeCl <sub>3</sub> · 6 H <sub>2</sub> O	
		0.1 g	Trisodium citrate · 2 H <sub>2</sub> O	
			<i>ad</i> 100 ml dH <sub>2</sub> O, sterile filter	
	10× MN base	136 g	K <sub>2</sub> HPO <sub>4</sub> · 3 H <sub>2</sub> O	
		60 g	KH <sub>2</sub> PO <sub>4</sub>	
		10 g	Trisodium citrate · 2 H <sub>2</sub> O	
			<i>ad</i> 11 dH <sub>2</sub> O, autoclave	
	10× MSMN base	106.1 g	Na <sub>2</sub> HPO <sub>4</sub> · 2 H <sub>2</sub> O	
		68.8 g	NaH <sub>2</sub> PO <sub>4</sub> · 2 H <sub>2</sub> O	
		10 g	Trisodium citrate · 2 H <sub>2</sub> O	
			<i>ad</i> 11 dH <sub>2</sub> O, autoclave	
	5× MSSM base	41 g	Na <sub>2</sub> HPO <sub>4</sub> · 2 H <sub>2</sub> O	
		18 g	NaH <sub>2</sub> PO <sub>4</sub> · 2 H <sub>2</sub> O	
		5 g	Trisodium citrate · 2 H <sub>2</sub> O	
		1 g	MgSO <sub>4</sub> · 7 H <sub>2</sub> O	
			<i>ad</i> 11 dH <sub>2</sub> O, autoclave	



Table 2.1: Formulations of bacterial growth media, stock solutions and additives.

Type	Name	Amount	Component/Procedure
	100× Trace elements	0.735 g	CaCl <sub>2</sub> · 2 H <sub>2</sub> O
		0.1 g	MnCl <sub>2</sub> · 4 H <sub>2</sub> O
		0.17 g	ZnCl <sub>2</sub>
		0.033 g	CuCl <sub>2</sub> · 2 H <sub>2</sub> O
		0.06 g	CoCl <sub>2</sub> · 6 H <sub>2</sub> O
		0.06 g	Na <sub>2</sub> MoO <sub>4</sub> · 2 H <sub>2</sub> O
			<i>ad</i> 1 l dH <sub>2</sub> O, sterile filter

<sup>a</sup> Standard formulations. Other nitrogen sources or concentrations are indicated in the text.

Table 2.2: Formulations of other buffers, stock solutions and solutions.

Type	Name	Amount	Component/Procedure	
Blotting solutions	10× Buffer III	121.14 g	Tris base	
		58.44 g	NaCl	
				pH 9.5 (NaOH)
				<i>ad</i> 1 l dH <sub>2</sub> O, autoclave
	10× Phosphate buffered saline (PBS)	26.8 g	Na <sub>2</sub> HPO <sub>4</sub> · 7 H <sub>2</sub> O	
		2.4 g	KH <sub>2</sub> PO <sub>4</sub> · 7 H <sub>2</sub> O	
		80 g	NaCl	
		2 g	KCl	
				pH 6.5 (HCl)
				<i>ad</i> 1 l dH <sub>2</sub> O, autoclave
10× Tris buffered saline (TBS)	60 g	Tris base		
	90 g	NaCl		
			pH 7.6 (HCl)	
			<i>ad</i> 1 l dH <sub>2</sub> O, autoclave	
Transfer buffer	15.1 g	Tris base		
	72.1 g	Glycine		
	750 ml	Methanol		
			<i>ad</i> 5 l dH <sub>2</sub> O, autoclave	
Blotto	25 g	Skim milk powder		
	100 ml	10× TBS		
	1 ml	TWEEN 20		
			<i>ad</i> 1 l dH <sub>2</sub> O	
Buffers	Buffer E	0.027 g	D-Desthiobiotin	
			<i>ad</i> 50 ml Buffer W	
	Buffer W	12.114 g	Tris base	
		8.77 g	NaCl	
		0.3722 g	Na <sub>2</sub> EDTA · 2 H <sub>2</sub> O	
			pH 8.0 (HCl)	
			<i>ad</i> 1 l dH <sub>2</sub> O, autoclave	

Table 2.2: Formulations of other buffers, stock solutions and solutions.

Type	Name	Amount	Component/Procedure
	10× CCR buffer	200 mM 30 mM 0.5 M 5 mM 0.4 mg/ml	Tris-HCl (pH 8.5) MgCl <sub>2</sub> KCl NAD <sup>+</sup> Bovine serum albumin (BSA)
	Membrane buffer M	12.80 g 8.89 g	NaH <sub>2</sub> PO <sub>4</sub> · H <sub>2</sub> O Na <sub>2</sub> HPO <sub>4</sub> · H <sub>2</sub> O pH 6.8 (NaOH) <i>ad</i> 11 dH <sub>2</sub> O, autoclave
	10× PAGE buffer	144 g 30 g 10 g	Glycine Tris base SDS <i>ad</i> 11 dH <sub>2</sub> O, autoclave
	50× TAE buffer	242 g 57.1 ml 100 ml	Tris base Glacial acetic acid EDTA (0.5 M, pH 8.0) <i>ad</i> 11 dH <sub>2</sub> O, autoclave
	TE buffer	10 ml 2 ml	Tris-HCl (1 M, pH 8.0) EDTA (0.5 M, pH 8.0) <i>ad</i> 11 dH <sub>2</sub> O, autoclave
	Transformation buffer (TB)	3.46 g 18.64 g 2.2 g 55 ml	PIPES KCl CaCl <sub>2</sub> · 2 H <sub>2</sub> O pH 6.7 (KOH) <i>ad</i> 11 dH <sub>2</sub> O, autoclave MnCl <sub>2</sub> (1 M)
	Washing buffer M	5 g	CHAPS <i>ad</i> 100 ml Membrane buffer M
	ZAP	6.057 g 11.68 g <i>x</i> mg	Tris base NaCl Imidazole, adjusted as indicated <i>ad</i> 11 dH <sub>2</sub> O, autoclave
	Z buffer	10.68 g 6.24 g 0.74 g 0.25 g	Na <sub>2</sub> HPO <sub>4</sub> · 2 H <sub>2</sub> O NaH <sub>2</sub> PO <sub>4</sub> · 2 H <sub>2</sub> O KCl MgSO <sub>4</sub> · 7 H <sub>2</sub> O <i>ad</i> 11 dH <sub>2</sub> O, autoclave
Staining	Coomassie destaining solution	50 ml 200 ml	Glacial acetic acid Ethanol <i>ad</i> 11 dH <sub>2</sub> O

Table 2.2: Formulations of other buffers, stock solutions and solutions.

Type	Name	Amount	Component/Procedure
	Coomassie staining solution	5 g 100 ml 450 ml	Coomassie Brilliant Blue G-250 Glacial acetic acid Methanol <i>ad</i> 1 l dH <sub>2</sub> O
	Developer solution	6 g 2 ml 50 µl	Na <sub>2</sub> CO <sub>3</sub> Thiosulfate solution Formaldehyde 37 % <i>ad</i> 100 ml dH <sub>2</sub> O
	FA-Fixation solution	55 ml 12 ml 100 µl	Methanol Glacial acetic acid Formaldehyde 37 % <i>ad</i> 100 ml dH <sub>2</sub> O
	Impregnator solution	0.2 g 37 µl	AgNO <sub>3</sub> Formaldehyde 37 % <i>ad</i> 100 ml dH <sub>2</sub> O
	Stop solution	1.86 g	Na <sub>2</sub> EDTA · 2 H <sub>2</sub> O <i>ad</i> 100 ml dH <sub>2</sub> O
	Thiosulfate solution	20 mg	Na <sub>2</sub> S <sub>2</sub> O <sub>3</sub> · 5 H <sub>2</sub> O <i>ad</i> 100 ml dH <sub>2</sub> O
Miscellaneous	5× DNA loading dye	5 ml 200 µl 10 mg 10 mg	Glycerol (99 %) 50× TAE buffer (pH 8.0) Bromphenol blue Xylene cyanol <i>ad</i> 10 ml dH <sub>2</sub> O
	Expression mix	500 µl 250 µl 50 µl 250 µl	Yeast extract (5 %) Casamino acids (10 %) L-Tryptophan (5 mg/ml) dH <sub>2</sub> O
	Expression mix modified	50 µl 700 µl 50 µl 200 µl	D-Glucose (50 %) Casamino acids (10 %) L-Tryptophan (5 mg/ml) dH <sub>2</sub> O
	10× GOGAT assay mix	100 µl 100 µl 100 µl 100 µl 100 µl 400 µl	Tris-HCl (0.5 M, pH 7.5) L-Glutamine (0.2 M) α-Ketoglutaric acid (0.35 M) <sup>a</sup> NADPH (1 mM) β-Mercaptoethanol (50 mM) dH <sub>2</sub> O

**Table 2.2: Formulations of other buffers, stock solutions and solutions.**

Type	Name	Amount	Component/Procedure
	LD-mix	100 mg 10 mg	Lysozyme DNase I <i>ad</i> 10 ml dH <sub>2</sub> O, sterile filter
	SDS-PAA running gel (12%) <sup>b</sup>	3.3 ml 4 ml 2.5 ml 100 µl 100 µl 8 µl	dH <sub>2</sub> O Rotiphorese Gel 30 (37.5:1) Tris-HCl (1.5 M, pH 8,8) SDS (10%) APS (10%) TEMED
	SDS-PAA stacking gel (5%)	6.83 ml 1.3 ml 0.87 ml 100 µl 100 µl 10 µl	dH <sub>2</sub> O Rotiphorese Gel 30 (37.5:1) Tris-HCl (1.5 M, pH 6,8) SDS (10%) APS (10%) TEMED
	5× SDS loading dye	1.3 ml 1.6 ml 2.5 ml 5 ml 20 mg	Tris-HCl (1.5 M, pH 6.8) β-Mercaptoethanol SDS (20%) Glycerol (99%) Bromophenol blue sodium salt

<sup>a</sup> Solved in Tris-HCl (0.5 M, pH 7.5).

<sup>b</sup> Percentage of Rotiphorese Gel 30 and dH<sub>2</sub>O was adjusted depending on the protein size.

### 2.1.3 Antibiotics

Antibiotics were prepared as 1000-fold concentrated stock solutions, except for tetracycline (500-fold). Ampicillin, kanamycin, lincomycin, spectinomycin and streptomycin were dissolved in deionized water. Chloramphenicol, erythromycin and tetracycline were dissolved in 70 % ethanol. All stock solutions were sterile filtrated (pore size: 0.22 µm) and stored at −20 °C. For the selection on resistance marker genes, antibiotics were added to the media prior to inoculation. Agar media were cooled down to approximately 50 °C before antibiotics were added. Selective concentrations are indicated in Table 2.3. For the selection on *ermC*, a combination of the antibiotics erythromycin and lincomycin (Griffith *et al.*, 1965) was used with their indicated concentrations (Commichau *et al.*, 2015b).

**Table 2.3: Antibiotics and selective concentrations.**

Organism	Antibiotic	Selective Concentration
<i>Bacillus subtilis</i>	Chloramphenicol	5 µg/ml
	Erythromycin	2 µg/ml
	Kanamycin	10 µg/ml
	Lincomycin	25 µg/ml
	Spectinomycin	150 µg/ml
	Tetracycline	12.5 µg/ml
<i>Escherichia coli</i>	Ampicillin	100 µg/ml
	Chloramphenicol	15 µg/ml
	Kanamycin	50 µg/ml
	Streptomycin	100 µg/ml

## 2.2 Methods

General methods used in this work that are described in the literature are listed in Table 2.4.

**Table 2.4: General methods.**

Method	Reference
Chain termination DNA sequencing	Sanger <i>et al.</i> , 1977
Coomassie staining of protein gels	Fazekas de St Groth <i>et al.</i> , 1963
Determination of optical density	Sambrook <i>et al.</i> , 1989
Determination of protein amounts	Bradford, 1976
Gel electrophoresis of DNA	Sambrook <i>et al.</i> , 1989
Gel electrophoresis of proteins (SDS-PAGE)	Laemmli, 1970
Ligation of DNA fragments	Sambrook <i>et al.</i> , 1989
Plasmid preparation from <i>E. coli</i>	Sambrook <i>et al.</i> , 1989
Precipitation of nucleic acids	Sambrook <i>et al.</i> , 1989

### 2.2.1 Cultivation of bacteria

Unless otherwise stated, *E. coli* was grown in LB or SOB medium at 37 °C, 28 °C or 16 °C and 220 rpm in tubes and Erlenmeyer flasks. *B. subtilis* was grown in LB, MNGE, MSMNGN

or MSSM medium with the indicated supplements at 37 °C or 28 °C and 220 rpm in tubes and Erlenmeyer flasks. If applicable, media additives or modifications are indicated. Fresh colonies from plates, frozen DMSO stocks or overnight liquid cultures were used for inoculation. Growth in liquid cultures was monitored by measuring the optical density at a wavelength of 600 nm (Sambrook *et al.*, 1989) using a UV-Visible Spectrophotometer Ultrospec 2100 pro (Amersham Biosciences). Suppressor mutants originating from strains with growth defects were isolated by re-streaking and cultivating them on medium agar plates which was repeated at least three times (Commichau *et al.*, 2015b).

### 2.2.2 Storage of bacteria

*E. coli* was kept on LB medium agar plates at 4 °C for up to four weeks. For long-term storage, bacterial stocks with a final concentration of 10 % (v/v) DMSO were prepared from overnight liquid cultures and stored at –80 °C. For long-term storage of *B. subtilis*, bacteria were kept on SP medium agar plates and tubes at room temperature, as well as in 10 % (v/v) DMSO stocks at –80 °C (Commichau *et al.*, 2015b).

### 2.2.3 Genetic modification of *Escherichia coli*

#### Preparation of chemically competent *E. coli* cells (Inoue *et al.*, 1990)

A single colony of *E. coli* DH5 $\alpha$  or XL1-Blue was used to inoculate 20 ml LB medium and grown for approximately 20 h at 28 °C and 220 rpm. A second culture of 250 ml SOB medium was inoculated with 6 ml of the preculture and cultivated for approximately 20–24 h at 16 °C and 220 rpm until an OD<sub>600</sub> of 0.5–0.9. The culture was cooled down on ice for 10 min and the cells were harvested by centrifugation for 10 min at 5000 rpm and 4 °C. The cell pellet was resuspended in 80 ml of ice-cold TB, again incubated on ice for 10 min and cells were harvested as before. Cells were resuspended in 20 ml of ice-cold TB and supplemented with a final concentration of 7 % (v/v) DMSO. Aliquots (200  $\mu$ l) of highly competent *E. coli* cells were frozen in liquid nitrogen and stored at –80 °C (Commichau *et al.*, 2015b).

#### Preparation of chemically competent *E. coli* cells (Lederberg and Cohen, 1974)

A 4 ml overnight culture of *E. coli* DH5 $\alpha$ , XL1-Blue or BL21(DE3) in LB medium was used to inoculate 50 ml LB medium to an OD<sub>600</sub> of 0.05. The culture was grown at 37 °C and 220 rpm until an OD<sub>600</sub> of 0.3–0.6 and the cells were harvested by centrifugation for 10 min at 5000 rpm and 4 °C. The cell pellet was resuspended in 5 ml of ice-cold 50 mM CaCl<sub>2</sub> solution

and incubated on ice for 30 min. The competent cells were again harvested as before and this time resuspended in 1 ml of ice-cold 50 mM CaCl<sub>2</sub> solution. An aliquot of 200 µl was used for subsequent transformation (Commichau *et al.*, 2015b).

### **Transformation of chemically competent *E. coli* cells**

An aliquot of 200 µl competent cells was either thawed on ice or kept on ice in the case of freshly prepared competent cells. The cells were carefully mixed with 10–100 ng of plasmid DNA and incubated on ice for 30 min. Samples were heat-shocked for 90 s at 42 °C and incubated on ice for another 5 min. After addition of 800 µl LB medium, the samples were incubated for 1 h at 37 °C and 220 rpm. 100 µl and the concentrated rest of the transformation sample were plated on LB medium agar plates with the appropriate antibiotics and transformants were grown overnight at 37 °C (Commichau *et al.*, 2015b).

### **2.2.4 Genetic modification of *Bacillus subtilis***

#### **Preparation of competent *B. subtilis* cells**

A 4 ml overnight culture of the desired *B. subtilis* strain in LB medium was used to inoculate 10 ml MNGE medium, supplemented with 0.1 % casamino acids, to an OD<sub>600</sub> of 0.1. The culture was grown at 37 °C and 220 rpm until an OD<sub>600</sub> of 1.3, diluted with 10 ml prewarmed (37 °C) MNGE medium without casamino acids and cultivated for an additional hour. An aliquot of 400 µl was used for subsequent transformation (Commichau *et al.*, 2015b). For the construction of strains lacking all three diadenylate cyclases, an adjusted protocol was used, since cyclic di-AMP is essential under most common laboratory growth conditions (Luo and Helmann, 2012; Mehne *et al.*, 2013). Competent cells of a strain already devoid of *cdaS* and *disA* were prepared as described before but MSMNGN medium was used. MSMNGN is similar to MNGE but the potassium salts are replaced by the corresponding sodium salts (potassium concentration is adjusted to 0.1 mM) and glutamate is replaced by ammonium, since high amounts of potassium as well as glutamate become toxic for a c-di-AMP-free *B. subtilis* strain (Gundlach, 2017; Gundlach *et al.*, 2017b).

#### **Transformation of competent *B. subtilis* cells**

An aliquot of 400 µl competent cells was carefully mixed with 0.1–1 µg of DNA and incubated for 30 min at 37 °C and 220 rpm. The sample was supplemented with 100 µl expression mix and incubated for an additional hour as before. 50 µl and the concentrated rest of the

transformation sample were plated on SP medium agar plates with the appropriate antibiotics and transformants were grown overnight at 37 °C (Commichau *et al.*, 2015b). For the deletion of the last diadenylate cyclase gene, competent cells of a strain already devoid of *cdaS* and *disA* were transformed with chromosomal DNA of GP94 ( $\Delta cdaA$ ) as described before but a modified expression mix was used. Most importantly, yeast extract was omitted since high amounts of potassium and glutamate become toxic for a c-di-AMP-free *B. subtilis* strain. Transformation samples were plated on MSSM medium agar plates with ammonium as the nitrogen source and 0.1 mM KCl, including the appropriate antibiotics. Transformants were grown for two days at 37 °C (Gundlach *et al.*, 2017b).

### 2.2.5 Growth analysis of *Bacillus subtilis*

#### Growth curves of *B. subtilis* in liquid cultures

Different amounts of a 4 ml LB medium pre-culture of a *B. subtilis* strain were used to inoculate 10 ml MSSM medium with a combination of either ammonium or L-glutamate as the nitrogen source and 0.1 or 5 mM KCl. Strains lacking all three diadenylate cyclases were cultivated in MSSM medium with ammonium as the nitrogen source and 0.1 mM KCl. The cultures were grown overnight at 37 °C and 220 rpm and the OD<sub>600</sub> was determined the next morning. Cultures with cells in the exponential growth phase with a similar OD<sub>600</sub> were selected and used to inoculate a 50 ml main culture with the same medium to an OD<sub>600</sub> of 0.1. The cultures were grown at 37 °C and 220 rpm and growth was analyzed by measuring the OD<sub>600</sub> every hour for 8 h.

#### Growth analysis of *B. subtilis* by serial drop dilution on medium agar

Different amounts of a 4 ml LB medium pre-culture of the respective *B. subtilis* strain were used to inoculate 4 ml MSSM medium with ammonium as the nitrogen source and 0.1 or 5 mM KCl as indicated. The cultures were grown overnight at 37 °C and 220 rpm and the OD<sub>600</sub> was determined the next morning. Cultures with cells in the exponential growth phase with a similar OD<sub>600</sub> were selected and cells were pelleted for 5 min at 5000 rpm and room temperature. The cell pellet was washed three times in a ten-fold volume of 1× MSSM base by resuspension in the appropriate volume and subsequent centrifugation for 5 min at 5000 rpm and room temperature. Cell pellets were resuspended in 1.5 ml 1× MSSM base, adjusted to an OD<sub>600</sub> of 1.0 and 4 µl of a serial dilution (10<sup>-1</sup> steps ranging from 1 up to 10<sup>-5</sup>) were spotted on MSSM medium agar plates with the indicated KCl concentration and either 30 mM ammonium or 15 mM L-glutamate, L-glutamine, L-arginine or L-proline as the nitrogen source. Pictures were taken after incubation for 48 h at 37 °C (adapted from Gundlach *et al.*, 2017a).



## 2.2.6 Preparation and detection of DNA

### Isolation of plasmid DNA from *E. coli*

Plasmid DNA was isolated from an overnight culture of *E. coli* carrying the desired plasmid (Sambrook *et al.*, 1989). Either 4 or 20 ml of culture were used for the preparation of low or high copy plasmids, respectively, using the NucleoSpin Plasmid Kit (Macherey-Nagel). The plasmid DNA was eluted with deionized, prewarmed (70 °C) water (Commichau *et al.*, 2015b).

### Isolation of genomic DNA from *B. subtilis*

Genomic DNA of the desired strain was isolated from an overnight culture using the peqGOLD Bacterial DNA Kit (PEQLAB Biotechnologie). By default, *B. subtilis* was grown in LB medium or in MSSM medium with ammonium as the nitrogen source and 0.1 mM KCl for strains lacking all diadenylate cyclases. Isolated suppressor mutants were grown in the medium from which they were isolated from. A sufficient amount of cells was used for isolation according to the manufacturer's protocol. The genomic DNA was eluted with deionized, prewarmed (70 °C) water (adapted from Commichau *et al.*, 2015b).

### Purification of DNA

Linear DNA fragments obtained after polymerase chain reaction, restriction digestion and/or dephosphorylation were purified using the QIAquick PCR purification kit (Qiagen) according to the manufacturer's protocol. Purified DNA was eluted with deionized, prewarmed (70 °C) water (Commichau *et al.*, 2015b).

### Quantification of nucleic acids

The concentration of nucleic acids in samples was determined at a wavelength of 260 nm using the NanoDrop ND-1000 UV-Visible spectrophotometer (PEQLAB Biotechnologie). Purity of the nucleic acid samples was verified by analyzing the 260/280 and 260/230 nm absorbance ratios according to the manufacturer's protocol (Commichau *et al.*, 2015b; Warburg and Christian, 1942).

### Agarose gel electrophoresis of DNA

For qualitative analysis, DNA fragments were separated via agarose gel electrophoresis in a TAE buffer system (Sambrook *et al.*, 1989). The gels were prepared as 1% (w/v) agarose in TAE buffer that was dissolved via heating. The agarose solution was supplemented with 1  $\mu$ l HDGreen Plus Safe DNA stain (INTAS Science Imaging Instruments) per 10 ml to facilitate staining of the DNA fragments. DNA samples were mixed with 5 $\times$  DNA loading dye and loaded onto the agarose gel. A voltage of 130 V was applied until the DNA fragments were sufficiently separated. The separated DNA was detected and documented by fluorescence of the DNA-bound HDGreen Plus Safe DNA stain under UV light ( $\lambda = 254$  nm) using the Molecular Imager Gel Doc XR+ system (Bio-Rad Laboratories). Self-made  $\lambda$ -phage DNA marker (BamHI and EcoRI digested), run on the same gel, served as a molecular weight marker to estimate the size of the DNA fragments (Commichau *et al.*, 2015b).

### Polymerase chain reaction (PCR)

DNA was amplified *in vitro* by polymerase chain reaction (PCR) with specific oligodeoxynucleotides (oligos) using chromosomal or plasmid DNA as template (Mullis and Faloona, 1987; Mullis *et al.*, 1986; Saiki *et al.*, 1985). PCR reactions were carried out in the thermocycler labcycler (SensoQuest) using Phusion High-Fidelity DNA Polymerase or DreamTaq DNA Polymerase (both Thermo Fisher Scientific) for cloning and sequencing purposes or check PCRs, respectively. Oligos were designed using the Geneious software 10.0.5 (Biomatters) and purchased from Sigma-Aldrich Chemie. All oligos created or used during this work are listed in the Appendix. PCR reactions were performed in a total volume of 50  $\mu$ l according to the manufacturer's protocol (Commichau *et al.*, 2015b).

### Long-flanking homology PCR (LFH-PCR)

Long-flanking homology PCR (LFH-PCR) was used for the construction of *B. subtilis* deletion mutants (Wach, 1996). During a two-step LFH-PCR a gene mediating selective antibiotic resistance is fused together with two DNA fragments of approximately 1 kb directly flanking the deletion target region on the chromosome, for example a gene. Subsequently, the obtained linear DNA fragment can be used to transform competent *B. subtilis* cells. Through homologous recombination, the genomic region between the 1 kb up- and downstream flanking parts is finally replaced by the employed selective resistance cassette. The genes mediating resistance against erythromycin/lincomycin, tetracycline and spectinomycin were amplified from pDG646, pDG1513 and pDG1726, respectively (Guérout-Fleury *et al.*, 1995). Resistance cassettes were amplified without the encoded terminator sequence if the deletion target region was within

an operon to ensure expression of downstream genes. The up- and downstream flanking regions were amplified from *B. subtilis* 168 chromosomal DNA and extended into the deletion target region to ensure intact expression of up- and downstream genes accordingly. All three fragments were amplified via PCR using the Phusion High-Fidelity DNA Polymerase (Thermo Fisher Scientific) and were purified afterwards. Fusion of the 3'-end of the upstream fragment and the 5'-end of the downstream fragment to the 5'- or 3'-end of the resistance cassette (respectively) was performed during the first step of the LFH-PCR. This was achieved by complementary sequences (*kanR*-tags) at the corresponding fragment ends, attached by the oligos used before. During the second step the final, joined fragment was amplified by addition of the outer oligos. LFH-PCR reactions were performed in a total volume of 50  $\mu$ l using the Phusion DNA Polymerase as described below. *B. subtilis* was transformed with 10  $\mu$ l of the LFH-PCR product. Correct recombination for the up- and downstream regions was verified by check PCRs, with one oligo binding within the resistance gene and one binding before the respective 1 kb fragment. The DNA sequence was verified by sequencing of the PCR products (adapted from Commichau *et al.*, 2015b).

LFH-PCR reaction mix:

10 $\mu$ l	Phusion HF buffer (5 $\times$ )
2 $\mu$ l	dNTPs (12.5 mM)
$x$ $\mu$ l	upstream flanking region (100 ng)
$y$ $\mu$ l	downstream flanking region (100 ng)
$z$ $\mu$ l	resistance gene (300 ng)
4 $\mu$ l	forward oligo (5 $\mu$ M) added at 2. step
4 $\mu$ l	reverse oligo (5 $\mu$ M) added at 2. step
2 $\mu$ l	Phusion DNA polymerase (2 U/ $\mu$ l)
ad 50 $\mu$ l	dH <sub>2</sub> O

	<b>Step</b>	<b>Time</b>	<b>Temperature</b>
10 $\times$	Initial Denaturation	2 min	98.5 °C
	Denaturation	15 s	98.5 °C
	Annealing	45 s	$T_m - 5$ °C
	Elongation	2 min 30 s	72 °C
	Hold	$\infty$	15 °C
	Addition of oligos		
21 $\times$	Denaturation	10 s	98.5 °C
	Annealing	45 s	$T_m - 5$ °C
	Elongation	4 min + 5 s / cycle	72 °C
	Final Elongation	5 min	72 °C
	Hold	$\infty$	15 °C

**Combined chain reaction PCR (CCR-PCR)**

For site-directed mutagenesis, a combined chain reaction PCR (CCR-PCR) with a mutagenic, intragenic-binding and 5'-phosphorylated oligodeoxynucleotide was used (Bi and Stambrook, 1998). The mutagenic oligo contained nucleotide point mutation(s) for the substitution of a single amino acid in the final protein that is encoded by the gene of interest (*goi*). The incorporation of the mutagenic oligo is facilitated by a stronger binding to the template DNA compared to the forward and reverse oligos which amplify the *goi*. During the CCR-PCR the thermostable DNA ligase Ampligase (Epicentre) ligates the phosphorylated 5'-end of the mutagenic primer to the 3'-OH end of the extended upstream oligo, thus closing the gap. Phusion High-Fidelity DNA Polymerase (Thermo Fisher Scientific), which exhibits no 5'-3'-exonuclease activity, was used to prevent a possible degradation of the extended oligos. Plasmid DNA containing the *goi* served as template (Commichau *et al.*, 2015b).

CCR-PCR reaction mix:

2 $\mu$ l	forward oligo (5 $\mu$ M)
2 $\mu$ l	reverse oligo (5 $\mu$ M)
4 $\mu$ l	mutagenic oligo (5 $\mu$ M)
1 $\mu$ l	plasmid template DNA (1 ng/ $\mu$ l)
5 $\mu$ l	CCR buffer (10 $\times$ )
1 $\mu$ l	Phusion DNA polymerase (2 U/ $\mu$ l)
3 $\mu$ l	Ampligase (5 U/ $\mu$ l)
2 $\mu$ l	dNTPs (12.5 mM)
2 $\mu$ l	BSA (20 $\mu$ g/ $\mu$ l)
<i>ad</i> 50 $\mu$ l	dH <sub>2</sub> O

	<b>Step</b>	<b>Time</b>	<b>Temperature</b>
30 $\times$ {	Initial Denaturation	5 min	95 °C
	Denaturation	1 min	95 °C
	Annealing	1 min	T <sub>m</sub> - 5 °C
	Elongation	2 min	68 °C
	Final Elongation	10 min	68 °C
	Hold	$\infty$	15 °C

**Digestion and dephosphorylation of DNA**

Linear DNA fragments (inserts) and vector DNA were digested using FastDigest restriction endonucleases in the supplied buffer (Thermo Fisher Scientific) according to the manufacturer's protocol. To prevent re-ligation, digested vectors were dephosphorylated at their 5'-end by using the FastAP thermosensitive alkaline phosphatase (Thermo Fisher Scientific) according to the manufacturer's protocol (Commichau *et al.*, 2015b).

## Ligation of DNA

A five- to tenfold excess of digested insert was ligated with 10–100 ng digested and dephosphorylated vector using the T4 DNA Ligase (Thermo Fisher Scientific) in the supplied buffer. The ligation mix was done according to the manufacturer's protocol and the ligation was carried out in the dark for either 2 h at room temperature, or overnight at 16 °C (Commichau *et al.*, 2015b).

## Sequencing and identification of suppressor mutations

DNA fragments and plasmids were sequenced externally by Microsynth SeqLab (Göttingen) based on the chain termination method (Sanger *et al.*, 1977) with fluorescently labeled dideoxynucleotides. Whole genome sequencing was performed internally by the Göttingen Genomics Laboratory via an Illumina sequencing approach (Bentley *et al.*, 2008). Sequencing data were mapped against the *B. subtilis* 168 strain reference genome (GenBank accession number: NC\_000964) (Barbe *et al.*, 2009) using the Geneious software 10.0.5 (Biomatters) (Kearse *et al.*, 2012). Significant single nucleotide polymorphisms with a total coverage above 25 reads and a minimum variant frequency of 80 % were verified by subsequent PCR amplification of the genomic region and chain termination sequencing (Sanger *et al.*, 1977) by Microsynth SeqLab (Göttingen) (Commichau *et al.*, 2015b).

### 2.2.7 Preparation and analysis of proteins

#### Overproduction of recombinant proteins in *E. coli*

A 80 ml overnight culture of *E. coli* DH5 $\alpha$  or BL21(DE3) carrying the desired plasmid(s) in LB medium was used to inoculate 1 l LB medium to an OD<sub>600</sub> of 0.1. The culture was grown at 37 °C and 220 rpm until an OD<sub>600</sub> of 0.6 and overproduction of the recombinant proteins was induced by addition of isopropyl- $\beta$ -D-thio-galactopyranoside (IPTG) with a final concentration of 1 mM. The cultures were incubated for another three hours as before. Cells were harvested by centrifugation for 15 min at 5000 rpm and 4 °C. The cell pellet was washed in the buffer that will be used for the subsequent purification of the proteins (His<sub>6</sub>: buffer W, Strep: ZAP with 10 mM imidazole), transferred to falcon tubes and harvested one last time for 5 min at 8500 rpm and 4 °C. The pellets were stored at –20 °C until further processing (Commichau *et al.*, 2015b).

### **Determination of protein amounts with the Bradford method**

The protein concentration of complex protein mixtures like cell extracts, purification fractions or samples of purified proteins was determined with the Bradford method (Bradford, 1976) and Roti-Quant (Roth) according to the manufacturer's protocol. A calibration curve with bovine serum albumin (AppliChem) served as a reference for the calculation (Commichau *et al.*, 2015b).

### **Cell disruption with a French pressure cell press**

Pellets of *E. coli* were resuspended in ice-cold ZAP with 10 mM imidazole or buffer W for subsequent purification of His<sub>6</sub>- or Strep-tagged proteins, respectively. Pellets of *B. subtilis* were resuspended in ice-cold buffer W or membrane buffer M for subsequent purification of Strep-tagged proteins or separation of cytosolic and membrane proteins, respectively. The cell suspension was filled in an ice-cold French pressure cell (Thermo Fisher Scientific) and remaining air was squeezed out. The disruption of the cells was carried out at 1241 bar (18,000 psi) and performed three times in total. The cell suspensions were always kept on ice (Commichau *et al.*, 2015b).

### **Cell disruption with LD-mix**

Pellets of *B. subtilis* were disrupted with LD-mix either for subsequent Western blotting or for subsequent determination of  $\beta$ -galactosidase activity. For Western blotting, pellets from 2 ml culture (OD<sub>600</sub> of 1.0) were resuspended in 45  $\mu$ l Z buffer supplemented with LD-mix (100  $\mu$ l LD-mix in 4 ml Z buffer) and incubated for 30 min at 37 °C and 500 rpm. For  $\beta$ -galactosidase activity assays, pellets from 1.5 ml culture (OD<sub>600</sub> of 0.6) were resuspended in 400  $\mu$ l buffer Z supplemented with  $\beta$ -mercaptoethanol and LD-mix (175  $\mu$ l  $\beta$ -mercaptoethanol and 250  $\mu$ l LD-mix in 50 ml Z buffer) and incubated for 10 min at 37 °C and 500 rpm. The cell suspensions were always kept on ice (Commichau *et al.*, 2015b).

### **Cell disruption with NaOH**

Pellets of *B. subtilis* were disrupted with NaOH for subsequent determination of the total protein amount per ml cell culture. This was used for the normalization of intracellular c-di-AMP amounts and done in technical duplicates for each sample. A pellet of 2 ml culture (OD<sub>600</sub> of 0.5) was resuspended with 800  $\mu$ l 0.2 M NaOH, incubated for 10 min at 98 °C and centrifuged for 10 min at 20,800  $\times g$  and 4 °C. The supernatant was transferred into a fresh

reaction tube and the above procedure was repeated with the remaining cell pellet. The two supernatants were pooled and the protein amount was determined from 50, 75 and 100  $\mu$ l with the Bradford method (adapted from Commichau *et al.*, 2015b).

### **Purification of His<sub>6</sub>-tagged proteins by affinity chromatography**

For the purification of His<sub>6</sub>-tagged proteins by affinity chromatography, frozen cell pellets were resuspended in ice-cold ZAP with 10 mM imidazole (5 ml / g pellet) and cells were disrupted using the French press method. The suspension was cleared of remaining cell debris and insoluble material by ultracentrifugation for 1 h at 35,000 rpm and 4 °C. The cell-free crude extract (supernatant) of a 1 l culture pellet was loaded onto a 1 ml Ni<sup>2+</sup>-NTA sepharose resin (IBA Lifesciences). Beforehand, the resin was assembled in a Poly-Prep chromatography column (Bio-Rad Laboratories) and equilibrated with 10 ml of ZAP with 10 mM imidazole. After all of the cell-free crude extract had been loaded, the column was washed three times with 8 ml of ZAP with 10 mM imidazole. The last washing step was analyzed with the Bradford method and washing was continued until no relevant protein amount was measurable anymore. The elution was done stepwise with 8 ml ZAP containing increasing imidazole concentrations (50, 75, 100 and 500 mM). The 100 and 500 mM steps were collected as two separate fractions. The purification fractions were analyzed by SDS-PAGE with subsequent Coomassie staining. Relevant fractions were pooled and eventually dialyzed against another buffer (if needed) as indicated (adapted from Commichau *et al.*, 2015b).

### **Purification of Strep-tagged proteins by affinity chromatography**

For the purification of Strep-tagged proteins by affinity chromatography, frozen cell pellets were resuspended in ice-cold buffer W (5 ml / g pellet) and cells were disrupted using the French press method. The suspension was cleared of remaining cell debris and insoluble material by ultracentrifugation for 1 h at 35,000 rpm and 4 °C. The cell-free crude extract (supernatant) of a 1 l culture pellet was loaded onto a 500  $\mu$ l Strep-Tactin sepharose resin (IBA Lifesciences). Beforehand, the resin was assembled in a Poly-Prep chromatography column (Bio-Rad Laboratories) and equilibrated with 5 ml of buffer W. After all of the cell-free crude extract had been loaded, the column was washed five times with 2.5 ml of buffer W. The last washing step was analyzed with the Bradford method and washing was continued until no relevant protein amount was measurable anymore. Strep-tagged proteins were eluted with buffer E and collected in three fractions (E1: 250  $\mu$ l, E2/3: 500  $\mu$ l each). The purification fractions were analyzed by SDS-PAGE with subsequent Coomassie staining. Relevant fractions were pooled and eventually dialyzed against another buffer (if needed) as indicated (adapted from Commichau *et al.*, 2015b).

### Dialysis of proteins

If needed, protein samples were dialyzed against a 1000-fold volume of the desired buffer. For this purpose, a sufficient part of MEMBRA-CEL dialysis tubing (SERVA) was boiled two times for 10 min in deionized water and soaked in 4 °C cold buffer afterwards. The protein sample was put into the tubing and dialyzed under stirring for 2 h at 4 °C and again overnight at 4 °C against fresh buffer (adapted from Commichau *et al.*, 2015b).

### Sodium dodecyl sulfate polyacrylamide gel electrophoresis (SDS-PAGE)

Proteins were analyzed by sodium dodecyl sulfate polyacrylamide gel electrophoresis (SDS-PAGE) based on their molecular weight (Laemmli, 1970). Running gels were prepared with 8–15 % (v/v) Rotiphorese Gel 30 depending on the mass of the expected proteins. Protein samples were denatured in SDS loading dye for 30 min at 95 °C and loaded onto the prepared gel. PageRuler Plus Prestained Protein Ladder (Thermo Fisher Scientific) or in-house prepared protein marker, run on the same gel, served as a reference to estimate the size of the proteins. The electrophoresis was carried out at 150 V in a Tris-glycine buffer system until the proteins were sufficiently separated. Proteins were visualized by Coomassie staining, silver staining or Western blotting (Commichau *et al.*, 2015b).

### Coomassie staining of polyacrylamide gels

Proteins separated in SDS polyacrylamide (SDS-PAA) gels, for example from purification elution fractions, were visualized using Coomassie Brilliant Blue G-250 (Sigma-Aldrich Chemie) (Fazekas de St Groth *et al.*, 1963). The gels were incubated in Coomassie staining solution for 30 min at room temperature on a horizontal reciprocating shaker at 50 rpm. Background staining of the gel was removed by further incubation in Coomassie destaining solution until the contrast between the background and the stained protein bands was sufficient. Stained gels were stored in deionized water and documented using the Molecular Imager Gel Doc XR+ system (Bio-Rad Laboratories) (Commichau *et al.*, 2015b).

### Silver staining of polyacrylamide gels

In order to detect even small amounts of proteins in SDS-PAA gels, separated proteins were visualized by silver (nitrate) staining (Merril *et al.*, 1981). All incubation steps were carried out at room temperature on a horizontal reciprocating shaker at 50 rpm. First, the proteins were fixated within the gel by incubation in fixation solution overnight. The gel was washed three



times with 50 % ethanol for 20 min and incubated for 90 s in thiosulfate solution (reduction). After washing three times with deionized water for 20 s, staining was carried out by incubation in impregnator solution for 25 min. The gel was again washed three times with deionized water for 20 s and the protein bands were visualized by incubation in developer solution until sufficient staining. The development was stopped by washing two times with deionized water for 20 s and incubation in stop solution for 10 min. Stained gels were stored in deionized water and documented using the Molecular Imager Gel Doc XR+ system (Bio-Rad Laboratories) (Commichau *et al.*, 2015b).

### **Western blotting**

Proteins were detected in cell-free crude extracts, membrane and cytosolic protein fractions or protein purification elution fractions by Western blotting (Towbin *et al.*, 1979). Wherever needed, protein concentrations were determined with the Bradford method beforehand and adjusted to the desired concentration. After previous separation by SDS-PAGE the proteins were transferred onto a methanol treated (30 s) Immun-Blot polyvinylidene fluoride (PVDF) membrane (Bio-Rad Laboratories) using a semi dry blotting system (G&P Kunststofftechnik), blotting paper sheets and transfer buffer. The blotting was carried out for 1 h with a current of 80 mA. Unless otherwise stated, all following incubation steps were carried out at room temperature on a horizontal reciprocating shaker at 50 rpm. The membrane was incubated for 1 h in blocking solution to minimize unspecific binding of the antibodies. The primary antibody raised against the protein of interest was diluted in blocking solution (see Appendix for dilutions) and binding was achieved by incubation overnight at 6 °C. Excess of the primary antibody was removed by washing the membrane three times with blocking solution for 30 min. The secondary antibody (Anti-Rabbit IgG (Fc), AP Conjugate; Promega) was diluted in blocking solution (1:100,000), added to the membrane and incubated for 30 min. The membrane was again washed three times with blocking solution for 20 min, shortly rinsed in deionized water and incubated in buffer III for 5 min to equilibrate the pH. Finally, protein detection was enabled by addition of 0.25 mM CDP-*Star* chemiluminescence substrate (Roche Diagnostics) in buffer III. Chemiluminescence emerging by substrate turnover was detected and documented using the ChemoCam Imager ECL (INTAS Science Imaging Instruments) (Commichau *et al.*, 2015b).

### **Separation of membrane and cytosolic proteins by ultracentrifugation**

To investigate the localization of DarA within the cells the respective *B. subtilis* strains were first grown in 250 ml MSSM medium with ammonium or glutamate as the nitrogen source and 0.1 or 5 mM KCl until an OD<sub>600</sub> of 1.0 as described. Cells of 200 ml culture were

harvested by centrifugation for 15 min at 5000 rpm and 4 °C. The cell pellet was washed in ice-cold membrane buffer M, transferred to falcon tubes and harvested one last time for 5 min at 8500 rpm and 4 °C. The pellets were stored at −20 °C until resuspension in 1.5 ml ice-cold membrane buffer M and disruption by using the French press method. The suspension was cleared of remaining cell debris and insoluble material by centrifugation for 15 min at 8500 rpm and 4 °C followed by a second centrifugation step for 30 min as before. A sample of the cell-free crude extract (supernatant) was kept, while the rest was transferred into 1.5 ml microcentrifuge tubes. The separation of cytosolic and membrane proteins was achieved by pelleting the membrane fraction for 1 h at 68,000 rpm and 4 °C. To minimize contamination of the cytosolic fraction with membrane proteins only the upper 80 % of the supernatant was carefully removed and kept as the cytosolic protein fraction while the remaining supernatant was discarded. The pellet containing the membrane proteins was washed twice to get rid of contamination by remaining cytosolic proteins. For this purpose, the pellet was resuspended in 20 ml ice-cold membrane buffer M, transferred to an ultracentrifuge tube and pelleted for 30 min at 35,000 rpm and 4 °C. After washing again as described before the membrane fraction pellet was resuspended in 200 µl ice-cold membrane buffer M supplemented with 5 % (w/v) CHAPS to solubilize the membrane proteins. The protein fractions were analyzed by SDS-PAGE with subsequent Western blotting (Commichau *et al.*, 2015b).

### **Strep-protein interaction experiment (SPINE)**

One way to detect protein–protein interactions *in vivo* is the Strep-protein interaction experiment (SPINE). This method relies on the *in vivo* crosslinking of adjacent proteins by treating growing bacterial cells with the heat-reversible crosslinker paraformaldehyde. A Strep-tagged protein of interest is then purified by affinity chromatography and eventually crosslinked proteins are co-eluted. The crosslinker is resolved by boiling of the protein samples in SDS loading dye and fractions can be analyzed by SDS-PAGE and subsequent silver staining and/or Western blotting (Herzberg *et al.*, 2007). The respective *B. subtilis* strain was grown in the indicated medium to an OD<sub>600</sub> of 1.0 as described. The culture was split and one half was harvested by centrifugation for 15 min at 5000 rpm and 4 °C. The other half was crosslinked with a final concentration of 0.6 % paraformaldehyde (4 % in PBS) for 20 min at 37 °C and 220 rpm and also harvested afterwards. Both cell pellets were washed in ice-cold buffer W, transferred to falcon tubes and again harvested for 5 min at 8500 rpm and 4 °C. The pellets were disrupted by using the French press method. The suspension was cleared of remaining cell debris and insoluble material by ultracentrifugation for 30 min at 35,000 rpm and 4 °C. The Strep-tagged protein was purified from the cell-free crude extract (supernatant) by affinity chromatography and the protein fractions were analyzed by SDS-PAGE with subsequent silver staining and/or Western blotting. Individual protein bands or whole lanes were eventually cut out from silver stained gels. The subsequent preparation by Trypsin in-gel

digestion and gas chromatography–mass spectrometry (GC/MS) analysis was done externally in the laboratory of Dr. Elke Hammer (Institute of Genetics and Functional Genomics, Department of Functional Genomics, University Greifswald) (Commichau *et al.*, 2015b).

### **Protein pull-down experiment**

A protein pull-down experiment can be used to study protein–protein interactions *in vitro* (Louche *et al.*, 2017). To analyze a possible interaction of GltAB with DarA, either GltAB-His<sub>6</sub> (pGP3031 and pGP3033) or GltAB-Strep (pGP3032 and pGP3033) were co-produced in *E. coli* BL21(DE3). In parallel, DarA was also overproduced in *E. coli* with either an N-terminal His<sub>6</sub>- (pGP2601) or Strep-tag (pGP2624). The following steps were done at room temperature. GltAB was loaded onto the respective column for the affinity purification and the column was washed until no significant amount of protein was measurable anymore in a Bradford assay. The differently tagged DarA versions were exhaustively dialyzed against the binding/washing buffer used for the respective GltAB purification. DarA was either saturated with a 2.5-fold excess of c-di-AMP for 30 min at room temperature or incubated with an equal amount of buffer and applied to the already washed GltAB purification columns. Strep-DarA or His<sub>6</sub>-DarA was always applied to the column with bound GltAB exhibiting another affinity tag to exclude tag-based interactions. Empty columns served as a negative control. The columns were washed again until no relevant protein amount was measurable anymore with the Bradford method. The proteins were eluted as described for the affinity chromatography before and the protein fractions were analyzed by SDS-PAGE with subsequent silver staining and Western blotting.

### **Size exclusion chromatography (SEC)**

Size exclusion chromatography (SEC) is a widely adopted method to discriminate proteins and their multimeric aggregates by their size/molecular weight. In short, this is achieved by the fact that smaller/lighter proteins are retained to a greater extent within a porous matrix compared to larger/heavier proteins or their multimeric aggregates (Hong *et al.*, 2012). Whether mutated DarA variants are able to form stable homotrimers was analyzed by SEC. First, the DarA variants were overproduced in *E. coli* BL21(DE3) and purified via an N-terminal His<sub>6</sub>-tag by affinity chromatography. SEC was carried out at room temperature using a SEC column HiLoad 16/600 Superdex connected with the ÄKTAprime plus chromatography system (both GE Healthcare). The column was equilibrated with ZAP and purified protein was applied. The elution was run at 1 ml/min, protein concentration was measured with a column-coupled spectrometer and 4 ml elution fractions were collected. The elution spectra of the mutated DarA variants were compared to the spectrum of the native DarA, known to

form stable trimers. The trimer fractions of each variant were pooled and checked again by SDS-PAGE and Coomassie staining. Further analysis of the variants was done by isothermal titration calorimetry (ITC).

### **Isothermal titration calorimetry (ITC)**

The c-di-AMP binding capacity of mutated DarA variants was checked, at least in technical duplicates, by isothermal titration calorimetry (ITC). ITC is a well established, highly sensitive method to determine the binding constant, stoichiometry, binding enthalpy and more of a ligand–protein or protein–protein interaction. The method is based on the temperature change during an endothermic or exothermic reaction and features a sample and a reference cell, placed inside an adiabatic jacket. A ligand is titrated to a protein of interest placed in the sample cell. If an interaction occurs the temperature inside the sample cell changes and thus is now different to the temperature in the reference cell. The system either cools or heats the sample cell to a thermal equilibrium, which is detected and quantified (Pierce *et al.*, 1999; Wiseman *et al.*, 1989). For the ITC, the sample cell was filled with 10  $\mu\text{M}$  His<sub>6</sub>-DarA in ZAP buffer. The titration syringe was put into identical ZAP buffer containing 150  $\mu\text{M}$  c-di-AMP. The measurements were carried out with a VP-ITC MicroCalorimeter (MicroCal) and the operating parameters were as follows: Temperature 20 °C, stirring speed 502 rpm, reference potential 12.5  $\mu\text{cal/s}$ . The injections were done with an interval of 300 s and a filter period of 2 s as follows: First injection with 5  $\mu\text{l}$  over 5 s, second injection until end with 15  $\mu\text{l}$  over 30 s. A titration of c-di-AMP in buffer served as a negative control which was subtracted from the actual data. Subsequent data analysis was done with the Origin 7 SR2 software assuming a one-site binding model (OriginLab) (adapted from Gundlach *et al.*, 2015a).

### **$\beta$ -Galactosidase activity assay**

A  $\beta$ -galactosidase activity assay was used to quantify the activity of the *gltAB* promoter in *B. subtilis* strains expressing different *gltC* variants (Miller, 1972). Before the actual assay, the respective strains were grown in MSSM medium with ammonium as the nitrogen source and 0.5 mM KCl until an OD<sub>600</sub> of 0.6 as described before. Cells of 1.5 ml culture were harvested by centrifugation for 5 min at 13,000 rpm and 4 °C. The cells were disrupted with LD-mix and the suspension was cleared of remaining cell debris and insoluble material by centrifugation for 2 min at 13,000 rpm and 4 °C. The cell-free crude extract (supernatant) was transferred to a fresh reaction tube. 100  $\mu\text{l}$  cell-free crude extract were mixed with 700  $\mu\text{l}$  of Z buffer supplemented with  $\beta$ -mercaptoethanol (175  $\mu\text{l}$   $\beta$ -mercaptoethanol in 50 ml Z buffer) by vortexing. 800  $\mu\text{l}$  of Z buffer with  $\beta$ -mercaptoethanol served as a negative control and reference. All samples were prewarmed for 5 min at 28 °C and the reaction was started

by addition of 200  $\mu\text{l}$  *o*-nitrophenyl- $\beta$ -D-galactopyranoside (ONPG) solution (4 mg/ml in Z buffer). Upon yellow coloration, the time was noted and the reaction was stopped by adding 500  $\mu\text{l}$  of 1 M  $\text{Na}_2\text{CO}_3$  solution to the sample and vortexing briefly. The absorption of the product *o*-nitrophenyl was measured at 420 nm. The protein amount of the used cell-free crude extracts was determined from 20  $\mu\text{l}$  with the Bradford method. All measurements were done from independent, biological triplicates. The specific  $\beta$ -galactosidase activity in Miller units resembles the activity of the promoter and was quantified by using the following equation (Commichau *et al.*, 2015b).

$$\frac{\text{Miller Units}}{\text{mg protein}} = \frac{1500 \cdot A_{420}}{\Delta t [\text{min}] \cdot A_{595}}$$

### Glutamine oxoglutarate aminotransferase (GOGAT) activity assay

Whether DarA regulates the activity of the glutamine 2-oxoglutarate aminotransferase (GOGAT) GltAB from *B. subtilis*, was determined in GOGAT activity assays. The GOGAT, also known as glutamate synthase, catalyzes the reductive, NADPH-dependent synthesis of two molecules of L-glutamate from the precursors L-glutamine and  $\alpha$ -ketoglutarate. The rate of the reaction can be analyzed by measuring the oxidation of the cofactor NADPH to  $\text{NADP}^+$  at 340 nm, resulting in decreasing absorption over time (Bohannon and Sonenshein, 1989). Prior to the GOGAT activity assay, *E. coli* BL21(DE3) was transformed with pGP3031 (GltB-His<sub>6</sub>) and subsequently with pGP3033 (GltA) or only with pGP2426 (Strep-DarA). The proteins were purified by affinity chromatography from cell pellets of 0.5 l or 3 l LB medium overexpression culture, respectively. Since the subunits GltA and GltB are known to interact with each other, both subunits were co-produced within one *E. coli* culture. GltB-His<sub>6</sub> was purified and GltB-bound, untagged GltA was co-eluted in the process (Agnelli *et al.*, 2005). The purification fractions of GltAB-His<sub>6</sub> and Strep-DarA were checked by SDS-PAGE with subsequent Coomassie staining. The protein solutions were exhaustively dialyzed against 50 mM Tris-HCl pH 7.5 buffer and protein amounts were determined with the Bradford method. The final reaction mixes for the GOGAT activity assay contained 50 mM Tris-HCl pH 7.5, 5 mM  $\beta$ -mercaptoethanol, 20 mM L-glutamine, 35 mM  $\alpha$ -ketoglutaric acid and 0.1 mM NADPH (adapted from Bohannon and Sonenshein, 1989). Functionality of the assay and of the GltAB dodecamer was first tested with a titration of 0–20 pmol of GltAB-His<sub>6</sub> preparation. For the actual assay, Strep-DarA was either saturated with a 2.5-fold excess of *c*-di-AMP for 30 min at room temperature or incubated with an equal amount of buffer immediately prior to the assay. Finally, 10 pmol GltAB-His<sub>6</sub> alone or together with a 10-fold excess (100 pmol) Strep-DarA (with or without *c*-di-AMP), or only with *c*-di-AMP were added to start the reaction. The reactions were measured every 10 min over the course of 2 h at 340 nm in the microplate reader Synergy M (BioTek Instruments). The reactions were corrected for calculated background

NADPH oxidation and control reactions without the substrates L-glutamine/ $\alpha$ -ketoglutaric acid or without GltAB-His<sub>6</sub> served as additional negative controls.



### 2.2.8 Bacterial adenylate cyclase-based two-hybrid (BACTH) system

The bacterial adenylate cyclase-based two-hybrid (BACTH) system is based on the reconstitution of the catalytic domain of the adenylate cyclase from *Bordetella pertussis* in *E. coli* (Karimova *et al.*, 1998). The genes encoding for two potentially interacting proteins are fused N- or C-terminally to the T18 or T25 fragment of the catalytic domain of the adenylate cyclase. A physical interaction of the two proteins reconstitutes a functional adenylate cyclase and the produced cAMP activates the transcription of the lactose operon.  $\beta$ -Galactosidase finally cleaves X-Gal and the initial interaction is indicated by blue colonies (Karimova *et al.*, 1998). The genes were each cloned into two high copy (pUT18, pUT18C) and two low copy vectors (p25-N, pKT25) using the *E. coli* XL1-blue strain. Since DarA is a c-di-AMP-binding protein, interactions could occur in a ligand-bound or -free state. However, c-di-AMP is not naturally present in *E. coli*. Thus, an additional plasmid facilitating low level c-di-AMP production (pGP2608) or the corresponding empty vector (pFDX4291) were used (Gundlach, 2014). The *E. coli* BTH101 strain was first transformed with the additional plasmid pGP2608 or pFDX4291. In a second transformation the resulting two strains were each co-transformed with plasmid combinations for the different T18 and T25 constructs. The plasmids pUT18C-Zip and pKT25-Zip, forming a leucine zipper, were used as a positive control. For the co-transformations, 200  $\mu$ l competent cells were mixed with 5  $\mu$ g plasmid DNA (2.5  $\mu$ g for each of the T18 and T25 construct plasmids). The transformation was carried out as described and the transformation samples were plated on LB medium agar plates supplemented with the appropriate antibiotics, X-Gal (80  $\mu$ g/ml) and IPTG (0.5 mM). The plates were incubated in the dark for 24 h at 28 °C. Colonies from the transformation plates were re-streaked together onto a big LB medium agar plate (supplemented with the appropriate antibiotics, X-Gal and IPTG). Pictures were taken after incubation in the dark for another 24–48 h at 28 °C (adapted from Gundlach, 2014 and Commichau *et al.*, 2015b).

### 2.2.9 Determination of intracellular metabolite amounts

For the determination of intracellular metabolite amounts, the *B. subtilis* wild type (168) and the *darA* deletion mutant (GP1712) were grown in MSSM medium with 0.1 mM KCl and ammonium as the nitrogen source until an OD<sub>600</sub> of 0.5–0.6 as described before. 1 mg wet weight biomass (4 ml with an OD<sub>600</sub> of 0.5) of the respective culture were transferred

onto an ash-free filter disk (pore size: 0.45  $\mu\text{m}$ ) and immediately transferred into 2 ml of a  $-20^\circ\text{C}$  cold mixture of 40:40:20 (vol.-%) acetonitrile:methanol:water. The samples were incubated for 30 min at  $-20^\circ\text{C}$  for extraction of the metabolites and vortexed before and after. 500  $\mu\text{l}$  were taken and remaining particles were pelleted for 15 min at 13,000 rpm and  $-9^\circ\text{C}$ . 400  $\mu\text{l}$  of each supernatant were stored at  $-80^\circ\text{C}$  until further processing (adapted from Guder *et al.*, 2017). All samples were prepared in technical duplicates and as independent biological quadruplets. Further processing and determination of the intracellular metabolites was done externally by the laboratory of Dr. Hannes Link (Dynamic Control of Metabolic Networks, Max Planck Institute for Terrestrial Microbiology, Marburg) as described in Guder *et al.* (2017) and Gundlach *et al.* (2017a) using liquid chromatography–mass spectrometry (LC/MS).

### 2.2.10 Determination of intracellular c-di-AMP amounts

For the determination of intracellular c-di-AMP amounts, the *B. subtilis* wild type (168) and the *darA* deletion mutant (GP1712) were grown in MSSM medium with 0.1 mM KCl and ammonium as the nitrogen source until an  $\text{OD}_{600}$  of 0.5–0.6 as described before. 20 ml of the respective culture were pelleted for 5 min at 8500 rpm and  $4^\circ\text{C}$ . The cell pellets were quickly frozen in liquid nitrogen and stored at  $-80^\circ\text{C}$ . The pellets were resuspended in 150  $\mu\text{l}$  of lysozyme solution (2 mg/ml in TE buffer), transferred to fresh reaction tubes and incubated for 30 min at  $25^\circ\text{C}$  and 750 rpm. The suspensions were shortly frozen in liquid nitrogen and incubated for 10 min at  $95^\circ\text{C}$ . 800  $\mu\text{l}$  of a 50:50 (vol.-%) acetonitrile:methanol mixture was added, samples were vigorously vortexed for 45 s and immediately transferred on ice. After a 15 min incubation on ice, the samples were centrifuged for 10 min at  $20,800 \times g$  and  $4^\circ\text{C}$ . The supernatant was collected in a fresh reaction tube and stored on ice. For a second extraction step, the remaining pellet of each sample was resuspended with 200  $\mu\text{l}$  of a 40:40:20 (vol.-%) acetonitrile:methanol:water mixture, vigorously vortexed for 45 s and again incubated on ice for 15 min. The samples were centrifuged again as described before and the supernatant of each sample was pooled with the previously collected one. The second extraction step was repeated as described before. The supernatants of all three extraction steps were pooled, incubated overnight at  $-20^\circ\text{C}$  and centrifuged for 20 min at  $20,800 \times g$  and  $4^\circ\text{C}$ . The supernatants were transferred into fresh reaction tubes and dried for 2 h at  $40^\circ\text{C}$  using a SpeedVac concentrator. All samples were prepared as independent, biological triplicates. The determination of c-di-AMP amounts was done externally in the laboratory of Prof. Dr. Volkhardt Kaefer (Research Service Centre Metabolomics, Hannover Medical School) using high performance liquid chromatography-coupled tandem mass spectrometry (HPLC-MS/MS) (Spangler *et al.*, 2010). For the normalization of the measured c-di-AMP (nM), the total protein amount per ml cell culture was determined from pellets of 2 ml culture. The cells were lysed with the NaOH method and the total protein amount per ml cell culture

was calculated. Finally, the c-di-AMP values were normalized to the protein content by using the following equation (adapted from Commichau *et al.*, 2015b).

$$\frac{c_{\text{c-di-AMP}} \cdot 0.2 \cdot M_w(\text{c-di-AMP})}{V_{\text{culture}} \cdot c_{\text{protein}}} = \frac{\text{ng c-di-AMP}}{\text{mg protein}}$$

### 2.2.11 Determination of intracellular potassium amounts

For the determination of intracellular potassium amounts, the *B. subtilis* wild type (168) and the *darA* deletion mutant (GP1712) were grown in MSSM medium with 0.1 mM KCl and ammonium as the nitrogen source until an OD<sub>600</sub> of 0.5–0.6 as described before. 100 ml of the respective culture were pelleted for 10 min at 5000 rpm and 4 °C. The cell pellet was resuspended in 1.8 ml 1× MSSM base and transferred onto an ash-free filter disk (pore size: 0.45 μm). The filter disks were first dried overnight at room temperature, and again overnight at 70 °C (adapted from Gundlach *et al.*, 2017b). All samples were prepared as independent, biological triplicates. Further processing and determination of the intracellular potassium amounts was done externally by the research group of Dr. Dietrich Hertel (Department of Plant Ecology and Ecosystems Research, University of Göttingen) using inductively coupled plasma optical emission spectrometry (ICP-OES) as described in Gundlach *et al.* (2017b).

### 2.2.12 Phenotype screening

Unbiased screening for metabolic phenotypes of a *B. subtilis darA* deletion mutant was performed using Phenotype MicroArray (PM) plates (Biolog). Each 96-well plate contained 96 different substrates like single carbon or nitrogen sources, di- or tri-peptides, phosphorus or sulfur sources, pH or salt stress conditions, for phenotypic analysis. The screening integrates the cellular respiration, thus growth and metabolic activity, and relies on the reduction of a tetrazolium based dye, like tetrazolium violet. Under normal environmental conditions the cells have to carry out a cascade of different processes in order to grow. These include nutrient transport, catabolism, anabolism, build up of cellular structures and more. While the cells grow, electrons from the carbon source will be transferred to NADH and flow down the cellular electron transport chain. Finally, these electrons will be transferred onto the oxidized form of the tetrazolium violet dye, reducing it to purple formazane. Since dye reduction is irreversible under physiological conditions, the purple formazane accumulates in the wells over time, thus integrating the cellular respiration. For quantitation, the purple coloration can easily be measured at a wavelength of 590 nm. Impairment of one or more processes in the cellular physiology, for example in a deletion mutant, will ultimately limit the electron flow rate onto the tetrazolium dye, thus leading to a decrease in purple color formation or even no color formation at all (Bochner *et al.*, 2001). For the described screening, a single colony



of the *B. subtilis* wild type (168) or of the *darA* deletion mutant (GP1712) was re-streaked twice from an SP medium agar master plate onto fresh plates. The strains were first grown for 24 h, then for 16 h at 37 °C to get rid of spores carried over from the master plate. A sufficient amount of cells was transferred into 1 ml 1× IF-0a (PM1–8) or 1× IF-10b (PM9/10) with a sterile loop and resuspended by stirring. The cell suspension was set to rest until remaining cell clumps had sedimented. The supernatant was adjusted to an OD<sub>600</sub> of 0.1 and used to inoculate a final 1× PM solution. All solutions were preheated to 37 °C. The respective PM plate was loaded with 100 µl 1× PM inoculation solution per well and dye reduction, thus respiration, was measured at a wavelength of 590 nm in the microplate reader Synergy Mx (BioTek Instruments) every 10 min over the course of 48 h at 37 °C and medium shaking. The additive and inoculation solutions were prepared as described by the manufacturer and are shown in the Tables 2.5 and 2.6 (Biolog).

**Table 2.5: Composition of 12× PM additive solutions.**

Components	1×	40–120×	12× PM				
			1,2	4	3,6–8	4	9–10
Tricarballic acid, pH 7.1 (NaOH)	20 mM	800 mM	–	30 ml	30 ml	30 ml	–
MgCl <sub>2</sub> · 6 H <sub>2</sub> O	2 mM	240 mM	10 ml	10 ml	10 ml	10 ml	10 ml
CaCl <sub>2</sub> · 2 H <sub>2</sub> O	1 mM	120 mM	–	–	–	–	–
L-Arginine hydrochloride	25 µM	3 mM	10 ml	–	10 ml	–	–
Monosodium L-glutamate	50 µM	6 mM	–	–	–	–	–
L-Cystine, pH 8.5 (NaOH)	12.5 µM	0.5 mM	30 ml	30 ml	–	–	–
5'-UMP-Na <sub>2</sub>	25 µM	1 mM	–	–	–	–	–
Yeast extract	0.005 %	0.6 %	10 ml	10 ml	10 ml	–	10 ml
Tween 80	0.005 %	0.6 %	10 ml	10 ml	10 ml	–	10 ml
D-Glucose	2.5 mM	300 mM	–	10 ml	10 ml	10 ml	10 ml
Monosodium pyruvate	5 mM	600 mM	–	–	–	–	–
Sterile dH <sub>2</sub> O	–	–	30 ml	–	20 ml	50 ml	60 ml

**Table 2.6: Final 1× PM inoculation solutions.**

Components	1× PM	
	1–8	9–10
1.2× IF-0a GN/GP	10 ml	–
1.2× IF-10b GN/GP	–	10 ml
100× Dye mix F	0.12 ml	0.12 ml
12× PM additive	1 ml	1 ml
Cells (OD <sub>600</sub> = 0.1 in 1× IF)	0.88 ml	0.88 ml

### 2.2.13 Rational bioinformatic search of interaction partners

A rational bioinformatic approach was chosen to get a broad, unbiased overview of proteins that are in theory suitable for an interaction with DarA. For this purpose, we analyzed the proteome of *B. subtilis* and several rational requirements were set beforehand. Namely, conservation among related bacteria, suitable protein amount, structure and localization. First, a putative interaction partner is most likely conserved among c-di-AMP-producing firmicutes also expressing *darA* or homologues. Consequently, the *Bacillus subtilis* 168 proteome (GenBank accession number: NC\_000964) was compared with the proteome of the related, well studied *Listeria monocytogenes* EGD-e and *Staphylococcus aureus subspecies aureus* NCTC 8325 (GenBank accession numbers: NC\_003210 and NC\_007795, respectively). All proteins not conserved between the three were discarded. Second, the total cellular protein amount of the potential target should be lower, since a regulation by binding of DarA would otherwise not be possible. Protein quantification data were taken from <http://www.subtiwiki.uni-goettingen.de> (Zhu and Stülke, 2018) and originated from Maass *et al.* (2011) and Maaß *et al.* (2014). Only proteins with a lower protein amount than DarA were chosen. Third, since DarA exhibits a trimeric, P<sub>II</sub>-like structure the mode of interaction is most likely similar to the well studied P<sub>II</sub> or other P<sub>II</sub>-like proteins. Thus, foremost proteins with a trimeric, hexameric or dodecameric structure were of high interest. Although less likely, monomeric and dimeric proteins were also kept. The structures were accessed at <http://www.rcsb.org> (Berman *et al.*, 2000). Finally, the cellular localization was accounted for by discarding all membrane bound or extracellular proteins, since DarA seems to be solely present in the cytosol (this thesis). Localization data were taken from <http://www.subtiwiki.uni-goettingen.de> (Zhu and Stülke, 2018). Entries for proteins that are conserved and less abundant than DarA, but lack localization and/or structural data were kept in the list, since they cannot be excluded for certain. The final list was analyzed for promising targets. A separate list of proteins with missing quantification data was kept since they also cannot be excluded completely. Missing protein quantification data might be attributed to membrane proteins, proteins that are not expressed, only expressed under very specific conditions or the protein amount of these is extremely low in general. In either case, the suitability for an interaction with DarA is arguably questionable.

## 3 Results

### 3.1 The genomic context of *darA* and its possible implications

Prior to this work, several different theses had tried to elucidate the function of DarA (Gundlach, 2014; Hach, 2015; Jäger, 2015). However, the function had remained enigmatic and interaction partners had escaped detection. One approach of the previous studies was the focus on the genomic arrangement of *darA*. The DarA protein itself is highly conserved among Gram-positive, c-di-AMP-producing firmicutes, such as *Bacillus* and closely related genera like *Staphylococcus*, *Listeria*, *Lactobacillus*, *Enterococcus* and *Clostridium*. Notable exceptions are *Streptococcus*, *Lactococcus*, *Geobacillus* and the *Bacillus cereus* group (this work and Gundlach *et al.*, 2015a). In addition, the genomic arrangement is also highly conserved. The essential gene *tmk* (coding for the thymidylate kinase) is located directly upstream of *darA*, regulated by its own promoter, while the essential gene *holB* (coding for the  $\delta'$  subunit of the DNA polymerase III) is located downstream of *darA* and under control of the same promoter as *darA* (Nicolas *et al.*, 2012). This arrangement is true for almost all bacteria expressing *darA* suggesting a functional linkage (Dandekar *et al.*, 1998). Intriguingly, no interaction of DarA with Tmk or HolB could be verified in the past, however, c-di-AMP-bound and -free states of DarA were not always exhaustively accounted for (Hach, 2015; Jäger, 2015).

Thus, as an additional approach a modified bacterial two-hybrid was performed in *E. coli* BTH101. The fact that *E. coli* does not produce c-di-AMP naturally was circumvented by using an additional third plasmid for expression of the *B. subtilis* diadenylate cyclase gene *cdaS* (pGP2608), or the empty vector (pFDX4291) accordingly. The *E. coli* BTH101 strain carrying either the *cdaS* expression plasmid (+ c-di-AMP) or the empty vector (– c-di-AMP) was transformed with the different T18/T25-construct plasmid combinations (Plasmids see Appendix: Tables 6.8 and 6.9). Transformants were re-streaked onto LB medium agar plates (containing antibiotics, X-Gal and IPTG) and pictures were taken after incubation in the dark for 24 h at 28 °C. DarA did not interact with Tmk and only self-interactions were observable, as shown in Figure 3.1. This is in agreement with additional isothermal titration calorimetry (ITC) experiments with purified His<sub>6</sub>-DarA (pGP2601) and Strep-Tmk (pGP1689), where no interaction was observed, irrespective of whether DarA was saturated with c-di-AMP beforehand or not. At first glance, HolB showed considerable interaction with DarA in the modified BACTH assay when c-di-AMP was present (T25–HolB and HolB–T18 with both DarA fusions). However, this was also partially observed when c-di-AMP was absent (T25–HolB with DarA–T18), indicating a false positive interaction. To check whether this potential interaction is indeed false-positive, a SPINE in *B. subtilis* (grown in MSSM medium with ammonium as the nitrogen source and 5 mM KCl) was performed with N- or C-terminally Strep-tagged HolB as bait (pGP2672 and pGP3028, respectively). However, DarA could not be detected in the SPINE elution fractions by Western blotting in both cases. Consequently, the HolB–DarA interactions observed in the BACTH assay are likely false positive. In summary,

although the genomic arrangement of *tmk-darA-holB* is highly conserved among most *Bacillus* species and closely related genera, no interactions could be detected. Consequently, neither c-di-AMP-bound nor -free DarA seems to interact with Tmk or HolB.

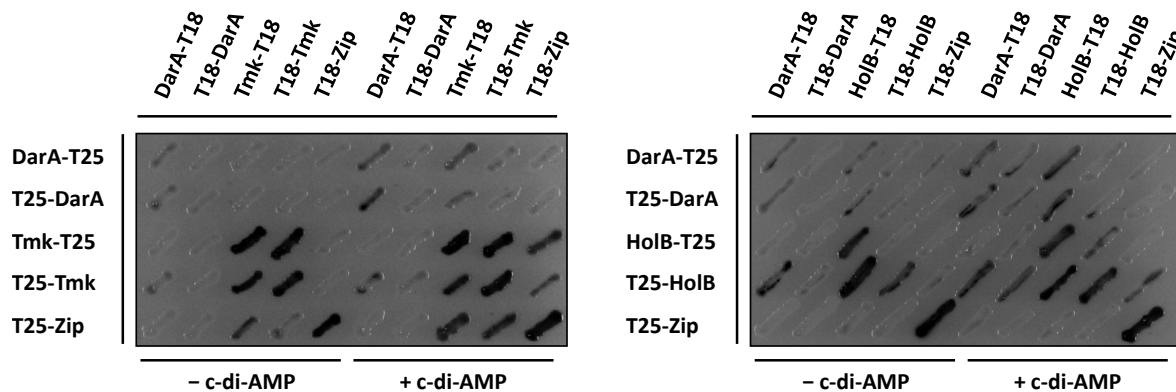


**Figure 3.1: DarA does not interact clearly with Tmk or HolB in a modified BACTH assay.** A modified bacterial two-hybrid assay in *E. coli* in the presence or absence of c-di-AMP. Dark colonies indicate an interaction. Tmk and DarA show only self-interactions. HolB and DarA show self-interactions and interact with and without c-di-AMP present, indicating a false positive result. Leucine zipper constructs (Zip) were used as a control.

### 3.2 Unbiased screening for *darA* mutant phenotypes

The work of several preceding coworkers did not identify the interaction partner of DarA and did not yield robust data about a putative cellular/metabolic context in general. We reasoned that a switch from the biased and directed experiments to a broad, unbiased approach might be necessary. One way to elucidate the function of a gene or gene product is to broadly screen for phenotypes of a deletion mutant. This can for instance be done using the Phenotype MicroArray (PM) system (Biolog). Briefly, the screening integrates the cellular respiration, thus growth and metabolic activity, and relies on the reduction of a tetrazolium violet dye. This reduction leads to a purple coloration which can be measured and quantified at a wavelength of 590 nm. Impairment of one or more processes in the cellular physiology in a deletion mutant will ultimately limit the electron flux onto the tetrazolium dye, which leads to a decrease in purple color formation or even no color formation at all (Bochner *et al.*, 2001).

To get an unbiased overview of DarA-related phenotypes, we compared the metabolic activity of a *darA* deletion mutant to the wild type using the described phenotype screening. The assay was carried out in 96-well plates which each contained 96 different substrates. The conditions included different carbon and nitrogen sources, phosphorus and sulfur sources, specific nutrient supplements, di- and tri-peptide nitrogen sources, osmolytes and pH conditions (PM plates 1–10). Briefly, the *B. subtilis* wild type (168) or the *darA* deletion mutant (GP1712) were re-streaked twice from an SP medium agar master plate onto fresh plates to get rid of spores carried over from the master plate. A sufficient amount of cells was transferred into the

respective inoculation fluid, the cell suspension adjusted to an  $OD_{600}$  of 0.1 and the  $1 \times$  PM solution was inoculated. The respective screening plate was loaded with 100  $\mu$ l final  $1 \times$  PM inoculation solution per well and dye reduction, thus respiration, was measured at a wavelength of 590 nm in a microplate reader every 10 min over the course of 48 h at 37 °C and medium shaking. Finally, the metabolic activity of the *B. subtilis darA* deletion mutant (GP1712) was compared to the activity of the wild type (168). A summary of all plates and tested conditions with their respective curves can be found in the Appendix (Figures 6.1 to 6.10). Despite screening 948 different conditions, no clear phenotype of the *darA* deletion mutant could be detected. Either, DarA acts in a very unique way that is not covered by the screening, or the function is redundant and masked or compensated for by other processes. In addition, it could be that only apo-DarA is interacting with a target. Therefore, a phenotype might have escaped detection because the screening was performed in the wild type background where c-di-AMP is present.

### 3.3 Construction of a c-di-AMP insensitive DarA variant

DarA was first identified in 2015 as a prominent c-di-AMP-binding receptor in *B. subtilis*. The protein forms stable trimers of identical subunits, where the ligand c-di-AMP is bound within a deep pocket between two subunits (1:1 stoichiometry) (Gundlach *et al.*, 2015a). Binding of c-di-AMP should lead to conformational changes within the homotrimeric protein. Although no crystal structure of an apo state of *B. subtilis* DarA is available, this has already been suggested through comparison of the ligand-bound form of *B. subtilis* DarA with a putative orthologue from *Pediococcus pentosaceus* in its apo state. Especially the B- and T-loops of DarA undergo substantial changes in orientation and flexibility (Gundlach *et al.*, 2015a). B- and T-loops of classical  $P_{II}$  proteins have already been analyzed in detail and are known to interact with their respective interaction partner and this will arguably greatly influence DarA's interaction as well (Conroy *et al.*, 2007; Forchhammer and Lüddecke, 2016; Ll acer *et al.*, 2007). However, c-di-AMP is essential and conditions allowing its dispensability had not been found at that point, preventing a clear discrimination of c-di-AMP-bound and apo-DarA *in vivo* (Luo and Helmann, 2012; Mehne *et al.*, 2013).

To investigate target interactions of DarA *in vivo* while accounting for a ligand-bound and -free state, a c-di-AMP-insensitive DarA variant was constructed. For this purpose, several single residues within the binding pocket were mutated by CCR-PCR. Target residues were F36 and R26 which perfectly sandwich one adenine ring of c-di-AMP (Gundlach *et al.*, 2015a). Both residues were mutated to E, thus supposedly breaking  $\pi$ - $\pi$  and cation- $\pi$  interactions, respectively, while also introducing a negative charge. Furthermore, the residues T28 and N41 were both mutated to R, supposedly hindering binding of the ribose and phosphate moieties of c-di-AMP and additionally introducing a positive charge (Gundlach *et al.*, 2015a). All changes were chosen for minimal disturbance of the overall trimeric structure of DarA. The four DarA

variants with the substitutions R26E, T28R, F36E and N41R were fused to an N-terminal His<sub>6</sub>-tag (pGP2798, pGP2799, pGP2800 and pGP3001, respectively), overproduced in *E. coli* and purified by affinity chromatography. Elution fractions were analyzed by SDS-PAGE and Coomassie staining. Figure 3.2 A shows the c-di-AMP (yellow) binding pocket of DarA between two subunits (brown and blue) of the homotrimer. The locations of the mutated residues are indicated (adapted from Gundlach *et al.*, 2015a). The purification of the native His<sub>6</sub>-DarA is shown in Figure 3.2 B and was similar for the other variants.

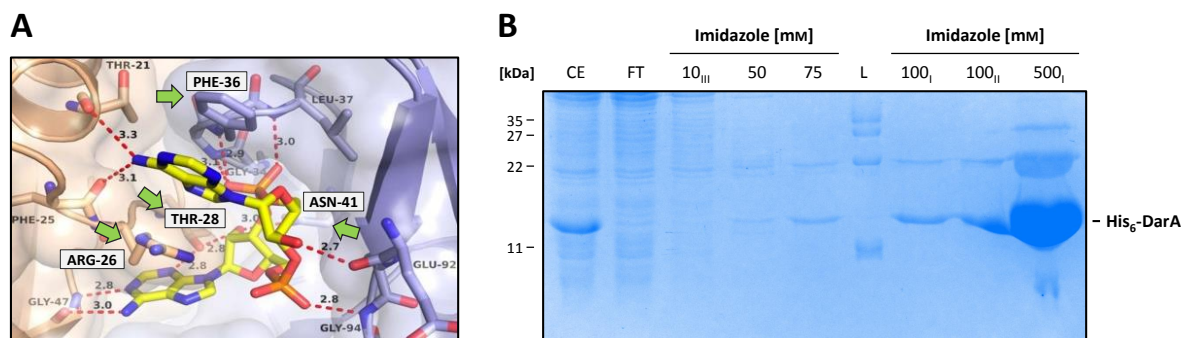


**Figure 3.2: Mutated residues in the c-di-AMP binding pocket of DarA and fractions of a His<sub>6</sub>-DarA purification.** (A) c-di-AMP (yellow) binding pocket between two DarA monomers (brown and blue) (adapted from Gundlach *et al.*, 2015a). Arrows indicate the residues mutated to R26, T28R, F36E and N41R. (B) Purification of His<sub>6</sub>-DarA by affinity chromatography. Cell extract (CE), flow-through (FT), in-house protein ladder (L).

The ability of the four DarA variants to form homotrimers was verified by comparing them with the purified native His<sub>6</sub>-DarA (pGP2601) by size exclusion chromatography (SEC). Proteins were eluted with ZAP and again analyzed by SDS-PAGE and Coomassie staining. SEC analysis revealed that all DarA variants were still able to form trimers. The data for DarA and DarA<sub>F36E</sub> are shown in Figure 3.3 A. Capability of c-di-AMP binding was analyzed at least in technical duplicates by isothermal titration calorimetry (ITC). For this purpose, 150 μM c-di-AMP dissolved in the same buffer were titrated to approximately 10 μM of the respective DarA variant in the sample cell. Figure 3.3 B shows the integrated ITC results for the His<sub>6</sub>-tagged c-di-AMP-insensitive DarA variant DarA<sub>F36E</sub> and the native His<sub>6</sub>-DarA. c-di-AMP titrated into the same buffer served as reference and was subtracted from the actual measurements. The recorded kcal per mole of injected c-di-AMP were plotted against the molar ratio of c-di-AMP : DarA assuming a one-site binding model. DarA<sub>R26E</sub> still showed minor c-di-AMP binding in ITC experiments, which was arguably not desired. The DarA variants DarA<sub>F36E</sub>, DarA<sub>T28R</sub> and DarA<sub>N41R</sub> did not show c-di-AMP binding in the ITC experiments. However, SEC peaks corresponding to the DarA trimer for DarA<sub>F36E</sub> were stronger compared to much weaker ones obtained for the latter two. The chromatogram for DarA<sub>F36E</sub> was quite similar to the one obtained for the native DarA. The weak trimer peaks for DarA<sub>T28R</sub> and DarA<sub>N41R</sub> might indicate that assembly of the monomers for these two variants is partially impaired. DarA<sub>F36E</sub> was thus chosen for future experiments.

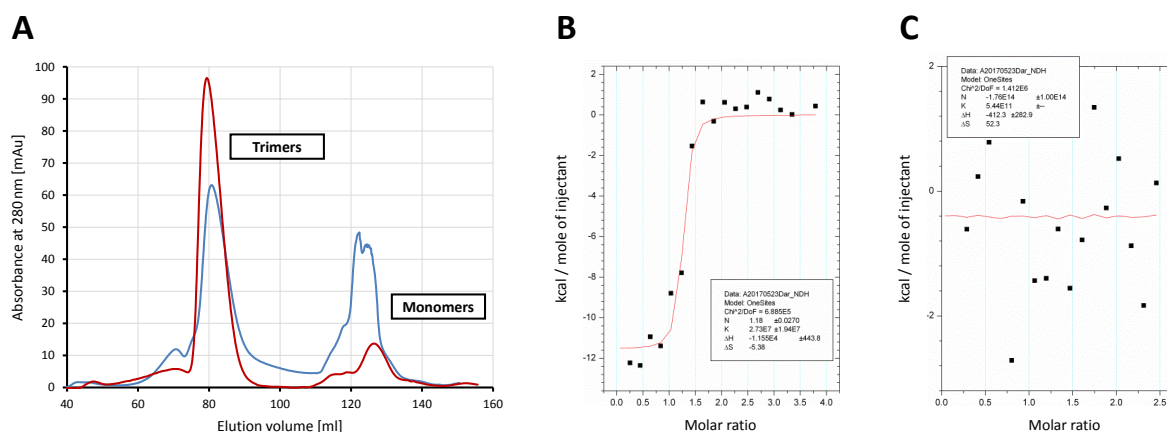


**Figure 3.3: The DarA<sub>F36E</sub> variant still forms trimers but is not able to bind c-di-AMP anymore.** (A) His<sub>6</sub>-DarA (pGP2601) and His<sub>6</sub>-DarA<sub>F36E</sub> (pGP2800) were overproduced in *E. coli* and purified by affinity chromatography. Subsequent SEC shows that the constructed His<sub>6</sub>-DarA<sub>F36E</sub> (red) variant still forms trimers like the native His<sub>6</sub>-DarA (blue). c-di-AMP binding ability is lost for His<sub>6</sub>-DarA<sub>F36E</sub> as demonstrated by ITC analysis for (B) the native DarA or (C) DarA<sub>F36E</sub>.

### 3.4 DarA – a link to glutamate and potassium homeostasis?

It has been shown that c-di-AMP synthesis in *B. subtilis* is dependent on the nitrogen source (Gundlach *et al.*, 2015b) and is controlled by the external potassium concentration (Gundlach *et al.*, 2017b). Recently, potassium homeostasis was shown to be a cause for c-di-AMP essentiality in *B. subtilis* (Gundlach *et al.*, 2017b). Since there is an intricate link between c-di-AMP, potassium and glutamate homeostasis, it is tempting to speculate that DarA integrates the cellular c-di-AMP signal and regulates a process in one of the latter two (Gundlach *et al.*, 2018). A decrease or increase in intracellular c-di-AMP levels could consequently shift DarA into a ligand-bound or -free state, thus altering its interactions. Integration of global cellular signals in bacteria has already been described exhaustively for the classical P<sub>II</sub> proteins. The typical P<sub>II</sub> proteins bind 2-oxoglutarate and ADP or ATP, and control nitrogen metabolism in bacteria (Arcondéguy *et al.*, 2001; Forchhammer and Lüddecke, 2016).

#### 3.4.1 DarA can inhibit growth at low potassium availability

Low levels of K<sup>+</sup> lead to reduced synthesis of c-di-AMP which is necessary to abolish inhibition of K<sup>+</sup> uptake by the high-affinity potassium importers KtrAB and KimA. In addition, when ammonium is used as the nitrogen source, c-di-AMP synthesis is also downregulated compared to glutamate-grown cells (Gundlach, 2017; Gundlach *et al.*, 2018; 2017b; 2015b). Consequently, interactions of c-di-AMP-binding proteins like DarA might be adjusted depending on potassium or nitrogen source availability.

To investigate this hypothesis, we compared the growth of a *darA* deletion mutant to the wild type in minimal medium with different KCl concentrations and with ammonium or glutamate as the nitrogen source. The *B. subtilis* wild type (168) and the *darA* deletion mutant (GP1712) were grown in MSSM medium with ammonium or glutamate as the nitrogen source and low (0.1 mM) or high (5 mM) amounts of KCl at 37 °C and 220 rpm. Growth curves were recorded by measuring the OD<sub>600</sub> every hour over a course of 8 h. Surprisingly, growth of the *darA* deletion mutant was not impaired but faster compared to the wild type when cells were grown in MSSM medium with ammonium as the nitrogen source and 0.1 mM KCl. This phenotype was lost at high potassium concentrations like 5 mM (concentrations up to 1.5 M were analyzed) or by changing the nitrogen source to glutamate (see Figure 3.4 A and B, respectively). Interestingly, both strains were able to slowly grow even when omitting external addition of potassium to the glutamate containing medium, however, a phenotypic difference was absent (data not shown). c-di-AMP levels are very low when cells are grown in MSSM medium with ammonium and 0.1 mM KCl (Gundlach *et al.*, 2017b). This could mean that DarA is acting on its target in a c-di-AMP-free state, at least under this condition.

Changing c-di-AMP levels (or the medium composition) could in principle alter *darA* expression by a yet unknown mechanism. To account for this possibility, the wild type was cultivated again in the different MSSM-based media. Cells were harvested at an OD<sub>600</sub> of 0.5, disrupted with LD-mix and the cell lysates cleared by ultracentrifugation. Total protein amounts were determined with the Bradford method and 10 µg of the cell-free crude extracts were used for SDS-PAGE. Presence of DarA was analyzed by Western blotting with primary antibodies raised against DarA. Antibodies raised against GapA served as a loading control. As shown in Figure 3.4 C, DarA amounts remained stable under the tested conditions. Apparently, the expression of *darA* is not governed by the nitrogen source or K<sup>+</sup> availability, and thus is likely also not affected by c-di-AMP.

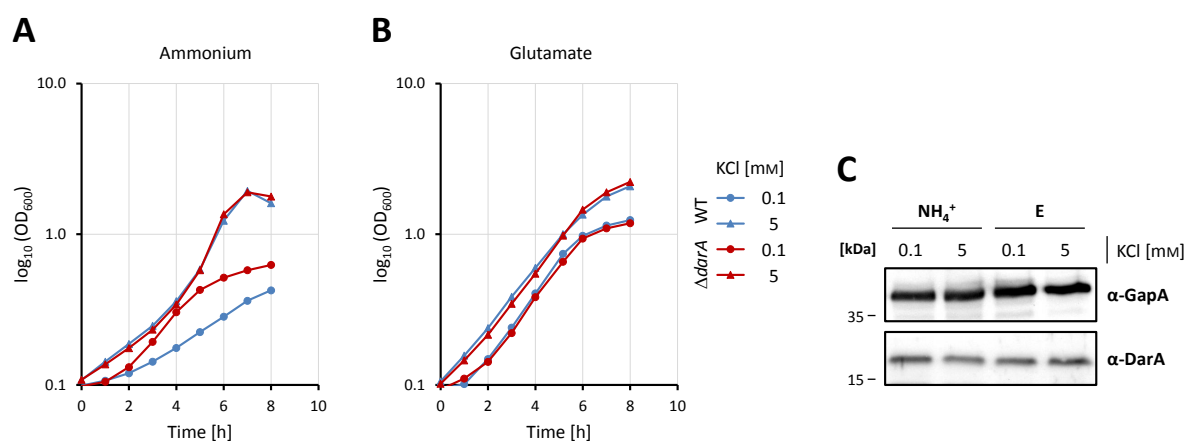


**Figure 3.4: DarA inhibits growth in minimal medium with ammonium as the nitrogen source and low amounts of potassium.** Growth of *B. subtilis* wild type (168) and *darA* deletion mutant (GP1712) in MSSM medium with low (0.1 mM) or high (5 mM) amounts of potassium and (A) ammonium or (B) glutamate as the nitrogen source. Curves are means of independent biological triplicates ( $n = 3$ ). (C) Protein amounts of DarA remain stable under all tested conditions.



The stable protein amounts of DarA are not surprising since *darA* shares its promoter with *holB*, located downstream of *darA*, which codes for the essential DNA polymerase III  $\delta'$  subunit (Nicolas *et al.*, 2012). To conclude all of the above, DarA has to interact with an unknown target in MSSM medium with ammonium and 0.1 mM KCl which inhibits growth. DarA might not be bound to c-di-AMP since intracellular c-di-AMP levels are very low under this condition (Gundlach *et al.*, 2017b). The results furthermore suggest, that DarA is either involved in potassium or nitrogen/glutamate homeostasis.

### 3.4.2 The ligand-bound DarA impairs growth in liquid medium

The condition under which DarA is inhibitory for growth (MSSM medium with ammonium and 0.1 mM KCl) only provokes very low-level c-di-AMP synthesis (Gundlach *et al.*, 2017b). As a result, deletion of the genes encoding all three c-di-AMP-synthesizing diadenylate cyclases in *B. subtilis* was possible and c-di-AMP is indeed dispensable under this condition (Gundlach *et al.*, 2017b). Since c-di-AMP is the natural ligand of DarA we wondered whether c-di-AMP-bound or -free DarA is causative for the slower growth of the wild type in MSSM medium with ammonium as the nitrogen source and low amounts of potassium.

To investigate this hypothesis, we checked whether deletion of *darA* is not only beneficial in the wild type but also in a c-di-AMP-free strain background when cells are grown in MSSM medium with ammonium and 0.1 mM KCl. In addition, we also checked whether both the native DarA and the c-di-AMP-insensitive DarA<sub>F36E</sub> inhibit growth in a wild-type background. First, a *darA* deletion mutant also devoid of the three diadenylate cyclases CdaA, DisA and CdaS (abbreviated *DAC*) was constructed (GP2420) using the protocol from Gundlach *et al.* (2017b). Second, a strain only expressing the c-di-AMP-insensitive *darA*<sub>F36E</sub> in the wild type background was constructed (GP2467) by integrating a ScaI linearized plasmid (pGP3006) into the *ganA* locus of the *darA* deletion mutant by double homologous recombination. As a control, another isogenic strain with the native *darA* (pGP3005) integrated into *ganA* was used (GP2467). The *darA* deletion mutant (GP1712) served as a reference. Growth curves of all strains were recorded as described before, but only in MSSM medium with ammonium as the nitrogen source and 0.1 mM KCl, since this is the condition where DarA inhibits growth of the cells. In addition, higher potassium concentrations and/or glutamate are toxic for the  $\Delta DAC$  strain (Gundlach, 2017; Gundlach *et al.*, 2017b). Interestingly, the deletion of *darA*, which is beneficial in the wild type background, had no impact on growth of a c-di-AMP-free strain. Growth of the  $\Delta DAC$  and  $\Delta DAC \Delta darA$  strains was identical (see Figure 3.5). This is in agreement with growth of the *darA* deletion mutant and of the strain only expressing the c-di-AMP insensitive *darA*<sub>F36E</sub> variant, which grew alike. Only the strain expressing the native *darA* showed slower growth than all the other strains. This strongly indicates that DarA has to act in a c-di-AMP-bound state in MSSM medium with ammonium and low amounts of potassium.

As an additional verification we also investigated the impact of c-di-AMP-bound DarA on growth on the same solidified medium by a drop dilution experiment. For this purpose, the indicated strains were grown until the exponential phase, adjusted to an  $OD_{600}$  of 1.0, serially diluted as indicated and spotted on MSSM medium agar with ammonium and 0.1 mM KCl. The picture was taken after three days at 37 °C. Intriguingly, c-di-AMP-bound DarA does not inhibit growth anymore when cells are grown on solid medium (see Figure 3.5 C). However, presence of c-di-AMP-binding DarA leads to a red/brownish coloration of the colonies which is not the case for the *darA* deletion mutant and the strain expressing only the insensitive *darA<sub>F36E</sub>*. This indicates that c-di-AMP-bound DarA leads to accumulation of metabolite(s) which, however, only inhibits growth under liquid culturing conditions.

In theory, changing residues in a protein may render it unstable *in vivo* and lead to subsequent degradation. To exclude such an artifact, the results for DarA<sub>F36E</sub> were validated by verifying the integrity of the variant in a Western Blot with primary antibodies raised against DarA. Similar specificity of the antibody to both DarA variants was verified in a Western Blot with purified, His<sub>6</sub>-tagged proteins. Figure 3.5 B shows that both variants are equally stable and verifies the integrity of DarA<sub>F36E</sub>.

To conclude all of the above, DarA most likely interacts with a target in a c-di-AMP-bound state in MSSM medium with ammonium as the nitrogen source and low amounts of potassium. Furthermore, this interaction inhibits growth in liquid medium. It is not obvious which compound(s) accumulate(s) when DarA is present (see also Sections 3.4.4.3 and 3.4.4.4) and why this does not inhibit growth of the cells on the same solidified medium.

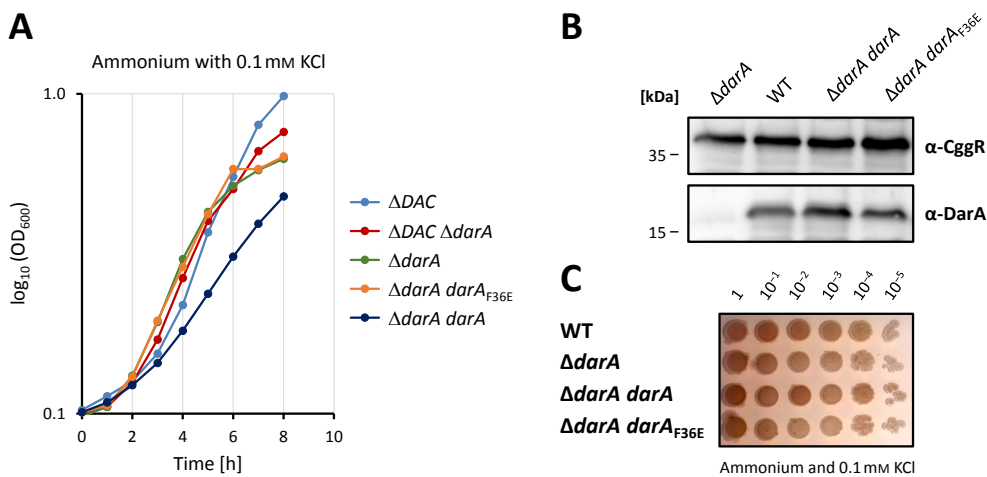


**Figure 3.5: The c-di-AMP-bound DarA inhibits growth in liquid minimal medium with ammonium as the nitrogen source and low amounts of potassium.** (A) Growth in indicated MSSM medium of a *B. subtilis* *DAC* deletion mutant (GP2222), isogenic *DAC darA* deletion mutant (GP2420) and of a *darA* deletion mutant expressing the native *darA* (GP2467) or the c-di-AMP-insensitive *darA<sub>F36E</sub>* (GP2468) from a neutral locus. Curves are means of independent biological triplicates ( $n = 3$ ). (B) Verification of expression and integrity of the DarA<sub>F36E</sub> variant. (C) Growth defect is lost on the same, solidified MSSM medium but the native DarA leads to a red/brownish coloration.

### 3.4.3 DarA is solely located in the cytosol

The classical P<sub>II</sub> proteins bind ATP/ADP and 2-oxoglutarate, thus integrating the energy, carbon and nitrogen status of the cell (Arcondéguy *et al.*, 2001). Especially P<sub>II</sub> proteins of the GlnK-type, like NrgB in *B. subtilis*, have been studied extensively. NrgB regulates the activity of the high affinity ammonium importer NrgA (AmtB). In response to a high external ammonium concentration, ammonium import is inhibited by binding of NrgB to NrgA (Detsch and Stülke, 2003). Crystal structures of the *E. coli* GlnK-AmtB complex showed that inhibition is achieved by protrusion of GlnK's T-loops into the core of the ammonium channel (Conroy *et al.*, 2007). Since DarA is a P<sub>II</sub>-like protein, although with different B- and T-loop lengths (Gundlach *et al.*, 2015a), an interaction with another type of transporter would be quite fitting. In response to the K<sup>+</sup> concentration and nitrogen source availability the c-di-AMP levels are adjusted which might recruit DarA to the membrane.

To investigate this hypothesis, the subcellular localization of DarA in response to c-di-AMP, nitrogen source and potassium concentration was determined. The *B. subtilis* wild type (168) was grown in MSSM medium with low (0.1 mM) or high (5 mM) amounts of KCl and ammonium (NH<sub>4</sub><sup>+</sup>) or glutamate (E) as the nitrogen source. To account for the c-di-AMP-free state of DarA, the *DAC* deletion mutant was cultivated alongside. However, the  $\Delta DAC$  strain was only grown in MSSM medium with 0.1 mM KCl and ammonium as the nitrogen source since higher potassium concentrations and/or glutamate are toxic for the strain (Gundlach, 2017; Gundlach *et al.*, 2017b). Cells were harvested at an OD<sub>600</sub> of 1.0 and disrupted with the French press method. Membrane proteins (ME) from the cell-free crude extracts (CE) were separated from cytosolic proteins (CY) by ultracentrifugation. Total protein amounts were determined with the Bradford method and 20  $\mu$ g of the fractions were used for SDS-PAGE. DarA was detected in the fractions by Western blotting with primary antibodies raised against DarA. Primary antibodies raised against the cytosolic CggR and the membrane-bound RNase Y protein served as separation controls. The localization of DarA is shown in Figure 3.6.

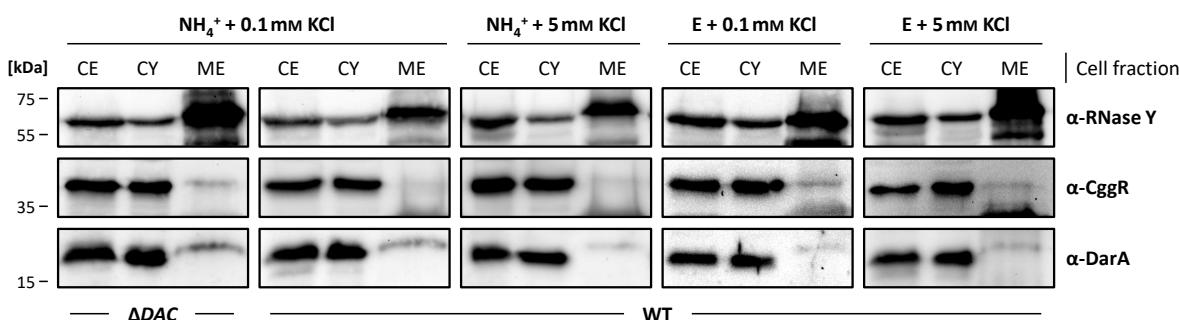


**Figure 3.6: DarA is localized in the cytosol irrespective of nitrogen source, potassium concentration and c-di-AMP presence.** The *B. subtilis* wild type (WT, 168) was grown in MSSM medium with ammonium (NH<sub>4</sub><sup>+</sup>) or glutamate (E) as the nitrogen source and low (0.1 mM) or high (5 mM) amounts of potassium. The c-di-AMP-free strain ( $\Delta DAC$ , GP2222) was only grown in MSSM medium with ammonium (NH<sub>4</sub><sup>+</sup>) and 0.1 mM KCl. Cells were harvested at an OD<sub>600</sub> of 1.0. 20  $\mu$ g of cell extract (CE), cytosolic fraction (CY) and membrane fraction (ME) were analyzed by Western blotting.

As shown in Figure 3.6, DarA was solely localized in the cytosol, irrespective of potassium concentration, nitrogen source and c-di-AMP presence. Furthermore, the results show that absence of c-di-AMP does apparently not alter *darA* expression. Consequently, DarA is most likely not acting on a membrane-bound protein or a transporter. The previously observed, inhibitory effect of c-di-AMP-bound DarA on growth in MSSM medium with ammonium and low amounts of potassium thus has to be caused by an interaction with a cytosolic partner.

In parallel to the above experiments, the novel high-affinity potassium importer KimA of *B. subtilis* was discovered. The expression of *kimA* is negatively regulated by c-di-AMP binding to the *kimA* riboswitch that is located upstream of the gene (Gundlach *et al.*, 2017b; Nelson *et al.*, 2013). However, regulation of the KimA protein by c-di-AMP had not been reported. The expression of *ktrAB*, the second high-affinity K<sup>+</sup> importer, is also negatively regulated by a *kimA* riboswitch. In addition, the activity of KtrAB is likely negatively regulated by direct binding of c-di-AMP to the RCK\_C domain of the KtrA protein (Albright *et al.*, 2006; Corrigan *et al.*, 2013; Gundlach *et al.*, 2017b). Intriguingly, KimA lacks obvious c-di-AMP-binding motifs like the RCK\_C domain. We reasoned that DarA could mediate a c-di-AMP-dependent regulation of the KimA transporter on a protein level which seemed to be missing. Expression of *kimA* only occurs at low potassium concentrations when glutamate is present and expression at high potassium concentrations might be unfavorable for the cells (Gundlach *et al.*, 2017b). Although DarA was not detected at the membrane before, artificial expression of *kimA* at high potassium concentrations might recruit DarA to the membrane to inhibit unnecessary, elevated K<sup>+</sup> import.

To address this hypothesis, the subcellular localization of DarA was investigated in a strain which constitutively expresses *kimA* (GP2403). The strain was constructed by replacing the promoter and riboswitch region upstream of *kimA* with a terminator-less *ermC* resistance cassette using LFH-PCR. The wild type (168) and the *kimA* overexpression strain were grown in MSSM medium with glutamate as the nitrogen source and low (0.1 mM) or high (5 mM) amounts of potassium until an OD<sub>600</sub> of 1.0. Fractions of membrane and cytosolic proteins were prepared and analyzed as described before. Again, DarA was not detected at the membrane in neither condition and results were similar to the ones shown in Figure 3.6. To validate the results, *kimA* overexpression was verified in another Western blot. For this purpose, *kimA* was additionally fused to a 3×FLAG-tag by transforming GP2403 or the 168 wild type with the integrative plasmid pGP2789 (yielding GP2404 and GP2405, respectively). The cells were cultivated again and crude extracts were prepared as described before. Constitutive overexpression was verified by detecting KimA-3×FLAG in a Western Blot using primary antibodies raised against the FLAG epitope. Primary antibodies raised against HPr served as a loading control. The successful overexpression was verified since KimA was detectable in the overexpression background at high amounts of potassium, but not in the wild type background (data not shown). The results indicate that DarA does not control KimA activity on a protein level. This is in agreement with recently reported binding of c-di-AMP to the

KimA protein which makes a regulation by DarA superfluous (Gundlach, 2017). In summary, all of the above strongly indicates that DarA's interaction partner is a cytosolic protein.

### 3.4.4 The cytosolic interaction partner of DarA

As described in the previous sections, c-di-AMP-bound DarA most likely interacts with a yet unknown cytosolic target which inhibits growth in MSSM medium with ammonium and low amounts of potassium. Two approaches to identify an interaction partner and the function of DarA came to mind. First, searching for interaction partners by using the SPINE protocol from Herzberg *et al.* (2007). Second, screening for arising suppressor mutants since *darA* expressing cells show a growth defect when compared to a *darA* deletion mutant.

#### 3.4.4.1 A search of DarA interaction partners by SPINE

Since DarA has to interact with a target in MSSM medium with ammonium and 0.1 mM KCl we tried to identify interaction partners with a SPINE *in vivo*. For this purpose, the *darA* deletion mutant (GP1712) was transformed with either a plasmid encoding an N-terminally Strep-tagged DarA (pGP2602) or the empty vector (pGP380). The functionality of N-terminally Strep-tagged DarA was verified by recording growth curves of both strains and the wild type (168) in MSSM medium with ammonium and 0.1 mM KCl. Strep-DarA complemented the *darA* deletion mutant and even resulted in slower growth compared to the wild type. For the SPINE, both strains were grown in MSSM medium with ammonium as the nitrogen source and 0.1 mM KCl. This was the condition where the presence c-di-AMP-bound DarA leads to slower growth. Cultures were split in half and were either harvested directly or first crosslinked with a final concentration of 0.6% paraformaldehyde. After disruption with the French press method, Strep-DarA (pGP2602) or only the Strep-tag (pGP380) were purified by affinity chromatography and fractions were analyzed by SDS-PAGE and silver staining. The silver stained lanes were very clean with almost no background compared to the empty vector control lanes. However, the results from the SPINE remained inconclusive. The interaction partner still escaped detection since no band above background (except DarA) could be identified. The same was true for a SPINE in the same medium, but with high (5 mM) amounts of potassium. Although DarA seems to interact with a target in a c-di-AMP-bound state in MSSM medium with ammonium and 0.1 mM KCl, this might not cover all of DarA's interactions. Thus, it was investigated whether expressing the c-di-AMP-insensitive DarA<sub>F36E</sub> in cells grown in rich medium might identify the interaction partner. After all, c-di-AMP-free DarA is not expected in rich medium with elevated c-di-AMP synthesis which might force an interaction to occur (Gundlach *et al.*, 2017b). For this purpose, a SPINE in LB medium was performed with the *darA* deletion mutant (GP1712) expressing either

N-terminally Strep-tagged, native *darA* or the c-di-AMP insensitive *darA*<sub>F36E</sub> from a plasmid (pGP2602 and pGP3008, respectively). At first, few potentially promising bands were detected in the elution fractions on the silver stained gel. However, GC/MS analysis of the whole lanes could not identify interacting proteins with high confidence. It might be that the interaction of DarA with its target is only weak/transient or that the protein complex hinders binding of Strep-DarA to the matrix, which either way leads to the interaction partner being washed away from the purification column. Taken together, all of the pursued SPINE approaches did not identify the interaction partner of DarA.

#### 3.4.4.2 Suppressor evolution to elucidate the function of DarA

Since several different SPINEs were not conclusive, we tried to elucidate the function of DarA by generating suppressor mutants under the condition where DarA inhibits growth of the cells. This was done by evolving and sequencing suppressor mutants of *darA* expressing strains grown in MSSM medium with ammonium as the nitrogen source and 0.1 mM KCl. To prevent isolation of mutations in *darA*, and to simultaneously increase the pressure on the cells, we first introduced a second *darA* copy into the genome of the wild type (168). The second copy of *darA* was introduced into the neutral *ganA* locus by transformation with the ScaI linearized pGP2790. For the evolution of suppressor mutants, the resulting *darA*<sup>+</sup> strain (GP2425) was grown overnight in MSSM medium with ammonium as the nitrogen source and 0.1 mM KCl. Fresh medium was reinoculated with 1/10 of the overnight culture the next day. This was repeated over ten passages and samples were plated on the same solidified medium. Suppressor mutants were distinguishable after around three days at 37°C and were isolated. The wild type (168) and the *darA* deletion mutant (GP1712) were carried along as controls. As an additional approach, the mentioned strains were solely grown on plates. First, overnight at 37°C, then at room temperature on MSSM medium agar plates with ammonium as the nitrogen source and 0.05, 0.075 or 0.1 mM KCl. Suppressor mutants were isolated after two weeks at room temperature. The acquired suppressor mutations were identified by whole genome sequencing (WGS +/-) and/or Sanger sequencing and are summarized in Table 3.1.

The evolution of the wild type,  $\Delta darA$  and *darA*<sup>+</sup> strain in liquid MSSM medium with ammonium as the nitrogen source and 0.1 mM KCl only promoted mutations in *ktrB* (see Table 3.1) which codes for the integral membrane unit of the high affinity potassium importer KtrAB (Holtmann *et al.*, 2003). This is not surprising, since all strains were cultivated in minimal medium with only very low amounts of potassium. Consequently, increasing the activity of a high affinity potassium importer would result in faster growth. This was indeed the case as documented by recorded growth curves in the same medium (data not shown). However, no other suppressor mutations were identified and similar mutations arose in the *darA* deletion strain. Hence, the mutations in *ktrB* are not a specific result of the DarA

phenotype in this medium. Apparently, the pressure to increase potassium import masks the function of DarA which is inhibitory for growth under this condition.

**Table 3.1: Suppressors isolated from solid or liquid MSSM medium with ammonium as the nitrogen source and low amounts of KCl.**

Strain	Background	Suppressor mutations	Isolation remarks	WGS
GP2449	<i>darA</i> <sup>+</sup>	<i>gltC</i> <sub>G230A</sub>	Solid, 0.1 mM KCl	+
GP2452	<i>darA</i> <sup>+</sup>	<i>odhA</i> <sub><math>\Delta</math><i>bp373</i></sub>	Solid, 0.1 mM KCl	+
GP2451	<i>darA</i> <sup>+</sup>	<i>odhA</i> <sub>Q523STOP</sub>	Solid, 0.1 mM KCl	-
GP2447	<i>darA</i> <sup>+</sup>	<i>odhA</i> <sub>N320H</sub>	Solid, 0.075 mM KCl	-
GP2448	<i>darA</i> <sup>+</sup>	<i>odhA</i> <sub>K64STOP</sub>	Solid, 0.075 mM KCl	-
GP2446	<i>darA</i> <sup>+</sup>	<i>ktrA</i> <sub>p(TAAATT→TAAACT)</sub>	Solid, 0.05 mM KCl	+
GP2450	<i>darA</i> <sup>+</sup>	<i>ktrA</i> <sub>p(TAAATT→TAAACT)</sub>	Solid, 0.1 mM KCl	-
GP2455	<i>darA</i> <sup>+</sup>	<i>ktrB</i> <sub>N184S</sub> <i>atpB</i> <sub>G93W</sub>	Liquid, 0.1 mM KCl	+
GP2454	<i>darA</i> <sup>+</sup>	<i>ktrB</i> <sub>G23V,N184S</sub>	Liquid, 0.1 mM KCl	-
GP2456	<i>darA</i> <sup>+</sup>	<i>ktrB</i> <sub>G23V,N184S</sub>	Liquid, 0.1 mM KCl	-
GP2457	WT	<i>ktrB</i> <sub>G23V,T394S</sub>	Liquid, 0.1 mM KCl	-
GP2458	WT	<i>ktrB</i> <sub>G23V</sub>	Liquid, 0.1 mM KCl	-
GP2459	WT	<i>ktrB</i> <sub>E116A</sub>	Liquid, 0.1 mM KCl	-
GP2466	WT	<i>ktrB</i> <sub>G23V,A64V,Q85H</sub>	Liquid, 0.1 mM KCl	-
GP2462	$\Delta$ <i>darA</i>	<i>ktrB</i> <sub>E116A,N184S,L299STOP</sub>	Liquid, 0.1 mM KCl	-
GP2463	$\Delta$ <i>darA</i>	<i>ktrB</i> <sub>L212Q</sub>	Liquid, 0.1 mM KCl	-
GP2464	$\Delta$ <i>darA</i>	<i>ktrB</i> <sub>64V,R331K</sub>	Liquid, 0.1 mM KCl	-
GP2465	$\Delta$ <i>darA</i>	<i>ktrB</i> <sub>G23V,V381G</sub>	Liquid, 0.1 mM KCl	-

Only the *darA*<sup>+</sup> strain acquired mutations on MSSM medium agar with ammonium as the nitrogen source and low amounts of KCl, which all lead to faster growth compared to the parental strain. In contrast, no suppressor mutants appeared for the wild type (168) and the *darA* deletion mutant (GP1712) under the same condition. Two independent suppressors harbored a point mutation in the promoter region of *ktrA* (*TAAATT*→*TAAACT*). This particular mutation has already been isolated in a different context and was demonstrated to increase expression of *ktrAB* (Gundlach *et al.*, 2017a). This is not surprising, since potassium amounts were quite low and mutations in *ktrB* which increase potassium import were also identified in suppressor mutants isolated from liquid medium. Although the *ktrA* mutation was only identified in the *darA*<sup>+</sup> strain, potassium homeostasis might only be indirectly affected by DarA since mutations in the other subunit *ktrB* were identified independently of DarA after evolution in liquid medium. One identified mutation was located in *gltC* (G230A) coding for the transcriptional activator of the glutamate synthase gene *gltAB* (Bohannon and Sonenshein, 1989). This proved to be a gain of function mutation as shown by  $\beta$ -galactosidase activity assays with *gltAB-lacZ* promoter fusions (Krammer, 2017). Consequently, *GltC*<sub>G230A</sub> leads to

elevated GltAB amounts, thus most likely elevated glutamate levels. However, neither direct interaction of DarA with GltC nor indirect influence of DarA on *gltAB* expression could be shown (Krammer, 2017). Four mutations were found in *odhA*, with three of them most likely being loss-of-function mutations since the final protein would be truncated (K64STOP and Q523STOP and  $\Delta bp373$ ). It is thus likely that the fourth mutation (N320H) also impairs the functionality of OdhA. *odhA* codes for the E1 subunit of the 2-oxoglutarate dehydrogenase complex which acts in the central carbon metabolism and catalyzes the decarboxylation of 2-oxoglutarate to succinyl coenzyme A (Carlsson and Hederstedt, 1989). Impairment of OdhA activity would abolish or at least slow the metabolic flux from 2-oxoglutarate to succinyl coenzyme A, thus increasing the available 2-oxoglutarate pool in the cells. The accumulating 2-oxoglutarate could potentially be used by the glutamate synthase GltAB and thus enhance glutamate production, just like the mutation found in *gltC*.

In summary, the evolution experiments in/on MSSM medium with ammonium as the nitrogen source and low amounts of potassium lead to identification of mutations affecting potassium import, which are likely not directly related to DarA, or *darA*<sup>+</sup> specific mutations which increase the glutamate pool. It is tempting to speculate that c-di-AMP-bound DarA inhibits the accumulation of glutamate or related amino acids when cells are grown in/on MSSM medium with ammonium and low amounts of potassium, and this has to be compensated for.

#### 3.4.4.3 Metabolite pools in a *darA* mutant

The growth experiments and suppressor mutants revealed that increasing the potassium or glutamate levels counteract a growth inhibitory function of DarA when cells are grown in MSSM medium with ammonium as the nitrogen source and low amounts of potassium. However, only the mutations that affect glutamate accumulation seemed to be DarA specific. Glutamate can be incorporated into proteins or used for the synthesis of other amino acids like proline, which functions as an osmoprotectant, or arginine (Gunka and Commichau, 2012; Hoffmann and Bremer, 2017; Whatmore *et al.*, 1990). Surprisingly, positively charged amino acids of the glutamate family like arginine, ornithine and citrulline can rescue growth of *B. subtilis* cells experiencing extreme K<sup>+</sup> limitation (Gundlach *et al.*, 2017a). This is of particular interest since a P<sub>II</sub> protein regulates arginine biosynthesis by interaction with the *N*-acetyl-L-glutamate kinase (NAGK) in the unicellular cyanobacterium *Synechococcus elongatus* (Maheswaran *et al.*, 2004).

The potential impact of DarA on glutamate and/or arginine metabolism was investigated by determination of glutamate, arginine and related metabolite amounts from cells grown in the minimal medium where absence of DarA is beneficial for growth. The *B. subtilis* wild type (168) and the *darA* deletion mutant (GP1712) were grown in MSSM medium with ammonium as the nitrogen source and low (0.1 mM) amounts of potassium to an OD<sub>600</sub> of



0.5. Intracellular metabolites were extracted, determined by liquid chromatography–mass spectrometry (LC/MS) and normalized to the  $OD_{600}$ . As shown in Figure 3.7, deletion of *darA* had no, or only minor impact on the intracellular concentration of amino acids from the glutamate family. The concentration of glutamate was only slightly affected with 230 and 182 mM for the WT and  $\Delta darA$  strain, respectively. This is in agreement with another study where no difference was detected under the same condition (Richts, 2018). Only the amount of citrulline was notably lower in the *darA* deletion mutant compared to the wild type (16.2 and 33.1 mM for  $\Delta darA$  and WT, respectively). However, the significance is questionable because the amounts of ornithine, which is the direct precursor of citrulline, and arginine, which originates from citrulline, were not affected. Glutamine and proline amounts were also not altered in the *darA* deletion mutant. This was also the case for the central metabolites citrate and acetyl coenzyme A (acetyl-CoA) which were determined alongside. Both are synthesized in the TCA cycle which is linked to glutamate metabolism, and acetyl-CoA is directly fed into the arginine biosynthesis (Cunin *et al.*, 1986; Gunka and Commichau, 2012).

In summary, the function of DarA, which inhibits growth in MSSM medium with ammonium as the nitrogen source and low amounts of potassium, could not be linked to altered, intracellular levels of glutamate or derived amino acids, which was also true for citrate and acetyl-CoA. This means that either DarA does not affect the metabolism of these metabolites or that the levels are tightly maintained and metabolic fluxes are adjusted independently of DarA.

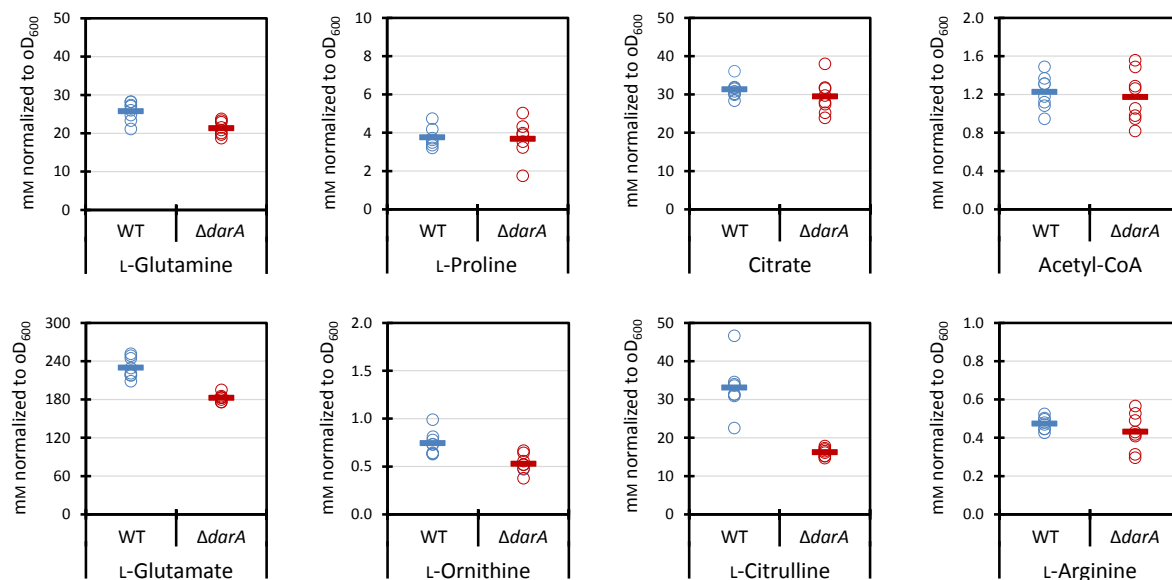


**Figure 3.7: Deletion of *darA* has only minor impact on glutamate and arginine metabolism.** The *B. subtilis* wild type (168) and the *darA* deletion mutant (GP1712) were grown in MSSM medium with ammonium and low (0.1 mM) amounts of potassium. Cells were harvested at an  $OD_{600}$  of 0.5. The amounts of extracted, intracellular metabolites were determined by LC/MS in the laboratory of Dr. Hannes Link (Marburg) and were normalized to the  $OD_{600}$ . Data points represent independent biological replicates, bars indicate the calculated means ( $n = 8$ ).

#### 3.4.4.4 Potassium and c-di-AMP amounts in a *darA* mutant

The cytosolic localization of DarA under several conditions strongly suggested that DarA does not regulate a (potassium) transporter by direct binding. Nevertheless, supplementation with higher amounts of KCl counteracted the inhibitory effect of DarA on growth in MSSM medium with ammonium as the nitrogen source and low amounts of potassium. It might be that DarA integrates the c-di-AMP signal to affect potassium homeostasis in another way under this condition, which had escaped detection before. Since c-di-AMP levels correspond to the potassium concentration to adjust import of  $K^+$  accordingly we also wondered whether DarA affects the levels of c-di-AMP (Gundlach, 2017; Gundlach *et al.*, 2017b). It should be noted that direct modulation of the cellular c-di-AMP homeostasis is not common for c-di-AMP targets. However, the c-di-AMP-binding TrkH family protein CabP was recently described to alter c-di-AMP levels in *Streptococcus pneumoniae* in a  $K^+$  independent manner (Zarrella *et al.*, 2018).

To investigate the above hypotheses, the intracellular amounts of  $K^+$  and c-di-AMP were determined from cells grown in the minimal medium where absence of DarA is beneficial for growth. For these purposes, the *B. subtilis* wild type (168) and the *darA* deletion mutant (GP1712) were grown as described for the metabolite determination in MSSM medium with ammonium and 0.1 mM KCl. The intracellular  $K^+$  amounts were determined by inductively coupled plasma optical emission spectrometry (ICP-OES) and normalized to the culture volume and  $OD_{600}$ . c-di-AMP was extracted from aliquots of the same cultures, quantified using high performance liquid chromatography-coupled tandem mass spectrometry (HPLC-MS/MS) and normalized to the total protein amount determined with the Bradford method. As shown in Figure 3.8, deletion of *darA* had no impact on the intracellular amounts of  $K^+$  or c-di-AMP.

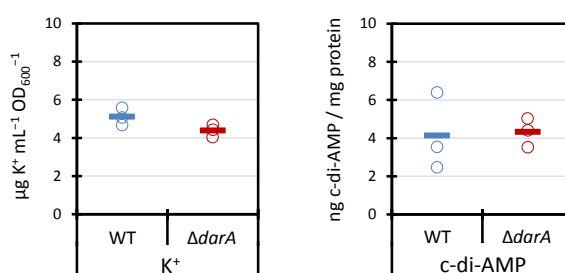


**Figure 3.8: Deletion of *darA* has no impact on c-di-AMP and potassium homeostasis.** The *B. subtilis* wild type (WT, 168) and the *darA* deletion mutant (GP1712) were grown in MSSM medium with ammonium and low (0.1 mM) amounts of potassium. Cells were harvested at an  $OD_{600}$  of 0.5. The intracellular amounts of potassium were determined by ICP-OES in the laboratory of Dr. Dietrich Hertel (Göttingen) and were normalized to the culture volume and  $OD_{600}$ . The amounts of extracted, intracellular c-di-AMP were determined by HPLC-MS/MS in the laboratory of Prof. Dr. Volkhardt Kaever (Hannover) and were normalized to the total cellular protein amount. Data points represent independent biological replicates, bars indicate the calculated means ( $n = 3$ ).

Apparently, DarA does not integrate the c-di-AMP signal to affect K<sup>+</sup> homeostasis, at least not under the condition where DarA inhibits growth (MSSM medium with ammonium and 0.1 mM KCl). Furthermore, DarA does not affect c-di-AMP homeostasis under the same condition. The results show that the inhibitory effect of DarA on growth in MSSM medium with ammonium and 0.1 mM KCl is not caused by a modulation of potassium or c-di-AMP homeostasis by DarA. In summary, several studies did not elucidate the reason for this phenotype. The most likely cytosolic interaction partner of (most likely c-di-AMP-bound) DarA still escaped detection despite pursuing a multitude of different approaches.

### 3.5 Rational bioinformatic search of interaction partners

The c-di-AMP-bound DarA most likely interacts with a cytosolic target in MSSM medium with ammonium and low amounts of potassium, which inhibits growth in liquid medium. Despite this specific phenotype and numerous experiments, the interaction partner still escaped detection. We reasoned that a rational bioinformatic search could provide an unbiased overview of proteins that are in theory suitable for an interaction with DarA.

For this purpose, we analyzed the proteome of *B. subtilis* to identify putative targets. Several rational requirements were set and proteins not matching them were discarded. First, a putative interaction partner is most likely conserved among c-di-AMP-producing firmicutes also expressing *darA* or homologues. Consequently, the *Bacillus subtilis* 168 proteome was compared with the proteome of the related, well studied firmicutes *Listeria monocytogenes* EGD-e and *Staphylococcus aureus subspecies aureus* NCTC 8325. Second, regulation by binding of DarA only makes sense if the interaction partner is less abundant than DarA. Third, DarA is a trimeric, P<sub>II</sub>-like protein. As a consequence, only proteins which structurally resemble known P<sub>II</sub> targets are highly suggestive of an interaction. These are foremost trimeric, hexameric or dodecameric. Fourth, our results strongly indicate that DarA is solely located in the cytosol and so should be the interaction partner. A list of the rational interaction partners can be found in the Appendix (see Table 6.1). It should be noted that 509 proteins were excluded since protein quantification data were missing, but a separate list was kept (see Appendix: Table 6.2). Missing protein quantification data might be attributed to membrane proteins, proteins that are not expressed, only expressed under very specific conditions or the protein amount of these is extremely low in general. In either case, suitability as an interaction partner of DarA is arguably questionable. We identified 160 proteins that were conserved, less abundant compared to DarA, and cytosolic or with unknown location. Structural data were not available for all of them but promising candidates were identified. Only eleven proteins matched all criteria (see Table 3.2).

Interestingly, again enzymes and proteins related to glutamate/arginine metabolism were found. Most notable hits were the dodecameric glutamate synthase GltAB and the hexameric *N*-acetyl-L-glutamate kinase (NAGK) ArgB. As mentioned before, the NAGK is regulated by

a P<sub>II</sub> protein in the cyanobacterium *S. elongatus* and catalyzes the second, rate limiting step in arginine biosynthesis (Burillo *et al.*, 2004; Maheswaran *et al.*, 2004). Furthermore, molecular docking of DarA to GltAB suggested that this enzyme is a promising interaction partner of DarA since both protein structures fit together perfectly (Richts, 2018). The other hits were not as suggestive of an interaction. The glutamate dehydrogenase GudB is not a suitable target since the enzyme is not functional in the laboratory strain 168 (Belitsky and Sonenshein, 1998). It should be noted that *B. subtilis* encodes a second glutamate dehydrogenase, RocG, but quantification data were missing for this protein. HprK, MecA, Rho and YojN fulfilled our rational criteria. However, analysis of their tertiary structure and symmetry suggested that an interaction with DarA is not very likely. The structures of YhfE, YtaG and YtoP might be suitable for an interaction with DarA, however, all three proteins are only poorly characterized and we have no additional experimental indications (as in the case for GltAB or ArgB) that suggest an interaction. Taken together, ArgB and GltAB were identified as promising interaction partners of DarA. However, it remained elusive why neither of the two was identified in prior experiments, despite linking DarA to glutamate metabolism.

**Table 3.2: Proteins that fulfilled our criteria for an interaction with DarA.**

Name	Description	Localization	Structure <sup>a</sup>
ArgB	<i>N</i> -Acetylglutamate 5-phosphotransferase	Cytoplasm	6-hom
GltA	Glutamate synthase (large subunit)	Cytoplasm	12-het
GltB	Glutamate synthase (small subunit)	Cytoplasm	12-het
GudB	Glutamate dehydrogenase, trigger enzyme	–	6-hom
HprK	PtsH-HPr kinase/ phosphorylase	–	6-hom
MecA	Adaptor protein	–	6-hom
Rho	Transcriptional termination protein	–	6-hom
YhfE	Similar to glucanase	–	12-hom
YojN	Similar to nitric-oxide reductase	–	6-hom
YtaG	Dephospho-CoA kinase	–	3-hom
YtoP	Similar to glutamyl aminopeptidase	–	12-hom

<sup>a</sup> hom: homomer, het: heteromer.

## 3.6 DarA and extreme potassium limitation

The hints from Section 3.5 raised the question why extensive research and a multitude of experiments could not identify ArgB or GltAB as an interaction partner of DarA. Perhaps, the conditions applied on the cells were not harsh enough for a putative interaction of DarA with the NAGK ArgB or the glutamate synthase GltAB to be particularly important. As mentioned before, Gundlach *et al.* (2017a) documented the role of positively charged amino acids of the arginine family during extreme potassium limitation. *B. subtilis* cells devoid of the high affinity potassium importers KtrAB and KimA are not able to grow with ammonium as the nitrogen source and low amounts of potassium. This can be compensated for by acquiring suppressor mutations that derepress arginine biosynthesis, starting from glutamate and acetyl-CoA. Accordingly, a *ktrAB kimA* deletion mutant also devoid of AhrC, the negative regulator of the arginine biosynthesis operons, is able to grow again (Gundlach *et al.*, 2017a).

### 3.6.1 DarA is needed during extreme potassium limitation

As mentioned, *B. subtilis* cells experiencing extreme K<sup>+</sup> limitation compensate the lack of the cation by accumulation of positively charged amino acids of the arginine family to stay viable (Gundlach *et al.*, 2017a). If arginine biosynthesis is so important at extreme potassium limitation, and DarA is involved in any step connected to glutamate or arginine production, this is an excellent condition to look for a phenotype of an isogenic *darA* deletion mutant. If DarA would interact with GltAB or ArgB (see Section 3.5) the deletion of *darA* might affect the growth of these cells negatively or positively, depending on whether the interaction is inhibitory or stimulating.

To investigate this hypothesis, we analyzed the growth of the *darA* deletion mutant in a *ktrAB kimA ahrC* deletion background. For this purpose, the *B. subtilis* wild type (WT, 168), a  $\Delta ktrAB \Delta kimA$  strain ( $\Delta K$ , GP2165) and isogenic deletion mutants for *ahrC* ( $\Delta K \Delta ahrC$ , GP2185), *darA* ( $\Delta K \Delta darA$ , GP2461) or both ( $\Delta K \Delta ahrC \Delta darA$ , GP2495) were grown overnight in MSSM medium with ammonium as the nitrogen source and 5 mM KCl. Cells were washed extensively to get rid of excess potassium and samples of a serial dilution were spotted on MSSM medium agar plates with low (0.5 mM) or high (5 mM) amounts of potassium and either ammonium, L-glutamate, L-glutamine, L-arginine or L-proline as the sole nitrogen source. Figure 3.9 shows the results of a representative drop dilution experiment after 48 h at 37 °C. The *ahrC* deletion restored growth of the *ktrAB kimA* deletion mutant as expected ( $\Delta K \Delta ahrC$ ). Growth of the *ktrAB kimA* deletion mutant was also rescued by increasing the potassium concentration or supplying the cells with glutamate, glutamine, arginine or proline. Although, glutamine supplementation was not as beneficial as the other nitrogen sources. Surprisingly, compensation of extreme potassium limitation by derepression of the arginine biosynthesis was barely possible in an isogenic *darA* mutant ( $\Delta K \Delta ahrC \Delta darA$ )

when cells were grown with ammonium and low amounts of potassium. Complementation of the  $\Delta K \Delta ahrC \Delta darA$  strain by introducing *darA* or *Strep-darA* into a neutral locus was shown by Fülleborn (2018). Growth of the  $\Delta K \Delta ahrC \Delta darA$  strain was restored by increasing the potassium concentration, which was expected. These results already suggest that DarA likely acts on a step within the arginine biosynthesis or at a metabolic step that feeds into it. In addition, changing the nitrogen source to glutamate, glutamine, arginine or proline also rescued growth of the  $\Delta K \Delta ahrC \Delta darA$  strain when grown with low amounts of potassium. This indicates that DarA has to act upstream of the arginine biosynthesis, since supplementation with glutamate or glutamine is already sufficient to restore growth of the strain. Consequently, the glutamate synthase GltAB might be a suitable target of DarA, which is not the case for the NAGK ArgB.

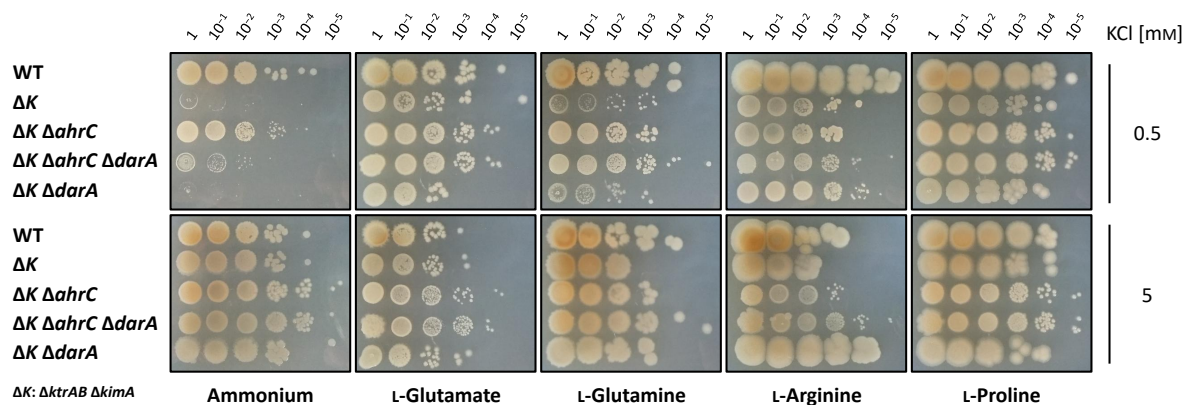


**Figure 3.9: DarA is needed to cope with extreme potassium limitation when cells are grown with ammonium as the nitrogen source.** Growth of *B. subtilis* wild type (WT, 168), a strain devoid of the high-affinity potassium importers KtrAB and KimA ( $\Delta K$ , GP2165), isogenic deletion mutants for *ahrC* ( $\Delta K \Delta ahrC$ , GP2185), *darA* ( $\Delta K \Delta darA$ , GP2461) or both ( $\Delta K \Delta ahrC \Delta darA$ , GP2495) on MSSM medium agar plates with indicated nitrogen source and KCl concentration after 48 h at 37 °C. Numbers on top indicate the spotted dilution of an  $OD_{600}$  of 1.0.

To extend the above indications, which exclude ArgB as an interaction partner of DarA, we performed a modified BACTH assay with DarA and ArgB. In addition we also checked whether the arginase RocF interacts with DarA in a BACTH assay. RocF is structurally suitable for an interaction with DarA and catalyzes the first step of arginine catabolism (Gardan *et al.*, 1995). However, it should be noted that RocF is only conserved between *B. subtilis* and *S. aureus*, but not present in *L. monocytogenes* and thus is not a rational interaction partner (see Section 3.5). The modified BACTH assay was performed as described before. DarA did not interact with ArgB or RocF, irrespective of c-di-AMP presence (see Figure 3.10). SPINEs conducted with Strep-tagged ArgB (pGP3010) (cells grown in MSSM medium with ammonium and 0.1 or 5 mM KCl) suggested the same, as did further *in vitro* experiments with purified ArgB by Richts (2018). All this is in agreement with the drop dilution experiments which strongly suggested that DarA interacts with a target upstream of the arginine biosynthesis. Taken together, DarA most likely enhances a metabolic flux towards

the arginine biosynthesis. It is tempting to speculate that DarA binds to the glutamate synthase GltAB (see Section 3.5) thus enhancing the synthesis of glutamate which is directly fed into the arginine biosynthesis pathway.

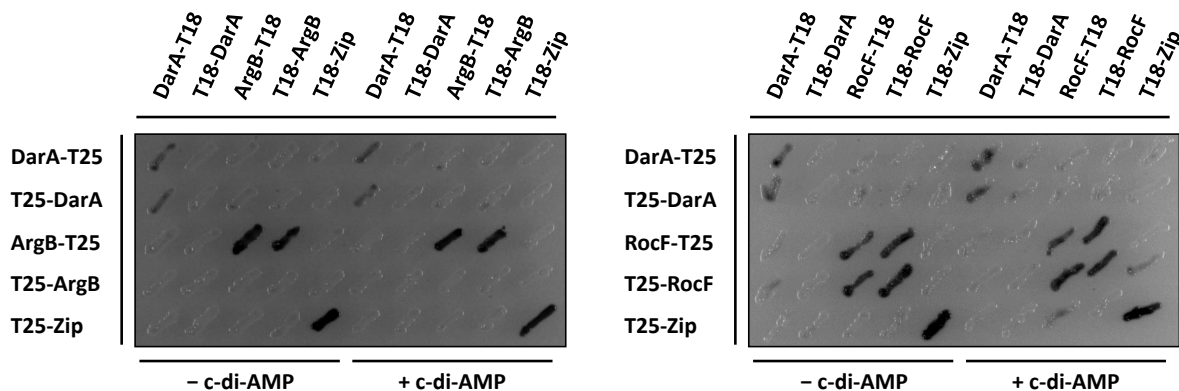


**Figure 3.10: DarA does not interact with ArgB or RocF in a modified BACTH assay.** A modified bacterial two-hybrid assay in *E. coli* in the presence or absence of c-di-AMP. Dark colonies indicate an interaction. ArgB, RocF and DarA show only self-interactions. Leucine zipper constructs (Zip) were used as a control.

### 3.6.2 Suppressor mutations that compensate the *darA* deletion

The *B. subtilis ktrAB kimA ahrC darA* deletion mutant was not able to grow on MSSM medium with ammonium as the nitrogen source and low (0.5 mM) amounts of potassium since  $K^+$  is extremely limited and this cannot be compensated for anymore by derepression of the arginine biosynthesis.

To investigate the function of DarA in this context we generated suppressor mutants of the  $\Delta ktrAB \Delta kimA \Delta ahrC \Delta darA$  strain by plating the washed cells on the aforementioned medium. Suppressors arising after around one week were isolated, their growth was analyzed in a serial drop dilution experiment as described before, and the acquired mutations were identified by whole genome sequencing (WGS +/-) and/or Sanger sequencing. Three independently isolated suppressors were able to grow again on MSSM medium with ammonium and low (0.5 mM) amounts of potassium (see Figure 3.11). However, suppressor 2 grew only slightly better, compared to the parental strain. Whole genome sequencing of suppressor 1 revealed a single point mutation in *gltC* leading to the amino acid exchange L201H. Interestingly, the exact same mutation was also found in the independently generated suppressor 3. GltC is the transcriptional activator of the *gltAB* operon and the mutation likely increases the transcription of *gltAB* to enhance the production of glutamate.

To verify this hypothesis, we compared the influence of GltC and GltC<sub>L201H</sub> on the expression of *gltAB* in a  $\beta$ -galactosidase activity assay. For this purpose, the genomic region of *gltC*<sub>L201H</sub> including the *gltAB* promoter was first cloned into pAC5 to generate a *gltAB-lacZ* promoter fusion with *gltC*<sub>L201H</sub> encoded in the reverse direction on the same plasmid. The

PstI linearized plasmid (pGP3030) was integrated into the *amyE* locus of a *B. subtilis* *gltC* transposon mutant (*gltC*<sup>-</sup> *gltC*<sub>L201H</sub>, GP3015). A strain constructed in the same way but with the wild type *gltC* was used as a reference (*gltC*<sup>-</sup> *gltC*, GP651). A strain where only the *gltAB-lacZ* promoter fusion was integrated served as an additional control (WT, GP669). Before the assay, the strains were grown in MSSM medium with ammonium as the nitrogen source and 0.5 mM KCl until an OD<sub>600</sub> of 0.6 as described. Cells were disrupted with LD-mix and the cell lysates cleared by ultracentrifugation. The cell-free crude extracts were used for a β-galactosidase activity assay and the activity of the *gltAB* promoter was determined. Indeed, *GltC*<sub>L201H</sub> is a hyperactive variant and *gltAB* expression was increased by more than 4-fold (see Figure 3.11 B). This indicates that the deletion of *darA*, which inhibits growth in a  $\Delta ktrAB \Delta kimA \Delta ahrC$  strain background on MSSM medium with ammonium and 0.5 mM KCl, might limit the accumulation of glutamate.

Suppressor 2 carried a mutation in *odhB* (W21C), coding for the E2 subunit of the 2-oxoglutarate dehydrogenase complex (ODH) (Carlsson and Hederstedt, 1989), and in the putative Shine Dalgarno sequence of *argG* (*GAGAGGGGA*→*GAGAGGGAA*). The *argGH* operon codes for the argininosuccinate synthase and lyase, enzymes required for the last steps of the arginine biosynthesis (Cunin *et al.*, 1986). The two mutations might arguably increase the available 2-oxoglutarate for glutamate synthesis (*odhB*<sub>W21C</sub>) and improve arginine biosynthesis (*argG*<sub>SD</sub>(*GAGAGGGGA*→*GAGAGGGAA*)). However, this was not further investigated since *GltC*<sub>L201H</sub> was more efficient in restoring growth, indicating that elevated glutamate synthesis is crucial for the  $\Delta K \Delta ahrC \Delta darA$  strain.

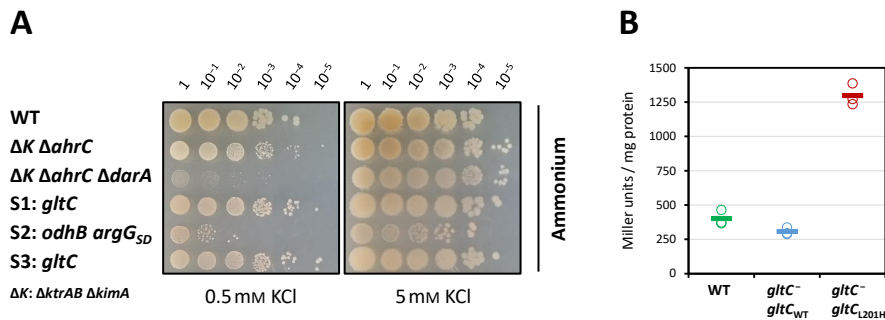


**Figure 3.11: Suppressor mutations that allow for growth of the *ktrAB kimA ahrC darA* mutant at extreme potassium limitation with ammonium as the nitrogen source. (A)** Growth of *B. subtilis* wild type (WT, 168), a strain devoid of the high-affinity potassium importers KtrAB and KimA and the transcription factor AhrC ( $\Delta K \Delta ahrC$ , GP2187), an isogenic *darA* deletion mutant ( $\Delta K \Delta ahrC \Delta darA$ , GP2495) and independently isolated suppressor mutants (S1–3) of the latter on MSSM medium agar with ammonium as the nitrogen source and indicated KCl concentration after 48 h at 37 °C. Numbers on top indicate the spotted dilution of an OD<sub>600</sub> of 1.0. A point mutation in *gltC* (L201H) restores growth for suppressor 1 and 3. Mutations in *odhB* (W21C) and in the putative Shine Dalgarno sequence of *argG* (*GAGAGGGGA*→*GAGAGGGAA*) restore growth partially for suppressor 2. **(B)** *GltC*<sub>L201H</sub> is hyperactive. Expression of *gltAB* is enhanced by more than 4-fold in a β-galactosidase activity assay. Data points represent independent biological replicates, bars indicate the calculated means ( $n = 3$ ).



To get further insights into the function of DarA during extreme potassium limitation, more suppressor mutants of the  $\Delta K \Delta ahrC \Delta darA$  strain were sequenced. These were generated independently as described before during another study and were able to grow on MSSM medium with ammonium and low amounts of KCl in contrast to the parental strain (Fülleborn, 2018). A summary of all identified mutations so far is shown below (see Table 3.3). Most of them seem to either increase glutamate or arginine synthesis. The effect of mutations in *bmr*, encoding a multidrug efflux transporter (Saier *et al.*, 2016), could not be deduced with high confidence. Taken together, our results indicate that DarA is needed for the accumulation of glutamate which is needed for the synthesis of arginine in cells experiencing extreme potassium limitation. It is tempting to speculate that the interaction partner of DarA is the glutamate synthase GltAB.

**Table 3.3: Suppressors of a *ktrAB kimA ahrC darA* mutant on MSSM medium with ammonium as the nitrogen source and low amounts of potassium.**

Strain	Mutations	Target/Effect	Compensation	WGS
GP3016	<i>gltC</i> <sub>L201H</sub> <sup>b</sup>	Hyperactive GltC, + <i>gltAB</i> expression	+ Glutamate <sup>a</sup>	+
GP3017	<i>odhB</i> <sub>W21C</sub> <i>argG</i> <sub>SD(GAGAGGGGA → GAGAGGGAA)</sub>	– OdhB/ODH activity <sup>a</sup> + <i>argGH</i> expression <sup>a</sup>	+ Glutamate <sup>a</sup> + Arginine <sup>a</sup>	+
GP3023	<i>argG</i> <sub>H116Y</sub> <i>cotE</i> <sub>5'UTR S610: bpC12A</sub>	+ ArgG activity <sup>a</sup> Spore coat protein <sup>a</sup>	+ Arginine <sup>a</sup> Not related <sup>a</sup>	+
GP3021	<i>bmr</i> <sub>bp578+T</sub>	– Multidrug efflux <sup>a</sup>	Unknown	+
GP3022	<i>bmr</i> <sub>G105S</sub>	– Multidrug efflux <sup>a</sup>	Unknown	–
5 more	Unknown	Unknown	Unknown	–

<sup>a</sup> Effect is deduced from the context. No experimental data.

<sup>b</sup> Identified in two independently evolved suppressors.

### 3.7 Interaction studies of DarA and the glutamate synthase

Previous growth analyses of a *B. subtilis ktrAB kimA ahrC darA* mutant strongly suggested that DarA has to act upstream of the arginine biosynthesis pathway, for example on the synthesis of glutamate. A rational bioinformatic approach already suggested the glutamate synthase GltAB as a fitting interaction partner. The hypothesis was supported by molecular docking of the DarA trimer to the dodecameric GltAB holoenzyme (Richts, 2018). The prior study tried to prove an interaction of DarA with GltAB in a glutamine oxoglutarate aminotransferase (GOGAT) activity assay with cell-free crude extracts from a *B. subtilis* wild type or a *darA* deletion mutant (Richts, 2018). This was not conclusive, however, the cell extracts were not from a *ktrAB kimA ahrC* deletion strain grown in MSSM medium with ammonium and low amounts of potassium, the condition where DarA is crucial for cell growth. Since growth of an isogenic *darA* deletion mutant under this condition is barely possible, we

decided to perform different *in vitro* experiments with purified GltAB and DarA to investigate a potential interaction.

To investigate if DarA interacts with GltAB, and likely promotes glutamate synthesis (see Section 3.6), we investigated whether DarA affects the enzymatic activity of GltAB *in vitro*. This was done using a GOGAT activity assay with purified proteins. For this purpose, GltAB and DarA had to be purified. *gltB* was C-terminally fused to a His<sub>6</sub>-tag, connected by a GGSG-linker, and cloned into pGP574 yielding pGP3031. *gltA*, together with a Shine Dalgarno sequence (of T7 gene 10 from pGP574), was cloned into pBAD33 yielding pGP3033. Both plasmids were introduced into the same *E. coli* strain and overexpressed simultaneously in LB medium by induction with 1 mM IPTG and 0.2% L-arabinose for 3 h. Cells were disrupted with the French press method and GltB-His<sub>6</sub> was purified by affinity chromatography where GltA was co-eluted with 50 mM imidazole in ZAP (see Figure 3.12 A). For the purification of DarA, a plasmid encoding Strep-DarA (pGP2624) was also introduced into *E. coli*, overexpressed and Strep-DarA was purified by affinity chromatography (see Figure 3.12 B).

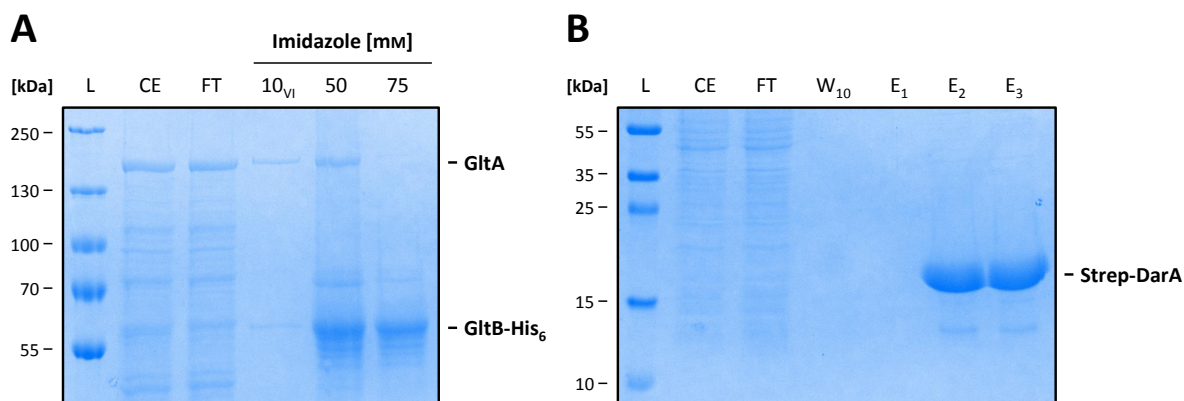


**Figure 3.12: Fractions of a GltAB-His<sub>6</sub> and Strep-DarA purification.** (A) GltB-His<sub>6</sub> and GltA were co-produced in one *E. coli* strain, purified and co-eluted by affinity chromatography. (B) Strep-DarA was overproduced in *E. coli* and purified by affinity chromatography. PageRuler Plus (L), cell extract (CE), flow-through (FT), wash fraction (W), elution fraction (E).

Relevant fractions of Strep-DarA and GltAB-His<sub>6</sub> were each pooled and exhaustively dialyzed together against 50 mM Tris-HCl pH 7.5. The integrity and functionality of the GltAB holoenzyme was verified by a titration of different amounts of the GltAB-His<sub>6</sub> preparation in a GOGAT activity assay. Briefly, NADPH oxidation by GltAB was measured over two hours at 280 nm in a microplate reader. Values were blanked against background NADPH oxidation and assay mixtures without NADPH served as a negative control. The GltAB-His<sub>6</sub> preparation indeed yielded functional GltAB holoenzyme (see Figure 3.13).

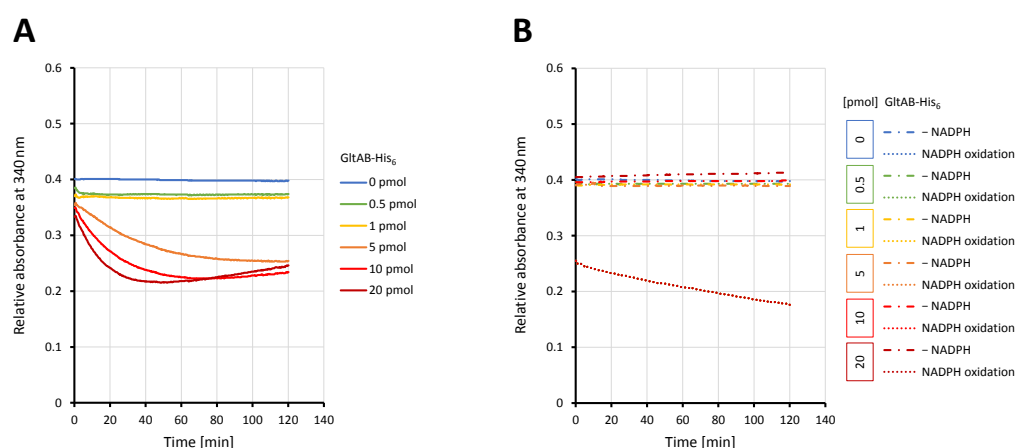


**Figure 3.13: Functionality of the GltAB-His<sub>6</sub> preparation in a GOGAT activity assay.** (A) GltB-His<sub>6</sub> and GltA were co-produced in *E. coli*, purified and co-eluted by affinity chromatography, and dialyzed against 50 mM Tris-HCl pH 7.5. The indicated pmol of the GltAB-His<sub>6</sub> preparation were used for the GOGAT activity assay. Curves are blanked against background NADPH oxidation. (B) Controls without the cofactor NADPH and calculated background NADPH oxidation.

For the GltAB–DarA interaction study, 10 pmol of the GltAB-His<sub>6</sub> preparation were chosen for a GOGAT activity assay. To account for the ligand-bound and -free DarA, Strep-DarA was either saturated with a 2.5-fold excess of c-di-AMP beforehand or incubated with an equal amount of buffer. GltAB-His<sub>6</sub> (10 pmol) was mixed with either buffer, only c-di-AMP (250 pmol) in buffer, or Strep-DarA (100 pmol) without or with c-di-AMP (250 pmol). The GOGAT activity assay was performed and values were blanked against background NADPH oxidation. Assay mixtures without either GltAB, the cofactor NADPH or the substrates  $\alpha$ -ketoglutaric acid ( $\alpha$ -KG) and L-glutamine (Gln) served as negative controls. As shown in Figure 3.14, neither c-di-AMP-bound nor -free DarA affected the activity of GltAB.

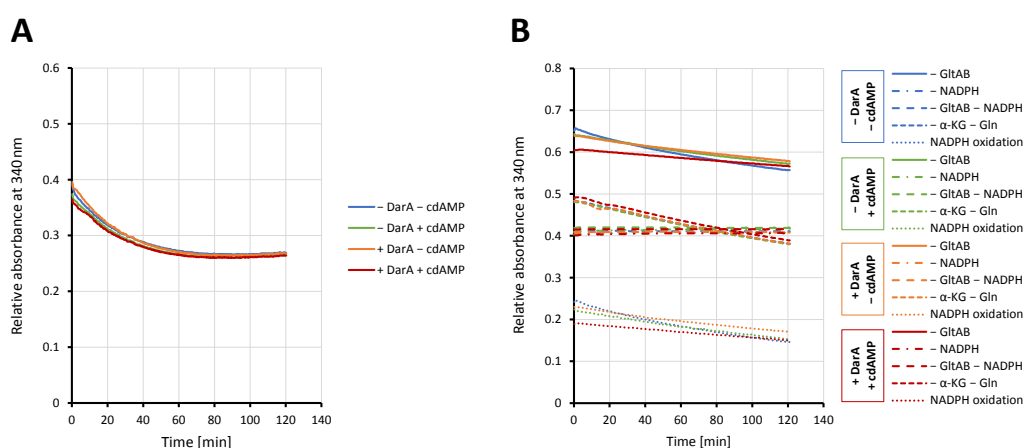


**Figure 3.14: DarA does not affect the activity of GltAB-His<sub>6</sub> in a GOGAT activity assay.** GltAB-His<sub>6</sub> (10 pmol) was mixed with either buffer, only c-di-AMP (250 pmol, cdAMP) in buffer, or Strep-DarA (100 pmol) without or with c-di-AMP (250 pmol). (A) Enzymatic activity of GltAB-His<sub>6</sub> is not altered irrespective of DarA/c-di-AMP presence. Values were blanked against calculated background NADPH oxidation. (B) Controls without either GltAB, the cofactor NADPH or the substrates  $\alpha$ -ketoglutaric acid ( $\alpha$ -KG) and L-glutamine (Gln), as well as the calculated background NADPH oxidation.

Functionality of GltAB-His<sub>6</sub> and the assay was apparent. Functionality of Strep-DarA had been verified before (see Section 3.4.4.1 and Fülleborn, 2018). On the one hand, the results indicate that there is no interaction of DarA with the glutamate synthase GltAB *in vitro*. On the other hand, this could also mean that unknown cofactors, ligands or interactions were missing. We conclude that an interaction of DarA with GltAB could not be shown, but can also not be excluded for certain.

The GOGAT activity assay did not yield conclusive results for a putative interaction of DarA with GltAB. As an additional approach, a pull-down assay with the purified proteins was chosen to identify an interaction. For this purpose, plasmid combinations for GltAB-His<sub>6</sub> (pGP3031 and pGP3033) or similarly constructed GltAB-Strep (pGP3032 and pGP3033) were each introduced into *E. coli*. Both variants were overproduced in LB medium as described before and cells were disrupted with the French press method. Cell-free crude extracts containing GltAB-His<sub>6</sub> or GltAB-Strep were loaded onto an appropriate column for affinity purification. The columns were washed until no protein was measurable anymore in the washing fractions with the Bradford method. In parallel, Strep-DarA (pGP2624) or His<sub>6</sub>-DarA (pGP2601) were overproduced in *E. coli* and purified by affinity chromatography. Both were exhaustively dialyzed against either Buffer W (His<sub>6</sub>-DarA) or ZAP (Strep-DarA). To account for the ligand-bound and -free DarA, both variants were either saturated with a 2.5-fold excess of *c*-di-AMP beforehand or incubated with an equal amount of buffer. For the pull-down assay, 40 nmol Strep-DarA or 100 nmol His<sub>6</sub>-DarA (each either *c*-di-AMP saturated or untreated) were loaded onto the columns with bound GltAB exhibiting another affinity tag. Empty columns served as negative controls. The columns were washed until no protein was measurable anymore in the washing fractions with the Bradford method and bound proteins were eluted. Samples were analyzed by SDS-PAGE and Western blotting or silver staining. 500 ng of the loaded DarA sample served as a positive control for the detection of DarA. Both Strep-DarA and His<sub>6</sub>-DarA bound unspecifically to each of the respective purification columns as shown in Figure 3.15.

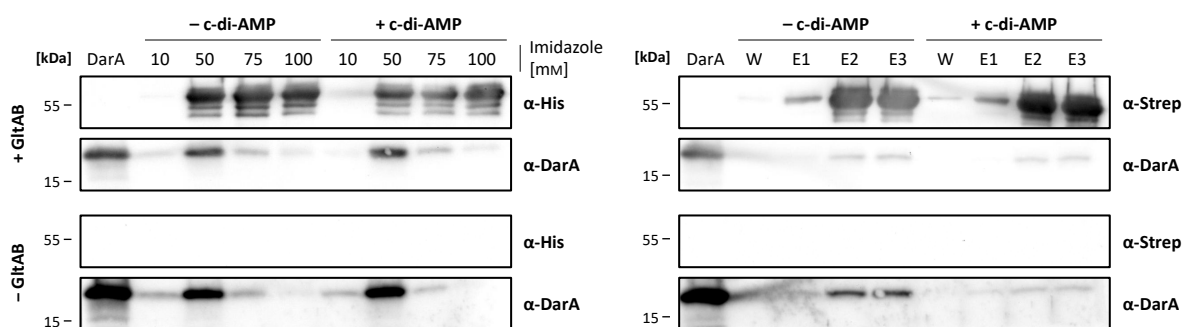


**Figure 3.15: Pull-down assay with purified GltAB and DarA shows only unspecific DarA binding.** Analysis of a pull-down assay with GltAB-His<sub>6</sub> (left) or GltAB-Strep (right) by Western blotting. Both DarA variants bound unspecifically to the respective purification column (- GltAB), preventing a clear interpretation. Eluted DarA amounts were not increased in the actual pull-down assay (+ GltAB). Wash fraction (W), elution fraction (E).

Eluted DarA amounts were not increased when GltAB was bound to the columns in the actual pull-down assay. Presence of co-eluted GltA was verified by SDS-PAGE and silver staining and revealed that GltA was present but not very abundant. Taken together, the pull-down assay was not entirely functional and thus not conclusive.

Interestingly, Fülleborn (2018) identified GltA in the elution fractions of a SPINE. This was done under conditions where DarA is needed for viability (a  $\Delta ktrAB \Delta kimA \Delta ahrC$  deletion strain grown in MSSM medium with ammonium as the nitrogen source and low amounts of KCl). This strongly indicated an interaction of DarA with GltAB. To verify these findings, the SPINE was repeated with an isogenic control strain (GP3003) expressing untagged DarA instead of Strep-DarA (GP3008). Bands likely corresponding to GltA also appeared in the control fractions as analyzed by SDS-PAGE and silver staining, but this was not validated by GC/MS analysis. This might indicate that the interaction of DarA with GltA in the SPINE by Fülleborn (2018) is a false positive hit, however background was quite strong and the presence of untagged DarA leads to partial unspecific binding of DarA to the matrix. Binding of DarA to GltA can consequently not be ruled out by this finding. A  $\Delta ktrAB \Delta kimA \Delta ahrC \Delta darA$  strain would have been a good control for the SPINE but this was not possible since the cells are not able to grow in MSSM medium with ammonium and low amounts of potassium when DarA is missing. Taken together, DarA does not interact with the glutamate synthase GltAB in the *in vitro* GOGAT activity assay. The pull-down assay suggested likewise but was not entirely functional. Consequently, unambiguous evidence for an interaction of DarA with the glutamate synthase GltAB is still pending and further approaches should be pursued.

### 3.8 Implications for DarA's function in a *DAC* mutant

Although c-di-AMP is the only known essential second messenger (Commichau *et al.*, 2015a; Luo and Helmann, 2012; Mehne *et al.*, 2013), recent research refined this classification. Indeed, c-di-AMP becomes dispensable under very specific growth conditions or by accumulation of suppressor mutations (Commichau *et al.*, 2018b). Mainly, prevention of toxic accumulation of potassium, osmolytes and/or amino acids seems to be the reason for this (Commichau *et al.*, 2018a). Recently, viable c-di-AMP-free mutants have been demonstrated for a variety of different bacteria, namely *B. subtilis*, *L. monocytogenes*, *S. aureus* and Group B *Streptococcus* (Devaux *et al.*, 2018; Gundlach *et al.*, 2017b; Whiteley *et al.*, 2015; Zeden *et al.*, 2018). Interestingly, accumulation of different suppressor mutations, including null mutations in *darA* (*pstA*), restored the viability of a *L. monocytogenes cdaA* mutant in rich medium (Gibhardt, unpublished; Whiteley *et al.*, 2015). This indicated that a function of DarA becomes toxic for the cells under this condition. Accordingly, deletion of *darA* in the *L. monocytogenes dacA* (*cdaA*) mutant is already sufficient to restore growth of the strain, which means that apo-DarA has to interact with a target when *Listeria* is grown in rich medium (Whiteley *et al.*, 2015).

We wondered whether this is also true for *B. subtilis* and might reveal more about DarA's function. For this purpose, we checked whether there is a medium in which the *B. subtilis* *DAC darA* deletion mutant is able to grow, in contrast to the parental  $\Delta DAC$  strain. We compared the growth of the *B. subtilis* *DAC* (GP2222) deletion mutant with an isogenic strain additionally devoid of *darA* (GP2420) in a range of different media. Among others, these included common rich media (like LB or BHI medium) but also minimal media like MSSM medium with ammonium or glutamate as the nitrogen source and elevated potassium concentrations (5 mM and higher). No growth differences were observed and both strains were not viable in almost all of the tested conditions (see also Section 3.9). Both strains neither grew nor formed suppressors in rich media. This indicates, that the interconnection of DarA with metabolism is more complex in *B. subtilis* compared to *L. monocytogenes* since deletion of *darA* does not easily restore growth of the  $\Delta DAC$  strain in rich medium.

During our studies, it was shown that c-di-AMP is dispensable for *S. aureus* in rich medium when cells are grown anaerobically, a condition where TCA cycle activity is reduced (Fuchs *et al.*, 2007; Zeden *et al.*, 2018). We wondered whether this is also true for *B. subtilis* and Krüger tried to grow the  $\Delta DAC$  strain (GP2222) on LB medium agar plates under aerobic and anaerobic conditions. However, neither growth nor formation of suppressor mutants was observed for the *DAC* deletion mutant in both cases (Krüger, unpublished). Surprisingly, generation of stable suppressor mutants of the isogenic *DAC darA* deletion mutant (GP2420) was possible, but only under anaerobic conditions.

An anaerobically evolved suppressor (GP2496) of the  $\Delta DAC \Delta darA$  strain (GP2420) was kindly provided by Krüger and we identified the compensatory mutations by sequencing. Fittingly to the essential function of c-di-AMP in *B. subtilis* (Gundlach *et al.*, 2017b), the anaerobically evolved *DAC darA* deletion mutant had acquired a point mutation in *ktrC* (see Table 3.4). KtrC is the cytoplasmic component of the low-affinity K<sup>+</sup> importer KtrCD which is supposed to be active under this culturing condition (Holtmann *et al.*, 2003). The mutation leads to an amino acid exchange in the RCK\_N domain of the protein, a domain that binds ADP/ATP and NAD<sup>+</sup>/NADH (Albright *et al.*, 2006). Inhibition of K<sup>+</sup> import by c-di-AMP is absent in the  $\Delta DAC$  strain. Accordingly, the mutation most likely impairs K<sup>+</sup> import by KtrCD (Gundlach *et al.*, 2017b). While the nature of the mutation in *ktrC* was obvious, the effect of the mutations in *yfkF* and *nusG* in the same strain could not be deduced with high confidence. YfkF is similar to multi-drug efflux transporters and belongs to the unknown major facilitator family-2. The altered residue is located in a transmembrane helix and might affect the transport activity or specificity of YfkF (Marger and Saier, 1993; Saier *et al.*, 2016). However, the substrates of YfkF in *B. subtilis* are not known so far. NusG functions as a sequence specific pause factor that recognizes specific T-rich sequences in the non-template DNA and interacts with and stalls movement of the RNA polymerase. The mutated residue T82(K) is the most important residue for pausing of RNA polymerase movement (Yakhnin *et al.*, 2016). However, compensatory effects of the *yfkF* and *nusG* mutations are not obvious and both might be “hitchhiker’s” with no functional correlation.

The anaerobic growth of the *DAC darA* suppressor on LB medium raised the question whether growth under aerobic conditions without c-di-AMP is now also possible. Consequently, we tried to grow the *DAC darA* suppressor mutant (GP2496) aerobically on LB medium agar plates at 37 °C. Indeed, we were able to generate suppressor mutants with the anaerobically evolved GP2496 suppressor strain, but not with the parental  $\Delta DAC \Delta darA$  strain (GP2420). The aerobically acquired mutations of three independently isolated suppressors were identified by whole genome sequencing (WGS +/-) and/or Sanger sequencing and are summarized in Table 3.4. All three suppressors acquired the exact same mutation in *kimA* (deletion of three base pairs). As a consequence, amino acid G112, located in a transmembrane helix, of the high-affinity K<sup>+</sup> importer KimA was excised (Gundlach *et al.*, 2017b). This is in agreement with the mutation in *ktrC* acquired under anaerobic conditions and most likely impairs K<sup>+</sup> import further. Interestingly, one suppressor (GP3010) carried a deletion of 155 base pairs in *ccpA* including 24 base pairs downstream of the STOP codon (*ccpA* <sub>$\Delta bp850-1005incl.24bp(3')$</sub> ). *ccpA* encodes the pleiotropic transcription factor CcpA which governs carbon catabolite repression in *B. subtilis* (Stülke and Hillen, 1999). The deletion most likely leads to a nonfunctional CcpA. Furthermore, the deletion leads to formation of a new STOP codon at the start of *motP* which is located downstream of *ccpA* (*motP*<sub>START1STOP</sub>). MotP is part of the stator MotPS which supports Na<sup>+</sup>-transport-driven flagellar movement. However, *B. subtilis* also contains the H<sup>+</sup>-type stator MotAB which seems to be more potent under various conditions (Ito *et al.*, 2004; Terahara *et al.*, 2017). The compensatory effect of the *ccpA/motP* mutation could not be deduced with high confidence.

Taken together, deletion of *darA* allowed the *DAC* deletion mutant to acquire suppressor mutations on rich medium when first grown anaerobically and then aerobically. The mutations emphasize the important function of c-di-AMP in K<sup>+</sup> homeostasis. The results furthermore indicate that apo-DarA interacts with a target in the c-di-AMP-free strain which inhibits growth on rich medium.

**Table 3.4: Suppressors of a *DAC darA* deletion mutant on LB medium.**

Strain	Background	Isolation	Additional mutations	Effect	WGS
GP2496	$\Delta DAC \Delta darA$	Anaerobic	<i>ktrC</i> <sub>G11C</sub> <i>yfkF</i> <sub>G294S</sub> <i>nusG</i> <sub>T82K</sub>	– K <sup>+</sup> import <sup>a</sup> Unknown Unknown	–
GP3011	GP2496	Aerobic	<i>kimA</i> <sub><math>\Delta G112</math></sub> <sup>b</sup>	– K <sup>+</sup> import <sup>a</sup>	–
GP3010	GP2496	Aerobic	<i>kimA</i> <sub><math>\Delta G112</math></sub> <i>ccpA</i> <sub><math>\Delta bp850-1005incl.24bp(3')</math></sub> <i>motP</i> <sub>START1STOP</sub>	– K <sup>+</sup> import <sup>a</sup> Unknown Unknown	+

<sup>a</sup> Effect is deduced from the context. No experimental data.

<sup>b</sup> Identified in two independently evolved suppressors.

### 3.9 Elevated potassium amounts stabilize a *DAC* mutant

As mentioned before, potassium homeostasis is an essential function of c-di-AMP in *B. subtilis*. Cells lacking the second messenger are not able to inhibit potassium import. Consequently, subjection to high (5 mM) instead of low (0.1 mM) potassium concentrations leads to toxic accumulation of the ion and cell lysis, presumably caused by concomitant water influx (Gundlach *et al.*, 2017b). In the aforementioned studies (see Section 3.8), we also analyzed growth of the *B. subtilis* *DAC* (GP2222) deletion mutant in a range of different media, including MSSM medium with ammonium and elevated potassium concentrations (5 mM and higher). Surprisingly, the c-di-AMP-free  $\Delta DAC$  strain was able to grow with very high (250 mM) amounts of potassium in MSSM medium with ammonium as the nitrogen source but not with 5 mM.

To verify and refine our initial observation, we investigated which potassium concentrations inhibit growth of the  $\Delta DAC$  strain on MSSM medium with ammonium as the nitrogen source in a drop dilution experiment. The  $\Delta DAC$  strain (GP2222) was first grown in MSSM medium with ammonium as the nitrogen source and low (0.1 mM) amounts of potassium and the wild type (168) was carried along as a control. Cells were washed extensively and samples of a serial dilution were spotted on MSSM medium agar plates with ammonium as the nitrogen source and the indicated potassium concentration (0.1 to 500 mM). Growth was documented after 48 h at 37 °C. Although elevated amounts of potassium were thought to be toxic for a c-di-AMP-free *B. subtilis* strain, the results shown in Figure 3.16 refine this postulation. Surprisingly, increasing the potassium concentration to 100 mM and more stabilized growth of the  $\Delta DAC$  strain. This is particularly interesting since the results are counterintuitive at first glance. Subjection of the  $\Delta DAC$  strain to 5 mM KCl already resulted in toxic accumulation of  $K^+$  and cell lysis, as documented before (Gundlach *et al.*, 2017b), but a 20- to 50-fold increase allows for growth again.

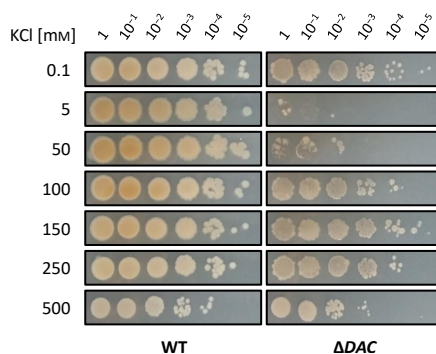


**Figure 3.16: Elevated potassium amounts stabilize growth of a c-di-AMP-free strain again.** Growth of *B. subtilis* wild type (WT, 168) and of a c-di-AMP-free deletion mutant devoid of *cdaA*, *disA* and *cdaS* ( $\Delta DAC$ , GP2222) on MSSM medium agar plates with ammonium as the nitrogen source and indicated KCl concentration after 48 h at 37 °C. Numbers on top indicate the spotted dilution of an  $OD_{600}$  of 1.0.



Growth at 500 mM KCl was slightly worse than growth at 250 mM for both the wild type and the  $\Delta DAC$  strain, most likely because the hyperosmotic condition leads to dehydration of the cells (Hoffmann and Bremer, 2017). It should be noted that unstressed *B. subtilis* cells accumulate potassium to around 300 mM (Whatmore *et al.*, 1990). The results indicate that, although c-di-AMP cannot inhibit  $K^+$  uptake anymore, increasingly abundant potassium amounts prevent the build-up of a huge  $K^+$  gradient which would then lead to increased water influx and cell lysis in the  $\Delta DAC$  strain.



## 4 Discussion

The second messenger c-di-AMP is essential for many bacteria that produce it and becomes dispensable only under very specific growth conditions or by accumulation of suppressor mutations (Commichau *et al.*, 2018b). DarA is a prominent c-di-AMP receptor in *B. subtilis* and is highly conserved among Gram-positive, c-di-AMP-producing firmicutes. Similar to other c-di-AMP targets, DarA is not essential (Gundlach *et al.*, 2015a). In the past, our and other groups tried to elucidate the function of DarA in *B. subtilis* and its homologue PstA in *L. monocytogenes* and *S. aureus*. Despite extensive research the function of DarA has remained enigmatic. In this thesis we showed that DarA is acting on a cytosolic target. Specific phenotypes of a *darA* deletion mutant were shown, several hypotheses could be ruled out and DarA was linked to glutamate homeostasis. This is especially interesting since the homeostases of c-di-AMP, potassium and glutamate seem to be intricately linked to each other (Gundlach *et al.*, 2018). So far, no target of c-di-AMP has been reported to be involved in the homeostasis of glutamate.

### 4.1 No apparent functional link within the *darA* operon

DarA is conserved among Gram-positive, c-di-AMP-producing firmicutes with only few exceptions (Gundlach *et al.*, 2015a). The genomic arrangement of DarA with the essential genes *tmk* (upstream, coding for the thymidylate kinase) and *holB* (downstream, coding for the  $\delta'$  subunit of the DNA polymerase III) is also highly conserved among bacteria that express *darA* hinting to a functional link (Dandekar *et al.*, 1998; Nicolas *et al.*, 2012). In addition, in almost all *Bacillus* species a gene of unknown function (*yaaR*) is located directly between *darA* and *holB*. However, the presence of *yaaR* is not conserved among the firmicutes, suggesting that there is no functional link between DarA and YaaR (Dandekar *et al.*, 1998; Nicolas *et al.*, 2012).

Conserved gene pairs or operons can often be attributed to ribosomal genes or genes involved in other fundamental cellular processes like cell division or cell wall synthesis and those likely originate from a common ancestral genome. In addition, many proteins encoded by conserved gene pairs appear to physically interact with each other. This allows for the prediction of functional linkages and protein–protein interactions (Dandekar *et al.*, 1998; Thomas *et al.*, 2000; Watanabe *et al.*, 1997). In fact, there are also examples of conserved genomic linkages and interactions of the gene products among P<sub>II</sub> proteins. For instance, the genes for the P<sub>II</sub> protein GlnK and the ammonium importer AmtB are encoded in a conserved operon in almost all bacteria that produce them. The physical interaction of GlnK with AmtB has been structurally resolved for *E. coli* and verified experimentally in different bacteria including *B. subtilis* (Conroy *et al.*, 2007; Coutts *et al.*, 2002; Detsch and Stülke, 2003).

Stimulated by the genetic linkage of *tmk*, *darA* and *holB*, earlier studies tried to prove physical interactions between the three. This has been especially interesting as DarA itself is not an essential target of the essential second messenger c-di-AMP but of course its interaction partner might as well be (Gundlach *et al.*, 2015b). Intriguingly, no interaction of DarA with HolB or Tmk could be verified. This work is in agreement with previous studies and accounted for c-di-AMP-bound and apo-DarA which was not always done before (Hach, 2015; Jäger, 2015). No specific interaction of DarA with Tmk or HolB could be detected in a variety of different experimental setups (see Section 3.1). These results, together with the preceding work, strongly indicate that there is no interaction present.

This raises the question: Why is there such a conserved genomic arrangement at all? One reason might be that this conservation does not reflect a physical interaction but rather an indirect functional linkage of the gene products as in the case of GlnB, the founding member of the P<sub>II</sub> protein family. GlnB indirectly regulates the glutamine synthetase (GS) GlnA, thus nitrogen assimilation, on a transcriptional and post-transcriptional level in many proteobacteria, and *glnA* and *glnB* are genetically linked in many diazotrophic  $\alpha$ -proteobacteria. It should be noted that this is not the case in the  $\gamma$ -proteobacterial model organism *E. coli*, although the GS is still regulated on a transcriptional and post-transcriptional level by GlnB (Arcondéguy *et al.*, 2001; Huergo *et al.*, 2013; Leigh and Dodsworth, 2007). The genomic conservation of the *darA* operon might point to a functional relation of the encoded proteins without physical interaction. However, there are no experimental indications for this and our results associate DarA with glutamate metabolism.

There is one report of P<sub>II</sub> proteins from the  $\alpha$ -proteobacterial *Rhodobacter capsulatus* where a yeast two-hybrid experiment showed an interaction of GlnB and GlnK with PcrA (helicase superfamily 1) and Era (Ras-like GTPase), respectively. This is quite unusual and would be the first time that a P<sub>II</sub> protein regulates the unwinding of the DNA (PcrA). The other protein, Era, is involved in several processes, among them ribosome assembly, energy metabolism and cell cycle regulation, and would be an unusual target for a P<sub>II</sub> protein as well (Pawlowski *et al.*, 2003). However, yeast two-hybrid analysis is prone to false positive indications and validation by other approaches is still missing (Brückner *et al.*, 2009).

## 4.2 DarA interacts with a cytosolic target

Regulation of transporters is a quite common regulatory mechanism of P<sub>II</sub> proteins. The P<sub>II</sub> protein GlnK is widely distributed over many different taxa including proteobacteria, firmicutes, archaea and actinobacteria (Sant'Anna *et al.*, 2009). It controls the activity of the ammonium importer AmtB and literally functions as a physical plug. When NH<sub>4</sub><sup>+</sup> is abundant import activity of AmtB is inhibited by direct binding of GlnK to the transporter (Coutts *et al.*, 2002; Detsch and Stülke, 2003; Heinrich *et al.*, 2006). The structure has been solved in detail for the *E. coli* GlnK–AmtB complex and reveals how the long flexible T-loops of

GlnK protrude deep into the core of the ammonium channel (Conroy *et al.*, 2007). A similar regulation has been reported for the P<sub>II</sub>-like protein SbtB in cyanobacteria and suggested for the structurally similar CP<sub>II</sub> in  $\beta$ -proteobacteria (Du *et al.*, 2014; Selim *et al.*, 2018; Wheatley *et al.*, 2016). The cyanobacterial SbtB was shown to inhibit bicarbonate uptake by binding to the HCO<sub>3</sub><sup>-</sup> transporter SbtA in a heterologous expression system in *E. coli*. Interestingly, SbtB not only binds ATP and ADP like classical P<sub>II</sub> proteins but also AMP and the second messenger cAMP. SbtB seems to be a novel P<sub>II</sub>-like protein that integrates the status of inorganic carbon through binding of cAMP. This is needed by the phototrophic *Synechocystis* to efficiently adapt to altered CO<sub>2</sub> conditions for subsequent fixation. Although SbtB regulates bicarbonate uptake, direct binding of bicarbonate or modulation of ligand-binding affinity has not been observed (Du *et al.*, 2014; Selim *et al.*, 2018). In contrast, the carboxysome-associated CP<sub>II</sub> protein from the  $\beta$ -proteobacteria is able to bind bicarbonate and membrane association has been suggested but needs further experimental validation (Wheatley *et al.*, 2016). More interactions of P<sub>II</sub> proteins with membrane proteins are under investigation. For example, GlnB from *Synechocystis* seems to interact with the poorly characterized putative membrane channel PamA (Osanai *et al.*, 2005; Osanai and Tanaka, 2007). GlnK from the  $\beta$ -proteobacterial *Azoarcus* seems to interact with Rnf1, a membrane complex which couples Na<sup>+</sup>/H<sup>+</sup> import with the reduction of ferredoxins and NADH (Sarkar *et al.*, 2012). Since DarA is a P<sub>II</sub>-like protein, although with different B- and T-loop lengths (Gundlach *et al.*, 2015a), one of our first ideas was that DarA might regulate another type of transporter. This hypothesis has been especially tempting since c-di-AMP itself already modulates import processes (potassium and osmolytes) in various bacteria (Commichau *et al.*, 2018b).

During this work, the novel high-affinity K<sup>+</sup> importer KimA in *B. subtilis* was discovered. Expression of *kimA* is regulated by binding of c-di-AMP to the *kimA* riboswitch located upstream of the gene (Gundlach *et al.*, 2017b). We immediately thought of KimA as a suitable target candidate for DarA since the KimA protein lacks obvious c-di-AMP-binding motifs. However, even artificial overexpression of *kimA* under conditions with high external K<sup>+</sup> concentrations (elevated K<sup>+</sup> import by KimA is not needed) did not recruit DarA to the membrane. This is in agreement with all of our additional localization studies and recently reported binding of c-di-AMP to the KimA protein (Gundlach, 2017). Interestingly, the transcriptional and post-transcriptional regulation of KimA is in excellent agreement with the similar regulation of the second high-affinity K<sup>+</sup> import system KtrAB in *B. subtilis* (Corrigan *et al.*, 2013; Gundlach, 2017; Gundlach *et al.*, 2017b). It will be especially interesting to resolve the structure and the residues of KimA that are involved in binding of the second messenger. This will aid the elucidation of novel structural c-di-AMP-binding motifs and thus additional targets and is currently in progress.

The concentration of K<sup>+</sup> and the nitrogen source are known to influence c-di-AMP levels which leads to the adjustment of potassium import and other cellular processes (Gundlach, 2017; Gundlach *et al.*, 2017b; 2015b). Our studies indicate that DarA is not regulating the activity of a transporter by direct binding in response to c-di-AMP, the external potassium

concentration or the nitrogen source and that DarA protein amounts remain constant (see Figure 3.6). Consequently, this work strongly suggests that DarA is solely located in the cytosol and interacts with a cytosolic target, irrespective of the c-di-AMP-binding state. However, it might be interesting to evaluate the subcellular localization of DarA and a possible formation of local foci has not been investigated yet. This could be checked easily by genetically fusing DarA to a fluorescent protein like GFP. However, this approach is prone to false negative/positive results. One DarA trimer is only about 35.4 kDa in size, while three GFPs (one GFP would be fused to one DarA monomer) have a size of 80.7 kDa. Arguably, this might have a great impact on protein–protein interactions and the localization. However, the structurally similar P<sub>II</sub> protein GlnB from *Synechococcus elongatus* has been successfully fused to a derivative of the yellow fluorescent protein in the past which did not inhibit its interaction with the *N*-acetyl-L-glutamate kinase (NAGK) (Lüddecke and Forchhammer, 2013).

Interactions with cytosolic targets are not uncommon for P<sub>II</sub> proteins. As already mentioned, the founding member of the P<sub>II</sub> protein family, GlnB from *E. coli*, interacts with the histidine protein kinase NtrB and the adenylyltransferase GlnE and thus controls nitrogen assimilation by the GS on a transcriptional and post-transcriptional level (Huergo *et al.*, 2013; Leigh and Dodsworth, 2007). Another prominent example is the *S. elongatus* P<sub>II</sub> protein which interacts with the cytosolic NAGK, increases its activity and relieves it from feedback inhibition by arginine (Maheswaran *et al.*, 2004). In the  $\alpha$ -proteobacterial *Azospirillum brasilense* the NifH component II of the nitrogenase is regulated by the ADP-ribosyltransferase DraT and the ADP-ribosylglycohydrolase DraG, which in turn are bound and regulated by GlnB and GlnK (GlnZ), respectively. While GlnB activates its target DraT, AmtB-bound GlnK inactivates DraG by sequestration to the membrane (Huergo *et al.*, 2013; 2006; 2009; 2007). In addition to enzymes or transporters, regulatory proteins like the transcription factor TnrA (nitrogen master regulator) in *B. subtilis* can be bound by a P<sub>II</sub> protein. In *B. subtilis* GlnK seems to stabilize active TnrA dimers during nitrogen limitation by acting as a kind of template which furthermore protects TnrA from proteolysis. As mentioned before, AmtB-bound GlnK is even able to sequester TnrA to the membrane in an inverse, ATP-dependent manner (Heinrich *et al.*, 2006; Kayumov *et al.*, 2011; Schumacher *et al.*, 2015). As discussed in the following, DarA seems to interact with a cytosolic protein involved in glutamate homeostasis, which of course fits to the conserved function of P<sub>II</sub> proteins in bacteria.

### 4.3 DarA allows to cope with extreme potassium limitation

A *B. subtilis* mutant devoid of the high affinity K<sup>+</sup> importers KtrAB and KimA is not able to grow on minimal medium with ammonium as the nitrogen source and low (0.5 mM) amounts of potassium. Interestingly, accumulation of positively charged amino acids derived from glutamate like ornithine, citrulline or arginine can compensate for the lack of sufficient intracellular K<sup>+</sup> amounts, most likely by partially taking over the function of K<sup>+</sup> in buffering

the negative charge of the DNA and adjusting the intracellular pH. Accordingly, an isogenic triple deletion mutant additionally devoid of AhrC, the negative regulator of the arginine biosynthesis operon, is able to grow again (Gundlach *et al.*, 2017a).

Surprisingly, we were able to show that DarA is needed for this compensatory mechanism (see Figure 3.9). Derepression of arginine biosynthesis by deletion of *ahrC* barely restores growth in a *ktrAB kimA darA* deletion mutant. In agreement with this, suppressor mutants of the  $\Delta ktrAB \Delta kimA \Delta ahrC \Delta darA$  strain compensate the loss of *darA* by directing a metabolic flux towards glutamate synthesis (*gltC*<sup>+</sup>, *odhB*<sup>-</sup>) and arginine production (*argG*<sup>+</sup>, *SD<sub>argG</sub>*<sup>+</sup>). Interestingly, the suppressor mutation leading to a hyperactive GltC (GltC<sub>L201H</sub>) was identified two times independently and restored growth completely. However, the compensatory effect of some suppressor mutations is not that obvious. Two suppressor mutants, independently isolated by Fülleborn (2018), deactivated the multidrug efflux transporter Bmr, which is able to export structurally highly diverse compounds, among them ethidium bromide and chloramphenicol (Ahmed *et al.*, 1993). We speculate that Bmr might also export either K<sup>+</sup>, glutamate or necessary precursors. However, this remains speculative. In addition, five suppressor mutants isolated by Fülleborn (2018) did not harbor any of the previously identified mutations and subjecting them to whole genome sequencing will be interesting.

This is the first time a severe growth defect of a *darA* deletion mutant has been reported and complementation by introducing *darA* into the strain has been shown (Fülleborn, 2018). The target of DarA under this condition is most likely cytosolic as discussed before. Catabolic enzymes of the arginine pathway cannot be a target of DarA since the inducer arginine is not present and the transcriptional activator AhrC of these genes is deleted (Gardan *et al.*, 1995). Furthermore, our results show that DarA has to act upstream of the arginine biosynthesis as changing the nitrogen source from ammonium to glutamate already restored growth of the  $\Delta ktrAB \Delta kimA \Delta ahrC \Delta darA$  strain under extreme K<sup>+</sup> limitation (see Figure 3.9). The same was true for glutamine and proline which can be easily converted into glutamate (Gunka and Commichau, 2012). Consequently, the putative target of DarA should feed into the arginine biosynthesis to enable accumulation of positively charged amino acids like ornithine, citrulline or arginine. As discussed in the following, it is tempting to speculate that DarA directly stimulates the synthesis of glutamate which is the starting point for arginine biosynthesis. However, at this point we cannot exclude other upstream compensatory mechanisms completely.

#### 4.3.1 Does DarA interact with the glutamate synthase?

Currently, the most promising target for an interaction with DarA is the glutamate synthase GltAB (GOGAT). Two independently acquired mutations in the transcriptional regulator *gltC* were identified but surprisingly no mutation in the *gltAB* operon itself. It is not entirely clear why this is the case but this might be due to the small sample size of the analyzed suppressors.

GltAB was identified in our bioinformatic analysis where we searched for putative interaction partners of DarA that fit rational criteria. As a reminder, these criteria were conservation among related species, cytosolic localization, promising structure and less abundance in relation to the putative regulator DarA. In *B. subtilis*, glutamate is synthesized by the glutamate synthase GltAB in a reductive, NADPH-dependent reaction out of glutamine and the TCA cycle intermediate 2-oxoglutarate (Gunka and Commichau, 2012). Subsequently, glutamate and acetyl coenzyme A (acetyl-CoA) are used as a starting point for the arginine biosynthesis (Cunin *et al.*, 1986). A stimulating interaction of DarA with GltAB would increase the available glutamate which then can be fed into the arginine biosynthesis.

An interaction is highly likely from a structural point of view. Inspired by our experimental and bioinformatic results parallel work by Richts (2018) nicely showed how perfectly the structures of DarA and GltAB fit together. Structural compatibility was visualized by molecular docking of the *B. subtilis* DarA trimer to the GltAB homologue from *Azospirillum brasilense* in its enzymatically active, dodecameric form. The DarA homotrimer exhibits a tripod-like tertiary structure formed by the unusually long B-loops that protrude from the protein core. The tips are negatively charged, 40 Å apart and nicely fit into three positively charged depressions that are formed by the big subunit GltA. These are located in an 60 Å central cavity of the GltAB holoenzyme. In this model two DarA trimers would sandwich the dodecameric GltAB holoenzyme by binding into two cavities formed by two GltA trimers (Richts, 2018). This proposed mechanism resembles the stimulating interaction of P<sub>II</sub> with the NAGK in *S. elongatus* (Llácer *et al.*, 2007). Availability of K<sup>+</sup> is reported by alterations in the c-di-AMP pool which can be integrated by DarA since binding of the ligand leads to changes in the orientations of the B-loops (Gundlach *et al.*, 2015a). Consequently, depending on the binding state of DarA a putative interaction with GltA(B) could easily be either facilitated or diminished. Nevertheless, the structural indications should be viewed critically. The *Azospirillum* GOGAT structure was only resolved at a resolution of 9.5 Å and was acquired by a combination of three-dimensional cryoelectron microscopy, small angle x-ray scattering and bioinformatic modeling with a structural similar dehydrogenase as a template (Cotteville *et al.*, 2008).

The transcriptional control of the GOGAT has been studied extensively in the past but, to our knowledge, post-translational control of a bacterial glutamate synthase has not been reported so far (Gunka and Commichau, 2012). However, post-translational regulation of an eukaryotic GOGAT has been reported recently for the model plant *Arabidopsis thaliana* (Takabayashi *et al.*, 2016). The bacterial GOGAT found in *E. coli* or *B. subtilis* is a NADPH-dependent type of glutamate synthase (NADPH-GOGAT). In addition, two other types exist in nature which either use NADH (NADH-GOGAT) or reduced ferredoxin (Fd-GOGAT) as the electron donor. The NADH-GOGAT can be found in yeast, lower eukaryotes and in the nonphotosynthetic tissues of plants, while the Fd-GOGAT is found in cyanobacteria, algae and in the photosynthetic tissue of plants (Suzuki and Knaff, 2005). ACR11, an ACT-domain-containing protein (acronym for aspartate kinase, chorismate mutase, and TyrA),



directly interacts with the Fd-GOGAT in *A. thaliana*. ACR11 seems to stabilize the enzyme complex which is reflected by reduced Fd-GOGAT activity in an *acr11* mutant (Takabayashi *et al.*, 2016). Interestingly, ACR11 also increases the activity of the glutamine synthetase by direct binding and thus seems to balance the GS/GOGAT activity (Osanai *et al.*, 2017). Considering the structural and mechanistic similarities between the GOGAT-types and the significant sequence similarity (> 40%) of the Fd-GOGAT to the big subunit GltA of the NADPH-GOGAT, GltAB might also be regulated on a post-translational level (Cotteville *et al.*, 2008; Suzuki and Knaff, 2005). Although, *gltAB* expression is slightly reduced at low K<sup>+</sup> concentrations, GS/GOGAT activity is not influenced by K<sup>+</sup> (Krüger, unpublished; Measures, 1975). Consequently, it would be reasonable for DarA to sense K<sup>+</sup> limitation depending on its c-di-AMP binding status and to adjust the activity of GltAB accordingly. Our results indicate this but unambiguous proof for an interaction of DarA with GltAB is still pending.

Up to now, several different experiments were not able to verify an interaction of DarA with GltAB. However, most of them were either not entirely functional or the negative results have to be interpreted carefully. Previous GOGAT activity assays with different *B. subtilis* cell-free crude extracts were inconclusive (Richts, 2018). However, the extracts were not from a *ktrAB kimA ahrC* deletion background which might explain the negative results since the interaction seems unnecessary under these conditions and DarA is still bound to c-di-AMP which likely inhibits an interaction (see Section 4.3.2). On the one hand, the GOGAT activity assay with purified proteins also suggests that c-di-AMP-un-/bound DarA does not influence the activity of GltAB *in vitro* (see Figure 3.14). On the other hand, the *in vitro* assay surely does not reflect the native cellular conditions like substrate and cofactor concentrations and unknown factors might even be missing. Furthermore, the assay relies on the oxidation of the cofactor NADPH which occurs at the NADPH site of the small subunit GltB. Consequently, binding of DarA to the big subunit GltA might not hinder the oxidation of NADPH but only affect the reaction at the glutaminase site or the synthase site, where glutamine or 2-oxoglutarate are converted to glutamate, respectively. Both are located in GltA (Agnelli *et al.*, 2005; Vanoni *et al.*, 1996). The pull-down assay was also not entirely functional since DarA did bind unspecifically to the matrix. A BACTH assay with DarA and GltA conducted by Fülleborn (2018) was not conclusive. However, the other subunit GltB was not present for complex formation resulting in only little self-interaction of GltA. The most promising experimental evidence is the SPINE from Fülleborn (2018) since he was able to reproducibly detect the big subunit GltA in a cross-linked SPINE elution fraction. However, this cannot be taken as a definite proof since suitable controls were missing. A perfect control for this does not exist since a strain lacking DarA is not able to grow under this condition and a strain expressing an untagged DarA leads to partial unspecific binding of DarA to the matrix. The SPINE fractions showed a lot of background which might indicate a false positive binding of GltA. This could be excluded by cultivation of the strain with high amounts of K<sup>+</sup> and using this as a methodological control.

Since GltAB is the most tempting target candidate for DarA, additional experimental setups should be pursued. For example, Förster resonance energy transfer (FRET) can be used as an *in vitro* or as an *in vivo* approach. For this purpose, DarA and GltA have to be genetically fused to derivatives of the cyan fluorescent protein (CFP) and yellow fluorescent protein (YFP) which in pair function as a donor and acceptor fluorophore, respectively (Miyawaki *et al.*, 1997). FRET has already been successfully used to show an interaction of the P<sub>II</sub> protein GlnB with the NAGK from *S. elongatus* (Lüddecke and Forchhammer, 2013). In addition, ITC with the purified proteins can be used to detect a possible interaction *in vitro* without relying on NADPH oxidation. Purification of functional GltAB was demonstrated in this work starting with simultaneous overexpression of His<sub>6</sub>-tagged *gltB* and untagged *gltA* using a two-plasmid approach with subsequent co-purification (see Figure 3.12). For illustration, the localization of GltAB within glutamate metabolism as well as the connection of glutamate to the TCA cycle and to the arginine biosynthesis are depicted in Figure 4.1.

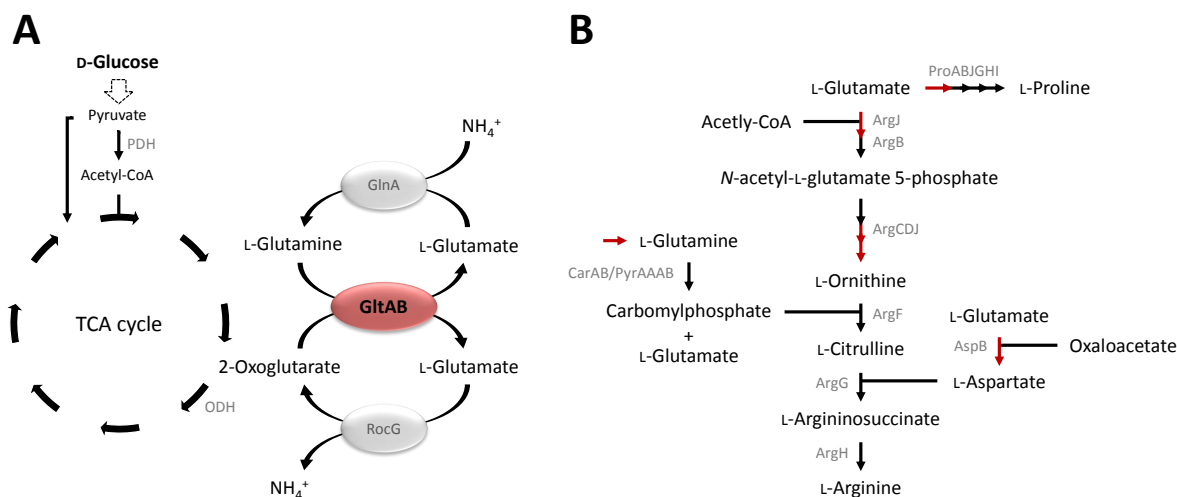


**Figure 4.1: Connection of central carbon and glutamate metabolism and overview of arginine biosynthesis.** (A) Localization of GltAB within glutamate metabolism and connection to the TCA cycle. (B) Arginine biosynthesis. Red arrows indicate glutamate dependent reactions. In both representations not all enzymes, steps, substrates and products are shown to ensure a good overview.

#### 4.3.2 Cyclic di-AMP – does it stimulate or inhibit DarA?

We hypothesize that the interaction of DarA with its main target is inhibited upon binding of c-di-AMP and that apo-DarA promotes glutamate synthesis. Especially the B-loops undergo major changes in orientation and flexibility upon ligand binding. This leads to a reduced accessibility of the otherwise flexible B-loops and has already been proposed to be inhibitory for PstA (DarA) interactions in *L. monocytogenes* (Campeotto *et al.*, 2015; Choi *et al.*, 2015; Gundlach *et al.*, 2015a; Whiteley *et al.*, 2017). This might also be the reason why no phenotype of a *darA* deletion in the wild type background was detectable in the huge Phenotype MicroArray screening, since an interaction was always inhibited.

A *B. subtilis*  $\Delta ktrAB \Delta kimA \Delta ahrC$  strain grown on minimal medium with ammonium as the nitrogen source and a low (0.5 mM) KCl concentration experiences extreme potassium limitation and the cells need DarA for viability.  $K^+$  limitation is sensed by the cells by a yet unknown mechanism which leads to reduced synthesis of c-di-AMP to abolish post-/transcriptional inhibition of  $K^+$  uptake by the high-affinity importers KtrAB and KimA (Gundlach, 2017; Gundlach *et al.*, 2017b). Since both transporters are absent in the strain,  $K^+$  uptake can only be partially facilitated by the low-affinity import system KtrCD (which is also regulated by c-di-AMP) (Corrigan *et al.*, 2013; Gundlach, 2017). Since  $K^+$  is extremely limited for the cells and the cations are even compensated by positively charged amino acids like arginine, we also expect extremely low intracellular levels of c-di-AMP (Gundlach *et al.*, 2017a). Consequently, DarA should be present in its apo-state under this condition but this has still to be verified. Data from *Listeria monocytogenes* showed that the affinity of DarA (PstA) to c-di-AMP is comparable to other targets of the second messenger like CbpA, CbpB (YkuL) or OpuCA and the dissociation constant is in the low  $\mu M$  range. Only phosphodiesterases like PgpH have a higher affinity to c-di-AMP (Huynh *et al.*, 2016; Sureka *et al.*, 2014). Although we deem it to be unlikely, we cannot exclude that DarA and/or other targets “soak up” residual amounts of c-di-AMP. Additional analysis using the c-di-AMP insensitive variant (DarA<sub>F36E</sub>) suggested that DarA acts in a c-di-AMP-bound state even under this condition, which is counterintuitive (Fülleborn, 2018). F36 was not changed to a smaller residue like alanine since a PstA<sub>F36A</sub> variant was already shown to partially retain ligand-binding capacity (Campeotto *et al.*, 2015). The introduced glutamate residue is similar in size to the native phenylalanine, but it might be that the novel negative charge disturbs necessary conformational changes and thus prevents an interaction. To verify the binding state of DarA in this context growth could be compared again in a  $\Delta DAC$  background. Alternatively, the variants DarA<sub>T28R</sub> or DarA<sub>N41R</sub> could be tested, although SEC analysis suggested weaker trimerisation of both variants compared to DarA<sub>F36E</sub>.

Additional evidence also strongly suggests that c-di-AMP inhibits a main function of DarA. Deletion of *darA* is beneficial for growth of the *B. subtilis*  $\Delta DAC$  strain on rich medium as suggested by isolated suppressors. It is especially interesting that the  $\Delta DAC$  strain does not form suppressors on rich medium (LB) but deletion of *darA* allows this when cells are grown anaerobically. Notably, TCA cycle activity is reduced under anaerobic conditions which influences the production and interconversion of many amino acids, including glutamate (Fuchs *et al.*, 2007; Nakano *et al.*, 1998). Interestingly, this was also possible with a  $\Delta DAC$  strain additionally lacking the uncharacterized c-di-AMP-binding protein YkuL (Krüger, unpublished). Furthermore, there seems to be a common scheme for the suppression mechanism in the  $\Delta DAC$  mutant. Several suppressors of both strains ( $\Delta DAC \Delta darA / \Delta DAC \Delta ykuL$ ) acquired a loss-of-function mutation in *ktrC* (anaerobically) and subsequently in *kimA* (aerobically), which shuts down the uncontrolled  $K^+$  import by KtrCD and KimA, respectively. Intriguingly, almost all of the  $\Delta DAC \Delta ykuL ktrC^- kimA^-$  mutants additionally acquired loss-of-function mutations in *darA* (Krüger, unpublished). Consequently, apo-DarA

interacts with a target in *B. subtilis* which is normally inhibited by c-di-AMP. Apparently, c-di-AMP governs multiple cellular processes which in combination cannot be overcome without pre-adaptation. In addition, this is intriguing since our results strongly suggest that DarA is involved in glutamate metabolism which is linked to K<sup>+</sup> homeostasis (Gundlach *et al.*, 2018). Furthermore, we already know that not only an elevated amount of K<sup>+</sup> but also glutamate is toxic for the *DAC* mutant (Gundlach, 2017; Gundlach *et al.*, 2017b). All the above suggests that apo-DarA increases glutamate production which, in combination with uncontrolled potassium import, is toxic for the  $\Delta DAC$  mutant on rich medium. It seems that glutamate, just like K<sup>+</sup>, leads to a change in turgor pressure which becomes lethal.

It is not immediately obvious though why glutamate can become toxic without c-di-AMP. Glutamate is the major counter-ion for K<sup>+</sup> and by far the most abundant amino acid in the cell (Bennett *et al.*, 2009; McLaggan *et al.*, 1994; Whatmore *et al.*, 1990). Potassium glutamate can act as a transcriptional inhibitor through binding to ribosomal promoters which might become toxic (Gralla and Vargas, 2006). However, the more obvious reason might be that glutamate, in addition to c-di-AMP, influences the export/uptake of K<sup>+</sup> and increases the accumulation of K<sup>+</sup> which becomes toxic. This would explain why glutamate is already toxic for the  $\Delta DAC$  strain, even when only low amounts of K<sup>+</sup> are present (Gundlach, 2017; Gundlach *et al.*, 2017b). Indeed, expression of *kimA* does not only depend on low, external K<sup>+</sup> amounts but also on the presence of glutamate, and more interconnections of glutamate and potassium homeostasis are expected (Gundlach, 2017; Gundlach *et al.*, 2017a; b).

The above is in agreement with reports for *Listeria*. In *L. monocytogenes*, accumulation of different suppressor mutations, including mutations in *pstA* (*darA*), restored the viability of a c-di-AMP-free strain on rich medium (Gibhardt, unpublished; Whiteley *et al.*, 2015). Indeed, deletion of *darA* in the *L. monocytogenes dacA* (*cdaA*) mutant was sufficient to restore growth of the strain on rich medium and suppressed sensitivity of the cells to the  $\beta$ -lactam antibiotic cefuroxime. This indicates that apo-DarA also interacts with a target in *Listeria* which influences the cellular turgor and prevents growth on rich medium. Similar to the observations by Krüger, growth was also restored by deletion of *cbpB* (*ykuL*) in the  $\Delta dacA$  strain, although cells were still sensitive to cefuroxime (Whiteley *et al.*, 2017). Interestingly, the deletion of *darA* was phenocopied by mutations blocking the allosteric activation of the pyruvate carboxylase PycA which replenishes the oxaloacetate pool in the TCA cycle. In *Listeria*, PycA is hyperactive without c-di-AMP and the cells accumulate toxic amounts of oxaloacetate, citrate and glutamate/glutamine (Jitrapakdee *et al.*, 2008; Sureka *et al.*, 2014; Whiteley *et al.*, 2017). However, the authors could not establish a direct link between PstA and PycA (Whiteley *et al.*, 2017). While PycA is of minor importance in *B. subtilis*, *L. monocytogenes* only contains a truncated TCA “cycle” and oxaloacetate is mainly produced by PycA (Schär *et al.*, 2010).

In addition to the above indications, our results suggest that c-di-AMP-bound DarA also interacts with a target. In MSSM medium with ammonium as the nitrogen source and low amounts of potassium a significant growth advantage of a *darA* deletion mutant was

shown (see Figure 3.4). However, this could not be linked to altered intracellular amounts of  $K^+$ , c-di-AMP, citrate, acetyl-CoA or amino acids of the glutamate/arginine family (see Sections 3.4.4.3 and 3.4.4.4). This either means that these processes are not influenced by DarA under this condition or that they can be sufficiently compensated for by other means. DarA most likely acts in a c-di-AMP-bound state under this condition since the phenotype is lost in a  $\Delta DAC$  background (see Figure 3.5). Intriguingly, the observed phenotype is lost when cells are grown on plates. However, presence of DarA leads to a more prominent red/brownish coloration of the colonies which we often observe more severely in strains that accumulate TCA cycle intermediates (Klewing, personal communication). Consequently, DarA might inhibit/facilitate a metabolic step connected to the TCA cycle. It is not clear why the phenotype in liquid is not visible for cells grown on the same solidified medium. Surely, a multitude of factors like osmotic pressure, nutrient availability/gradient, oxygen supply and gene expression are different but the root cause is not obvious right now.

It is tempting to speculate that c-di-AMP-bound DarA does not stimulate glutamate synthesis under this condition but even inhibits it since changing the nitrogen source to glutamate or deleting all diadenylate cyclases (apo-DarA likely stimulates glutamate synthesis) relieves the phenotype again (see Section 3.4 and Richts, 2018). The liquid evolution of the wild type,  $\Delta darA$  and  $darA^+$  strain indicates that the osmotic pressure to increase the potassium uptake masks a function of DarA which is inhibitory for growth in liquid medium since only mutations in *ktrB* were identified in all three strains. Furthermore, the *odhA*<sup>-</sup> and *gltC*<sup>+</sup> suppressor mutations in the  $darA^+$  strain direct a metabolic flux towards glutamate synthesis which we hypothesise is not stimulated by c-di-AMP-bound DarA. In addition, this also implies that elevated amounts of c-di-AMP-bound DarA under this condition restrict a metabolic flux towards glutamate and precursors from the TCA cycle might accumulate. This would be in agreement with the observation on solid medium. It is tempting to speculate that this is achieved by an altered, inhibitory interaction with GltAB. Since, the wild type did not acquire such suppressor mutations, the likely glutamate restricting action of DarA can be sufficiently adjusted by redirecting a metabolic flux towards glutamate by other metabolic adjustments.

Almost all well characterized P<sub>II</sub> and P<sub>II</sub>-like proteins are able to bind more than one ligand. The typical P<sub>II</sub> proteins like GlnB and GlnK bind antagonistically ATP or ADP and synergistically 2-oxoglutarate and ATP (Forchhammer and Lüddecke, 2016). As already mentioned, this allows one P<sub>II</sub> to interact with different types of targets. One of many examples is the P<sub>II</sub> from *S. elongatus* which, depending on the ATP/ADP and 2-oxoglutarate levels, either interacts with the NAGK to promote arginine biosynthesis or binds the NtcA-coactivator PipX and by that influences the expression of nitrogen assimilation genes (Llácer *et al.*, 2007; 2010). There might be additional factors that modulate the function of DarA in addition to c-di-AMP that explain the findings more convincingly since the phenotype is totally reversed when the cells experience extreme  $K^+$  limitation. However, this remains to be investigated.

### 4.3.3 Are there additional putative targets?

It has been argued previously that the NAGK ArgB would be a suitable interaction target for DarA since the context as well as the structure fit nicely (Richts, 2018). The NAGK catalyzes the rate-limiting step of arginine biosynthesis and is already known to be regulated by a P<sub>II</sub> protein in unicellular cyanobacteria. It has been shown that binding of P<sub>II</sub> to the NAGK increases the activity of the enzyme and releases it from feedback inhibition by arginine in *S. elongatus* (Maheswaran *et al.*, 2004). NAGK–P<sub>II</sub> interactions have also been reported for P<sub>II</sub> homologues in eukaryotes like the microalgae *Myrmecia incisa*, the red algae *Porphyra purpurea* and different plants (Burillo *et al.*, 2004; Chen *et al.*, 2006; Lapina *et al.*, 2018; Li *et al.*, 2017; Sugiyama *et al.*, 2004). Our results exclude ArgB as a potential target candidate for an interaction since DarA has to act upstream of the arginine biosynthesis pathway. This is in agreement with BACTH assays with and without c-di-AMP present and SPINEs where no interaction of DarA with ArgB was detectable. Several *in vivo* and *in vitro* experiments conducted in parallel suggest the same (Richts, 2018).

At a glance, suitable possibilities for DarA to promote arginine synthesis by modulating glutamate production appear to be sparse (see also Figure 4.1 for an overview about the metabolic context). For example, DarA neither interacts with the transcriptional activator GltC nor influences the expression of *gltAB* in SPINEs and  $\beta$ -galactosidase activity assays, respectively (Krammer, 2017). However, the experiments by Krammer (2017) were not done under genetic/experimental conditions where an interaction with DarA is crucial which should be repeated immediately. Similar to the interaction of GlnK with ThrA, DarA could potentially stabilize GltC and thus enhance the transcription of *gltAB* (Schumacher *et al.*, 2015).

The glutamine synthetase GlnA works in concert with GltAB (GS/GOGAT system) and utilizes glutamate and  $\text{NH}_4^+$  as substrates. In *B. subtilis*  $\text{NH}_4^+$  assimilation is solely achieved by the GS/GOGAT system and not by a glutamate dehydrogenase (Gunka and Commichau, 2012). Recently, GlnA was linked to c-di-AMP and  $\text{K}^+$  homeostasis via the c-di-AMP regulated, high-affinity  $\text{K}^+$  importer KimA. Expression of *kimA* was increased by 4-fold in a  $\Delta\text{glnA}$  strain when cells were grown with low amounts of potassium in the presence of ammonium and glutamine (Gundlach, 2017). Initially, expression of *kimA* has been described to be glutamate dependent (Gundlach *et al.*, 2017b). Although the interplay needs more clarification, this adds yet another facet to the already highly complex regulation of glutamate and c-di-AMP metabolism and even DarA might contribute to this. However, GlnA belongs to the 100 most abundant proteins in *B. subtilis* and DarA protein amounts are lower by roughly 10 to 100-fold which makes a regulation by physical interaction impossible (Eymann *et al.*, 2004; Maass *et al.*, 2011; Maaß *et al.*, 2014). As mentioned before, activity of the GS in enteric bacteria like *E. coli* is governed by its adenylation state and the enzyme is inactive when fully adenylation (van Heeswijk *et al.*, 2013). This process is regulated by the P<sub>II</sub> protein GlnB which interacts with the ATase GlnE and either stimulates (unmodified) or inhibits (uridylylated) the adenylation of the GS (Leigh and Dodsworth, 2007). However, in

*B. subtilis* the GS is not regulated by adenylation but instead by feedback inhibition (Fisher, 1999). When glutamine is present, GS activity is not needed and feedback inhibited by binding of glutamine to the GS (FBI-GS). Furthermore, the FBI-GS binds the transcriptional repressor GlnR and in complex represses the expression of the *glnAR* operon by binding to the promoter region, thus regulating its own expression (Fisher, 1999; Fisher and Wray, 2008).

In principle, inhibition of the glutamate degrading GDH by DarA could increase the available glutamate and indeed the hexameric RocG also fits structurally (Gunka *et al.*, 2010). However, *rocG* is not expressed under the conditions where DarA is needed since the cells are growing with glucose and ammonium as the carbon and nitrogen source, respectively. In the presence of glucose *rocG* is subject to CCR to prevent futile, ATP-consuming cycling of glutamate synthesis and degradation. This is achieved by the pleiotropic transcription factor CcpA. Under this condition CcpA forms a complex with the histidine-carrier protein HPr from the phosphotransferase system and inhibits the transcription of *rocG* and many other catabolic genes (Belitsky *et al.*, 2004; Commichau *et al.*, 2008; Görke and Stülke, 2008). Furthermore, CcpA inhibits transcription of the alternative sigma factor  $\sigma^L$  which is needed for *rocG* expression (Choi and Saier, 2005; Débarbouillé *et al.*, 1991; Gunka and Commichau, 2012). In addition, the transcription factors AhrC and RocR are needed to activate transcription of *rocG* when arginine is present (Belitsky and Sonenshein, 1999; Belitsky and Sonenshein, 1998; Commichau *et al.*, 2007). However, arginine is not present in the medium and *ahrC* is deleted in the strain. In summary, RocG cannot be a target of DarA. Although *B. subtilis* additionally encodes GudB, this second GDH can also be excluded. In the laboratory strain 168, a perfect direct repeat is inserted in the *gudB* gene and the enzyme is not functional (Belitsky and Sonenshein, 1998).

In one suppressor of the *ktrAB kimA ahrC darA* deletion mutant we also found a mutation in *odhB* which codes for the E2 subunit of the 2-oxoglutarate dehydrogenase complex (ODH). The *B. subtilis* ODH is composed of several monomers from the subunits OdhA (E1), OdhB (E2) and PdhD (E3) and catalyzes the oxidative decarboxylation of 2-oxoglutarate to succinyl coenzyme A in the TCA cycle (Carlsson and Hederstedt, 1989). The mutation in *odhB* leads to an amino acid exchange within the lipoyl-binding domain and might impair the function of OdhB/ODH (Saier *et al.*, 2016). This would arguably increase the available 2-oxoglutarate pool for glutamate synthesis by GltAB. However, inhibition of the huge ODH by DarA to promote glutamate synthesis seems highly unlikely from a structural point of view. In *E. coli* the structure has been resolved and the stoichiometry has been determined to 12:24:12 of the subunits E1:E2:E3, respectively (Pettit *et al.*, 1973). In Gram-positive bacteria 2-oxo acid dehydrogenase complexes even show a 30:60:6 subunit arrangement, although no structure for *Bacillus* ODH is available (Mattevi *et al.*, 1992; Neveling *et al.*, 1998). In addition, the genes for all three subunits are highly expressed and the proteins are way more abundant than DarA even when the genes are subject to CCR (Blencke *et al.*, 2003; Maass *et al.*, 2011; Maaß *et al.*, 2014).

Recently, the pyruvate dehydrogenase complex (PDH) has been suggested as a potential target of PstA (DarA) in *L. monocytogenes* since subunits interacted with PstA in yeast two-hybrid and pull-down assays (Whiteley *et al.*, 2017). The PDH catalyzes the oxidative decarboxylation of pyruvate to form acetyl-CoA which is fed into the TCA cycle, thus linking it with glycolysis (Gao *et al.*, 2002). As mentioned before, the authors found mutations blocking the allosteric activation of the pyruvate carboxylase PycA by acetyl-CoA. These mutations phenocopied the deletion of *pstA* in the  $\Delta dacA$  strain which rescued growth on rich medium. Since no interaction of PstA with PycA was detectable, it was argued that a stimulating effect of apo-PstA on acetyl-CoA production might be reasonable (Whiteley *et al.*, 2017). However, a physical interaction of DarA with the PDH is highly unlikely. Similar to the ODH, PDHs are enormous multienzyme complexes of 5 to 10 MDa. In Gram-positive bacteria like the close relative *Bacillus stearothermophilus* the PDH consists of a dodecahedron-like core composed of 60 E2 subunits that bind 30 E1 and 6 E3 subunits (Mattevi *et al.*, 1992; Neveling *et al.*, 1998). In addition, all subunits are among the 100 most abundant proteins in *B. subtilis* which makes regulation by physical binding of DarA impossible (Eymann *et al.*, 2004).

In the aforementioned report the authors suggested that misregulation of the TCA cycle in the absence of c-di-AMP leads to a detrimental alteration of osmotic pressure. In *L. monocytogenes* PycA is hyperactive without c-di-AMP and the cells accumulate oxaloacetate, citrate and glutamate/glutamine which can be prevented by deletion of *citZ* (coding for the citrate synthase) (Sureka *et al.*, 2014; Whiteley *et al.*, 2017). Interestingly, Whiteley *et al.* (2017) showed that a lack of the citrate synthase, but not a lack of aconitase or isocitrate dehydrogenase which catalyze the next steps in the TCA cycle, also phenocopies the  $\Delta dacA \Delta pstA$  strain. Consequently, the authors stated that the accumulation of citrate and not downstream metabolites like glutamate is toxic for the  $\Delta dacA$  strain. However, *L. monocytogenes* only contains a truncated TCA cycle and oxaloacetate is mainly produced by PycA, which is not the case for *B. subtilis* so the phenotypes are likely to be different (Schär *et al.*, 2010). Unfortunately, intracellular amounts of citrate or glutamate of the  $\Delta dacA \Delta pstA$  strain were not provided by the authors so it is not clear which metabolite is causative for the  $\Delta pstA$  phenotype.

Several reports of P<sub>II</sub> protein interactions suggest that there is a unified mechanism by which these small proteins interact with their targets. In almost all cases, the loop regions play a pivotal role and govern the interaction. The B-loops of DarA are unusually long and even longer than the usual T-loops in GlnK. Furthermore, they are reoriented upon c-di-AMP binding which suggests these are most crucial for an interaction (Gundlach *et al.*, 2015a; Müller *et al.*, 2015). As mentioned, prime targets of P<sub>II</sub> proteins are often trimeric or hexameric and interactions with AmtB or the NAGK have been analyzed extensively (Forchhammer and Lüddecke, 2016). Interestingly, even interactions with monomeric targets are mechanistically similar, like the interaction of P<sub>II</sub> with PipX, the cyanobacterial coactivator of NtcA. One P<sub>II</sub> trimer binds three PipX monomers between the protruding T-loops (Llácer *et al.*, 2010; Zhao *et al.*, 2010). In cyanobacteria NtcA, together with the coactivator PipX, acts as global



transcriptional regulator for genes involved in nitrogen assimilation and P<sub>II</sub> competes with NtcA for the binding of PipX (Espinosa *et al.*, 2014). Only few exceptional mechanisms have been resolved. For example the previously mentioned interaction of P<sub>II</sub> with three monomers of the ADP-ribosylglycohydrolase DraG in *Azospirillum brasilense*. In this unique case the loop regions are not involved in target-binding but the lateral body of P<sub>II</sub> (Rajendran *et al.*, 2011). Another example is the aforementioned interaction of *B. subtilis* GlnK with ThrA where the T-loop regions are again not involved and the lateral  $\alpha$ -helices mediate the interaction which stabilizes the global nitrogen regulator. This interaction is also exceptional since ThrA is bound as an active dimer (Schumacher *et al.*, 2015). To conclude, the primary target of most known P<sub>II</sub> proteins appears to be trimeric/hexameric which of course fits to their structural assembly. However, some examples of interactions with monomers and even dimers have been reported in the last years. The results of the unbiased *in silico* screening for putative DarA interaction partners, together with future experiments, might yield more promising candidates in addition to GltAB and one should be open for potential monomeric/dimeric targets. However, there data on the structure and/or localization for many proteins are missing. After accounting for our rational requirements still 160 proteins were in our list of putative target candidates simply because we could not exclude more of them for certain.

#### 4.4 Too much potassium is not enough without c-di-AMP

High external K<sup>+</sup> concentrations (5 mM) are toxic for a *B. subtilis* *DAC* deletion mutant since c-di-AMP cannot inhibit K<sup>+</sup> import anymore and the ion accumulates to toxic levels (Gundlach *et al.*, 2017b). Surprisingly, high amounts of K<sup>+</sup> do not inhibit growth when the cation is abundant to an even greater extent (100–250 mM; see Figure 3.16). At first glance the results are counterintuitive to the essential function of c-di-AMP in control of the K<sup>+</sup> homeostasis (Gundlach *et al.*, 2017b). However, it is quite obvious why this is the case when one considers the reason for K<sup>+</sup> toxicity. When K<sup>+</sup> uptake cannot be inhibited anymore by c-di-AMP, the cation is imported until the gradient between the intra- and extracellular environment is so high that the concomitant water influx induces swelling which culminates in cell lysis. However, if the cells are not able to build up such a high gradient the water flux remains moderate and the cells stay viable. Although some bacteria have aquaporins to accelerate water fluxes (*B. subtilis* does not possess any), no bacterium can actively pump water in or out of the cell so they rely on the ion and solute gradient to adjust the turgor (Hoffmann and Bremer, 2017). Apparently, the *DAC* mutant is not able to generate a toxic K<sup>+</sup> gradient as long as the extracellular K<sup>+</sup> concentration is high enough. It should be noted that *B. subtilis* cells usually accumulate potassium to around 300 mM and that the cells are thus growing under nearly isotonic conditions (Whatmore *et al.*, 1990).

The stabilizing effect might not only be true for K<sup>+</sup> but also for Na<sup>+</sup> or other osmolytes that counteract the K<sup>+</sup> gradient and contribute to maintaining the cellular turgor by directing

the water flow (Hoffmann and Bremer, 2017). Increasing the KCl concentration in the medium also increases the total osmolarity and supplementation with NaCl has the same effect. Indeed, the *DAC* mutant is not viable on the same minimal medium with 250 mM K<sup>+</sup> when the Na<sup>+</sup> concentration is lowered from 125 mM to 10 mM (our unpublished data). It might be interesting whether the opposite is also true and increasing the Na<sup>+</sup> concentration allows the  $\Delta DAC$  strain to grow with 5 mM K<sup>+</sup>, which is otherwise toxic.

Taken together, the above contributes to the recently proposed and accepted model that the superordinate function of c-di-AMP is maintaining the cellular turgor (Commichau *et al.*, 2018a). Similarly, addition of sucrose or Mg<sup>2+</sup> also stabilizes the growth of *B. subtilis* cells that are depleted for c-di-AMP (Luo and Helmann, 2012). Furthermore, stabilization of a *dacA* (*cdA*) mutant by addition of KCl or NaCl to the medium has also been reported for other bacteria. Growth of *L. monocytogenes* and *S. aureus* *dacA* mutants was stabilized on rich medium by addition of 0.2–0.8 M or 0.4–1.6 M salt, respectively (Whiteley *et al.*, 2015; Zeden *et al.*, 2018).

## 4.5 Outlook

The search of the function of DarA has proven to be much more complicated than we initially thought. Nevertheless, we were able to show that DarA most likely interacts with a cytosolic target. The results strongly suggest that apo-DarA enhances a metabolic flux towards glutamate and subsequent arginine synthesis. This is especially interesting since c-di-AMP, K<sup>+</sup> and glutamate homeostasis are somehow intricately intertwined but no c-di-AMP target has been proposed to be involved in glutamate homeostasis until this thesis (Gundlach, 2017; Gundlach *et al.*, 2018). The function of DarA was revealed when cells experience extreme potassium limitation, a condition where the accumulation of positively charged amino acids like citrulline, ornithine and arginine is needed for viability. Although our work suggests GltAB as the most promising target of DarA, unambiguous evidence has still to be provided. Furthermore, we cannot completely exclude other compensatory processes at this time.

It is intriguing that *darA* is expressed constitutively (Nicolas *et al.*, 2012). This might allow the cells to rapidly adapt the glutamate homeostasis to altered conditions like extreme potassium downshifts that are reported by c-di-AMP. Hypoosmotic shocks have not been addressed yet. Only growth analyses after hyperosmotic shocks (NaCl and KCl) or c-di-AMP upshock by inducible expression of *cdsS* have been conducted, albeit inconclusive.

Determination of the metabolite pools or transcriptional profiling in a genetic  $\Delta ktrAB \Delta kimA \Delta ahrC$  strain will be crucial to strengthen our hypotheses. However, the isogenic *darA* deletion mutant is not able to grow on minimal medium with ammonium and low amounts of K<sup>+</sup>. Either comparing a *darA* overexpression with the wild type situation or conditional depletion of *darA* using an inducible promoter construct might circumvent this problem and still show the influence of DarA. Furthermore, repeating the growth analyses

in a c-di-AMP-free strain or determination of the c-di-AMP pools could corroborate our hypothesis that DarA acts in its apo-state under this condition. The toxic effect of DarA in a  $\Delta DAC$  strain already shows that an important function of DarA is inhibited by c-di-AMP. In addition, some of our studies also suggest that DarA might inhibit glutamate accumulation in its c-di-AMP-bound state, although this is less clear.

Special focus should be directed to the glutamate synthase GltAB and additional experiments like the mentioned FRET and ITC approaches could provide more evidence for an interaction. In addition, it might still be that DarA regulates another process upstream of glutamate synthesis. It could be checked whether overexpression or deletion of key genes involved in glutamate or central metabolism phenocopy the deletion of *darA* in a *ktrAB kimA ahrC* deletion background. The results of the *in silico* search of rational targets will aid additional future analysis.



## 5 Bibliography

- Agnelli, P., Dossena, L., Colombi, P., Mulazzi, S., Morandi, P., Tedeschi, G., *et al.* (2005) The unexpected structural role of glutamate synthase  $[4\text{Fe-4S}]^{+1,+2}$  clusters as demonstrated by site-directed mutagenesis of conserved C residues at the N-terminus of the enzyme  $\beta$ -subunit. *Arch Biochem Biophys* **436**: 355–366.
- Agostoni, M., Logan-Jackson, A. R., Heinz, E. R., Severin, G. B., Bruger, E. L., Waters, C. M., *et al.* (2018) Homeostasis of second messenger cyclic-di-AMP is critical for cyanobacterial fitness and acclimation to abiotic stress. *Front Microbiol* **9**: 1121.
- Ahmed, M., Borsch, C. M., Neyfakh, A. A., and Schuldiner, S. (1993) Mutants of the *Bacillus subtilis* multidrug transporter Bmr with altered sensitivity to the antihypertensive alkaloid reserpine. *J Biol Chem* **268**: 11086–11089.
- Albright, R. A., Ibar, J.-L. V., Kim, C. U., Gruner, S. M., and Morais-Cabral, J. H. (2006) The RCK domain of the KtrAB  $\text{K}^+$  transporter: Multiple conformations of an octameric ring. *Cell* **126**: 1147–1159.
- Ali, M. K., Li, X., Tang, Q., Liu, X., Chen, F., Xiao, J., *et al.* (2017) Regulation of inducible potassium transporter KdpFABC by the KdpD/KdpE two-component system in *Mycobacterium smegmatis*. *Front Microbiol* **8**: 570.
- Andrade, W. A., Firon, A., Schmidt, T., Hornung, V., Fitzgerald, K. A., Kurt-Jones E. A. Trieu-Cuot, P., *et al.* (2016) Group B *Streptococcus* degrades cyclic-di-AMP to modulate STING-dependent type I interferon production. *Cell Host Microbe* **20**: 49–59.
- Arcondéguy, T., Rachael, J., and Merrick, M. (2001)  $\text{P}_{\text{II}}$  signal transduction proteins, pivotal players in microbial nitrogen control. *Microbiol Mol Biol Rev* **65**: 80–105.
- Bai, Y., Yang, J., Eisele, L. E., Underwood, A. J., Koestler, B. J., Waters, C. M., *et al.* (2013) Two DHH subfamily 1 proteins in *Streptococcus pneumoniae* possess cyclic di-AMP phosphodiesterase activity and affect bacterial growth and virulence. *J Bacteriol* **195**: 5123–5132.
- Bai, Y., Yang, J., Zarrella, T. M., Zhang, Y., Metzger, D. W., and Bai, G. (2014) Cyclic di-AMP impairs potassium uptake mediated by a cyclic di-AMP binding protein in *Streptococcus pneumoniae*. *J Bacteriol* **196**: 614–623.
- Bai, Y., Yang, J., Zhou, X., Ding, X., Eisele, L. E., and Bai, G. (2012) *Mycobacterium tuberculosis* Rv3586 (DacA) is a diadenylate cyclase that converts ATP or ADP into c-di-AMP. *PLOS ONE* **7**: 1–10.

- Ballal, A., Basu, B., and Apte, S. K. (2007)** The Kdp-ATPase system and its regulation. *J Biosci* **32**: 559–568.
- Barbe, V., Cruveiller, S., Kunst, F., Lenoble, P., Meurice, G., Sekowska, A., et al. (2009)** From a consortium sequence to a unified sequence: The *Bacillus subtilis* 168 reference genome a decade later. *Microbiology* **155**: 1758–1775.
- Barbieri, G., Voigt, B., Albrecht, D., Hecker, M., Albertini, A. M., Sonenshein, A. L., et al. (2015)** CodY regulates expression of the *Bacillus subtilis* extracellular proteases Vpr and Mpr. *J Bacteriol* **197**: 1423–1432.
- Bedrunka, P. and Graumann, P. L. (2017)** Subcellular clustering of a putative c-di-GMP-dependent exopolysaccharide machinery affecting macro colony architecture in *Bacillus subtilis*. *Environ Microbiol Rep* **9**: 211–222.
- Belitsky, B. R. and Sonenshein, A. L. (1999)** An enhancer element located downstream of the major glutamate dehydrogenase gene of *Bacillus subtilis*. *Proc Natl Acad Sci USA* **96**: 10290–10295.
- Belitsky, B. R., Kim, H.-J., and Sonenshein, A. L. (2004)** CcpA-dependent regulation of *Bacillus subtilis* glutamate dehydrogenase gene expression. *J Bacteriol* **186**: 3392–3398.
- Belitsky, B. R. and Sonenshein, A. L. (1998)** Role and regulation of *Bacillus subtilis* glutamate dehydrogenase genes. *J Bacteriol* **180**: 6298–6305.
- Bennett, B. D., Kimball, E. H., Osterhout, R., Van Dien, S. J., and Rabinowitz, J. D. (2009)** Absolute metabolite concentrations and implied enzyme active site occupancy in *Escherichia coli*. *Nat Chem Biol* **5**: 593–599.
- Bentley, D. R., Balasubramanian, S., Swerdlow, H. P., Smith, G. P., Milton, J., Brown, C. G., et al. (2008)** Accurate whole human genome sequencing using reversible terminator chemistry. *Nature* **456**: 53–59.
- Berman, H. M., Westbrook, J., Feng, Z., Gilliland, G., Bhat, T. N., Weissig, H., et al. (2000)** The protein data bank. *Nucleic Acids Res* **28**: 235–242.
- Bi, W. and Stambrook, P. J. (1998)** Site-directed mutagenesis by combined chain reaction. *Anal Biochem* **256**: 137–140.
- Biville, F. and Guiso, N. (1989)** Evidence for the presence of cAMP, cAMP receptor and transcription termination factor Rho in different Gram-negative bacteria. *J Gen Microbiol* **131**: 2953–2960.

- Blencke, H.-M., Homuth, G., Ludwig, H., Mäder, U., Hecker, M., and Stülke, J. (2003)** Transcriptional profiling of gene expression in response to glucose in *Bacillus subtilis*: Regulation of the central metabolic pathways. *Metab Eng* **5**: 133–149.
- Blötz, C., Treffon, K., Kaefer, V., Schwede, F., Hammer, E., and Stülke, J. (2017)** Identification of the components involved in cyclic di-AMP signaling in *Mycoplasma pneumoniae*. *Front Microbiol* **8**: 1328.
- Bochner, B. R., Gadzinski, P., and Panomitros, E. (2001)** Phenotype MicroArrays for high-throughput phenotypic testing and assay of gene function. *Genome Res* **11**: 1246–1255.
- Bohannon, D. E. and Sonenshein, A. L. (1989)** Positive regulation of glutamate biosynthesis in *Bacillus subtilis*. *J Bacteriol* **171**: 4718–4727.
- Bowman, L., Zeden, M. S., Schuster, C. F., Kaefer, V., and Gründling, A. (2016)** New insights into the cyclic di-adenosine monophosphate (c-di-AMP) degradation pathway and the requirement of the cyclic-dinucleotide for acid stress resistance in *Staphylococcus aureus*. *J Biol Chem* **291**: 26970–26986.
- Bradford, M. M. (1976)** A rapid and sensitive method for the quantitation of microgram quantities of protein utilizing the principle of protein-dye binding. *Anal Biochem* **72**: 248–254.
- Brill, J., Hoffmann, T., Bleisteiner, M., and Bremer, E. (2011)** Osmotically controlled synthesis of the compatible solute proline is critical for cellular defense of *Bacillus subtilis* against high osmolarity. *J Bacteriol* **193**: 5335–5346.
- Brown, M. S., Segal, A., and Stadtman, E. R. (1971)** Modulation of glutamine synthetase adenylation and deadenylation is mediated by metabolic transformation of the P<sub>II</sub>-regulatory protein. *Proc Natl Acad Sci USA* **68**: 2949–2953.
- Brückner, A., Polge, C., Lentze, N., Auerbach, D., and Schlattner, U. (2009)** Yeast two-hybrid, a powerful tool for systems biology. *Int J Mol Sci* **10**: 2763–2788.
- Burillo, S., Luque, I., Fuentes, I., and Contreras, A. (2004)** Interactions between the nitrogen signal transduction protein P<sub>II</sub> and *N*-acetyl glutamate kinase in organisms that perform oxygenic photosynthesis. *J Bacteriol* **186**: 3346–3354.
- Campeotto, I., Zhang, Y., Mladenov, M. G., Freemont, P. S., and Gründling, A. (2015)** Complex structure and biochemical characterization of the *Staphylococcus aureus* cyclic diadenylate monophosphate (c-di-AMP)-binding protein PstA, the founding member of a new signal transduction protein family. *J Biol Chem* **290**: 2888–2901.

- Carlsson, P. and Hederstedt, L. (1989)** Genetic characterization of *Bacillus subtilis* *odhA* and *odhB*, encoding 2-oxoglutarate dehydrogenase and dihydrolipoamide transsuccinylase, respectively. *J Bacteriol* **171**: 3667–3672.
- Chambert, R., Pereira, Y., and Petit-Glatron, M.-F. (2003)** Purification and characterization of YfkN, a trifunctional nucleotide phosphoesterase secreted by *Bacillus subtilis*. *J Biochem* **134**: 655–660.
- Chen, Y. M., Ferrar, T. S., Lohmeir-Vogel, E., Morrice, N., Mizuno, Y., Berenger, B., et al. (2006)** The P<sub>II</sub> signal transduction protein of *Arabidopsis thaliana* forms an arginine-regulated complex with plastid *N*-acetyl glutamate kinase. *J Biol Chem* **281**: 5726–5733.
- Chin, K.-H., Liang, J.-M., Yang, J.-G., Shih, M.-S., Tu, Z.-L., Wang, Y.-C., et al. (2015)** Structural insights into the distinct binding mode of cyclic di-AMP with Sa-CpaA\_RCK. *Biochemistry* **54**: 4936–4951.
- Cho, K. H. and Kang, S. O. (2013)** *Streptococcus pyogenes* c-di-AMP phosphodiesterase, GdpP, influences SpeB processing and virulence. *PLOS ONE* **8**: e69425.
- Choi, P. H., Sureka, K., Woodward, J. J., and Tong, L. (2015)** Molecular basis for the recognition of cyclic-di-AMP by PstA, a P<sub>II</sub>-like signal transduction protein. *MicrobiologyOpen* **4**: 361–374.
- Choi, P. H., Vu, T. M. N., Pham, H. T., Woodward, J. J., Turner, M. S., and Tong, L. (2017)** Structural and functional studies of pyruvate carboxylase regulation by cyclic di-AMP in lactic acid bacteria. *Proc Natl Acad Sci USA* **114**: E7226–E7235.
- Choi, S.-K. and Saier, M. H. (2005)** Regulation of *sigL* expression by the catabolite control protein CcpA involves a roadblock mechanism in *Bacillus subtilis*: Potential connection between carbon and nitrogen metabolism. *J Bacteriol* **187**: 6856–6861.
- Claessen, D., Emmins, R., Hamoen, L. W., Daniel, R. A., Errington, J., and Edwards, D. H. (2008)** Control of the cell elongation-division cycle by shuttling of PBP1 protein in *Bacillus subtilis*. *Mol Microbiol* **68**: 1029–1046.
- Commichau, F. M., Dickmanns, A., Gundlach, J., Ficner, R., and Stülke, J. (2015a)** A jack of all trades: The multiple roles of the unique essential second messenger cyclic di-AMP. *Mol Microbiol* **97**: 189–204.
- Commichau, F. M., Wacker, I., Schleider, J., Blencke, H.-M., Reif, I., Tripal, P., et al. (2007)** Characterization of *Bacillus subtilis* mutants with carbon source-independent glutamate biosynthesis. *J Mol Microbiol Biotechnol* **12**: 106–113.



- Commichau, F. M. (2006)** Regulation der Glutamatsynthese in *Bacillus subtilis* durch die Glutamatdehydrogenase RocG und das Aktivatorprotein GltC. Ph D thesis. Georg-August-University Göttingen.
- Commichau, F. M., Blötz, C., and Stülke, J. (2015b)** Methods in molecular biology of bacteria. *Department of General Microbiology: Georg-August-University Göttingen, Göttingen.*
- Commichau, F. M., Gibhardt, J., Halbedel, S., Gundlach, J., and Stülke, J. (2018a)** A delicate connection: c-di-AMP affects cell integrity by controlling osmolyte transport. *Trends Microbiol* **26**: 175–185.
- Commichau, F. M., Gunka, K., Landmann, J. J., and Stülke, J. (2008)** Glutamate metabolism in *Bacillus subtilis*: Gene expression and enzyme activities evolved to avoid futile cycles and to allow rapid responses to perturbations of the system. *J Bacteriol* **190**: 3557–3564.
- Commichau, F. M., Heidemann, J. L., Ficner, R., and Stülke, J. (2018b)** Making and breaking of an essential poison: The cyclases and phosphodiesterases that produce and degrade the essential second messenger cyclic di-AMP in bacteria. *J Bacteriol*: JB.00462–18.
- Conroy, M. J., Durand, A., Lupo, D., Li, X.-D., Bullough, P. A., Winkler, F. K., et al. (2007)** The crystal structure of the *Escherichia coli* AmtB-GlnK complex reveals how GlnK regulates the ammonia channel. *Proc Natl Acad Sci USA* **104**: 1213–1218.
- Corrigan, R. M., Bowman, L., Willis, A. R., Kaeffer, V., and Gründling, A. (2015)** Cross-talk between two nucleotide-signaling pathways in *Staphylococcus aureus*. *J Biol Chem* **290**: 5826–5839.
- Corrigan, R. M., Campeotto, I., Jeganathan, T., Roelofs, K. G., Lee, V. T., and Gründling, A. (2013)** Systematic identification of conserved bacterial c-di-AMP receptor proteins. *Proc Natl Acad Sci USA* **110**: 9084–9089.
- Corrigan, R. M. and Gründling, A. (2013)** Cyclic di-AMP: Another second messenger enters the fray. *Nat Rev Microbiol* **11**: 513–524.
- Cotteville, M., Larquet, E., Jonic, S., Petoukhov, M. V., Caprini, G., Paravisi, S., et al. (2008)** The subnanometer resolution structure of the glutamate synthase 1.2-MDa hexamer by cryoelectron microscopy and its oligomerization behavior in solution: Functional implications. *J Biol Chem* **283**: 8237–8249.

- Coutts, G., Thomas, G., Blakey, D., and Merrick, M. (2002) Membrane sequestration of the signal transduction protein GlnK by the ammonium transporter AmtB. *EMBO J* **21**: 536–545.
- Csonka, L. N., Ikeda, T. P., Fletcher, S. A., and Kustu, S. (1994) The accumulation of glutamate is necessary for optimal growth of *Salmonella typhimurium* in media of high osmolality but not induction of the *proU* operon. *J Bacteriol* **176**: 6324–6333.
- Cunin, R., Glansdorff, N., Piérard, A., and Stalon, V. (1986) Biosynthesis and metabolism of arginine in bacteria. *Microbiol Rev* **50**: 314–352.
- Dandekar, T., Snel, B., Huynen, M., and Bork, P. (1998) Conservation of gene order: a fingerprint of proteins that physically interact. *Trends Biochem Sci* **23**: 324–328.
- Davies, B. W., Bogard, R. W., Young, T. S., and Mekalanos, J. J. (2012) Coordinated regulation of accessory genetic elements produces cyclic di-nucleotides for *V. cholerae* virulence. *Cell* **149**: 358–370.
- Débarbouillé, M., Martin-Verstraete, I., Kunst, F., and Rapoport, G. (1991) The *Bacillus subtilis sigL* gene encodes an equivalent of  $\sigma^{54}$  from gram-negative bacteria. *Proc Natl Acad Sci USA* **88**: 9092–9096.
- Detsch, C. and Stülke, J. (2003) Ammonium utilization in *Bacillus subtilis*: Transport and regulatory functions of NrgA and NrgB. *Microbiology* **149**: 3289–3297.
- Devaux, L., Sleiman, D., Mazzuoli, M.-V., Gominet, M., Lanotte, P., Trieu-Cuot, P., *et al.* (2018) Cyclic di-AMP regulation of osmotic homeostasis is essential in Group B *Streptococcus*. *PLOS Genet* **14**: 1–23.
- Diethmaier, C., Newman, J. A., Kovács, Á. T., Kaefer, V., Herzberg, C., Rodrigues, C., *et al.* (2014) The YmdB phosphodiesterase is a global regulator of late adaptive responses in *Bacillus subtilis*. *J Bacteriol* **196**: 265–275.
- Dodsworth, J. A. and Leigh, J. A. (2006) Regulation of nitrogenase by 2-oxoglutarate-reversible, direct binding of a P<sub>II</sub>-like nitrogen sensor protein to dinitrogenase. *Proc Natl Acad Sci USA* **103**: 9779–9784.
- Du, J., Förster, B., Rourke, L., Howitt, S. M., and Price, G. D. (2014) Characterisation of cyanobacterial bicarbonate transporters in *E. coli* shows that SbtA homologs are functional in this heterologous expression system. *PLOS ONE* **9**: 1–25.
- Durand, A., Sinha, A. K., Dard-Dascot, C., and Michel, B. (2016) Mutations affecting potassium import restore the viability of the *Escherichia coli* DNA Polymerase III *hold* mutant. *PLOS Genet* **12**: e1006114.

- Ennis, H. L. and Lubin, M. (1961)** Dissociation of ribonucleic acid and protein synthesis in bacteria deprived of potassium. *Biochim Biophys Acta* **50**: 399–402.
- Epstein, W. (2003)** The roles and regulation of potassium in bacteria. *Prog Nucleic Acid Res Mol Biol* **75**: 293–320.
- Espinosa, J., Rodríguez-Mateos, F., Salinas, P., Lanza, V. F., Dixon, R., Cruz, F. de la, et al. (2014)** PipX, the coactivator of NtcA, is a global regulator in cyanobacteria. *Proc Natl Acad Sci USA* **111**: E2423–E2430.
- Eymann, C., Dreisbach, A., Albrecht, D., Bernhardt, J., Becher, D., Gentner, S., et al. (2004)** A comprehensive proteome map of growing *Bacillus subtilis* cells. *Proteomics* **4**: 2849–2876.
- Fazekas de St Groth, S., Webster, R. G., and Datyner, A. (1963)** Two new staining procedures for quantitative estimation of proteins on electrophoretic strips. *Biochim Biophys Acta* **71**: 377–391.
- Firon, A., Dinis, M., Raynal, B., Poyart, C., Trieu-Cuot, P., and Kaminski, P. A. (2014)** Extracellular nucleotide catabolism by the Group B *Streptococcus* ectonucleotidase NudP increases bacterial survival in blood. *J Biol Chem* **289**: 5479–5489.
- Fisher, S. H. (1999)** Regulation of nitrogen metabolism in *Bacillus subtilis*: *Vive la différence!* *Mol Microbiol* **32**: 223–232.
- Fisher, S. H. and Wray, L. V. (2008)** *Bacillus subtilis* glutamine synthetase regulates its own synthesis by acting as a chaperone to stabilize GlnR–DNA complexes. *Proc Natl Acad Sci USA* **105**: 1014–1019.
- Forchhammer, K. (2008)** P<sub>II</sub> signal transducers: Novel functional and structural insights. *Trends Microbiol* **16**: 65–72.
- Forchhammer, K. and Lüddecke, J. (2016)** Sensory properties of the P<sub>II</sub> signalling protein family. *FEBS J* **283**: 425–437.
- Fuchs, S., Pané-Farré, J., Kohler, C., Hecker, M., and Engelmann, S. (2007)** Anaerobic gene expression in *Staphylococcus aureus*. *J Bacteriol* **189**: 4275–4289.
- Fujisawa, M., Ito, M., and Krulwich, T. A. (2007)** Three two-component transporters with channel-like properties have monovalent cation/proton antiport activity. *Proc Natl Acad Sci USA* **104**: 13289–13294.

- Fujisawa, M., Wada, Y., and Ito, M. (2004)** Modulation of the K<sup>+</sup> efflux activity of *Bacillus subtilis* YhaU by YhaT and the C-terminal region of YhaS. *FEMS Microbiol Lett* **231**: 211–217.
- Fülleborn, J. A. (2018)** Funktionelle Analyse des c-di-AMP Bindeproteins DarA in *Bacillus subtilis*. B Sc thesis. Georg-August-University Göttingen.
- Gándara, C. and Alonso, J. C. (2015)** DisA and c-di-AMP act at the intersection between DNA-damage response and stress homeostasis in exponentially growing *Bacillus subtilis* cells. *DNA Repair* **27**: 1–8.
- Gándara, C., Lucena, D. K. d., Torres, R., Serrano, E., Altenburger, S., Graumann, P. L., et al. (2017)** Activity and in vivo dynamics of *Bacillus subtilis* DisA are affected by RadA/Sms and by Holliday junction-processing proteins. *DNA Repair* **55**: 17–30.
- Gao, H., Jiang, X., Pogliano, K., and Aronson, A. I. (2002)** The E1 $\beta$  and E2 subunits of the *Bacillus subtilis* pyruvate dehydrogenase complex are involved in regulation of sporulation. *J Bacteriol* **184**: 2780–2788.
- Gardan, R., Rapoport, G., and Débarbouillé, M. (1995)** Expression of the *rocDEF* operon involved in arginine catabolism in *Bacillus subtilis*. *J Mol Biol* **249**: 843–856.
- Gomelsky, M. (2011)** cAMP, c-di-GMP, c-di-AMP and now cGMP: Bacteria use them all! *Mol Microbiol* **79**: 562–565.
- Görke, B. and Stülke, J. (2008)** Carbon catabolite repression in bacteria: Many ways to make the most out of nutrients. *Nat Rev Microbiol* **6**: 613–624.
- Gralla, J. D. and Vargas, D. R. (2006)** Potassium glutamate as a transcriptional inhibitor during bacterial osmoregulation. *EMBO J* **25**: 1515–1521.
- Grant, S. G. N., Jessee, J., Bloom, F. R., and Hanahan, D. (1990)** Differential plasmid rescue from transgenic mouse DNAs into *Escherichia coli* methylation-restriction mutants. *Proc Natl Acad Sci USA* **87**: 4645–4649.
- Greie, J.-C. (2011)** The KdpFABC complex from *Escherichia coli*: A chimeric K<sup>+</sup> transporter merging ion pumps with ion channels. *Eur J Cell Biol* **90**: 705–710.
- Griffith, L. J., Ostrander, W. E., Mullins, C. G., and Beswick, D. E. (1965)** Drug antagonism between lincomycin and erythromycin. *Science* **147**: 746–747.

- Guder, J., Schramm, T., Sander, T., and Link, H. (2017)** Time-optimized isotope ratio LCMS/MS for high-throughput quantification of primary metabolites. *Anal Chem* **89**: 1624–1631.
- Guérout-Fleury, A.-M., Shazand, K., Frandsen, N., and Stragier, P. (1995)** Antibiotic-resistance cassettes for *Bacillus subtilis*. *Gene* **167**: 335–336.
- Gundlach, J. (2014)** Potential influence of c-di-AMP on membrane proteins involved in cell wall synthesis in *Bacillus subtilis*. MSc thesis. Georg-August-University Göttingen.
- Gundlach, J. (2017)** Cyclic di-AMP signaling in *Bacillus subtilis*. PhD thesis. Georg-August-University Göttingen.
- Gundlach, J., Commichau, F. M., and Stülke, J. (2018)** Of ions and messengers: An intricate link between potassium, glutamate, and cyclic di-AMP. *Curr Genet* **64**: 191–195.
- Gundlach, J., Dickmanns, A., Schröder-Tittmann, K., Neumann, P., Kaesler, J., Kampf, J., et al. (2015a)** Identification, characterization, and structure analysis of the cyclic di-AMP-binding P<sub>II</sub>-like signal transduction protein DarA. *J Biol Chem* **290**: 3069–3080.
- Gundlach, J., Herzberg, C., Hertel, D., Thürmer, A., Daniel, R., Link, H., et al. (2017a)** Adaptation of *Bacillus subtilis* to life at extreme potassium limitation. *mBio* **8**: e00861–17.
- Gundlach, J., Herzberg, C., Kaefer, V., Gunka, K., Hoffmann, T., Weiß, M., et al. (2017b)** Control of potassium homeostasis is an essential function of the second messenger cyclic di-AMP in *Bacillus subtilis*. *Sci Signal* **10**: eaal3011.
- Gundlach, J., Mehne, F. M. P., Herzberg, C., Kampf, J., Valerius, O., Kaefer, V., et al. (2015b)** An essential poison: Synthesis and degradation of cyclic di-AMP in *Bacillus subtilis*. *J Bacteriol* **197**: 3265–3274.
- Gunka, K., Newman, J. A., Commichau, F. M., Herzberg, C., Rodrigues, C., Hewitt, L., et al. (2010)** Functional dissection of a trigger enzyme: Mutations of the *Bacillus subtilis* glutamate dehydrogenase RocG that affect differentially its catalytic activity and regulatory properties. *J Mol Biol* **400**: 815–827.
- Gunka, K. and Commichau, F. M. (2012)** Control of glutamate homeostasis in *Bacillus subtilis*: A complex interplay between ammonium assimilation, glutamate biosynthesis and degradation. *Mol Microbiol* **85**: 213–224.

- Gunka, K., Stannek, L., Care, R. A., and Commichau, F. M. (2013)** Selection-driven accumulation of suppressor mutants in *Bacillus subtilis*: The apparent high mutation frequency of the cryptic *gudB* gene and the rapid clonal expansion of *gudB*<sup>+</sup> suppressors are due to growth under selection. *PLoS ONE* **8**: 1–15.
- Guzman, L.-M., Belin, D., Carson, M. J., and Beckwith, J. (1995)** Tight regulation, modulation, and high-level expression by vectors containing the arabinose P<sub>BAD</sub> promoter. *J Bacteriol* **177**: 4121–4130.
- H., A. S. and Wong, K.-P. (1986)** The role of magnesium and potassium ions in the molecular mechanism of ribosome assembly: Hydrodynamic, conformational, and thermal stability studies of 16 S RNA from *Escherichia coli* ribosomes. *Arch Biochem Biophys* **249**: 137–147.
- Hach, C. A. (2015)** Neue Einblicke in das *darA* Operon. BSc thesis. Georg-August-University Göttingen.
- Hauryliuk, V., Atkinson, G. C., Murakami, K. S., Tenson, T., and Gerdes, K. (2015)** Recent functional insights into the role of (p)ppGpp in bacterial physiology. *Nat Rev Microbiol* **13**: 298–309.
- Heinrich, A., Woyda, K., Brauburger, K., Meiss, G., Detsch, C., Stülke, J., et al. (2006)** Interaction of the membrane-bound GlnK-AmtB complex with the master regulator of nitrogen metabolism ThrA in *Bacillus subtilis*. *J Biol Chem* **281**: 34909–34917.
- Hengge, R., Gründling, A., Jenal, U., Ryan, R., and Yildiz, F. (2016)** Bacterial signal transduction by cyclic di-GMP and other nucleotide second messengers. *J Bacteriol* **198**: 15–26.
- Herzberg, C., Weidinger, L. A. F., Dörrbecker, B., Hübner, S., Stülke, J., and Commichau, F. M. (2007)** SPINE: A method for the rapid detection and analysis of protein-protein interactions *in vivo*. *Proteomics* **7**: 4032–4035.
- Hoffmann, T. and Bremer, E. (2017)** Guardians in a stressful world: The Opu family of compatible solute transporters from *Bacillus subtilis*. *Biol Chem* **398**: 193–214.
- Holtmann, G., Bakker, E. P., Uozumi, N., and Bremer, E. (2003)** KtrAB and KtrCD: Two K<sup>+</sup> uptake systems in *Bacillus subtilis* and their role in adaptation to hypertonicity. *J Bacteriol* **185**: 1289–1298.
- Hong, P., Koza, S., and Bouvier, E. S. P. (2012)** Size-exclusion chromatography for the analysis of protein biotherapeutics and their aggregates. *J Liq Chromatogr Relat Technol* **35**: 2923–2950.

- Huergo, L. F., Chandra, G., and Merrick, M. (2013) P<sub>II</sub> signal transduction proteins: Nitrogen regulation and beyond. *FEMS Microbiol Rev* **37**: 251–283.
- Huergo, L. F., Chubatsu, L. S., Souza, E. M., Pedrosa, F. O., Steffens, M. B., and Merrick, M. (2006) Interactions between P<sub>II</sub> proteins and the nitrogenase regulatory enzymes DraT and DraG in *Azospirillum brasilense*. *FEBS Lett* **580**: 5232–5236.
- Huergo, L. F., Merrick, M., Monteiro, R. A., Chubatsu, L. S., Steffens, M. B. R., Pedrosa, F. O., *et al.* (2009) *In vitro* interactions between the P<sub>II</sub> proteins and the nitrogenase regulatory enzymes dinitrogenase reductase ADP-ribosyltransferase (DraT) and dinitrogenase reductase-activating glycohydrolase (DraG) in *Azospirillum brasilense*. *J Biol Chem* **284**: 6674–6682.
- Huergo, L. F., Merrick, M., Pedrosa, F. O., Chubatsu, L. S., Araujo, L. M., and Souza, E. M. (2007) Ternary complex formation between AmtB, GlnZ and the nitrogenase regulatory enzyme DraG reveals a novel facet of nitrogen regulation in bacteria. *Mol Microbiol* **66**: 1523–1535.
- Huynh, T. N., Choi, P. H., Sureka, K., Ledvina, H. E., Campillo, J., Tong, L., *et al.* (2016) Cyclic di-AMP targets the cystathionine beta-synthase domain of the osmolyte transporter OpuC. *Mol Microbiol* **102**: 233–243.
- Huynh, T. N. and Woodward, J. J. (2016) Too much of a good thing: Regulated depletion of c-di-AMP in the bacterial cytoplasm. *Curr Opin Microbiol* **30**: 22–29.
- Inoue, H., Nojima, H., and Okayama, H. (1990) High efficiency transformation of *Escherichia coli* with plasmids. *Gene* **96**: 23–28.
- Ito, M., Hicks, D. B., Henkin, T. M., Guffanti, A. A., Powers, B. D., Zvi, L., *et al.* (2004) MotPS is the stator-force generator for motility of alkaliphilic *Bacillus*, and its homologue is a second functional Mot in *Bacillus subtilis*. *Mol Microbiol* **53**: 1035–1049.
- Jäger, N. (2015) Characterization of c-di-AMP interaction partners in *Bacillus subtilis*. MSc thesis. Georg-August-University Göttingen.
- Jenal, U., Reinders, A., and Lori, C. (2017) Cyclic di-GMP: Second messenger extraordinaire. *Nat Rev Microbiol* **15**: 271–284.
- Jitrapakdee, S., St Maurice, M., Rayment, I., Cleland, W. W., Wallace, J. C., and Attwood, P. V. (2008) Structure, mechanism and regulation of pyruvate carboxylase. *Biochem J* **413**: 369–387.

- Kalamorz, F., Reichenbach, B., März, W., Rak, B., and Görke, B. (2007)** Feedback control of glucosamine-6-phosphate synthase GlmS expression depends on the small RNA GlmZ and involves the novel protein YhbJ in *Escherichia coli*. *Mol Microbiol* **65**: 1518–1533.
- Kampf, J. and Stülke, J. (2017)** Cyclic-di-GMP signalling meets extracellular polysaccharide synthesis in *Bacillus subtilis*. *Environ Microbiol Rep* **9**: 182–185.
- Kampf, J. (2014)** Identification of cyclic di-AMP exporters and interaction partners in *Bacillus subtilis*. MSc thesis. Georg-August-University Göttingen.
- Kampf, J., Gundlach, J., Herzberg, C., Treffon, K., and Stülke, J. (2017)** Identification of c-di-AMP-binding proteins using magnetic beads. In: Sauer, K. (eds.) c-di-GMP signaling. Methods in molecular biology. **1657**. Humana Press: New York: 347–359.
- Karimova, G., Pidoux, J., Ullmann, A., and Ladant, D. (1998)** A bacterial two-hybrid system based on a reconstituted signal transduction pathway. *Proc Natl Acad Sci USA* **95**: 5752–5756.
- Kayumov, A., Heinrich, A., Fedorova, K., Ilinskaya, O., and Forchhammer, K. (2011)** Interaction of the general transcription factor TnrA with the P<sub>II</sub>-like protein GlnK and glutamine synthetase in *Bacillus subtilis*. *FEBS J* **278**: 1779–1789.
- Kearse, M., Moir, R., Wilson, A., Stones-Havas, S., Cheung, M., Sturrock, S., et al. (2012)** Geneious Basic: An integrated and extendable desktop software platform for the organization and analysis of sequence data. *Bioinformatics* **28**: 1647–1649.
- Kellenberger, C. A., Chen, C., Whiteley, A. T., Portnoy, D. A., and Hammond, M. C. (2015)** RNA-based fluorescent biosensors for live cell imaging of second messenger cyclic di-AMP. *J Am Chem Soc* **137**: 6432–6435.
- Klewing, A. (2013)** Minimizing the genome of *Bacillus subtilis*: Consequences due to the loss of the citric acid cycle. BSc thesis. Georg-August-University Göttingen.
- Koo, B.-M., Kritikos, G., Farelli, J. D., Todor, H., Tong, K., Kimsey, H., et al. (2017)** Construction and analysis of two genome-scale deletion libraries for *Bacillus subtilis*. *Cell Systems* **4**: 291–305.e7.
- Krammer, T. K. (2017)** Functional analysis of the c-di-AMP binding proteins DarA and YkuL in *Bacillus subtilis*. MSc thesis. Georg-August-University Göttingen.
- Laemmli, U. K. (1970)** Cleavage of structural proteins during the assembly of the head of bacteriophage T4. *Nature* **227**: 680–685.



- Lapina, T., Selim, K. A., Forchhammer, K., and Ermilova, E. (2018) The P<sub>II</sub> signaling protein from red algae represents an evolutionary link between cyanobacterial and Chloroplastida P<sub>II</sub> proteins. *Sci Rep* **8**: 790.
- Lederberg, E. M. and Cohen, S. N. (1974) Transformation of *Salmonella typhimurium* by plasmid deoxyribonucleic acid. *J Bacteriol* **119**: 1072–1074.
- Lehnik-Habrink, M., Pförtner, H., Rempeters, L., Pietack, N., Herzberg, C., and Stülke, J. (2010) The RNA degradosome in *Bacillus subtilis*: Identification of CshA as the major RNA helicase in the multiprotein complex. *Mol Microbiol* **77**: 958–971.
- Leigh, J. A. and Dodsworth, J. A. (2007) Nitrogen regulation in bacteria and archaea. *Annu Rev Microbiol* **61**: 349–377.
- Li, Y., Liu, W., Sun, L.-P., and Zhou, Z.-G. (2017) Evidence for P<sub>II</sub> with NAGK interaction that regulates Arg synthesis in the microalga *Myrmecia incisa* in response to nitrogen starvation. *Scientific Reports* **7**: 16291.
- Linder, J. U. (2010) cGMP production in bacteria. *Mol Cell Biochem* **334**: 215–219.
- Liu, K., Bittner, A. N., and Wang, J. D. (2015) Diversity in (p)ppGpp metabolism and effectors. *Curr Opin Microbiol* **24**: 72–79.
- Liu, S., Bayles, D. O., Mason, T. M., and Wilkinson, B. J. (2006) A cold-sensitive *Listeria monocytogenes* mutant has a transposon insertion in a gene encoding a putative membrane protein and shows altered (p)ppGpp levels. *Appl Environ Microbiol* **72**: 3955–3959.
- Llácer, J. L., Contreras, A., Forchhammer, K., Marco-Marín, C., Gil-Ortiz, F., Maldonado, R., *et al.* (2007) The crystal structure of the complex of P<sub>II</sub> and acetylglutamate kinase reveals how P<sub>II</sub> controls the storage of nitrogen as arginine. *Proc Natl Acad Sci USA* **104**: 17644–17649.
- Llácer, J. L., Espinosa, J., Castells, M. A., Contreras, A., Forchhammer, K., and Rubio, V. (2010) Structural basis for the regulation of NtcA-dependent transcription by proteins PipX and P<sub>II</sub>. *Proc Natl Acad Sci USA* **107**: 15397–15402.
- Louche, A., Salcedo, S. P., and Bigot, S. (2017) Protein–protein interactions: Pull-down assays. In: Journet, L. and Cascales, E. (eds.) Bacterial protein secretion systems. Methods in molecular biology. **1615**. Humana Press: New York: 247–255.
- Lüddecke, J. and Forchhammer, K. (2013) From P<sub>II</sub> signaling to metabolite sensing: A novel 2-oxoglutarate sensor that details P<sub>II</sub> - NAGK complex formation. *PLOS ONE* **8**: e83181.

- Luo, Y. and Helmann, J. D. (2012)** Analysis of the role of *Bacillus subtilis*  $\sigma^M$  in  $\beta$ -lactam resistance reveals an essential role for c-di-AMP in peptidoglycan homeostasis. *Mol Microbiol* **83**: 623–639.
- Maass, S., Sievers, S., Zühlke, D., Kuzinski, J., Sappa, P. K., Muntel, J., et al. (2011)** Efficient, global-scale quantification of absolute protein amounts by integration of targeted mass spectrometry and two-dimensional gel-based proteomics. *Anal Chem* **83**: 2677–2684.
- Maaß, S., Wachlin, G., Bernhardt, J., Eymann, C., Fromion, V., Riedel, K., et al. (2014)** Highly precise quantification of protein molecules per cell during stress and starvation responses in *Bacillus subtilis*. *Mol Cell Proteomics* **13**: 2260–2276.
- Mach, H., Hecker, M., and Mach, F. (1984)** Evidence for the presence of cyclic adenosine monophosphate in *Bacillus subtilis*. *FEMS Microbiol Lett* **22**: 27–30.
- Magasanik, B. (1961)** Catabolite repression. *Cold Spring Harb Symp Quant Biol* **26**: 249–256.
- Maheswaran, M., Urbanke, C., and Forchhammer, K. (2004)** Complex formation and catalytic activation by the P<sub>II</sub> signaling protein of *N*-acetyl-L-glutamate kinase from *Synechococcus elongatus* strain PCC 7942. *J Biol Chem* **279**: 55202–55210.
- Makman, R. S. and Sutherland, E. W. (1965)** Adenosine 3',5'-phosphate in *Escherichia coli*. *J Biol Chem* **240**: 1309–1314.
- Manikandan, K., Sabareesh, V., Singh, N., Saigal, K., Mechold, U., and Sinha, K. M. (2014)** Two-step synthesis and hydrolysis of cyclic di-AMP in *Mycobacterium tuberculosis*. *PLOS ONE* **9**: e86096.
- Manikandan, K., Prasad, D., Srivastava, A., Singh, N., Dabeer, S., Krishnan, A., et al. (2018)** The second messenger cyclic di-AMP negatively regulates the expression of *Mycobacterium smegmatis* recA and attenuates DNA strand exchange through binding to the C-terminal motif of mycobacterial RecA proteins. *Mol Microbiol* **109**: 600–614.
- Marden, J. N., Dong, Q., Roychowdhury, S., Berleman, J. E., and Bauer, C. E. (2011)** Cyclic GMP controls *Rhodospirillum centenum* cyst development. *Mol Microbiol* **79**: 600–615.
- Marger, M. D. and Saier, J. M. H. (1993)** A major superfamily of transmembrane facilitators that catalyse uniport, symport and antiport. *Trends Biochem Sci* **18**: 13–20.

- Martin-Verstraete, I., Débarbouillé, M., Klier, A., and Rapoport, G. (1992)** Mutagenesis of the *Bacillus subtilis* “-12, -24” promoter of the levanase operon and evidence for the existence of an upstream activating sequence. *J Mol Biol* **226**: 85–99.
- Martin-Verstraete, I., Débarbouillé, M., Klier, A., and Rapoport, G. (1994)** Interactions of wild-type and truncated LevR of *Bacillus subtilis* with the upstream activating sequence of the levanase operon. *J Mol Biol* **241**: 178–192.
- Mattevi, A., Obmolova, G., Schulze, E., Kalk, K. H., Westphal, A. H., de Kok, A., et al. (1992)** Atomic structure of the cubic core of the pyruvate dehydrogenase multienzyme complex. *Science* **255**: 1544–1550.
- McLaggan, D., Naprstek, J., Buurman, E. T., and Epstein, W. (1994)** Interdependence of  $K^+$  and glutamate accumulation during osmotic adaptation of *Escherichia coli*. *J Biol Chem* **269**: 1911–1917.
- Measures, J. C. (1975)** Role of amino acids in osmoregulation of non-halophilic bacteria. *Nature* **257**: 398–400.
- Mehne, F. M. P., Gunka, K., Eilers, H., Herzberg, C., Kaever, V., and Stülke, J. (2013)** Cyclic di-AMP homeostasis in *Bacillus subtilis*: Both lack and high level accumulation of the nucleotide are detrimental for cell growth. *J Biol Chem* **288**: 2004–2017.
- Mehne, F. M. P., Schröder-Tittmann, K., Eijlander, R. T., Herzberg, C., Hewitt, L., Kaever, V., et al. (2014)** Control of the diadenylate cyclase CdaS in *Bacillus subtilis*: An autoinhibitory domain limits cyclic di-AMP production. *J Biol Chem* **289**: 21098–21107.
- Mengin-Lecreulx, D. and van Heijenoort, J. (1996)** Characterization of the essential gene *glmM* encoding phosphoglucosamine mutase in *Escherichia coli*. *J Biol Chem* **271**: 32–39.
- Merrick, M. (2015)** Post-translational modification of  $P_{II}$  signal transduction proteins. *Front Microbiol* **5**: 763.
- Merril, C. R., Goldman, D., Sedman, S. A., and Ebert, M. H. (1981)** Ultrasensitive stain for proteins in polyacrylamide gels shows regional variation in cerebrospinal fluid proteins. *Science* **211**: 1437–1438.
- Merzbacher, M., Detsch, C., Hillen, W., and Stülke, J. (2004)** *Mycoplasma pneumoniae* HPr kinase/phosphorylase. *Eur J Biochem* **271**: 367–374.

- Miller, J. (1972) Experiments in molecular genetics. *Cold Spring Harbor Laboratory Press*: Cold Spring Harbor, New York.
- Miyawaki, A., Llopis, J., Heim, R., McCaffery, J. M., Adams, J. A., Ikura, M., *et al.* (1997) Fluorescent indicators for Ca<sup>2+</sup> based on green fluorescent proteins and calmodulin. *Nature* **388**: 882–887.
- Moscoso, J. A., Schramke, H., Zhang, Y., Tosi, T., Dehbi, A., Jung, K., *et al.* (2016) Binding of cyclic di-AMP to the *Staphylococcus aureus* sensor kinase KdpD occurs via the universal stress protein domain and downregulates the expression of the Kdp potassium transporter. *J Bacteriol* **198**: 98–110.
- Müller, M., Hopfner, K.-P., and Witte, G. (2015) c-di-AMP recognition by *Staphylococcus aureus* PstA. *FEBS Lett* **589**: 45–51.
- Mullis, K. B. and Faloona, F. A. (1987) Specific synthesis of DNA *in vitro* via a polymerase-catalyzed chain reaction. *Methods Enzymol* **155**: 355–350.
- Mullis, K. B., Faloona, F. A., Scharf, S., K., S. R., Horn, G. T., and Erlich, H. A. (1986) Specific enzymatic amplification of DNA *in vitro*: The polymerase chain reaction. *Cold Spring Harb Symp Quant Biol* **51**: 263–273.
- Nakano, M. M., Zuber, P., and Sonenshein, A. L. (1998) Anaerobic regulation of *Bacillus subtilis* krebs cycle genes. *J Bacteriol* **180**: 3304–3311.
- Nelson, J. W., Sudarsan, N., Furukawa, K., Weinberg, Z., Wang, J. X., and Breaker, R. R. (2013) Riboswitches in eubacteria sense the second messenger c-di-AMP. *Nat Chem Biol* **9**: 834–839.
- Neveling, U., Bringer-Meyer, S., and Sahm, H. (1998) Gene and subunit organization of bacterial pyruvate dehydrogenase complexes. *Biochim Biophys Acta* **1385**: 367–372.
- Nicolas, P., Mäder, U., Dervyn, E., Rochat, T., Leduc, A., Pigeonneau, N., *et al.* (2012) Condition-dependent transcriptome reveals high-level regulatory architecture in *Bacillus subtilis*. *Science* **335**: 1103–1106.
- Nissen, P., Hansen, J., Ban, N., Moore, P. B., and Steitz, T. A. (2000) The structural basis of ribosome activity in peptide bond synthesis. *Science* **289**: 920–930.
- Orr, M. W. and Lee, V. T. (2017) Differential radial capillary action of ligand assay (DRaCALA) for high-throughput detection of protein–metabolite interactions in bacteria. In: Nordenfelt, P. and Collin, M. (eds.) Bacterial pathogenesis. Methods in molecular biology. **1535**. *Humana Press*: New York: 25–41.

- Osanai, T., Kuwahara, A., Otsuki, H., Saito, K., and Hirai, M. Y. (2017) ACR11 is an activator of plastid-type glutamine synthetase GS2 in *Arabidopsis thaliana*. *Plant Cell Physiol* **58**: 650–657.
- Osanai, T., Sato, S., Tabata, S., and Tanaka, K. (2005) Identification of PamA as a P<sub>II</sub>-binding membrane protein important in nitrogen-related and sugar-catabolic gene expression in *Synechocystis sp.* PCC 6803. *J Biol Chem* **280**: 34684–34690.
- Osanai, T. and Tanaka, K. (2007) Keeping in touch with P<sub>II</sub>: P<sub>II</sub>-interacting proteins in unicellular cyanobacteria. *Plant Cell Physiol* **48**: 908–914.
- Parkinson, J. S. (1993) Signal transduction schemes of bacteria. *Cell* **73**: 857–871.
- Pawlowski, A., Riedel, K.-U., Klipp, W., Dreiskemper, P., Groß, S., Bierhoff, H., *et al.* (2003) Yeast two-hybrid studies on interaction of proteins involved in regulation of nitrogen fixation in the phototrophic bacterium *Rhodobacter capsulatus*. *J Bacteriol* **185**: 5240–5247.
- Pettit, F. H., Hamilton, L., Munk, P., Namihira, G., Eley, M. H., Willms, C. R., *et al.* (1973)  $\alpha$ -Keto acid dehydrogenase complexes: XIX. Subunit structure of the *Escherichia coli*  $\alpha$ -ketoglutarate dehydrogenase complex. *J Biol Chem* **248**: 5282–5290.
- Pham, H. T., Nhiep, N. T. H., Vu, T. N. M., Huynh, T. N., Zhu, Y., Huynh, A. L. D., *et al.* (2018) Enhanced uptake of potassium or glycine betaine or export of cyclic-di-AMP restores osmoresistance in a high cyclic-di-AMP *Lactococcus lactis* mutant. *PLOS Genet* **14**: 1–23.
- Pierce, M. M., Raman, C. S., and Nall, B. T. (1999) Isothermal titration calorimetry of protein–protein interactions. *Methods* **19**: 213–221.
- Prindle, A., Liu, J., Asally, M., Ly, S., Garcia-Ojalvo, J., and Süel, G. M. (2015) Ion channels enable electrical communication within bacterial communities. *Nature* **527**: 59–63.
- Radchenko, M. V., Tanaka, K., Waditee, R., Oshimi, S., Matsuzaki, Y., Fukuhara, M., *et al.* (2006a) Potassium/Proton antiport system of *Escherichia coli*. *J Biol Chem* **281**: 19822–19829.
- Radchenko, M. V., Waditee, R., Oshimi, S., Fukuhara, M., Takabe, T., and Nakamura, T. (2006b) Cloning, functional expression and primary characterization of *Vibrio parahaemolyticus* K<sup>+</sup>/H<sup>+</sup> antiporter genes in *Escherichia coli*. *Mol Microbiol* **59**: 651–663.

- Rajendran, C., Gerhardt, E. C. M., Bjelic, S., Gasperina, A., Scarduelli, M., Pedrosa, F. O., et al. (2011)** Crystal structure of the GlnZ-DraG complex reveals a different form of P<sub>II</sub>-target interaction. *Proc Natl Acad Sci USA* **108**: 18972–18976.
- Rall, T. W. and Sutherland, E. W. (1958)** Formation of a cyclic adenine ribonucleotide by tissue particles. *J Biol Chem* **232**: 1065–1076.
- Rao, F., Ji, Q., Soehano, I., and Liang, Z. X. (2011)** Unusual heme-binding PAS domain from YybT family proteins. *J Bacteriol* **193**: 1543–1551.
- Rao, F., See, R. Y., Zhang, D., Toh, D. C., Ji, Q., and Liang, Z.-X. (2010)** YybT is a signaling protein that contains a cyclic dinucleotide phosphodiesterase domain and a GGDEF domain with ATPase activity. *J Biol Chem* **285**: 473–482.
- Reuß, D. (2017)** Large-scale genome reduction in bacteria: From *Bacillus subtilis* to *Mini-Bacillus*. Ph D thesis. Georg-August-University of Göttingen.
- Richts, B. (2018)** Interaction studies of the P<sub>II</sub>-like protein DarA. MSc thesis. Georg-August-University Göttingen.
- Rismondo, J., Gibhardt, J., Rosenberg, J., Kaefer, V., Halbedel, S., and Commichau, F. M. (2016)** Phenotypes associated with the essential diadenylate cyclase CdaA and its potential regulator CdaR in the human pathogen *Listeria monocytogenes*. *J Bacteriol* **198**: 416–426.
- Romeo, Y., Obis, D., Bouvier, J., Guillot, A., Fourçans, A., Bouvier, I., et al. (2003)** Osmoregulation in *Lactococcus lactis*: BusR, a transcriptional repressor of the glycine betaine uptake system BusA. *Mol Microbiol* **47**: 1135–1147.
- Römling, U., Galperin, M. Y., and Gomelsky, M. (2013)** Cyclic di-GMP: The first 25 years of a universal bacterial second messenger. *Microbiol Mol Biol Rev* **77**: 1–52.
- Rosenberg, J., Dickmanns, A., Neumann, P., Gunka, K., Arens, J., Kaefer, V., et al. (2015)** Structural and biochemical analysis of the essential diadenylate cyclase CdaA from *Listeria monocytogenes*. *J Biol Chem* **290**: 6596–6606.
- Rubin, B. E., Huynh, T. N., Welkie, D. G., Diamond, S., Simkovsky, R., Pierce, E. C., et al. (2018)** High-throughput interaction screens illuminate the role of c-di-AMP in cyanobacterial nighttime survival. *PLoS Genet* **14**: 1–21.
- Saier, M. H. J., Reddy, V. S., Tsu, B. V., Ahmed, M. S., Li, C., and Moreno-Hagelsieb, G. (2016)** The Transporter Classification Database (TCDB): Recent advances. *Nucleic Acids Res* **44**: D372–D379.

- Saiki, R. K., Scharf, S., Faloona, F. A., Mullis, K. B., Horn, G. T., Erlich, H. A., *et al.* (1985) Enzymatic amplification of  $\beta$ -globin genomic sequences and restriction site analysis for diagnosis of sickle cell anemia. *Science* **230**: 1350–1354.
- Sambrook, J., Fritsch, E. F., and Maniatis, T. (1989) Molecular cloning: A laboratory manual. 2nd ed. *Cold Spring Harbor Laboratory Press*: Cold Spring Harbor, New York.
- Sanger, F., Nicklen, S., and Coulson, A. R. (1977) DNA sequencing with chain-terminating inhibitors. *Proc Natl Acad Sci USA* **74**: 5463–5467.
- Sant’Anna, F. H., Trentini, D. B., de Souto Weber, S., Cecagno, R., da Silva, S. C., and Schrank, I. S. (2009) The P<sub>II</sub> superfamily revised: A novel group and evolutionary insights. *J Mol Evol* **68**: 322–336.
- Sarenko, O., Klauck, G., Wilke, F. M., Pfiffer, V., Richter, A. M., Herbst, S., *et al.* (2017) More than enzymes that make or break cyclic di-GMP—local signaling in the interactome of GGDEF/EAL domain proteins of *Escherichia coli*. *mBio* **8**: e01639–17.
- Sarkar, A., Köhler, J., Hurek, T., and Reinhold-Hurek, B. (2012) A novel regulatory role of the Rnf complex of *Azoarcus sp.* strain BH72. *Mol Microbiol* **83**: 408–422.
- Saum, S. H., Sydow, J. F., Palm, P., Pfeiffer, F., Oesterhelt, D., and Müller, V. (2006) Biochemical and molecular characterization of the biosynthesis of glutamine and glutamate, two major compatible solutes in the moderately halophilic bacterium *Halobacillus halophilus*. *J Bacteriol* **188**: 6808–6815.
- Schär, J., Stoll, R., Schauer, K., Loeffler, D. I. M., Eylert, E., Joseph, B., *et al.* (2010) Pyruvate carboxylase plays a crucial role in carbon metabolism of extra- and intracellularly replicating *Listeria monocytogenes*. *J Bacteriol* **192**: 1774–1784.
- Schilling, O., Herzberg, C., Hertrich, T., Vörsmann, H., Jessen, D., Hübner, S., *et al.* (2006) Keeping signals straight in transcription regulation: Specificity determinants for the interaction of a family of conserved bacterial RNA–protein couples. *Nucleic Acids Res* **34**: 6102–6115.
- Schirmer, F., Ehrt, S., and Hillen, W. (1997) Expression, inducer spectrum, domain structure, and function of MopR, the regulator of phenol degradation in *Acinetobacter calcoaceticus* NCIB8250. *J Bacteriol* **179**: 1329–1336.
- Schumacher, M. A., Chinnam, N. b., Cuthbert, B., Tonthat, N. K., and Whitfill, T. (2015) Structures of regulatory machinery reveal novel molecular mechanisms controlling *B. subtilis* nitrogen homeostasis. *Genes Dev* **29**: 451–464.

- Schuster, C. F., Bellows, L. E., Tosi, T., Campeotto, I., Corrigan, R. M., Freemont, P., *et al.* (2016) The second messenger c-di-AMP inhibits the osmolyte uptake system OpuC in *Staphylococcus aureus*. *Sci Signal* **9**: ra81–ra81.
- Selim, K. A., Haase, F., Hartmann, M. D., Hagemann, M., and Forchhammer, K. (2018) P<sub>II</sub>-like signaling protein SbtB links cAMP sensing with cyanobacterial inorganic carbon response. *Proc Natl Acad Sci USA* **115**: E4861–E4869.
- Severin, G. B., Ramliden, M. S., Hawver, L. A., Wang, K., Pell, M. E., Kieninger, A.-K., *et al.* (2018) Direct activation of a phospholipase by cyclic GMP-AMP in *El Tor Vibrio cholerae*. *Proc Natl Acad Sci USA* **115**: E6048–E6055.
- Shapiro, B. M. (1969) Glutamine synthetase deadenylylating enzyme system from *Escherichia coli*. Resolution into two components, specific nucleotide stimulation, and cofactor requirements. *Biochemistry* **8**: 659–670.
- Spangler, C., Böhm, A., Jenal, U., Seifert, R., and Kaefer, V. (2010) A liquid chromatography-coupled tandem mass spectrometry method for quantitation of cyclic di-guanosine monophosphate. *J Microbiol Methods* **81**: 226–231.
- Studier, F. W., Daegelen, P., Lenski, R. E., Maslov, S., and Kim, J. F. (2009) Understanding the differences between genome sequences of *Escherichia coli* B strains REL606 and BL21(DE3) and comparison of the *E. coli* B and K-12 genomes. *J Mol Biol* **394**: 653–680.
- Studier, F. W. and Moffatt, B. A. (1986) Use of bacteriophage T7 RNA polymerase to direct selective high-level expression of cloned genes. *J Mol Biol* **189**: 113–130.
- Stülke, J. and Hillen, W. (1999) Carbon catabolite repression in bacteria. *Curr Opin Microbiol* **2**: 195–201.
- Sugiyama, K., Hayakawa, T., Kudo, T., Ito, T., and Yamaya, T. (2004) Interaction of *N*-acetylglutamate kinase with a P<sub>II</sub>-like protein in rice. *Plant Cell Physiol* **45**: 1768–1778.
- Sun, L., Wu, J., Du, F., Chen, X., and Chen, Z. J. (2012) Cyclic GMP-AMP synthase is a cytosolic DNA sensor that activates the type I interferon pathway. *Science* **339**: 786–791.
- Sureka, K., Choi, P. H., Precit, M., Delince, M., Pensinger, D. A., Huynh, T. N., *et al.* (2014) The cyclic dinucleotide c-di-AMP is an allosteric regulator of metabolic enzyme function. *Cell* **158**: 1389–1401.



- Sutherland, E. W. and Rall, T. W. (1958)** Fractionation and characterization of a cyclic adenine ribonucleotide formed by tissue particles. *J Biol Chem* **232**: 1077–1091.
- Suzuki, A. and Knaff, D. B. (2005)** Glutamate synthase: Structural, mechanistic and regulatory properties, and role in the amino acid metabolism. *Photosynth Res* **83**: 191–217.
- Takabayashi, A., Niwata, A., and Tanaka, A. (2016)** Direct interaction with ACR11 is necessary for post-transcriptional control of GLU1-encoded ferredoxin-dependent glutamate synthase in leaves. *Sci Rep* **6**: 29668.
- Terahara, N., Noguchi, Y., Nakamura, S., Kami-ike, N., Ito, M., Namba, K., et al. (2017)** Load- and polysaccharide-dependent activation of the Na<sup>+</sup>-type MotPS stator in the *Bacillus subtilis* flagellar motor. *Sci Rep* **7**: 46081.
- Thomas, G., Coutts, G., and Merrick, M. (2000)** The *glnKamtB* operon. A conserved gene pair in prokaryotes. *Trends Genet* **16**: 11–14.
- Towbin, H., Staehelin, T., and Gordon, J. (1979)** Electrophoretic transfer of proteins from polyacrylamide gels to nitrocellulose sheets: Procedure and some applications. *Proc Natl Acad Sci USA* **76**: 4350–4354.
- Ullmann, A. and Monod, J. (1968)** Cyclic AMP as an antagonist of catabolite repression in *Escherichia coli*. *FEBS Lett* **2**: 57–60.
- van Heeswijk, W. C., Wen, D., Clancy, P., Jaggi, R., Ollis, D. L., Westerhoff, H. V., et al. (2000)** The *Escherichia coli* signal transducers P<sub>II</sub> (GlnB) and GlnK form heterotrimers *in vivo*: Fine tuning the nitrogen signal cascade. *Proc Natl Acad Sci USA* **97**: 3942–3947.
- van Heeswijk, W. C., Westerhoff, H. V., and Boogerd, F. C. (2013)** Nitrogen assimilation in *Escherichia coli*: Putting molecular data into a systems perspective. *Microbiol Mol Biol Rev* **77**: 628–695.
- Vanoni, M. A., Verzotti, E., Zanetti, G., and Curti, B. (1996)** Properties of the recombinant  $\beta$  subunit of glutamate synthase. *Eur J Biochem* **236**: 937–946.
- Wach, A. (1996)** PCR-synthesis of marker cassettes with long flanking homology regions for gene disruptions in *S. cerevisiae*. *Yeast* **12**: 259–265.
- Wakeman, C. A., Goodson, J. R., Zacharia, V. M., and Winkler, W. C. (2014)** Assessment of the requirements for magnesium transporters in *Bacillus subtilis*. *J Bacteriol* **196**: 1206–1214.

- Wang, H., Baldwin, K. A., O’Sullivan, D. J., and McKay, L. L. (2000)** Identification of a gene cluster encoding krebs cycle oxidative enzymes linked to the pyruvate carboxylase gene in *Lactococcus lactis* ssp. *lactis* C2<sup>1,2</sup>. *J Dairy Sci* **83**: 1912–1918.
- Warburg, O. and Christian, W. (1942)** Isolation and crystallization of enolase. *Biochem Z* **310**: 384–421.
- Watanabe, H., Mori, H., Itoh, T., and Gojobori, T. (1997)** Genome plasticity as a paradigm of eubacteria evolution. *J Mol Evol* **44** (Suppl. 1): 57–64.
- Whatmore, A. M., Chudek, J. A., and Reed, R. H. (1990)** The effects of osmotic upshock on the intracellular solute pools of *Bacillus subtilis*. *J Gen Microbiol* **136**: 2527–2535.
- Wheatley, N. M., Eden, K. D., Ngo, J., Rosinski, J. S., Sawaya, M. R., Cascio, D., et al. (2016)** A P<sub>II</sub>-like protein regulated by bicarbonate: Structural and biochemical studies of the carboxysome-associated CP<sub>II</sub> protein. *J Mol Biol* **428**: 4013–4030.
- Whiteley, A. T., Garelis, N. E., Peterson, B. N., Choi, P. H., Tong, L., Woodward, J. J., et al. (2017)** c-di-AMP modulates *Listeria monocytogenes* central metabolism to regulate growth, antibiotic resistance and osmoregulation. *Mol Microbiol* **104**: 212–233.
- Whiteley, A. T., Pollock, A. J., and Portnoy, D. A. (2015)** The PAMP c-di-AMP is essential for *Listeria monocytogenes* growth in rich but not minimal media due to a toxic increase in (p)ppGpp. *Cell Host Microbe* **17**: 788–798.
- Wiseman, T., Williston, S., Brandts, J. F., and Lin, L.-N. (1989)** Rapid measurement of binding constants and heats of binding using a new titration calorimeter. *Anal Biochem* **179**: 131–137.
- Witte, G., Hartung, S., Büttner, K., and Hopfner, K.-P. (2008)** Structural biochemistry of a bacterial checkpoint protein reveals diadenylate cyclase activity regulated by DNA recombination intermediates. *Mol Cell* **30**: 167–178.
- Wohlhueter, R. M., Schutt, H., and Holzer, H. (1973)** Regulation of glutamine synthesis *in vivo* in *E. coli*. In: Prusiner, S. and Stadtman, E. R. (eds.) The enzymes of glutamine metabolism. Academic Press: New York: 45–64.
- Wu, J., Sun, L., Chen, X., Du, F., Shi, H., Chen, C., et al. (2013)** Cyclic GMP-AMP is an endogenous second messenger in innate immune signaling by cytosolic DNA. *Science* **339**: 826–830.

- Yakhnin, A. V., Murakami, K. S., and Babitzke, P. (2016)** NusG is a sequence-specific RNA polymerase pause factor that binds to the non-template DNA within the paused transcription bubble. *J Biol Chem* **291**: 5299–5308.
- Ye, M., Zhang, J.-J., Fang, X., Lawlis, G. B., Troxell, B., Zhou, Y., et al. (2014)** DhhP, a cyclic di-AMP phosphodiesterase of *Borrelia burgdorferi*, is essential for cell growth and virulence. *Infect Immun* **82**: 1840–1849.
- Zarella, T. M., Metzger, D. W., and Bai, G. (2018)** Stress suppressor screening leads to detection of regulation of cyclic di-AMP homeostasis by a Trk Family effector protein in *Streptococcus pneumoniae*. *J Bacteriol* **200**: e00045–18.
- Zeden, M. S., Schuster, C. F., Bowman, L., Zhong, Q., Williams, H. D., and Gründling, A. (2018)** Cyclic di-adenosine monophosphate (c-di-AMP) is required for osmotic regulation in *Staphylococcus aureus* but dispensable for viability in anaerobic conditions. *J Biol Chem* **293**: 3180–3200.
- Zhang, L. and He, Z.-G. (2013)** Radiation-sensitive gene A (RadA) targets DisA, DNA integrity scanning protein A, to negatively affect cyclic di-AMP synthesis activity in *Mycobacterium smegmatis*. *J Biol Chem* **288**: 22426–22436.
- Zhang, L., Li, W., and He, Z.-G. (2013)** DarR, a TetR-like transcriptional factor, is a cyclic di-AMP-responsive repressor in *Mycobacterium smegmatis*. *J Biol Chem* **288**: 3085–3096.
- Zhao, M.-X., Jiang, Y.-L., Xu, B.-Y., Chen, Y., Zhang, C.-C., and Zhou, C.-Z. (2010)** Crystal structure of the cyanobacterial signal transduction protein P<sub>II</sub> in complex with PipX. *J Mol Biol* **402**: 552–559.
- Zheng, C., Wang, J., Luo, Y., Fu, Y., Su, J., and He, J. (2013)** Highly efficient enzymatic preparation of c-di-AMP using the diadenylate cyclase DisA from *Bacillus thuringiensis*. *Enzyme Microb Technol* **52**: 319–324.
- Zhu, B. and Stülke, J. (2018)** SubtiWiki in 2018: From genes and proteins to functional network annotation of the model organism *Bacillus subtilis*. *Nucleic Acids Res* **46**: D743–D748.
- Zhu, Y., Pham, T. H., Nhiep, T. H. N., Vu, N. M. T., Marcellin, E., Chakrabortti, A., et al. (2016)** Cyclic-di-AMP synthesis by the diadenylate cyclase CdaA is modulated by the peptidoglycan biosynthesis enzyme GlmM in *Lactococcus lactis*. *Mol Microbiol* **99**: 1015–1027.



## 6 Appendix

### 6.1 Supplementary data

#### Rational bioinformatic search of interaction partners

All proteins listed in Table 6.1 are conserved between *Bacillus subtilis*, *Listeria monocytogenes* and *Staphylococcus aureus*. Furthermore, all proteins are less abundant than DarA in the cell and localized in the cytoplasm (or with unknown location). A separate list of proteins with missing quantification data was kept since they cannot be excluded completely (Table 6.2). Proteins that exhibit a tri-, hexa- or dodecameric structure are best suited for an interaction with DarA. Monomeric or dimeric proteins might also be suitable.

**Table 6.1: Bioinformatic search of rational DarA interaction partners.**

Name	Description	Localization	Structure <sup>a</sup>
AccC	Acetyl-CoA carboxylase (biotin carboxylase subunit)	–	2-hom
AcoL	Acetoin dehydrogenase (E3 dihydrolipoamide dehydrogenase)	Cytoplasm	–
ArgB	<i>N</i> -Acetylglutamate 5-phosphotransferase	Cytoplasm	6-hom
AroB	3-Dehydroquinate synthase	Cytoplasm	2-hom
AroC	3-Dehydroquinate dehydratase	–	2-hom
AroD	Shikimate dehydrogenase	–	1
AroK	Shikimate kinase	Cytoplasm	1
BglA	6-Phospho-beta-glucosidase)	–	2-hom
BkdAB	2-Oxoisovalerate dehydrogenase (E1 $\beta$ -subunit)	–	–
CatR	MarR/DUF24 family transcription repressor	–	–
CcpC	Transcriptional repressor (LysR family)	–	–
CggR	Central glycolytic genes regulator	Cytoplasm	2-hom
CinA	Unknown	Nucleoid	–
ClpC	AAA unfoldase, ATPase of ClpC-ClpP protease	Cytoplasm	1
ClpY	Two-component ATP-dependent protease, ATPase subunit	–	–
CodY	Transcriptional pleiotropic repressor	Cytoplasm	2-hom
CspR	tRNA (Um34/Cm34) methyltransferase homolog	–	2-hom
DltA	D-Alanyl-D-alanine carrier protein ligase	Cytoplasm	1
Dxs	1-Deoxyxylulose-5-phosphate synthase	–	2-hom
ExuR	Transcriptional repressor (LacI family)	–	–
FabHB	Beta-ketoacyl-acyl carrier protein synthase III	Cytoplasm	2-hom
FapR	Transcriptional repressor	–	2-hom
Fbp	Fructose-1,6-bisphosphatase	–	–
Fmt	Methionyl-tRNA formyltransferase	–	1
FolD	Methylenetetrahydrofolate dehydrogenase (NADP)	Cytoplasm	2-hom
Fur	Transcriptional repressor Fur family	Cytoplasm	–
GidA	tRNA uridine 5-carboxymethylaminomethyl modification enzyme	Cytoplasm	2-hom
GlmS	Glutamine-fructose-6-phosphate transaminase	Cytoplasm	1
GlpD	Glycerol-3-phosphate dehydrogenase (menaquinone 7)	Cytoplasm	1

**Table 6.1: Bioinformatic search of rational DarA interaction partners.**

Name	Description	Localization	Structure <sup>a</sup>
GlpK	Glycerol kinase	–	2-hom
GltA	Glutamate synthase (large subunit)	Cytoplasm	12-het
GltB	Glutamate synthase (small subunit)	Cytoplasm	12-het
GntK	Gluconokinase	–	1
GntZ	6-Phosphogluconate dehydrogenase	–	2-hom
GpsA	Glycerol-3-phosphate dehydrogenase (NAD)	Cytoplasm	2-hom
GsaB	Glutamate-1-semialdehyde aminotransferase	Cytoplasm	2-hom
GudB	Glutamate dehydrogenase, trigger enzyme	–	6-hom
GyrA	DNA gyrase (subunit A)	Nucleoid	2-hom
GyrB	DNA gyrase (subunit B)	Nucleoid	2-hom
HisH	Imidazole glycerol phosphate synthase (glutaminase subunit)	Cytoplasm	2-het
HprK	PtsH-HPr kinase/ phosphorylase	–	6-hom
HypO	NAD(P)H-flavin nitroreductase	–	–
IlvA	Threonine dehydratase	–	2-hom
InfB	Initiation factor IF-2	Cytoplasm	1
IolU	Minor NADP-dependent scyllo-inositol dehydrogenase	–	2-hom
KatX	Catalase (major catalase in spores)	Cytoplasm	–
KsgA	rRNA adenine dimethyltransferase	–	1
LepA	Elongation factor 4	Cytoplasm	–
LexA	Transcriptional repressor of the SOS regulon	–	2-hom
LigA	DNA ligase (NAD-dependent)	–	1
LpdV	2-Oxoisovalerate dehydrogenase (E3 dihydrolipoamide dehydrogenase)	–	2-hom
LplJ	Lipoate:protein ligase	–	–
LysS	Lysyl-tRNA synthetase	Cytoplasm	1
MalR	Two-component response regulator	Cytoplasm	–
Map	Methionine aminopeptidase	Cytoplasm	1
MecA	Adaptor protein	–	6-hom
MlpA	Specific processing protease	–	–
MnaA	UDP- <i>N</i> -acetylglucosamine 2-epimerase	Cytoplasm	2-hom
MoaB	Unknown	–	–
MoeA	Molybdopterin molybdenumtransferase	–	–
MraW	<i>S</i> -Adenosyl-L-methionine-dependent methyltransferase	Cytoplasm	2-hom
MsrA	Peptide methionine sulfoxide reductase	–	1
MsrB	Peptide methionine sulfoxide reductase	–	1
MurB	UDP- <i>N</i> -acetylenolpyruvoylglucosamine reductase	Banded	1
MurD	UMAG synthetase	Cytoplasm	–
MurE	UDP-Aagm-diaminoheptanedioate synthetase	Banded	1
MurF	UDP- <i>N</i> -acetylmuramoyl-L-alanyl-D-glutamyl- <i>meso</i> -2,6-diaminopimeloyl-D-alanyl-D-alanine synthetase	Cytoplasm, banded	1
MutL	DNA mismatch repair	Midcell foci	2-hom
MutY	A/G-specific adenine glycosylase	–	1
NagB	Glucosamine-6-phosphate deaminase	–	1
Nfo	Type IV apurinic/apyrimidinic endonuclease	Cytoplasm	1
NfrA	FMN-containing NADPH-linked nitro/flavin reductase	–	2-hom
NifS	Cysteine desulfurase	Cytoplasm	–

**Table 6.1: Bioinformatic search of rational DarA interaction partners.**

<b>Name</b>	<b>Description</b>	<b>Localization</b>	<b>Structure<sup>a</sup></b>
NrdE	Ribonucleoside-diphosphate reductase (major subunit)	–	2-hom
ParC	Subunit of DNA topoisomerase IV	Cytoplasm	1
PgcA	Alpha-phosphoglucomutase	–	–
PksC	Bacillaene synthase trans-acting acyltransferase	–	–
PncB	Putative nicotinate phosphoribosyltransferase	–	2-hom
PolX	DNA polymerase X	–	–
PpaC	Inorganic pyrophosphatase	Cytoplasm	2-hom
ProS	Prolyl-tRNA synthetase	Cytoplasm	2-hom
PurK	Phosphoribosylaminoimidazole carboxylase (ATP-dependent)	–	2-hom
PurN	Phosphoribosylglycinamide formyltransferase	–	2-hom
QueA	<i>S</i> -Adenosylmethionine tRNA ribosyltransferase	–	1
RecJ	Single-strand DNA-specific exonuclease	Cytoplasm	1
RecN	Unknown	Nucleoid, evenly	1
ResD	Two-component response regulator OmpR family	Cytoplasm	2-hom
Rho	Transcriptional termination protein	–	6-hom
Rnz	Endoribonuclease Z	–	2-hom
RplC	Ribosomal protein L3 (BL3)	Cytoplasm	–
RplF	Ribosomal protein L6 (BL8)	–	1
RpsC	Ribosomal protein S3 (BS3)	–	–
SdaAB	L-Serine deaminase (beta chain)	–	–
SigB	RNA polymerase sigma factor	–	3-het
SpeA	Arginine decarboxylase	Cytoplasm	–
Spo0A	Phosphorelay response regulator	–	1
SufU	Iron-sulfur cluster scaffold protein	–	1
Sul	Dihydropteroate synthase	–	1
TagD	Glycerol-3-phosphate cytidylyltransferase	Cytoplasm	2-hom
ThiD	HMP-PP kinase	–	2-hom
ThiE	Thiamine-phosphate pyrophosphorylase	–	1
ThiI	Sulfuryl transferase	Cytoplasm	2-hom
ThrS	Threonyl-tRNA synthetase (major)	–	1
ThrZ	Threonyl-tRNA synthetase (minor)	Cytoplasm	1
TrmB	tRNA (m7G46) methyltransferase	–	2-hom
TrmFO	tRNA:m(5)U-54 methyltransferase	Cytoplasm	1
TrmK	tRNA:m1A22 methyl transferase	–	1
TruB	tRNA pseudouridine 5S synthase	–	–
TrxB	thioredoxin reductase (NADPH)	Cytoplasm	2-hom
TsaB	tRNA modification enzyme	–	2-hom
Udk	Uridine kinase	–	–
UppS	Undecaprenyl pyrophosphate synthetase	–	2-hom
YabC	16S rRNA methyltransferase	–	2-hom
YbfQ	Unknown	–	–
YbxB	Unknown	–	–
YcgT	NADPH:ferredoxin oxidoreductase	–	2-hom
YdaD	Unknown	–	1
YdcI	Unknown	–	1

Table 6.1: Bioinformatic search of rational DarA interaction partners.

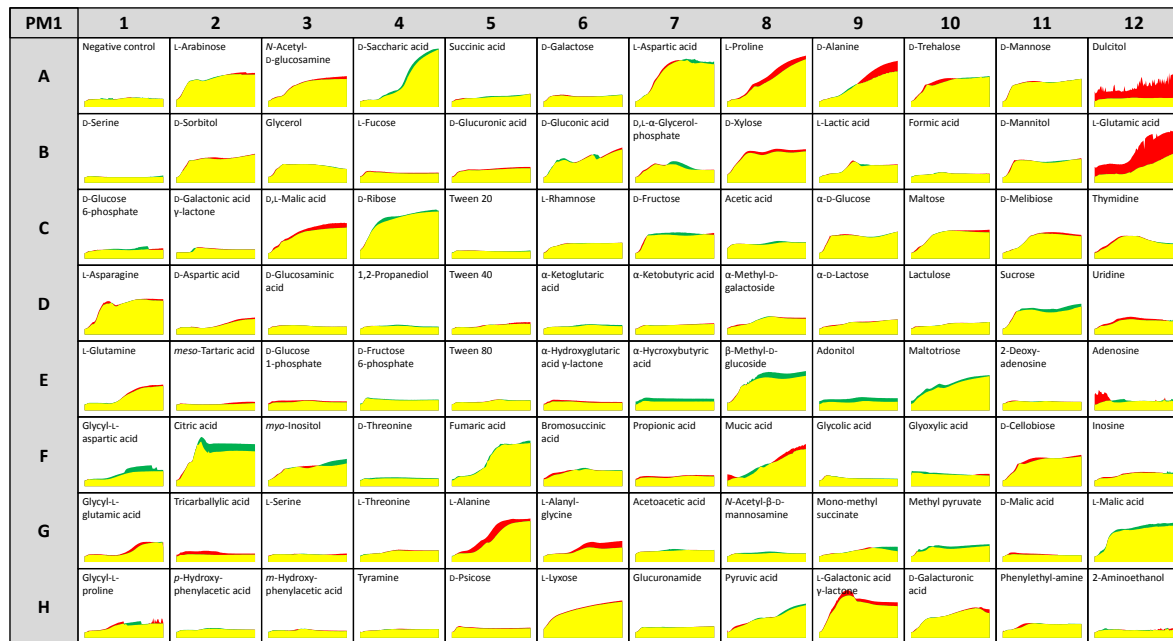
Name	Description	Localization	Structure <sup>a</sup>
YfmT	Vanillin dehydrogenase	–	2-hom
YhaM	RNase YhaM	Cytoplasm	–
YhcW	Unknown	–	1
YhfE	Similar to glucanase	–	12-hom
YhfK	Unknown	–	–
YisK	Modulator of Mbl activity	–	2-hom
YitS	Unknown	–	1
YitU	Unknown	–	–
YjcH	Unknown	–	–
YjgC	Formate dehydrogenase	–	–
YkaA	Unknown	–	–
YkrA	Unknown	–	1
YlaG	Unknown	–	1
YlbN	Unknown	–	–
YlmB	<i>N</i> -Formyl-4-amino-5-aminomethyl-2-methylpyrimidine deformylase	–	–
YlmE	Unknown	–	1
YlnD	Probable uroporphyrin-III C-methyltransferase	–	2-hom
YloV	Unknown	–	–
YlyB	Unknown	–	1
YojN	Similar to nitric-oxide reductase	–	6-hom
YpgQ	Mn <sup>2+</sup> -dependent pyrophosphohydrolase	–	2-hom
YphC	GTPase	Cytoplasm	1
YpiB	Unknown	–	–
YqeH	GTPase	–	1
YqeK	Predicted HD superfamily hydrolase (NAD metabolism)	–	2-hom
YqeU	Unknown	–	2-hom
YqiD	Geranyltransferase	–	2-hom
YqiK	Cytoplasmic glycerophosphodiester phosphodiesterase	Cytoplasm	2-hom
YqkF	NADPH-dependent 4-Hydroxy-2,3- <i>trans</i> -nonenal reductase	–	1
YrrO	Similar to protease	–	–
YsnA	ITPase	–	2-hom
YtaG	Dephospho-CoA kinase	–	3-hom
YtjP	Similar to succinyl-diaminopimelate disuccinylase	–	–
YtoP	Similar to glutamyl aminopeptidase	–	12-hom
YtsP	Unknown	–	2-hom
YumB	Unknown	–	–
YutD	Unknown	–	1
YutF	<i>p</i> -Nitrophenyl phosphatase	–	1
YvcK	UDP-sugar binding cell shape determinant	Helical-like	2-hom
YwtE	Unknown	–	1
YxiE	Unknown	–	–
YybB	Unknown	–	–

<sup>a</sup> hom: homomer, het: heteromer.

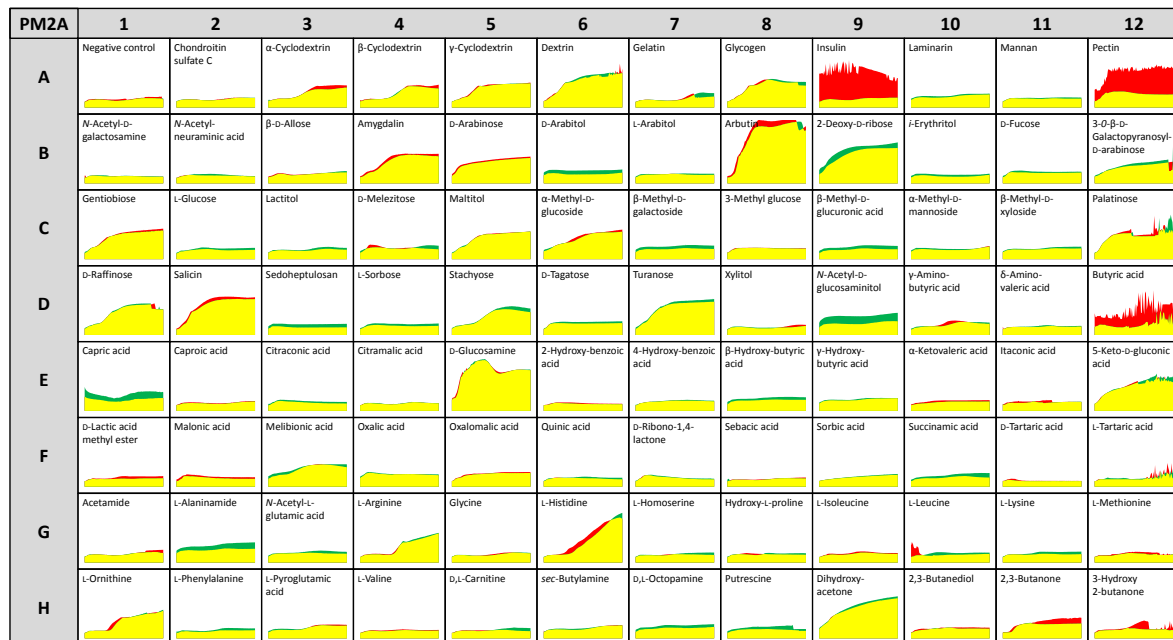


Table 6.2: Proteins with missing quantification data excluded from Table 6.1.

Aag	AcoA	AcpS	AdaB	AddA	AddB	AdhA	AdhR	AhrC	AlaS
AlaT	AlbF	AldY	Alr	AmhX	AnsA	AraL	AraR	ArgF	ArgJ
ArsC	AscR	BacC	BceR	BirA	BkdB	BmrU	BsaA	BsdA	CatE
Cca	CcpB	CcpN	CdaS	CheB	CitA	ClpX	CmoO	CodV	CpgA
CshB	CsoR	CssR	CtpA	CtsR	CysE	Dck	DctR	DeaD	DegV
DhbA	DinG	DltD	DltE	DnaA	DnaC	DnaE	DnaG	DnaJ	DnaN
DprA	Drm	EpsH	Era	FdhD	FolK	FrlR	FruK	FruR	GabT
GamA	GamR	GanR	GbsB	GcaD	GcvH	GcvPA	GdpP	GerE	GgaA
GidB	GlcT	GlmM	GlnL	GlnR	GlpP	GltC	GmuD	GmuF	GmuR
GuaD	GutB	HemC	HemN	HepT	Hfq	HolA	HolB	HrcA	InfC
Int	IolD	IolJ	IspE	KdgR	KinA	KinE	LcfA	LcfB	LiaR
LicR	LicT	LipL	LnrK	LutR	Maa	MalL	ManA	ManR	MccA
MenE	MenH	Mfd	MgsR	MhqE	MhqO	MiaA	MmgD	Moaa	MobA
MobB	MoeB	MrnC	MsmR	Mta	MtlF	MtnE	MtnU	MurP	MutM
MutS	MutTA	NadB	NadD	NagA	NasB	NasD	NasF	NdoA	NifZ
NrdEB	NrdR	NtdA	NtdC	Nth	NusB	OatA	Obg	Ogt	OhrR
PaiA	ParB	ParE	PcrB	Pdp	PepT	PerR	PhoR	PksE	PksG
PksJ	PksN	Pmi	PolA	PolC	PolY1	PpsA	PpsB	PpsC	PpsD
PrfA	PriA	Prp	PrpC	PsdR	PstBB	QueG	RacE	RadA	RadC
RbfA	RbgA	RbsR	RecF	RecG	RecQ	RecR	RecU	RelA	Rex
RhaEW	RhaR	RibC	RibR	RicA	RicF	RicT	RipX	RlmCD	RluB
Rnc	RnhB	RnhC	RnmV	RnpA	Rnr	RocG	RplB	RplI	RplK
RplN	RplO	RplP	RplQ	RplS	RplU	RplX	RpmA	RpmB	RpmC
RpmD	RpmE	RpmEB	RpmGA	RpmH	RpmI	RpmJ	RpoE	RpsH	RpsI
RpsJ	RpsK	RpsL	RpsM	RpsN	RpsNB	RpsO	RpsP	RpsR	RpsS
RpsT	RpsU	RuvB	SbcD	ScpB	SdaAA	SigE	SigG	SmpB	SnaB
SndA	Spo0F	SpoVB	SpoVC	SpsJ	SpsK	Spx	TenI	ThdF	ThiM
ThrD	ThyA	ThyB	TilS	Tmk	TnrA	TopA	TopB	TreA	TrmD
TrpB	TrpC	TrpD	TrpF	TrpS	TruA	TsaC	TsaD	TsaE	TuaG
Ung	UvrA	UvrB	UvrC	UvrX	Veg	WalJ	WalR	XpaC	XtmB
YaaA	YaaJ	YaaK	YaaN	YaaO	YabB	YabO	YabR	YacF	YacL
YacO	YacP	YbdJ	YbgE	YcbL	YccK	YceB	YckE	YclJ	YcnD
YcsD	YcsN	YcxD	YdaB	YdcK	YddN	YdeE	YdeF	YdeI	YdeL
YdfD	YdfI	YdfK	YdhC	YdiD	YdiG	YdiL	YerC	YesN	YfhP
YfiH	YfjN	YfjO	YfkH	YfkJ	YflK	YflL	YflN	YfmL	YgaC
YgzD	YhaO	YhcF	YhcR	YhcT	YhcY	YhcZ	YhdI	YhdW	YheB
YhfW	YhjE	YhxC	YisV	YitW	YizB	YjbH	YjbO	YjcF	YjcK
YjdI	YjmD	YjmF	YkgA	YkoG	YkrP	YktA	YkuR	YkvS	YkvZ
YkwD	YlaN	YlbC	YlbH	YlbI	YlbM	YlmG	YlmH	YloA	YloH
YloI	YloM	YloN	YloS	YloU	YlxM	YlxR	YmfC	YnbA	YneI
YneN	YneP	YngB	YngH	YngI	YnzC	YobH	YobT	YodB	YodT
YojE	YonN	YorL	YozK	YpcP	YplQ	YprA	YpsA	YpsC	YqeC
YqeG	YqeI	YqeL	YqeM	YqeT	YqgN	YqgS	YqhH	YqiB	YqjA
YqxD	YrbF	YrhD	YrhE	YrkA	YrkP	YrkQ	YrpB	YrpC	YrrK
YrrM	YrrN	YrvJ	YrvO	YrzB	YrzL	YsgA	YtbE	YtcB	YtcI
YtfP	YthA	YtjA	YtkP	YtlR	YtmI	YtmP	YtnP	YtoI	YtpP
YtqA	YtqB	YtrA	YttB	YtxM	YtzG	YueD	YugP	YugS	YugT
YunD	YunE	YunF	YutI	YuzB	YuzD	YvaG	YvbT	YvbU	YvdE
YvfU	YvrC	YvrD	YvrHb	YvyE	YwbD	YwbI	YwcH	YwdK	YwfO
YwhB	YwkE	YwlE	YwoG	YwoH	YwpD	YwpJ	YxaA	YxdJ	YxjL
YyaN	YyaT	YybA	YybD	YybJ	YydA	YyzE	YyzM	Zur	

Phenotype MicroArray screening for *darA* deletion phenotypes

**Figure 6.1: Phenotype screening for carbon sources.** Using the Biolog screening system PM1 plate, the utilization of different carbon sources was tracked over a time course of 48 h at 37 °C by measuring the OD<sub>590</sub>. Data for *B. subtilis* wild type (168, ■), *darA* deletion mutant (GP1712, ■) and overlay (■). No significant differences were observed. Difference for well A12 is an artifact, difference for well B12 could not be reproduced.



**Figure 6.2: Phenotype screening for carbon sources.** Using the Biolog screening system PM2A plate, the utilization of different carbon sources was tracked over a time course of 48 h at 37 °C by measuring the OD<sub>590</sub>. Data for *B. subtilis* wild type (168, ■), *darA* deletion mutant (GP1712, ■) and overlay (■). No significant differences were observed. Differences for wells A9, A12 and D12 are artifacts.

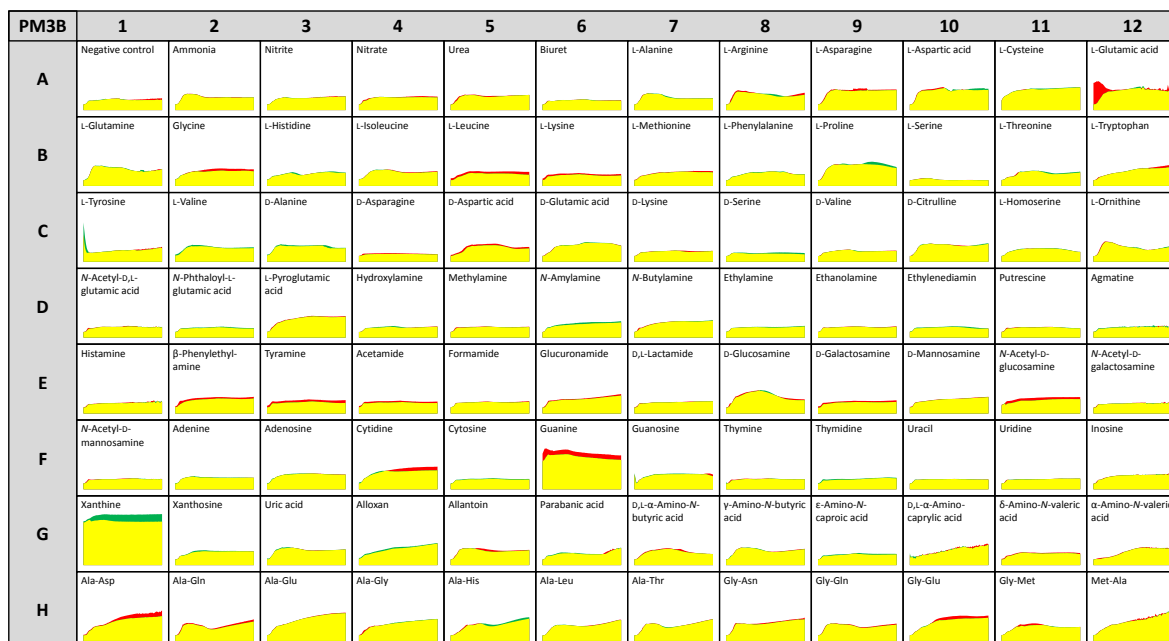


**Figure 6.3: Phenotype screening for nitrogen sources.** Using the Biolog screening system PM3B plate, the utilization of different nitrogen sources was tracked over a time course of 48 h at 37 °C by measuring the OD<sub>590</sub>. Data for *B. subtilis* wild type (168, ■), *darA* deletion mutant (GP1712, ■) and overlay (■). No significant differences were observed.

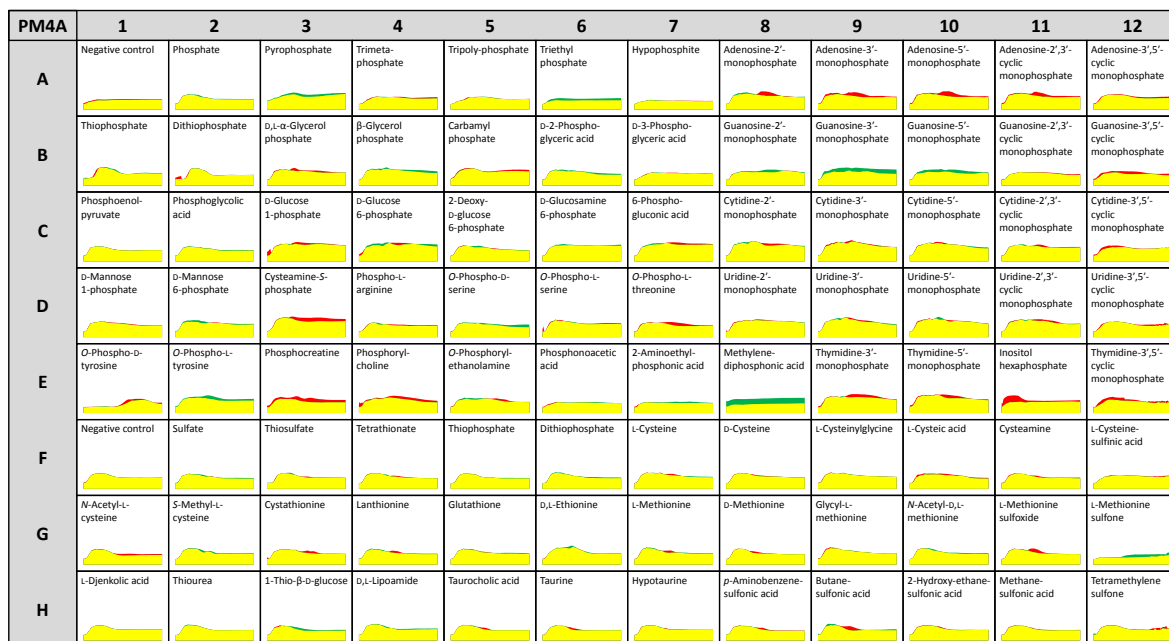


**Figure 6.4: Phenotype screening for phosphorus and sulfur sources.** Using the Biolog screening system PM4A plate, the utilization of different phosphorus and sulfur sources was tracked over a time course of 48 h at 37 °C by measuring the OD<sub>590</sub>. Data for *B. subtilis* wild type (168, ■), *darA* deletion mutant (GP1712, ■) and overlay (■). No significant differences were observed.



**Figure 6.5: Phenotype screening for nutrient supplements.** Using the Biolog screening system PM5 plate, the utilization of different nutrient supplements was tracked over a time course of 48 h at 37 °C by measuring the OD<sub>590</sub>. Data for *B. subtilis* wild type (168, ■), *darA* deletion mutant (GP1712, ■) and overlay (■). No significant differences were observed.

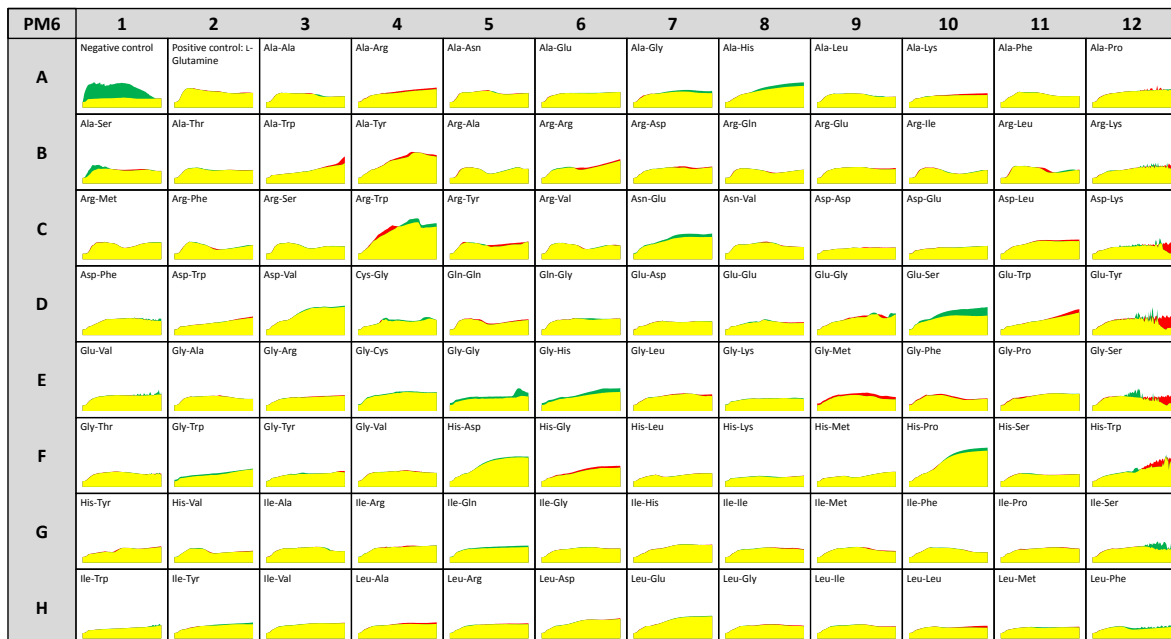


**Figure 6.6: Phenotype screening for peptide nitrogen sources.** Using the Biolog screening system PM6 plate, the utilization of different peptide nitrogen sources was tracked over a time course of 48 h at 37 °C by measuring the OD<sub>590</sub>. Data for *B. subtilis* wild type (168, ■), *darA* deletion mutant (GP1712, ■) and overlay (■). No significant differences were observed.

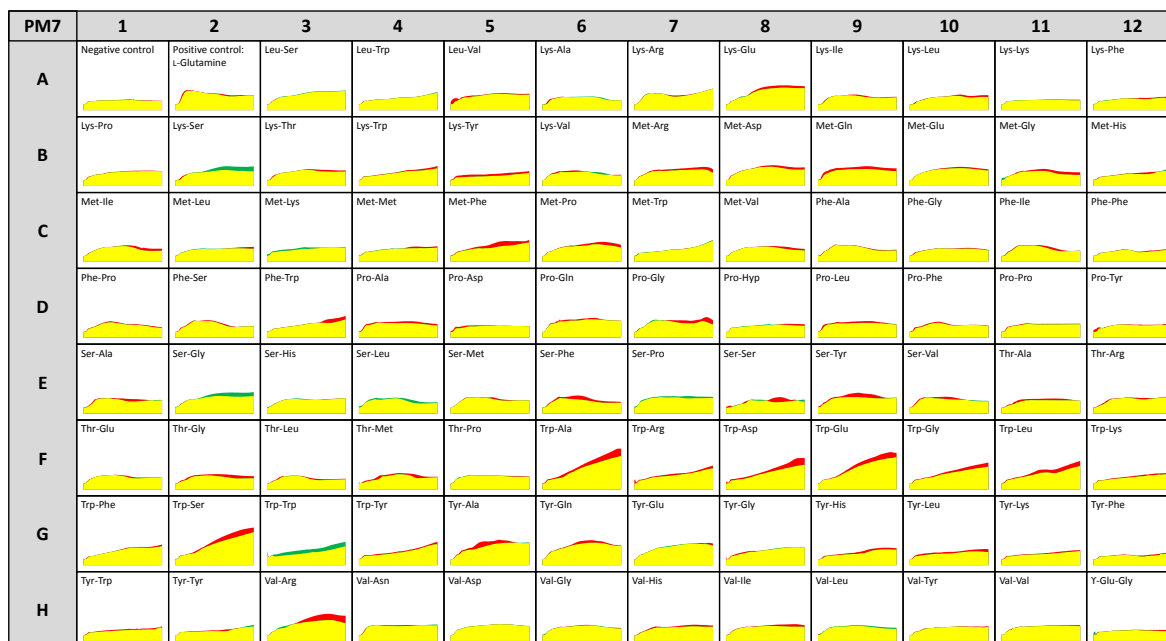


**Figure 6.7: Phenotype screening for peptide nitrogen sources.** Using the Biolog screening system PM7 plate, the utilization of different peptide nitrogen sources was tracked over a time course of 48 h at 37 °C by measuring the OD<sub>590</sub>. Data for *B. subtilis* wild type (168, ■), *darA* deletion mutant (GP1712, ■) and overlay (■). No significant differences were observed.

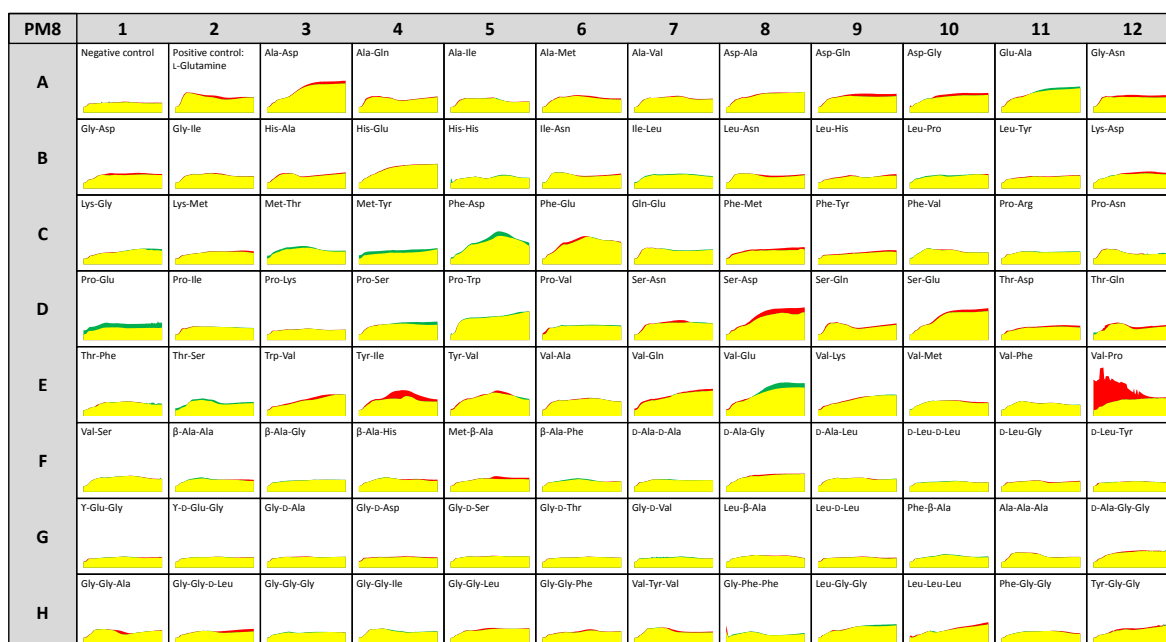


**Figure 6.8: Phenotype screening for peptide nitrogen sources.** Using the Biolog screening system PM8 plate, the utilization of different peptide nitrogen sources was tracked over a time course of 48 h at 37 °C by measuring the OD<sub>590</sub>. Data for *B. subtilis* wild type (168, ■), *darA* deletion mutant (GP1712, ■) and overlay (■). No significant differences were observed. Difference for well A12 is an artifact.

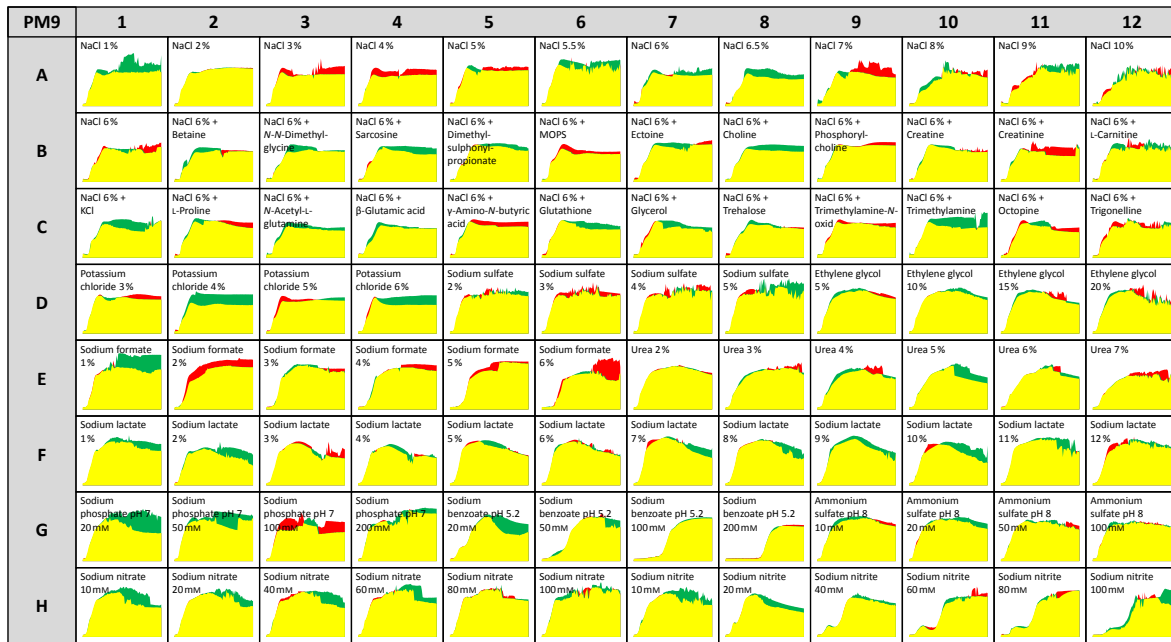


**Figure 6.9: Phenotype screening for osmolytes.** Using the Biolog screening system PM9 plate, the metabolic activity under different osmolyte conditions was tracked over a time course of 48 h at 37 °C by measuring the OD<sub>590</sub>. Data for *B. subtilis* wild type (168, ■), *darA* deletion mutant (GP1712, ■) and overlay (■). No significant differences were observed.

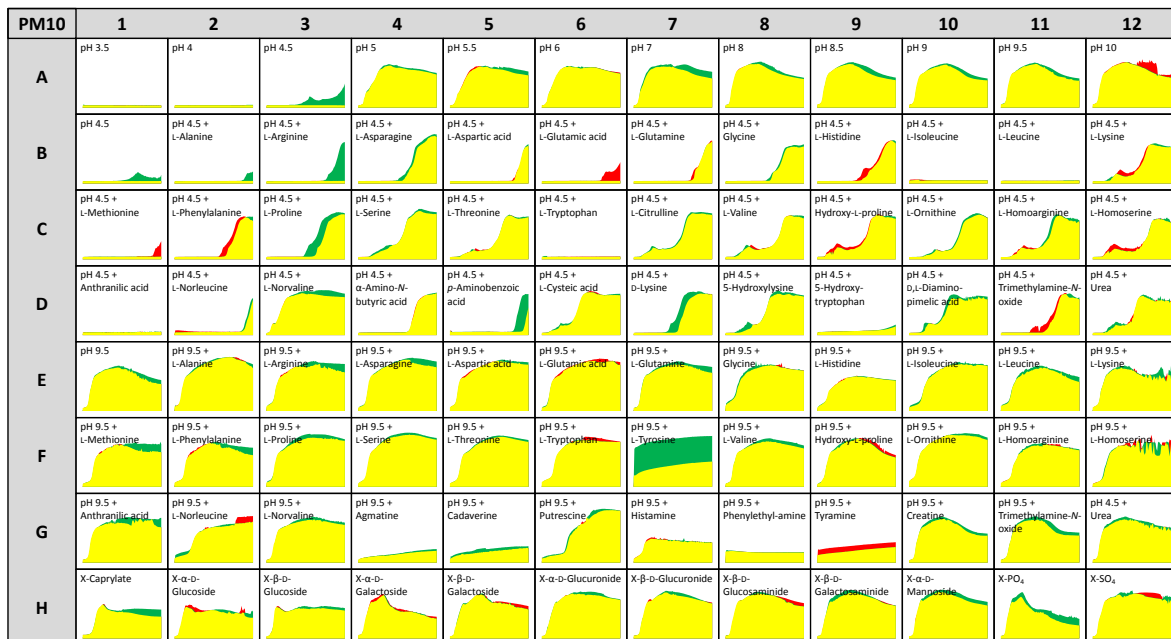


**Figure 6.10: Phenotype screening for pH.** Using the Biolog screening system PM10 plate, the metabolic activity under different pH conditions was tracked over a time course of 48 h at 37 °C by measuring the OD<sub>590</sub>. Data for *B. subtilis* wild type (168, ■), *darA* deletion mutant (GP1712, ■) and overlay (■). No significant differences were observed. Differences for wells A3, B3 and F7 are artifacts.

## 6.2 Bacterial strains

**Table 6.3: Bacterial strains created in this work.**

Name	Genotype	Construction
GP2401	<i>trpC2 tmk-3</i> × <i>FLAG spc</i>	pGP2786 → 168
GP2402	<i>trpC2 ermC-kimA</i>	LFH-PCR → 168
GP2403	<i>trpC2 ermC-kimA</i> Δ <i>darA::cat</i>	GP1712 → GP2402
GP2404	<i>trpC2 ermC-kimA-3</i> × <i>FLAG spc</i>	pGP2789 → GP2402
GP2406	<i>trpC2</i> Δ <i>darA::ermC</i>	LFH-PCR → 168
GP2407	<i>trpC2 amyE::(p<sub>kimA</sub>-RS-lacZ cat)</i> Δ <i>darA::ermC</i>	GP2406 → BP144
GP2408	<i>trpC2 amyE::(p<sub>kimA</sub>-lacZ cat)</i> Δ <i>darA::ermC</i>	GP2406 → GP2182
GP2409	<i>trpC2</i> Δ <i>oppABCDF::aphA3</i> Δ <i>darA::cat kinA<sub>E551</sub>STOP</i>	GP2097 → GP1712
GP2410	<i>trpC2</i> Δ <i>oppABCDF::aphA3</i> Δ <i>darA::cat kinA<sub>E551</sub>STOP</i> Δ <i>cdaS::ermC</i>	GP983 → GP2409
GP2411	<i>trpC2</i> Δ <i>oppABCDF::aphA3</i> Δ <i>darA::cat kinA<sub>E551</sub>STOP</i> Δ <i>cdaS::ermC</i> Δ <i>cdaA::spc</i>	GP94 → GP2410
GP2412	<i>trpC2</i> Δ <i>oppABCDF::aphA3</i> Δ <i>darA::cat kinA<sub>E551</sub>STOP</i> Δ <i>cdaS::ermC</i> Δ <i>disA::tet</i>	GP987 → GP2410
GP2413	<i>trpC2</i> Δ <i>cdaS::ermC</i> Δ <i>disA::tet</i> Δ <i>darA::cat</i>	GP1712 → GP991
GP2414	<i>trpC2 gudB1 amyE::(gltA-lacZ aphA3)</i> Δ <i>darA::cat</i>	GP1712 → GP804
GP2415	<i>trpC2</i> Δ <i>darA::spc</i>	LFH-PCR → 168
GP2416	<i>trpC2 lacA::(p<sub>deg</sub> Strep-darA aphA3)</i> Δ <i>darA::cat</i>	pGP2790 → GP1712
GP2417	<i>trpC2</i> Δ <i>darA::cat</i>	pGP2790 → GP1712
GP2418	<i>trpC2</i> Δ <i>cdaS::ermC</i> Δ <i>disA::tet</i> Δ <i>darA::cat lacA::(p<sub>deg</sub></i> <i>Strep-darA aphA3)</i>	GP2416 → GP2413
GP2419	<i>trpC2</i> Δ <i>cdaS::ermC</i> Δ <i>disA::tet</i> Δ <i>darA::cat lacA::(p<sub>deg</sub></i> <i>darA-Strep aphA3)</i>	GP2010 → GP2413
GP2420	<i>trpC2</i> Δ <i>cdaS::ermC</i> Δ <i>disA::tet</i> Δ <i>darA::cat</i> Δ <i>cdaA::spc</i> <i>ykoX<sub>K218</sub>STOP</i>	GP94 → GP2413
GP2421	<i>trpC2</i> Δ <i>cdaS::ermC</i> Δ <i>disA::tet</i> Δ <i>darA::cat lacA::(p<sub>deg</sub></i> <i>Strep-darA aphA3)</i> Δ <i>cdaA::spc</i>	GP94 → GP2418
GP2422	<i>trpC2</i> Δ <i>cdaS::ermC</i> Δ <i>disA::tet</i> Δ <i>darA::cat lacA::(p<sub>deg</sub></i> <i>darA-Strep aphA3)</i> Δ <i>cdaA::spc</i>	GP94 → GP2419
GP2423	<i>trpC2</i> Δ <i>ahrC::aphA3</i> Δ <i>darA::cat</i> several SNPs	GP1712 → GP729
GP2424	<i>trpC2</i> Δ <i>khtSTU::aphA3</i> Δ <i>darA::cat</i>	GP1712 → GP2078
GP2425	<i>trpC2 lacA::(p<sub>deg</sub> Strep-darA aphA3)</i>	pGP2790 → 168
GP2426	<i>trpC2 lacA::(p<sub>deg</sub> darA-Strep aphA3)</i>	pGP2630 → 168
GP2427	<i>trpC2 gudB amyE::(cfp cat)</i> Δ <i>darA::ermC</i>	GP2406 → BP52
GP2428	<i>trpC2 gudB amyE::(cfp cat)</i> Δ <i>oppABCDF::aphA3</i>	GP2097 → BP52
GP2429	<i>trpC2 gudB amyE::(cfp cat)</i> Δ <i>darA::ermC</i> Δ <i>oppABCDF::aphA3</i>	GP2428 → GP2427
GP2430	<i>trpC2</i> Δ <i>darA::cat</i> Δ <i>oppABCDF::aphA3</i>	GP2097 → GP1712
GP2431	<i>trpC2</i> Δ <i>oppABCDF::aphA3</i> Δ <i>darA::cat kinA<sub>E551</sub>STOP gudB1</i> <i>appA<sub>pos.468</sub> (A)7 → (A)8</i>	GP2409 suppressor <sup>a</sup>

Table 6.3: Bacterial strains created in this work.

Name	Genotype	Construction
GP2432	<i>trpC2 khtU-3×FLAG spc</i>	pGP2791 → 168
GP2433	<i>trpC2 ΔdarA::cat khtU-3×FLAG spc</i>	pGP2791 → GP1712
GP2434	<i>trpC2 ktrD-3×FLAG spc</i>	pGP2792 → 168
GP2435	<i>trpC2 ΔdarA::cat ktrD-3×FLAG spc</i>	pGP2792 → GP1712
GP2436	<i>trpC2 nhaK-3×FLAG spc</i>	pGP2793 → 168
GP2437	<i>trpC2 ΔdarA::cat nhaK-3×FLAG spc</i>	pGP2793 → GP1712
GP2438	<i>trpC2 yjbQ-3×FLAG spc</i>	pGP2794 → 168
GP2439	<i>trpC2 ΔdarA::cat yjbQ-3×FLAG spc</i>	pGP2794 → GP1712
GP2440	<i>trpC2 yrvD-3×FLAG spc</i>	pGP2795 → 168
GP2441	<i>trpC2 ΔdarA::cat yrvD-3×FLAG spc</i>	pGP2795 → GP1712
GP2442	<i>trpC2 yugO-3×FLAG spc</i>	pGP2796 → 168
GP2443	<i>trpC2 ΔdarA::cat yugO-3×FLAG spc</i>	pGP2796 → GP1712
GP2444	<i>trpC2 ktrAB::spc</i>	GP2716 → GP1712
GP2445	<i>trpC2 lacA::(p<sub>deg</sub> Strep-darA aphA3) ktrAB::spc</i>	GP2716 → GP2425
GP2446	<i>trpC2 lacA::(p<sub>deg</sub> Strep-darA aphA3) ktrA<sub>p(TAAA<math>\underline{T}</math>T→TAAA<math>\underline{C}</math>T)</sub></i>	GP2425 suppressor <sup>a</sup>
GP2447	<i>trpC2 lacA::(p<sub>deg</sub> Strep-darA aphA3) odhA<sub>N320H</sub></i>	GP2425 suppressor <sup>b</sup>
GP2448	<i>trpC2 lacA::(p<sub>deg</sub> Strep-darA aphA3) odhA<sub>K64STOP</sub></i>	GP2425 suppressor <sup>b</sup>
GP2449	<i>trpC2 lacA::(p<sub>deg</sub> Strep-darA aphA3) gltC<sub>G230A</sub></i>	GP2425 suppressor <sup>a</sup>
GP2450	<i>trpC2 lacA::(p<sub>deg</sub> Strep-darA aphA3) ktrA<sub>p(TAAA<math>\underline{T}</math>T→TAAA<math>\underline{C}</math>T)</sub></i>	GP2425 suppressor <sup>b</sup>
GP2451	<i>trpC2 lacA::(p<sub>deg</sub> Strep-darA aphA3) odhA<sub>Q523STOP</sub></i>	GP2425 suppressor <sup>b</sup>
GP2452	<i>trpC2 lacA::(p<sub>deg</sub> Strep-darA aphA3) odhA<sub>Δbp373</sub></i>	GP2425 suppressor <sup>a</sup>
GP2453	<i>trpC2 lacA::(p<sub>deg</sub> Strep-darA aphA3) ktrB<sub>G23V,A64T</sub></i>	GP2425 suppressor <sup>b</sup>
GP2454	<i>trpC2 lacA::(p<sub>deg</sub> Strep-darA aphA3) ktrB<sub>G23V,N184S</sub></i>	GP2425 suppressor <sup>b</sup>
GP2455	<i>trpC2 lacA::(p<sub>deg</sub> Strep-darA aphA3) ktrB<sub>N184S atpB<sub>G93W</sub></sub></i>	GP2425 suppressor <sup>a</sup>
GP2456	<i>trpC2 lacA::(p<sub>deg</sub> Strep-darA aphA3) ktrB<sub>G23V,N184S</sub></i>	GP2425 suppressor <sup>b</sup>
GP2457	<i>trpC2 ktrB<sub>G23V,T394S</sub></i>	168 suppressor <sup>b</sup>
GP2458	<i>trpC2 ktrB<sub>G23V</sub></i>	168 suppressor <sup>b</sup>
GP2459	<i>trpC2 ktrB<sub>E116A</sub></i>	168 suppressor <sup>b</sup>
GP2460	<i>trpC2 ΔdarA::cat ΔcdaA::spc ΔcdaS::ermC</i>	GP983 → GP1715
GP2461	<i>trpC2 ΔktrAB::aphA3 ΔkimA::cat ΔdarA::spc</i>	GP2415 → GP2165
GP2462	<i>trpC2 ΔdarA::cat ktrB<sub>E116A,N184S,L299STOP</sub></i>	GP1712 suppressor <sup>b</sup>
GP2463	<i>trpC2 ΔdarA::cat ktrB<sub>L212Q</sub></i>	GP1712 suppressor <sup>b</sup>
GP2464	<i>trpC2 ΔdarA::cat ktrB<sub>64V,R331K</sub></i>	GP1712 suppressor <sup>b</sup>
GP2465	<i>trpC2 lacA::(p<sub>deg</sub> Strep-darA aphA3) ktrB<sub>G23V,V381G</sub></i>	GP2425 suppressor <sup>b</sup>
GP2466	<i>trpC2 ktrB<sub>G23V,A64V,Q85H</sub></i>	168 suppressor <sup>b</sup>
GP2467	<i>trpC2 ΔdarA::cat lacA::(p<sub>deg</sub> darA aphA3)</i>	pGP3005 → GP1712
GP2468	<i>trpC2 ΔdarA::cat lacA::(p<sub>deg</sub> darA<sub>F36E</sub> aphA3)</i>	pGP3006 → GP1712
GP2469	<i>trpC2 ΔdarA::cat lacA::(p<sub>deg</sub> darA<sub>R26E</sub> aphA3)</i>	pGP3007 → GP1712
GP2470	<i>trpC2 ΔpycA::cat ΔdarA::spc</i>	GP793 → GP2415
GP2471	<i>trpC2 lacA::(p<sub>deg</sub> darA aphA3)</i>	pGP3005 → 168



Table 6.3: Bacterial strains created in this work.

Name	Genotype	Construction
GP2472	<i>trpC2 lacA::(p<sub>deg</sub> Strep-darA aphA3) ΔdarA::cat ΔahrC::ermC</i>	GP2185 → GP2416
GP2473	<i>trpC2 ΔcodY::spc</i>	BB1043 → 168
GP2474	<i>trpC2 ΔdarA::cat ΔcodY::spc</i>	BB1043 → GP1712
GP2475	<i>trpC2 ΔcodY::spc ΔahrC::aphA3</i>	GP729 → GP2473
GP2476	<i>trpC2 ΔcodY::spc ΔahrC::ermC</i>	GP2185 → GP2473
GP2477	<i>trpC2 ΔdarA::cat ΔcodY::spc ΔahrC::aphA3</i>	GP729 → GP2474
GP2478	<i>trpC2 ΔdarA::cat ΔcodY::spc ΔahrC::ermC</i>	GP2185 → GP2474
GP2479	<i>trpC2 ΔdarA::cat lacA::(p<sub>deg</sub> darA aphA3) ΔahrC::ermC</i>	GP2185 → GP2467
GP2480	<i>trpC2 ΔdarA::cat lacA::(p<sub>deg</sub> darA<sub>F36E</sub> aphA3) ΔahrC::ermC</i>	GP2185 → GP2468
GP2481	<i>trpC2 ΔargB::ermC</i>	BKE11210 → 168
GP2482	<i>trpC2 ΔdarA::cat ΔargB::ermC</i>	GP2481 → GP1712
GP2483	<i>trpC2 ΔahrC::aphA3 ΔargB::ermC</i>	GP2481 → GP729
GP2484	<i>trpC2 ΔdarA::cat ΔahrC::aphA3 ΔargB::ermC</i>	GP2481 → GP2423
GP2485	<i>trpC2 ΔdarA::cat ΔahrC::ermC</i>	GP2485 → GP1712
GP2486	<i>trpC2 ΔdarA::cat ΔglnA::ermC</i>	GP2263 → GP1712
GP2487	<i>trpC2 ΔdarA::cat ΔahrC::aphA3</i>	GP729 → GP1712
GP2488	<i>trpC2 ΔdarA::cat spo0A<sub>A178T</sub> yvdK<sub>Δbp699</sub></i>	GP1712 suppressor <sup>a</sup>
GP2489	<i>trpC2 ΔdarA::cat spo0B<sub>R29Q</sub> putP<sub>Y337C</sub></i>	GP1712 suppressor <sup>a</sup>
GP2490	<i>trpC2 ΔdarA::cat spo0A<sub>P167S</sub></i>	GP1712 suppressor <sup>b</sup>
GP2491	<i>trpC2 ΔdarA::cat lacA::(p<sub>deg</sub> Strep-darA<sub>F36E</sub> aphA3)</i>	pGP3026 → GP1712
GP2492	<i>trpC2 ΔpycA::cat Δpta::aphA3</i>	GP668 → GP793
GP2493	<i>trpC2 ΔpycA::cat ΔackA::aphA3</i>	GP1902 → GP793
GP2494	<i>trpC2 ΔpycA::cat ΔcdaA::spc</i>	GP94 → GP793
GP2495	<i>trpC2 ΔktrAB::aphA3 ΔkimA::cat ΔdarA::spc ΔahrC::ermC</i>	GP2185 → GP2461
GP2496	<i>trpC2 ΔcdaS::ermC ΔdisA::tet ΔdarA::cat ΔcdaA::spc ykoX<sub>K218STOP</sub> ktrC<sub>G11C</sub> yfkF<sub>G294S</sub> nusG<sub>T82K</sub></i>	GP2420 suppressor <sup>b</sup>
GP2497	<i>trpC2 ΔdarA::tet</i>	LFH → 168
GP2498	<i>trpC2 ΔkimA::cat ΔktrAB::spc</i>	GP2716 → GP93
GP2499	<i>trpC2 ΔkimA::cat ΔktrAB::spc ΔdarA::tet</i>	GP2497 → GP2498
GP2500	<i>trpC2 ΔkimA::cat ΔktrAB::spc ΔdarA::tet lacA::(p<sub>deg</sub> darA aphA3)</i>	GP2471 → GP2499
GP3001	<i>trpC2 ΔkimA::cat ΔktrAB::spc ΔahrC::ermC</i>	GP2185 → GP2498
GP3002	<i>trpC2 ΔkimA::cat ΔktrAB::spc ΔdarA::tet ΔahrC::ermC</i>	GP2185 → GP2499
GP3003	<i>trpC2 ΔkimA::cat ΔktrAB::spc ΔdarA::tet lacA::(p<sub>deg</sub> darA aphA3) ΔahrC::ermC</i>	GP2185 → GP2500
GP3004	<i>trpC2 ΔkimA::cat ΔktrAB::spc lacA::(p<sub>deg</sub> darA aphA3)</i>	GP2471 → GP2498
GP3005	<i>trpC2 ΔkimA::cat ΔktrAB::spc lacA::(p<sub>deg</sub> darA aphA3) ΔahrC::ermC</i>	GP2185 → GP3004

**Table 6.3: Bacterial strains created in this work.**

Name	Genotype	Construction
GP3006	<i>trpC2</i> $\Delta$ <i>kimA::cat</i> $\Delta$ <i>ktrAB::spc</i> $\Delta$ <i>darA::tet</i> <i>lacA::(p<sub>deg</sub> Strep-darA aphA3)</i>	GP2425 → GP2499
GP3007	<i>trpC2</i> $\Delta$ <i>kimA::cat</i> $\Delta$ <i>ktrAB::spc</i> $\Delta$ <i>darA::tet</i> <i>lacA::(p<sub>deg</sub> darA-Strep aphA3)</i>	GP2426 → GP2499
GP3008	<i>trpC2</i> $\Delta$ <i>kimA::cat</i> $\Delta$ <i>ktrAB::spc</i> $\Delta$ <i>darA::tet</i> <i>lacA::(p<sub>deg</sub> Strep-darA aphA3)</i> $\Delta$ <i>ahrC::ermC</i>	GP2185 → GP3006
GP3009	<i>trpC2</i> $\Delta$ <i>kimA::cat</i> $\Delta$ <i>ktrAB::spc</i> $\Delta$ <i>darA::tet</i> <i>lacA::(p<sub>deg</sub> darA-Strep aphA3)</i> $\Delta$ <i>ahrC::ermC</i>	GP2185 → GP3007
GP3010	<i>trpC2</i> $\Delta$ <i>cdaS::ermC</i> $\Delta$ <i>disA::tet</i> $\Delta$ <i>darA::cat</i> $\Delta$ <i>cdaA::spc</i> <i>ykoX<sub>K218STOP</sub></i> <i>ktrC<sub>G11C</sub></i> <i>yfkF<sub>G294S</sub></i> <i>nusG<sub>T82K</sub></i> <i>kimA<math>\Delta</math><sub>G112</sub></i> <i>ccpA<math>\Delta</math><sub>bp850-1005incl.24bp(3')</sub></i> <i>motP<sub>START1STOP</sub></i>	GP2420 suppressor <sup>a</sup>
GP3011	<i>trpC2</i> $\Delta$ <i>cdaS::ermC</i> $\Delta$ <i>disA::tet</i> $\Delta$ <i>darA::cat</i> $\Delta$ <i>cdaA::spc</i> <i>ykoX<sub>K218STOP</sub></i> <i>ktrC<sub>G11C</sub></i> <i>yfkF<sub>G294S</sub></i> <i>nusG<sub>T82K</sub></i> <i>kimA<math>\Delta</math><sub>G112</sub></i>	GP2420 suppressor <sup>b</sup>
GP3015	<i>trpC2</i> <i>gltC::Tn10</i> <i>spc amyE::(gltC<sub>L201H</sub> gltA' - 'lacZ cat)</i>	pGP3030 → GP738
GP3016	<i>trpC2</i> $\Delta$ <i>ktrAB::aphA3</i> $\Delta$ <i>kimA::cat</i> $\Delta$ <i>darA::spc</i> $\Delta$ <i>ahrC::ermC</i> <i>gltC<sub>L201H</sub></i>	GP2495 suppressor <sup>a</sup>
GP3017	<i>trpC2</i> $\Delta$ <i>ktrAB::aphA3</i> $\Delta$ <i>kimA::cat</i> $\Delta$ <i>darA::spc</i> $\Delta$ <i>ahrC::ermC</i> <i>odhB<sub>W21C</sub></i> <i>argG<sub>SD(GAGAGGGGA→GAGAGGGAA)</sub></i>	GP2495 suppressor <sup>a</sup>
GP3018	<i>trpC2</i> $\Delta$ <i>ktrAB::aphA3</i> $\Delta$ <i>kimA::cat</i> $\Delta$ <i>darA::spc</i> $\Delta$ <i>ahrC::ermC</i> <i>spo0B<sub>K109STOP</sub></i>	GP2495 suppressor <sup>a</sup>
GP3019	<i>trpC2</i> $\Delta$ <i>ktrAB::aphA3</i> $\Delta$ <i>kimA::cat</i> $\Delta$ <i>darA::spc</i> $\Delta$ <i>ahrC::ermC</i> <i>spo0B<sub>Q46STOP</sub></i>	GP2495 suppressor <sup>b</sup>
GP3020	<i>trpC2</i> $\Delta$ <i>ktrAB::aphA3</i> $\Delta$ <i>kimA::cat</i> $\Delta$ <i>darA::spc</i> $\Delta$ <i>ahrC::ermC</i> <i>spo0B<sub>Y94STOP</sub></i>	GP2495 suppressor <sup>b</sup>
GP3021	<i>trpC2</i> $\Delta$ <i>ktrAB::aphA3</i> $\Delta$ <i>kimA::cat</i> $\Delta$ <i>darA::spc</i> $\Delta$ <i>ahrC::ermC</i> <i>bmr<sub>bp578+T</sub></i>	GP2495 suppressor <sup>a</sup>
GP3022	<i>trpC2</i> $\Delta$ <i>ktrAB::aphA3</i> $\Delta$ <i>kimA::cat</i> $\Delta$ <i>darA::spc</i> $\Delta$ <i>ahrC::ermC</i> <i>bmr<sub>G105S</sub></i>	GP2495 suppressor <sup>b</sup>
GP3023	<i>trpC2</i> $\Delta$ <i>ktrAB::aphA3</i> $\Delta$ <i>kimA::cat</i> $\Delta$ <i>darA::spc</i> $\Delta$ <i>ahrC::ermC</i> <i>argG<sub>H116Y</sub></i> <i>cotE<sub>5'UTR S610: bpC12A</sub></i>	GP2495 suppressor <sup>a</sup>

<sup>a</sup> SNPs identified by whole genome sequencing and verified by sequencing of a PCR product.

<sup>b</sup> SNPs identified by sequencing of a PCR product.

**Table 6.4: Foreign *B. subtilis* strains used in this work.**

Name	Genotype	Reference
168	<i>trpC2</i>	Laboratory Collection
BB1043	<i>codY::(erm::spc)</i>	Barbieri <i>et al.</i> , 2015
BKE11210	<i>trpC2</i> $\Delta$ <i>argB::ermC</i>	Koo <i>et al.</i> , 2017
BP52	<i>trpC2</i> <i>gudB amyE::(cfp cat)</i>	Gunka <i>et al.</i> , 2013
BP144	<i>trpC2</i> <i>amyE::(p<sub>kimA</sub>-RS-lacZ cat)</i>	Gundlach <i>et al.</i> , 2017b

Table 6.4: Foreign *B. subtilis* strains used in this work.

Name	Genotype	Reference
GP93	<i>trpC2</i> $\Delta kimA::cat$	Gundlach <i>et al.</i> , 2017b
GP94	<i>trpC2</i> $\Delta cdaA::spc$	Gundlach <i>et al.</i> , 2017b
GP651	<i>trpC2</i> <i>gltC::Tn10</i> <i>spc amyE::(gltC gltA' - lacZ cat)</i>	Commichau, 2006
GP668	<i>trpC2</i> $\Delta pta::aphA3$	Commichau, 2006
GP669	<i>trpC2 amyE::(gltA' - lacZ cat)</i>	Commichau, 2006
GP729	<i>trpC2</i> $\Delta ahrC::aphA3$	Commichau, 2006
GP738	<i>trpC2</i> <i>gltC::Tn10</i> <i>spc</i>	Commichau, 2006
GP793	<i>trpC2</i> $\Delta pycA::cat3$	Klewing, 2013
GP804	<i>trpC2</i> <i>gudB1 amyE::(gltA-lacZ aphA3)</i>	Commichau <i>et al.</i> , 2008
GP983	<i>trpC2</i> $\Delta cdaS::ermC$	Mehne <i>et al.</i> , 2013
GP987	<i>trpC2</i> $\Delta disA::tet radA_{K436K}$	Mehne <i>et al.</i> , 2013
GP991	<i>trpC2</i> $\Delta cdaS::ermC \Delta disA::tet radA_{K436K, F258S}$	Mehne <i>et al.</i> , 2013
GP1712	<i>trpC2</i> $\Delta darA::cat$	Kampf, 2014
GP1715	<i>trpC2</i> $\Delta darA::cat \Delta cdaA::spc$	Kampf, 2014
GP1902	<i>trpC2</i> $\Delta pycA::cat \Delta ackA::aphA3$	Reuß, 2017
GP2010	<i>trpC2</i> <i>lacA::(p<sub>deg</sub> darA-Strep aphA3) \Delta darA::cat</i>	Gundlach, 2014
GP2078	<i>trpC2</i> $\Delta khSTU::aphA3$	Gundlach, 2017
GP2097	<i>trpC2</i> $\Delta oppABCDF::aphA3$	Gundlach, 2017
GP2165	<i>trpC2</i> $\Delta ktrAB::aphA3 \Delta kimA::cat$	Gundlach <i>et al.</i> , 2017a
GP2182	<i>trpC2</i> <i>amyE::(p<sub>kimA</sub>-lacZ cat)</i>	Gundlach <i>et al.</i> , 2017b
GP2185	<i>trpC2</i> $\Delta ahrC::ermC$	Gundlach <i>et al.</i> , 2017a
GP2187	<i>trpC2</i> $\Delta ktrAB::aphA3 \Delta kimA::cat \Delta ahrC::ermC$	Gundlach <i>et al.</i> , 2017a
GP2222	<i>trpC2</i> $\Delta cdaA::cat \Delta cdaS::ermC \Delta disA::tet$	Gundlach <i>et al.</i> , 2017b
GP2263	<i>trpC2</i> $\Delta glnA::ermC$	Gundlach, 2017
GP2405	<i>trpC2</i> <i>kimA-3</i> $\times$ <i>FLAG spc</i>	Gundlach <i>et al.</i> , 2017b
GP2716	<i>trpC2</i> $\Delta ktrAB::spc$	Gundlach <i>et al.</i> , 2017b

Table 6.5: Foreign *E. coli* strains used in this work.

Name	Genotype	Reference
BL21(DE3)	B F <sup>-</sup> <i>lon ompT hsdS</i> (r <sub>B</sub> <sup>-</sup> , m <sub>B</sub> <sup>-</sup> ) <i>gal dem lacI lacUV5-T7</i> <i>gene1 ind1 sam7 nin5 [mal<sup>+</sup>]<sub>K-12</sub>(<math>\lambda^S</math>)</i>	Studier and Moffatt, 1986, Studier <i>et al.</i> , 2009
BTH101	F <sup>-</sup> <i>cya-99 araD139 galE15 galK16 rpsL1 (Str<sup>R</sup>) hsdR2 mcrA1</i> <i>mcrB1</i>	Euromedex (Souffelweyersheim, FR)
DH5 $\alpha$	F <sup>-</sup> <i>endA1 hsdR17</i> (r <sub>K</sub> <sup>-</sup> , m <sub>K</sub> <sup>+</sup> ) <i>supE44 thi-1</i> $\lambda^-$ <i>recA1 gyrA96</i> <i>relA1 deoR \Delta(lacZYA-argF)U169 \phi80\Delta lacZ\Delta M15</i>	Grant <i>et al.</i> , 1990
XL1-Blue	<i>recA1 endA1 gyrA96 thi-1 hsdR17 supE44 relA1</i> <i>lac[F' proAB lacI<sup>q</sup>Z\Delta M15 Tn10 (Tet<sup>r</sup>)]</i>	Stratagene (La Jolla, California, USA)

### 6.3 Oligodeoxynucleotides

Oligodeoxynucleotides (desalted) were purchased from Sigma-Aldrich Chemie (Steinheim) and were either constructed during this work or originated from the in-house laboratory collection of the AG Stülke or AG Commichau. The description might not cover all of the actual uses in this work. Underlined bases are restriction sites for endonucleases, bold bases are introduced mutations. Bases for reading frame adjustments, START/STOP codons, Shine-Dalgarno sequences, overlapping regions for LFH-PCR (*kanR*-tags) or additional cut sites are in italics. 5'-extensions (usually AAA or TTT) were added to the restriction sites to ensure efficient restriction digestion (New England Biolabs).

**Table 6.6: Oligodeoxynucleotides constructed in this work.**

Name	Sequence (5'–3')	Description
MW01	AAA <u>GGATCC</u> GACCCAAAAACAGAAGCTCTCTTATATG	fwd, <i>tmk</i> , BamHI
MW02	TTT <u>GTCGAC</u> CAATTGAATTTTTTTTCAACGCTTCATCG	rev, <i>tmk</i> , Sall
MW03	AAA <u>GGATCC</u> <i>ATG</i> AAAAATCACTATACTGCGGTTGGTG	fwd, <i>kimA</i> <sub>451–607</sub> , BamHI, START codon
MW04	TTT <u>CTGCAG</u> TTACTTTTTTAAAATGATACGGCAGTGTG	rev, <i>kimA</i> <sub>451–607</sub> , PstI,
MW05	AAA <u>GGTACC</u> <i>G ATG</i> AAAAATCACTATACTGCGGTTGGTG	fwd, <i>kimA</i> <sub>451–607</sub> , KpnI, START codon
MW06	TTT <u>GGATCC</u> TTACTTTTTTAAAATGATACGGCAGTGTG	rev, <i>kimA</i> <sub>451–607</sub> , BamHI
MW07	<i>CCTATCACCTCAAATGGTTCGCTG</i> GCCTCTGTTTTATTCTGTATCTGTCTTT	rev, <i>kimA</i> <sub>RS/p</sub> , <i>kanR</i> -tag, LFH up
MW08	CGCTTAAACTGAAAAAGTCTGAAACG	fwd, <i>kimA</i> <sub>RS/p</sub> , LFH up
MW09	<i>CCGAGCGCCTACGAGGAATTTGTATCG</i> CGCATAACAGAGACATCATAGCAGA	fwd, <i>kimA</i> <sub>RS/p</sub> , <i>kanR</i> -tag, LFH down
MW10	GCCCAAAGGTTTCGGACG	rev, <i>kimA</i> <sub>RS/p</sub> , LFH down
MW11	GCCGACAAAACATCTTCAGCA	fwd, <i>kimA</i> , LFH check
MW12	CGGGAAGGCTGAGAATCCC	rev, <i>kimA</i> , LFH check
MW13	AAA <u>GGATCC</u> GCGGCTCTGATATCATTATGGTTC	fwd, <i>kimA</i> , BamHI
MW14	TTT <u>GTCGAC</u> CTTTTTAAAATGATACGGCAGTGTGG	rev, <i>kimA</i> , Sall
MW15	GTCCAGGTCATTCTTCGGGA	fwd, <i>kinA</i> , sequencing
MW16	CAATGGACACGCTGAGAGAAG	rev, <i>kinA</i> , sequencing
MW17	AAA <u>GAGCTC</u> CTGTTGAACAACTGTTGGACATTC	fwd, <i>khtU</i> , SacI
MW18	TTT <u>GGATCC</u> TCCCTGTTTTTTTTCGGGGC	rev, <i>khtU</i> , BamHI
MW19	AAA <u>GAGCTC</u> GCCCTGGAAGCAAACCATG	fwd, <i>ktrD</i> , SacI
MW20	TTT <u>GGATCC</u> TCCGATAATCACTCTTTCCTTCGG	rev, <i>ktrD</i> , BamHI
MW21	AAA <u>GAGCTC</u> CAGTATACATCATCTAATCGCATTAAAGAAGC	fwd, <i>nahK</i> , SacI

Table 6.6: Oligodeoxynucleotides constructed in this work.

Name	Sequence (5'–3')	Description
MW22	TTT <u>GGATCC</u> TTCGCCGCCTTCAAGCAT	rev, <i>nahK</i> , BamHI
MW23	AAA <u>GAGCTC</u> CCTGTCACACTCGAATTGCCA	fwd, <i>yjbQ</i> , SacI
MW24	TTT <u>GGATCC</u> TCCTTCCAATGTTTTCTTAAGATCCG	rev, <i>yjbQ</i> , BamHI
MW25	AAA <u>GAGCTC</u> GTCATTGACGAAGGCGATACAC	fwd, <i>yrvD</i> , SacI
MW26	TTT <u>GGATCC</u> GTCTTTTTTCTCAATCATGGCTGATG	rev, <i>yrvD</i> , BamHI
MW27	AAA <u>GAGCTC</u> CTTTTGAAGGACCTTCAGCTTGC	fwd, <i>yugO</i> , SacI
MW28	TTT <u>GGATCC</u> GATGGCAAGGAATTGATCTGTTTCG	rev, <i>yugO</i> , BamHI
MW29	AAA <u>TCTAGA</u> ATGAACACACCTTTATATAAAGCATTAAATTCAAC	fwd, <i>yaaO</i> , XbaI
MW30	TTT <u>GTCGAC</u> TCATGATTTCTCCTCTTCTATATAAACAAGTAGT	rev, <i>yaaO</i> , SalI
MW31	AAA <u>TCTAGA</u> AAAGGAGGAAACAATC ATGAACACACCTTTATATAAAGCATTAAATTCAAC	fwd, <i>yaaO</i> , XbaI, <i>SD<sub>gapA</sub></i>
MW32	TTT <u>GTCGAC</u> TGATTTCTCCTCTTCTATATAAACAAGTAGTTG	rev, <i>yaaO</i> , SalI
MW33	<i>CCTATCACCTCAAATGGTTTCGCTG</i> GAATTTCTTCTCGCATGTTGAATTAATGC	rev, <i>yaaO</i> , <i>kanR</i> -tag, LFH up
MW34	CGAAATACTTGGAGAGCTGATGAAAAA	fwd, <i>yaaO</i> , LFH up
MW35	<i>CGAGCGCCTACGAGGAATTTGTATCG</i> GTGCAAAAGCTCAGCCGC	fwd, <i>yaaO</i> , <i>kanR</i> -tag, LFH down
MW36	CGTTTTCTTTAATGAGACTCAACGCT	rev, <i>yaaO</i> , LFH down
MW37	GCAAAGCATTGTCTTATACGGTTCA	fwd, <i>yaaO</i> , LFH check
MW38	CCTTAACGGATCACAACCTC <b>GA</b> AGTCACAAAGCTTGCAACGAC	fwd, <i>darA</i> , mutagenesis, AG to GA, <i>DarA<sub>R26E</sub></i>
MW39	CGGATCACAACCTCAGAGTCA <b>G</b> AAAGCTTGCAACGACAGGAGG	fwd, <i>darA</i> , mutagenesis, C to G, <i>DarA<sub>T28R</sub></i>
MW40	AGCTTGCAACGACAGGAGGA <b>GAG</b> CTTAAATCAGGCAATACAAC	fwd, <i>darA</i> , mutagenesis, TTT to GAG, <i>DarA<sub>F36E</sub></i>
MW41	GAGGATTTCTTAAATCAGGCA <b>GA</b> ACAACGTTTATGATCGGTGT	fwd, <i>darA</i> , mutagenesis, AT to GA, <i>DarA<sub>N41R</sub></i>
MW42	AAA <u>GGATCC</u> AAAGGAGGAAACAATC ATGAAATTGATAGTGGCAGTTGTACAAGATCAG	fwd, <i>darA</i> , BamHI, <i>SD<sub>gapA</sub></i>
MW43	AAA <u>GGATCC</u> ATGAAGAAAACAATCGTTTTTAAATGCGG	fwd, <i>argB</i> , BamHI
MW44	TTT <u>CTGCAG</u> TCATGAAACAGCCTCCTTTGCT	rev, <i>argB</i> , PstI
MW45	AAA <u>GGATCC</u> AAAGGAGGAAACAATC ATGAAGAAAACAATCGTTTTTAAATGCGG	fwd, <i>argB</i> , BamHI, <i>SD<sub>gapA</sub></i>
MW46	TTT <u>CTGCAG</u> TGAAACAGCCTCCTTTGCTTTG	rev, <i>argB</i> , PstI, no STOP codon
MW47	AAA <u>GGTACC</u> G ATGAAGAAAACAATCGTTTTTAAATGCGG	fwd, <i>argB</i> , KpnI
MW48	TTT <u>GGATCC</u> TCATGAAACAGCCTCCTTTGCT	rev, <i>argB</i> , BamHI

Table 6.6: Oligodeoxynucleotides constructed in this work.

Name	Sequence (5'–3')	Description
MW49	AAA <u>GGTCTC</u> <i>ATGGT</i> ATGAAGAAAACAATCGTTTTTAAATGCGG	fwd, <i>argB</i> , BsaI, SUMO-overhang
MW50	TTT <u>CTCGAG</u> TCATGAAACAGCCTCCTTTGCT	rev, <i>argB</i> , XhoI
MW51	GAAGACCAGGCAGATACCGC	fwd, <i>argC–F</i> , LFH up
MW52	<i>CCTATCACCTCAAATGGTTTCGCTG</i> GCCTCCATATCCTGTAGCACC	rev, <i>argC–F</i> , <i>kanR</i> -tag, LFH up
MW53	<i>CGAGCGCCTACGAGGAATTTGTATCG</i> GCTGAAGGCCATTTTATATAAAGGGG	fwd, <i>argC–F</i> , <i>kanR</i> -tag, LFH down
MW54	GATTGCTGTTAAAAAGAGTGTATCCTTCA	rev, <i>argC–F</i> , LFH down
MW55	CATTACGATCCGCTACGTGCA	fwd, <i>argC–F</i> , LFH check
MW56	CTTCGGATTGAGGATTTCTGCT	rev, <i>argC–F</i> , LFH check
MW57	GTGGAAGTCAGAGAACCGCT	fwd, <i>argG–H</i> , LFH up
MW58	<i>CCTATCACCTCAAATGGTTTCGCTG</i> GTATCAAGACCTCCTGAGTATGCTAAT	rev, <i>argC–F</i> , <i>kanR</i> -tag, LFH up
MW59	<i>CGAGCGCCTACGAGGAATTTGTATCG</i> GTGGAACAGGCGCTTGAAAAA	fwd, <i>argC–F</i> , <i>kanR</i> -tag, LFH down
MW60	GATCTTCCTATCGGCGTTTTTTCTTT	rev, <i>argG–H</i> , LFH down
MW61	CGCAAGCAGAATCCACAAATACA	fwd, <i>argG–H</i> , LFH check
MW62	CTTGTTAATGACATTGAGGCCTCC	rev, <i>argG–H</i> , LFH check
MW63	AAA <u>GGTACC</u> <i>G</i> TTGCTGACATTAGAAAATGTCTCGAAA	fwd, <i>opuBA</i> , KpnI
MW64	TTT <u>CCCGGG</u> CTATGACAATGCTGCGAGCTG	rev, <i>opuBA</i> , SmaI
MW65	AAA <u>GGATCC</u> <i>G</i> ATGAAGAAAACAATCGTTTTTAAATGCGG	fwd, <i>argB</i> , BamHI, BACTH
MW66	TTT <u>GGTACC</u> <i>CG</i> TGAACAGCCTCCTTTGCTTTG	rev, <i>argB</i> , KpnI, BACTH
MW67	AAA <u>GGATCC</u> <i>G</i> ATGAACAAAGGCCAGAGGCATATTA	fwd, <i>ahrC</i> , BamHI, BACTH
MW68	TTT <u>GGTACC</u> <i>CG</i> CAGCAGTTCAAGGAGCCTGT	rev, <i>ahrC</i> , KpnI, BACTH
MW69	AAA <u>GGATCC</u> <i>G</i> ATGGATAAAACGATTTTCGGTTATTGGAA	fwd, <i>rocF</i> , BamHI, BACTH
MW70	TTT <u>GGTACC</u> <i>CG</i> CAGCAGCTTCTTCCCTAACAGG	rev, <i>rocF</i> , KpnI, BACTH
MW71	AAA <u>GGATCC</u> ATGAAGGCTATGCGCTATGAGC	fwd, <i>cdsS</i> , BamHI
MW72	TTT <u>GACGTC</u> <i>TTA</i> TTACGTTCTTGGTGAAATTAACGGATATAA	rev, <i>cdsS</i> , AatII, 2nd STOP codon
MW73	AAA <u>GGATCC</u> <i>AAAGGAGGAAACAATC</i> ATGGCAATATCCTGGAAGGAAATGA	fwd, <i>holB</i> , BamHI, <i>SD<sub>gapA</sub></i>
MW74	TTT <u>CTGCAG</u> TCCCTCCTGCAACATTAACACC	rev, <i>holB</i> , PstI
MW75	TTT <u>GGTACC</u> <i>CTA</i> TAAAATTGATGAAATTCATCGACTGGAAGG	rev, <i>darA</i> , KpnI, 2nd STOP codon
MW76	GGTGAAATAGCTCCTTTTTTATGACTTG	fwd, <i>yfkF</i> , sequencing
MW77	GGGATATCGTGATGACCAAGCATA	rev, <i>yfkF</i> , sequencing
MW78	GGCTAAAATGAAAGTTATCATAGGCTTG	fwd, <i>nusG</i> , sequencing

Table 6.6: Oligodeoxynucleotides constructed in this work.

Name	Sequence (5'–3')	Description
MW79	CCTCCCACTCAAGGTTTCATTCT	rev, <i>nusG</i> , sequencing
MW80	CAGAACCGATCAACCGTTCGA	fwd, <i>ccpA</i> , sequencing
MW81	CAGATCAAGAAAAGAGCGGAAACC	rev, <i>ccpA</i> , sequencing
MW82	AAGTGTCAACAAGAAAACAAAGGCTC	fwd, <i>spo0IIP</i> , sequencing
MW83	GTGGTTTGCCTGCTGCATG	rev, <i>spo0IIP</i> , sequencing
MW84	CTGCAAATCAACCAAAGCCAGA	fwd, <i>spo0B</i> , sequencing
MW85	TCGGCACATATTTTTTCACGGC	rev, <i>spo0B</i> , sequencing
MW86	AAA <u>GAGCTC</u> <i>TTAACTTTAAGAAGGAGATATACATA</i> ATGACGTACAATCAAATGCCAAAAG	fwd, <i>gltA</i> , SacI, SD <sub>T7 gene 10</sub>
MW87	TTT <u>TCTAGA</u> <i>TCA</i> TTACTGTACTACCGCTTGTTTTTGTG	rev, <i>gltA</i> , XbaI, 2nd STOP codon
MW88	AAA <u>GAGCTC</u> GGGAAACCAACTGGATTTATGGAGA	fwd, <i>gltB</i> , SacI, w/o START codon
MW89	TTT <u>GGATCC</u> <i>CTATCA GTGATGGTGATGGTGATG</i> <i>ACCCGAACCACC</i> CGGAAGAACTGAACTCCCCATC	rev, <i>gltB</i> , w/o STOP codon, GGSG-Linker, His <sub>6</sub> -tag, 2×STOP codon
MW90	TTT <u>GGATCC</u> <i>ACCACCACC</i> CGGAAGAACTGAACTCCCCATC	rev, <i>gltB</i> , w/o STOP codon, GGG-linker part
MW91	CTGTCATAAGGCTTTAGAAAGATTTTGC	fwd, <i>bmr</i> , sequencing
MW92	CCCCAATTGAGTAATACGATTCCTTC	rev, <i>bmr</i> , sequencing
MW93	GGCTTGAAAAAACGAAACGTAATTG	fwd, <i>argG</i> , sequencing
MW94	GTCTTCAGCAACTAAATTTTGGTCAAAT	rev, <i>argG</i> , sequencing

Table 6.7: Foreign oligodeoxynucleotides used in this work.

Name	Sequence (5'–3')	Description
Catchcheck rev	GTCTGCTTTCTTCATTAGAAATCAATCC	rev, <i>cat</i> , check/sequencing
CB242	AGCTAACGGAAGGGAGCG	fwd, pHT01, sequencing
CB243	ATAAGCCGATATTAGCCTCGTATG	rev, pHT01, sequencing
CZ68	<i>CGATACAAATTCCCTCGTAGGCGCTCGG</i> TTACTTATTAATAATTTATAGCTATTG	rev, <i>ermC</i> , <i>kanR</i> -tag, w/o terminator, LFH down
DR367	TGGGCCTGCAAAGAGATAAGC	fwd, <i>ackA</i> , LFH up
DR368	<i>CCTATCACCTCAAATGGTTTCGCTG</i> ATCGCATGAAAGCACATTCTCTTG	rev, <i>ackA</i> , <i>kanR</i> -tag, LFH up
FC02	AAA <u>GAATTC</u> TTATTGATACTGCTCCAGCTTAGAGAAA	rev, <i>gltA-gltC</i> , EcoRI
FC38	TGAGAGCACGTGAGCAGCAATTTG	fwd, <i>gltA</i> , sequencing
FC41	GGACATGTTACACAGGCAGAG	fwd, <i>gltA</i> , sequencing
FC43	TGCGATGTCATTCGGGTCCTTGA	fwd, <i>gltA</i> , sequencing

Table 6.7: Foreign oligodeoxynucleotides used in this work.

Name	Sequence (5'-3')	Description
FC45	CAGAGCTTCGCAAAAAGTTCATGGG	fwd, <i>gltA</i> , sequencing
FC48	CGCAATGGACTACCTCACACTTG	rev, <i>gltB</i> , sequencing
FC66	CTCCTGTAAAACCGTAAGCCCGC	rev, <i>ahrC</i> , sequencing
FC73	AGCACTGGAAAGCAAGCCAGCTTG	fwd, <i>gltA</i> , sequencing
FM35	AAA <u>TCTAGA</u> <i>G</i> ATGGCGGAAATTAAGGTACCTGAATTAGC	fwd, <i>odhB</i> , XbaI, BACTH
FM37	TTT <u>GAATTC</u> TTATCCTTCTAATAAAAAGCTGTTTCAGGATCTTCC	rev, <i>odhB</i> , EcoRI, BACTH
FM46	AAA <u>TCTAGA</u> <i>G</i> ATGTTTCAAATAGTATGAAACAAC- GAATGAATTGGGAAG	fwd, <i>odhA</i> , XbaI, BACTH
FM47	TTT <u>GGTACC</u> <i>CG</i> GTTTTTGCAGTCAAGCTATCAGATACAATACG	rev, <i>odhA</i> , KpnI, BACTH
FM48	GAGCGCGAGTGGCTGACAAGAAAG	fwd, <i>odhB</i> , sequencing
FM49	GGAGACGCTGCATCCCTGGG	fwd, <i>odhB</i> , sequencing
FM57	CCTCGCTCACCTCTTGTGCAGC	rev, <i>odhB</i> , sequencing
FR81	<i>CCGAGCGCCTACGAGGAATTTGTATCG</i> GCCCAAACGTGCAGCAAAGC	fwd, <i>acuC</i> , <i>kanR</i> -tag, LFH down
FX15	AAA <u>GGATCC</u> GCGGAATTTAAGCGTTCTCCAGTGCC	fwd, <i>ccpA</i> , BamHI
FX20	GGGGCGAAACACGAGTTAG	fwd, <i>disA</i> , qRT
FX21	GTCCACCACTTCTTTTACTTTATC	rev, <i>disA</i> , qRT
FX22	GCGTTCAAGGGGAAAATACAG	fwd, <i>cdsA</i> , qRT
FX23	GGATGCAATCCCCTGCATG	rev, <i>cdsA</i> , qRT
FX24	GATATATAAATTGATTATGGTGATACGC	fwd, <i>cdsA</i> , qRT
FX25	AATCCCCATGTTATCGCTTGGT	rev, <i>cdsA</i> , qRT
FX125	GGCTCGTATGTTGTGTGG	rev, pBQ200, sequencing
iGEM_90	GGCTATGCTTTCTCAGATG	fwd, <i>kimA</i> , qRT
IR01	ACG <u>CGTCGA</u> <i>CCTGGTTCCGCGTGGTTCC</i> ATGGAGCTGCGCAAACCTG	fwd, <i>gltC</i> , SalI, thrombin cleavage site
IR02	CCC <u>AAGCTT</u> TTATTATTGATACTGCTCCAGCTTAG	rev, <i>gltC</i> , HindIII
IW02	AAA <u>GGATCC</u> TGAGCTTTTGGCATTGATTGTACGC	fwd, <i>gltA-gltC</i> , BamHI
IW03	AAA <u>GAATTC</u> GAGTATCTTGACCCGCATCGC	fwd, <i>gltC</i> , EcoRI
IW04	AAA <u>GGATCC</u> GGAAACGAGAGGAGCAAAGCC	rev, <i>gltC</i> , BamHI
JG69	<i>CGATACAAATTCCTCGTAGGCGCTCG</i> GTTCCAC CATTTTTTCAATTTTTTTATAATTTTTTTAATCTG	rev, <i>spc</i> , <i>kanR</i> -tag, w/o terminator, LFH down
JG298	GATCCCTCTTCACTTCTCAGAATACATACG	fwd, <i>spo0A</i> , sequencing
JG299	CTTAATATTCTTCTCCATACTACAAATGTCCC	rev, <i>spo0A</i> , sequencing
JK20	TTT <u>CTGCAG</u> CTACATCCCTTCGTTTTTCAAACGTTTAATATCC	rev, <i>ktrA</i> , PstI
JK37	GGATAACAATTATAATAGATTCAATTGTGAGCGGAT AAC	fwd, pWH844, sequencing



Table 6.7: Foreign oligodeoxynucleotides used in this work.

Name	Sequence (5'–3')	Description
JK45	AAA <u>GGATCC</u> ATGAAATTGATAGTGGCAGTTGTACAAGATCAG	fwd, <i>darA</i> , BamHI
JK46	TTT <u>CTGCAG</u> TAAAATTGATGAAATTCATCGACTG GAAGGACAAATAC	rev, <i>darA</i> , PstI
JK47	CCATTGGGAGGAAAACGGAGAATAAACG	fwd, <i>darA</i> , LFH check
JK48	CAGACGTTTGTCTGCAGAATGGGG	fwd, <i>darA</i> , LFH up
JK49	<i>CCTATCACCTCAAATGGTTGCTG</i> GACTCTGAAGTTGTGATCCGTTAAGGTTTTTC	rev, <i>darA</i> , <i>kanR</i> -tag, LFH up
JK50	<i>CGAGCGCCTACGAGGAATTTGTATCG</i> TATGTCCCTTATCCAGTCGAAGTTGAAGTTG	fwd, <i>darA</i> , <i>kanR</i> -tag, LFH down
JK52	GCTGCAAAGGCTGAAAAGGAAGGGT	rev, <i>darA</i> , LFH down
JK53	ATTAGTCATGTTGGCCAGAAGCCTTGC	rev, <i>darA</i> , LFH check
JK56	AAA <u>GGATCC</u> ATGAAATTGATAGTGGCAGTTGTACAAGATCAG	fwd, <i>darA</i> , BamHI
JK57	TTT <u>CTGCAG</u> <i>CTA</i> TAAAATTGATGAAATTCATCGA CTGGAAGGACAAATAC	rev, <i>darA</i> , PstI, 2nd STOP codon
JK58	AAA <u>GGATCC</u> AATCTAAAGGAGGCCTTCACAGATGAAATTG	fwd, <i>darA</i> , BamHI, <i>SD<sub>darA</sub></i>
JK163	<i>CGATACAAATTCTCTGTTAGGCGCTCGG</i> TTAGAAATCCCTTTGAGAATGTTTATATACATTC	rev, <i>tet</i> , <i>kanR</i> -tag, w/o terminator, LFH down
JK230	<i>CGATACAAATTCTCTGTTAGGCGCTCG</i> GAGAAAGAAAGTAAAGATTACCTCATAAATTG	fwd, <i>ytzE</i> , <i>kanR</i> -tag, LFH down
JK231	GCGGCTACCGATTAGGATTTT	rev, <i>ytzE</i> , LFH down
JK271	<i>CCTATCACCTCAAATGGTTGCTG</i> CATAACTGCTTCCAACAAAACCC	rev, <i>ldh</i> , <i>kanR</i> -tag, LFH up
JN54	GTGAAAAATGAGCCGAAAGCAG	fwd, pBQ200, sequencing
JN154	TTT <u>GGTACC</u> <i>GC</i> TGTGTAAGGTTAATTAATAAACCTTTTATTTTCGC	rev, <i>yaaR</i> , KpnI, BACTH
JN159	AAA <u>GGATCC</u> ATGAGCGGTTTATTTATTACATTCGAAGG	fwd, <i>tmk</i> , BamHI
JN182	GCCCCGCCTCAGCAC	fwd, <i>ktrC</i> , qRT “ <i>RS</i> region”
JN199	GCGATTTTAGCCTCTGTTTTTTTATTTTTG	fwd, <i>kimA</i> , <i>RS</i> probe
JN201	CACTCCTCCGACTCAGCCT	fwd, <i>ktrA</i> , sequencing
JN245	GTTGCCCGCACAGCTTTG	fwd, <i>appA</i> , sequencing
JN246	CATTCCACCCGATGTACACATAACT	rev, <i>appA</i> , sequencing
JN286	ACCCGGATGAGCTTCTTTCAA	fwd, <i>khtT</i> , sequencing
JN290	TCGTGATGGTCGGTGTGAAG	fwd, <i>yjbQ</i> , sequencing
JN292	AGGTATTTGGTGGGCTGTGCG	fwd, <i>yugO</i> , sequencing
JN294	ATGACGGACGGAGAGAGCTT	fwd, <i>yrvC</i> , sequencing
JN460	TTT <u>CTGCAG</u> CTATTTTGTATGAAGAACTCTTTTTTTCGAAAC	rev, <i>ktrC</i> , PstI

Table 6.7: Foreign oligodeoxynucleotides used in this work.

Name	Sequence (5'–3')	Description
JN470	GAGCGGAATTCCCATTGAACAG	fwd, <i>argC</i> , sequencing
JN471	GCTATGTCACACAATTTACTATAGAAAGGA	fwd, <i>ygaE</i> , sequencing
JN472	CGCAGTCTTTCCGGATGATACGT	rev, <i>ygaE</i> , sequencing
JN473	GCATAATAGAAAACGGCAATGTTTACACTT	fwd, <i>pyrH</i> , sequencing
JN474	GCCGTCACCTTGTGTTGGTGTAAAG	rev, <i>pyrH</i> , sequencing
JN475	GACAAAGGAGATGATTGGAAATGAAAGA	fwd, <i>pepT</i> , sequencing
JN476	CGGAGGACGTGTTTAAAATGTTTCAT	rev, <i>pepT</i> , sequencing
JN495	CTGATGCCACCAAAGACACAC	fwd, <i>ahrC</i> , LFH up
JN497	CATTAAGTCGCGTCTCAATATAGTTCAG	rev, <i>ahrC</i> , LFH down
JN501	CACAGCCGGAAACCTCACG	fwd, <i>spoIIIF</i> , sequencing
JN502	GCCGTCCTTCGTTTGTCCC	rev, <i>spoIIIF</i> , sequencing
JN634	GTTATCTTTAACGACACTGCCATCA	fwd, <i>nhaK</i> , sequencing
JN646	CTTTAGAATAATTACCGTACTTAAAAAGAGAGGC	fwd, <i>ktrD</i> , sequencing
JN702	GATTGCCTGGTGATCATGGG	fwd, <i>ktrB</i> , sequencing
JN703	CTCATATCGAATCATAAAAAATCCGGC	rev, <i>ktrB</i> , sequencing
JN715	TAAGCCGGTAAGATGAGGATAACC	rev, <i>argC</i> , sequencing
KG01	<i>CCTATCACCTCAAATGGTTCCG</i> GGCCGATTCCGCATGCATCATGTTT	rev, <i>gltA</i> , <i>kanR</i> -tag, LFH up
KG35	TTT <u>GGTACC</u> <i>CG</i> TTGATACTGCTCCAGCTTAGAGAAAAATTG	rev, <i>gltC</i> , KpnI, BACTH
KG64	TATCAGGGCCTCGACTACA	rev, <i>ganA</i> , check/sequencing
KG65	CGCTGATTAAATACAGCATCGG	fwd, <i>ganA</i> , check/sequencing
KG163	CCCAAACCGTAATACATAAGGC	rev, <i>gudB</i> , sequencing
KG196	GGCTGATCGCTCTGACAT	fwd, <i>gudB</i> , sequencing
KG289	<i>CCTATCACCTCAAATGGTTCCGCTG</i> GGCCGTACAGGCAATTAGAATAGATAAACATATGA	rev, <i>dgcW</i> , <i>kanR</i> -tag, LFH up
KG292	GAATTCAGGCATGCCAACAAAGCCGAT	rev, <i>ykoX</i> , sequencing
M13_ pUC_fwd	GTAAAACGACGGCCAGTG	fwd, pBS/pUC, sequencing
M13_ pUC_rev	GGAAACAGCTATGACCATG	rev, pBS/pUC, sequencing
ML84	CTAATGGGTGCTTTAGTTGAAGA	rev, <i>cat</i> , check/sequencing
ML85	CTCTATTCAGGAATTGTCAGATAG	fwd, <i>cat</i> , check/sequencing
ML103	CTCTTGCCAGTCACGTTAC	rev, <i>spc</i> , check/sequencing
ML104	TCTTGGAGAGAATATTGAATGGAC	fwd, <i>spc</i> , check/sequencing
ML107	GCTTCATAGAGTAATTCTGTAAAGG	rev, <i>aphA3</i> , check/sequencing
ML108	GACATCTAATCTTTTCTGAAGTACATCC	fwd, <i>aphA3</i> , check/sequencing
ML109	GTCTAGTGTGTTAGACTTTATGAAATC	rev, <i>ermC</i> , check/sequencing
ML112	ACA <u>GGATCC</u> GAATTTAAGCGTTCTCCAGTGC	fwd, <i>ccpA</i> , BamHI

Table 6.7: Foreign oligodeoxynucleotides used in this work.

Name	Sequence (5'–3')	Description
mls- check-fwd	CCTTAAAACATGCAGGAATTGACG	fwd, <i>ermC</i> , check/sequencing
mls-fwd (kan)	<i>CAGCGAACCATTGAGGTGATAGG</i> GATCCTTTAACTCTGGCAACCCTC	fwd, <i>ermC</i> , <i>kanR</i> -tag, LFH up
pBAD- fwd	ATGCCATAGCATTTTTATCC	fwd, pBAD33, sequencing
pBAD- rev	GATTTAATCTGTATCAGG	rev, pBAD33, sequencing
pKT fwd	CGACTCGGCGCGCAGTTCCG	fwd, pKT25, sequencing
pKT rev	GCAAGGCGATTAAGTTGGGTAACGC	rev, pKT25, sequencing
p25-N fwd	GCTTCCGGCTCGTATGTTGTGTG	fwd, p25-N, sequencing
p25-N rev	GCCATCGAGTACGGCTGCGG	rev, p25-N, sequencing
pUT18C fwd	GAAGTTCTCGCCGATGTACTGG	fwd, pUT18C, sequencing
pUT18C rev	CGGGTGTTGGCGGGTGTCG	rev, pUT18C, sequencing
pUT18 fwd	CTTCCGGCTCGTATGTTGTGTGG	fwd, pUT18, sequencing
pUT18 rev	GCCGGCGCGAGCGATTTTCC	rev, pUT18, sequencing
SK34	GGC <u>GGATCC</u> ATGAGCAATATTACGATCTACGATGTA	fwd, <i>ccpA</i> , BamHI
SK35	GGCC <u>GTCGAC</u> TTTTCTTATGACTTGGTTGACTTTCTAAGC	rev, <i>ccpA</i> , Sall
spec-fwd (kan)	<i>CAGCGAACCATTGAGGTGATAGG</i> GACTGGCTCGC TAATAACGTAACGTGACTGGCAAGAG	fwd, <i>spc</i> , <i>kanR</i> -tag, LFH up
Tc-check- fwd	CGGCTACATTGGTGGGATACTTGTTG	fwd, <i>tet</i> , check/sequencing
Tc-check- rev	CATCGGTCATAAAATCCGTAATGC	rev, <i>tet</i> , check/sequencing
Tc-fwd2 (kan)	<i>CAGCGAACCATTGAGGTGATAGG</i> GCTTATCAACGTAGTAAGCGTGG	fwd, <i>tet</i> , <i>kanR</i> -tag, LFH up
T7-Prom.	TAATACGACTCACTATAGGG	fwd, T7 promoter, sequencing
T7-Term.	GCTAGTTATTGCTCAGCGG	rev, T7 terminator, sequencing

## 6.4 Plasmids

Table 6.8: Plasmids constructed in this work.

Name	Vector	Insert
pGP2786	pGP1331/ BamHI+Sall	<i>tmk</i> , MW01/02/ BamHI+Sall
pGP2787	pWH844/ BamHI+PstI	<i>kimA</i> <sub>451-607</sub> , MW03/04/ BamHI+PstI
pGP2788	pGP172/ KpnI+BamHI	<i>kimA</i> <sub>451-607</sub> , MW05/06/ KpnI+BamHI
pGP2790	pGP1459/ BamHI+PstI	<i>darA</i> , pGP2602/ BamHI+PstI+ScaI
pGP2791	pGP1331/ SacI+BamHI	<i>khtU</i> , MW17/18/ SacI+BamHI
pGP2792	pGP1331/ SacI+BamHI	<i>ktrD</i> , MW19/20/ SacI+BamHI
pGP2793	pGP1331/ SacI+BamHI	<i>nahK</i> , MW21/22/ SacI+BamHI
pGP2794	pGP1331/ SacI+BamHI	<i>yjbQ</i> , MW21/22/ SacI+BamHI
pGP2795	pGP1331/ SacI+BamHI	<i>yrvD</i> , MW23/24/ SacI+BamHI
pGP2796	pGP1331/ SacI+BamHI	<i>yugO</i> , MW25/26/ SacI+BamHI
pGP2797	pBQ200/ BamHI+PstI	<i>darA</i> , JK58/57/ BamHI+PstI
pGP2798	pWH844/ BamHI+PstI	<i>darA</i> <sub>R26E</sub> , JK45/MW38/JK46/ BamHI+PstI
pGP2799	pWH844/ BamHI+PstI	<i>darA</i> <sub>T28R</sub> , JK45/MW39/JK46/ BamHI+PstI
pGP2800	pWH844/ BamHI+PstI	<i>darA</i> <sub>F36E</sub> , JK45/MW40/JK46/ BamHI+PstI
pGP3001	pWH844/ BamHI+PstI	<i>darA</i> <sub>N41R</sub> , JK45/MW41/JK46/ BamHI+PstI
pGP3002	pBQ200/ BamHI+PstI	<i>darA</i> , MW42/JK57/ BamHI+PstI
pGP3003	pBQ200/ BamHI+PstI	<i>darA</i> <sub>F36E</sub> , MW42/JK57/ BamHI+PstI
pGP3004	pBQ200/ BamHI+PstI	<i>darA</i> <sub>R26E</sub> , MW42/JK57/ BamHI+PstI
pGP3005	pGP1460/ BamHI+PstI	<i>darA</i> , MW42/JK57/ BamHI+PstI
pGP3006	pGP1460/ BamHI+PstI	<i>darA</i> <sub>F36E</sub> , MW42/JK57/ BamHI+PstI
pGP3007	pGP1460/ BamHI+PstI	<i>darA</i> <sub>R26E</sub> , pGP3004/ BamHI/PstI/ScaI
pGP3008	pGP380/ BamHI+PstI	<i>darA</i> <sub>F36E</sub> , JK56/JK57/ BamHI+PstI
pGP3009	pGP380/ BamHI+PstI	<i>darA</i> <sub>R26E</sub> , JK56/JK57/ BamHI+PstI
pGP3010	pGP380/ BamHI+PstI	<i>argB</i> , MW43/MW44/ BamHI+PstI
pGP3011	pWH844/ BamHI+PstI	<i>argB</i> , MW43/MW44/ BamHI+PstI
pGP3012	pGP172/ KpnI+BamHI	<i>argB</i> , MW43/MW44/ KpnI+BamHI
pGP3013	pGP172/ KpnI+SmaI	<i>opuBA</i> , MW63/MW64/ KpnI+SmaI
pGP3014	pUT18/ BamHI+KpnI	<i>argB</i> , MW65/MW66/ BamHI+KpnI
pGP3015	pUT18C/ BamHI+KpnI	<i>argB</i> , MW65/MW66/ BamHI+KpnI
pGP3016	pKT25/ BamHI+KpnI	<i>argB</i> , MW65/MW66/ BamHI+KpnI
pGP3017	p25-N/ BamHI+KpnI	<i>argB</i> , MW65/MW66/ BamHI+KpnI
pGP3018	pUT18/ BamHI+KpnI	<i>ahrC</i> , MW67/MW68/ BamHI+KpnI
pGP3019	pUT18C/ BamHI+KpnI	<i>ahrC</i> , MW67/MW68/ BamHI+KpnI
pGP3020	pKT25/ BamHI+KpnI	<i>ahrC</i> , MW67/MW68/ BamHI+KpnI
pGP3021	p25-N/ BamHI+KpnI	<i>ahrC</i> , MW67/MW68/ BamHI+KpnI
pGP3022	pUT18/ BamHI+KpnI	<i>rocF</i> , MW69/MW70/ BamHI+KpnI
pGP3023	pUT18C/ BamHI+KpnI	<i>rocF</i> , MW69/MW70/ BamHI+KpnI
pGP3024	pKT25/ BamHI+KpnI	<i>rocF</i> , MW69/MW70/ BamHI+KpnI

**Table 6.8: Plasmids constructed in this work.**

Name	Vector	Insert
pGP3025	p25-N/ BamHI+KpnI	<i>rocF</i> , MW69/MW70/ BamHI+KpnI
pGP3026	pGP1459/ BamHI+KpnI	<i>darA</i> <sub>F36E</sub> , pGP3008/ BamHI/PstI/ScaI
pGP3027	pHT01/ BamHI+AatII	<i>cdaS</i> , MW71/MW72/ BamHI+AatII
pGP3028	pGP382/ BamHI+PstI	<i>holB</i> , MW73/MW74/ BamHI+PstI
pGP3029	pGP574/ SacI+BamHI	<i>gltB</i> -(His) <sub>6</sub> - <i>gltA</i> / pGP3034/ SacI+BamHI <sup>a</sup>
pGP3030	pAC5/ BamHI+EcoRI	<i>gltC</i> <sub>L201H</sub> , IW2/FC2/ BamHI+EcoRI
pGP3031	pGP574/ SacI+BamHI	<i>gltB</i> , MW88/MW89/ SacI+BamHI
pGP3032	pGP574/ SacI+BamHI	<i>gltB</i> , MW88/MW90/ SacI+BamHI
pGP3033	pBAD33/ SacI+XbaI	<i>gltA</i> , MW86/MW87/ SacI+XbaI
pGP3034	pMS/ AscI+PacI	<i>gltB</i> -(His) <sub>6</sub> - <i>gltA</i> / AscI+PacI, synthetic construct <sup>a</sup>

<sup>a</sup> Construction by Thermo Fisher Scientific Geneart, Regensburg. For details contact Prof. Dr. J. Stülke.

**Table 6.9: Foreign plasmids used in this work.**

Name	Description	Reference
pAC5	Construction of translational <i>lacZ</i> fusions, integrates into <i>B. subtilis amyE</i> site	Martin-Verstraete <i>et al.</i> , 1992
pBAD33	L-Arabinose inducible overexpression of a protein in <i>E. coli</i>	Guzman <i>et al.</i> , 1995
pBQ200	Constitutive overexpression of a protein in <i>B. subtilis</i>	Martin-Verstraete <i>et al.</i> , 1994
pDG646	Template for amplification of <i>ermC</i> , Erythromycin resistance cassette for LFH-PCR	Guérout-Fleury <i>et al.</i> , 1995
pDG1513	Template for amplification of <i>tet</i> , Tetracycline resistance cassette for LFH-PCR	Guérout-Fleury <i>et al.</i> , 1995
pDG1726	Template for amplification of <i>aad9</i> ( <i>spe</i> ), Spectinomycin resistance cassette for LFH-PCR	Guérout-Fleury <i>et al.</i> , 1995
pFDX4291	Expression of a third protein for a BACTH assay, very low copy plasmid	Kalamorz <i>et al.</i> , 2007
pGP172	Fusion of a Strep-tag to the N-terminus of a protein for IPTG inducible overexpression in <i>E. coli</i>	Merzbacher <i>et al.</i> , 2004
pGP380	Fusion of a Strep-tag to the N-terminus of a protein for constitutive overexpression in <i>B. subtilis</i>	Herzberg <i>et al.</i> , 2007
pGP382	Fusion of a Strep-tag to the C-terminus of a protein for constitutive overexpression in <i>B. subtilis</i>	Herzberg <i>et al.</i> , 2007
pGP574	Fusion of a Strep-tag to the C-terminus of a protein for IPTG inducible overexpression in <i>E. coli</i>	Schilling <i>et al.</i> , 2006
pGP1331	Fusion of a 3×FLAG-tag to the C-terminus of a protein for integration into native site in <i>B. subtilis</i>	Lehnik-Habrink <i>et al.</i> , 2010
pGP1459	Constitutive overexpression of an N-terminally Strep-tagged protein in <i>B. subtilis</i> , integrates into <i>lacA</i> site	Mehne <i>et al.</i> , 2013
pGP1460	Constitutive overexpression of a C-terminally Strep-tagged protein in <i>B. subtilis</i> , integrates into <i>lacA</i> site	Mehne <i>et al.</i> , 2013

Table 6.9: Foreign plasmids used in this work.

Name	Description	Reference
pGP1689	pGP172:: <i>tmk</i>	Jäger, 2015
pGP2601	pWH844:: <i>darA</i>	Kampf, 2014
pGP2602	pGP380:: <i>darA</i>	Kampf, 2014
pGP2604	pUT18:: <i>darA</i>	Gundlach, 2014
pGP2605	pUT18C:: <i>darA</i>	Gundlach, 2014
pGP2606	pKT25:: <i>darA</i>	Gundlach, 2014
pGP2607	p25-N:: <i>darA</i>	Gundlach, 2014
pGP2608	pFDX4291:: <i>cdaS</i> , additional third BACTH plasmid for the production of c-di-AMP	Gundlach, 2014
pGP2624	pGP172:: <i>darA</i>	Gundlach, 2014
pGP2630	pGP1460:: <i>darA</i>	Gundlach, 2014
pGP2659	pUT18:: <i>tmk</i>	Hach, 2015
pGP2660	pUT18C:: <i>tmk</i>	Hach, 2015
pGP2661	pKT25:: <i>tmk</i>	Hach, 2015
pGP2662	p25-N:: <i>tmk</i>	Hach, 2015
pGP2663	pUT18:: <i>holB</i>	Hach, 2015
pGP2664	pUT18C:: <i>holB</i>	Hach, 2015
pGP2665	pKT25:: <i>holB</i>	Hach, 2015
pGP2666	p25-N:: <i>holB</i>	Hach, 2015
pGP2672	pGP380:: <i>holB</i>	Hach, 2015
pGP2789	pGP1331:: <i>kimA</i>	Gundlach <i>et al.</i> , 2017b
pHT01	IPTG inducible overexpression of a protein in <i>B. subtilis</i>	MoBiTec (Göttingen)
pMS	Simple cloning vector based on pUC-like cloning vectors but without unnecessary promoters	Thermo Fisher Scientific Geneart (Regensburg)
pUT18	N-terminal fusion of the target protein to the T18 fragment of the adenylate cyclase for a BACTH assay	Karimova <i>et al.</i> , 1998
pUT18C	C-terminal fusion of the target protein to the T18 fragment of the adenylate cyclase for a BACTH assay	Karimova <i>et al.</i> , 1998
pUT18zip	Control plasmid carrying a leucine zipper fused to the T18 fragment of the adenylate cyclase for a BACTH assay	Karimova <i>et al.</i> , 1998
p25-N	N-terminal fusion of the target protein to the T25 fragment of the adenylate cyclase for a BACTH assay	Claessen <i>et al.</i> , 2008
pKT25	C-terminal fusion of the target protein to the T25 fragment of the adenylate cyclase for a BACTH assay	Karimova <i>et al.</i> , 1998
pKT25zip	Control plasmid carrying a leucine zipper fused to the T25 fragment of adenylate cyclase for a BACTH assay	Karimova <i>et al.</i> , 1998
pWH844	Fusion of a His <sub>6</sub> -tag to the N-terminus of a protein for IPTG inducible overexpression in <i>E. coli</i>	Schirmer <i>et al.</i> , 1997

## 6.5 Materials

Chemicals and compounds were purchased, if applicable, in purity *p.a.* or higher. Chemicals and compounds not listed in the following were purchased from Carl Roth (Karlsruhe), Sigma-Aldrich Chemie (Steinheim), Merck (Darmstadt) and SERVA Electrophoresis (Heidelberg).

**Table 6.10: Chemicals and Compounds.**

Name	Supplier
Acetic acid (glacial)	Th. Geyer, Renningen
Acetonitrile	Carl Roth, Karlsruhe
Agar-Agar	Carl Roth, Karlsruhe
AgNO <sub>3</sub>	Carl Roth, Karlsruhe
Albumin Fraction V, pH 7.0 (BSA)	AppliChem, Darmstadt
α-Ketoglutaric acid (2-oxoglutarate)	Sigma-Aldrich Chemie, Steinheim
Ammonium iron(III) citrate (14.5–16 % Fe basis, RT)	Sigma-Aldrich Chemie, Steinheim
Ammonium peroxydisulfate (APS)	Carl Roth, Karlsruhe
Ampicillin sodium salt	Carl Roth, Karlsruhe
Bacto Agar	Becton, Dickinson & Co., Le Pont de Claix, FR
Brilliant Blue G-250	Sigma-Aldrich Chemie, Steinheim
Bromophenol blue sodium salt	Sigma-Aldrich Chemie, Steinheim
CaCl <sub>2</sub> · 2 H <sub>2</sub> O	Carl Roth, Karlsruhe
Casein hydrolysate (acid) (Casamino acids)	Oxoid, Basingstoke, UK
c-di-AMP (3',5'-)	Biolog Life Science Institute, Bremen
CDP- <i>Star</i> Chemiluminescence substrate (25 mM)	Roche Diagnostics, Mannheim
CHAPS	Roche Diagnostics, Mannheim
Chloramphenicol	Carl Roth, Karlsruhe
CoCl <sub>2</sub> · 6 H <sub>2</sub> O	Merck, Darmstadt
CuCl <sub>2</sub>	Merck, Darmstadt
D-Desthiobiotin	IBA Lifesciences, Göttingen
DMSO	Carl Roth, Karlsruhe
D(+)-Glucose monohydrate	Carl Roth, Karlsruhe
dNTP mix	Roche Diagnostics, Mannheim
EDTA disodium salt hydrate	Carl Roth, Karlsruhe
Erythromycin	Sigma-Aldrich Chemie, Steinheim
Ethanol absolute	VWR International, Rue Carnot, FR
FeCl <sub>3</sub> · 6 H <sub>2</sub> O	Aldrich Chemical Company, Milwaukee, USA
5'-UMP-Na <sub>2</sub>	Sigma-Aldrich Chemie, Steinheim
Formaldehyde solution (37 %)	Carl Roth, Karlsruhe
Glycerol	Carl Roth, Karlsruhe
Glycine	Carl Roth, Karlsruhe
HCl	VWR International, Rue Carnot, FR
Imidazole	Carl Roth, Karlsruhe

Table 6.10: Chemicals and Compounds.

Name	Supplier
IPTG	Carl Roth, Karlsruhe
Kanamycin sulfate	AppliChem, Darmstadt
KCl	Carl Roth, Karlsruhe
$\text{KH}_2\text{PO}_4$	Carl Roth, Karlsruhe
$\text{K}_2\text{HPO}_4$	Carl Roth, Karlsruhe
$\text{K}_2\text{HPO}_4 \cdot 2\text{H}_2\text{O}$	Sigma-Aldrich Chemie, Steinheim
KOH	Carl Roth, Karlsruhe
$\lambda$ DNA (0.3 $\mu\text{g}/\mu\text{l}$ )	Thermo Fisher Scientific, Vilnius, LT
L-Arginine	Carl Roth, Karlsruhe
L-Arginine monohydrochloride	Sigma-Aldrich Chemie, Steinheim
L-Cystine	Sigma-Aldrich Chemie, Steinheim
Lincomycin hydrochloride	Sigma-Aldrich Chemie, Steinheim
L-Glutamic acid	Carl Roth, Karlsruhe
L-Glutamic acid monosodium salt hydrate	Sigma-Aldrich Chemie, Steinheim
L-Glutamine	Sigma-Aldrich Chemie, Steinheim
L-Proline	Sigma-Aldrich Chemie, Steinheim
L-Tryptophan	Carl Roth, Karlsruhe
Methanol	VWR International, Rue Carnot, FR
$\text{MgCl}_2 \cdot 6\text{H}_2\text{O}$	Carl Roth, Karlsruhe
$\text{MgSO}_4 \cdot 7\text{H}_2\text{O}$	Carl Roth, Karlsruhe
$\text{MnCl}_2 \cdot 4\text{H}_2\text{O}$	Carl Roth, Karlsruhe
NaCl	Carl Roth, Karlsruhe
$\text{Na}_2\text{CO}_3$	Carl Roth, Karlsruhe
$\text{NAD}^+$ sodium salt	Sigma-Aldrich Chemie, Steinheim
NADPH tetra(cyclohexylammonium) salt	Sigma-Aldrich Chemie, Steinheim
$\text{NaH}_2\text{PO}_4 \cdot 2\text{H}_2\text{O}$	Carl Roth, Karlsruhe
$\text{Na}_2\text{HPO}_4 \cdot 2\text{H}_2\text{O}$	Carl Roth, Karlsruhe
$\text{Na}_2\text{MoO}_4 \cdot 2\text{H}_2\text{O}$	Merck, Darmstadt
NaOH	Carl Roth, Karlsruhe
$\text{Na}_2\text{S}_2\text{O}_3 \cdot 5\text{H}_2\text{O}$	Merck, Darmstadt
$(\text{NH}_4)_2\text{SO}_4$	Carl Roth, Karlsruhe
Ni-NTA Sepharose (50 % suspension)	IBA Lifesciences, Göttingen
Nutrient broth	Carl Roth, Karlsruhe
PageRuler Plus Prestained Protein Ladder	Thermo Fisher Scientific, Vilnius, LT
Paraformaldehyde	Carl Roth, Karlsruhe
peqGOLD Universal Agarose	VWR International, Erlangen
Rotiphorese <sup>R</sup> Gel 30 (37.5:1)	Carl Roth, Karlsruhe
Roti <sup>R</sup> -Quant (5 $\times$ )	Carl Roth, Karlsruhe
PIPES disodium salt	SERVA Electrophoresis, Heidelberg
Powdered milk	Carl Roth, Karlsruhe



**Table 6.10: Chemicals and Compounds.**

<b>Name</b>	<b>Supplier</b>
Propan-2-ol	VWR International, Rue Carnot, FR
SDS Pellets	Carl Roth, Karlsruhe
Sodium pyruvate	Sigma-Aldrich Chemie, Steinheim
Spectinomycin dihydrochloride pentahydrate	Sigma-Aldrich Chemie, Steinheim
Strep-Tactin Sepharose (50 % suspension)	IBA Lifesciences, Göttingen
Streptomycin sulfate	Sigma-Aldrich Chemie, Steinheim
Tetracycline hydrochloride	Sigma-Aldrich Chemie, Steinheim
Tricarballic acid	Sigma-Aldrich Chemie, Steinheim
TEMED	Carl Roth, Karlsruhe
Tris	Carl Roth, Karlsruhe
Trisodium citrate dihydrate	Carl Roth, Karlsruhe
Tryptone/Peptone ex casein	Carl Roth, Karlsruhe
TWEEN 20/80	Sigma-Aldrich Chemie, Steinheim
2-Mercaptoethanol	Carl Roth, Karlsruhe
ONPG	AppliChem, Darmstadt
Yeast extract	Oxoid, Basingstoke, UK
X-Gal	Thermo Fisher Scientific, Vilnius, LT
Xylene cyanol FF	Sigma-Aldrich Chemie, Steinheim
ZnCl <sub>2</sub>	Carl Roth, Karlsruhe

**Table 6.11: Enzymes and Antibodies.**

<b>Name</b>	<b>Supplier</b>
Ampligase thermostable DNA ligase	Epicentre, Madison, USA
Anti-DarA [1:10,000]	Microsynth SeqLab, Göttingen
Anti-CggR [1:10,000]	Microsynth SeqLab, Göttingen
Anti-GapA [1:30,000]	Eurogentec, Cologne
Anti-Rabbit IgG (Fc), AP Conjugate [1:100,000]	Promega, Madison, USA
Anti-RnY [1:100,000]	Jan Maarten van Dijl, Groningen, NL
Anti-Strep-tag (StrepMAB-Classic)	IBA Lifesciences, Göttingen
Anti-His-tag (ABIN1573880)	<a href="http://www.antibodies-online.de">http://www.antibodies-online.de</a>
DNase I (from bovine pancreas, grade II)	Roche Diagnostics, Mannheim
DreamTaq DNA Polymerase (5 U/μl)	Thermo Fisher Scientific, Vilnius, LT
FastAP Thermosensitive Alkaline Phosphatase (1 U/μl)	Thermo Fisher Scientific, Vilnius, LT
FastDigest restriction endonucleases	Thermo Fisher Scientific, Vilnius, LT
Lysozyme (chicken egg white, min. 100,000 U/mg)	SERVA Electrophoresis, Heidelberg
Phusion High-Fidelity DNA Polymerase (2 U/μl)	Thermo Fisher Scientific, Vilnius, LT
T4 DNA Ligase (5 U/μl)	Thermo Fisher Scientific, Vilnius, LT

**Table 6.12: Commercial Systems.**

Name	Supplier
NucleoSpin Plasmid Kit	Macherey-Nagel, Düren
peqGOLD Bacterial DNA Kit	PEQLAB Biotechnologie, Erlangen
QIAquick PCR purification Kit	Qiagen, Hilden
Phenotype MicroArrays for microbial cells (PM1–10)	Biolog, Hayward, USA

**Table 6.13: Auxiliary materials.**

Name	Supplier
Beakers (50–5000 ml, DURAN)	DURAN Group, Wertheim/Main
Blotting paper sheets (BF 2, 195 g/m <sup>2</sup> )	Sartorius, Göttingen
Centrifuge bottles Nalgene (500/1000 ml, PPCO)	Thermo Fisher Scientific, Bonn
Concentrator Vivaspin Turbo 15 (5000 MWCO)	Sartorius, Göttingen
Cryo boxes (9×9, PC)	Sarstedt, Nürmbrecht
Culture Tubes (1 ml, borosilicate glass, disposable)	Kimble Chase, Vineland, USA
Cuvettes (semi-micro, PS)	Sarstedt, Nürmbrecht
Dewer carrying flask 26 B	KGW Isotherm, Karlsruhe
Dialysis tubing MEMBRA-CEL (MWCO 3500)	Serva, Heidelberg
Disposal bags	Sarstedt, Nürmbrecht
Erlenmeyer flasks (100–2000 ml, DURAN, un/-baffled)	DURAN Group, Wertheim/Main
Falcon centrifuge tubes (15/50 ml, PP, sterile)	Sarstedt, Nürmbrecht
Glas pipettes (1, 5, 10, 25 ml graduated)	Brand, Wertheim
Glas sample vials (4 ml)	Wheaton, Millville, USA
Immun-Blot PVDF membrane	Bio-Rad Laboratories, München
Inoculation loops (1 µl, sterile)	Sarstedt, Nürmbrecht
Laboratory film Parafilm M	Bemis, Neenah, USA
Laboratory flasks (100–5000 ml, DURAN)	DURAN Group, Wertheim/Main
Magnetic stirring bars (PTFE)	Brand, Wertheim
Measuring cylinders (100–2000 ml, DURAN)	DURAN Group, Wertheim/Main
Membrane filters S-Pak (0.45 µm, sterile)	Millipore, Molsheim, FR
Microcentrifuge tubes (1.5 ml, PP)	Beckman Coulter, Brea, USA
Microliter pipettes Research (2.5, 20, 200, 1000, 5000 µl)	Eppendorf, Hamburg
Microliter pipette Research (8-channel, 100 µl)	Eppendorf, Hamburg
Microtest plate 96 well, F	Sarstedt, Nürmbrecht
Protein LoBind tubes (1.5 ml)	Eppendorf, Hamburg
Reaction tubes (1.5/2 ml, PP)	Sarstedt, Nürmbrecht
Reaction tubes GeneAmp (0.5 ml, PP)	PerkinElmer, Weiterstadt
Scalpel Cutfix (sterile)	B. Braun, Tuttlingen
Test tubes (DURAN)	DURAN Group, Wertheim/Main

**Table 6.13: Auxiliary materials.**

Name	Supplier
Test tubes with white cap (5 ml)	Malvern Panalytical, Westborough, USA
Ultracentrifuge tubes (26 ml, PC)	Beckman Coulter, Brea, USA
Filtration unit Filtropur S/BT50 (0.2 µm)	Sarstedt, Nürmbrecht
Petri dishes with cams (60×15 /150×20 mm, PS)	Sarstedt, Nürmbrecht
Pipette tips (10, 200, 1000, 5000 µl)	Sarstedt, Nürmbrecht
Poly-Prep chromatography columns	Bio-Rad Laboratories, München
Syringes (1–50 ml, sterile)	Terumo Europe, Leuven, BE

**Table 6.14: Instruments.**

Name	Supplier
ÄKTAprime plus chromatography system	GE Healthcare, Uppsala, Schweden
Analytical balance MSE224S-100-DU Cubis	Sartorius, Göttingen
Autoclave LTA 2x3x4	Zirbus Technology, Bad Grund
Centrifuge Heraeus Biofuge primo R	Thermo Fisher Scientific, Bonn
Centrifuge Heraeus Megafuge 16R	Thermo Fisher Scientific, Bonn
ChemoCam Imager ECL	INTAS Science Imaging Instruments, Göttingen
Degassing Station ThermoVac	MicroCal, Northhampton, USA
French pressure cell FA-003 (20 k Mini)	Thermo Fisher Scientific, Bonn
French pressure cell FA-032 (40 k Standard)	Thermo Fisher Scientific, Bonn
French pressure cell press HTU-DIGI-Press	G. Heinemann, Schwäbisch Gmünd
French pressure cell press FA078E1	SLM Aminco, Lorch
Gel electrophoresis device	Waasetec, Göttingen
Hamilton GASTIGHT syringe 1002 (2.5 ml)	Altmann Analytik, München
Horizontal reciprocating shaker 3006	GFL, Burgwedel
Ice flaker MF36	Scotsman, Suffolk, UK
Incubator shaker Innova 44R	New Brunswick Scientific, Edison, USA
Liquid nitrogen container Apollo	Messer Cryotherm, Kirchen (Sieg)
Magnetic stirrer REO basic C	IKA-Werke, Staufen im Breisgau
Microbial incubator Heraeus B12	Thermo Fisher Scientific, Bonn
Microcentrifuge Heraeu Fresco 21	Thermo Fisher Scientific, Bonn
Microplate reader Synergy Mx	BioTek Instruments, Bad Friedrichshall
Microwave Privileg 8020	Quelle, Fürth
Mini centrifuge NG002R	Nippon Genetics Europe, Düren
Mini-PROTEAN Tetra System	Bio-Rad Laboratories, München
Molecular Imager Gel Doc XR+ system	Bio-Rad Laboratories, München
UV-Vis spectrophotometer NanoDrop ND-1000	PEQLAB Biotechnologie, Erlangen
UV-Vis spectrophotometer Ultrospec 2100 <i>pro</i>	Amersham Biosciences, Freiburg im Breisgau
pH-Meter 766 Calimatic	Knick, Berlin

**Table 6.14: Instruments.**

Name	Supplier
Power pack P25 T	Biometra, Göttingen
Rotor FIBERLite F50L-8x39	Thermo Fisher Scientific, Bonn
Rotor FIBERLite F9-4x1000y	Thermo Fisher Scientific, Bonn
Rotor FIBERLite F10-6x500y	Thermo Fisher Scientific, Bonn
Rotor TLA-110	Beckman Coulter, Brea, USA
SEC column HiLoad 16/600 Superdex 200 pg	GE Healthcare, Uppsala, Schweden
Scale CP2202S	Sartorius, Göttingen
SpeedVac concentrator Savant SPD111V-230	Thermo Fisher Scientific, Bonn
Sterile bench HERAsafe KS 12	Thermo Fisher Scientific, Bonn
Superspeed centrifuge Sorvall RC 6+	Thermo Fisher Scientific, Bonn
Thermocycler Labcycler	SensoQuest, Göttingen
ThermoMixer C	Eppendorf, Hamburg
Ultracentrifuge Optima MAX-E	Beckman Coulter, Palo Alto, USA
Ultracentrifuge Sorvall WX Ultra 80	Thermo Fisher Scientific, Bonn
Ultra-low temperature freezer MDF-594	Sanyo Electric Biomedical, Osaka, JP
Vacuum system MZ 2C +NT+AK	Vacuubrand, Wertheim
Vortex Genius 3	IKA-Werke, Staufen im Breisgau
VP-ITC MicroCalorimeter	MicroCal, Northhampton, USA
Washer-disinfector G 7893	Miele, Gütersloh
Water desalination plant Milli-Q Academic	Millipore, Schwalbach
Western blot semidry blotting system	G&P Kunststofftechnik, Kassel

**Table 6.15: Software and Websites.**

Name	Provider/Reference	Purpose
ChemoStar Imager 0.2.37	INTAS Science Imaging Instruments, Göttingen	Western blot imaging and documentation
Geneious 10.0.5	Biomatters, Auckland, NZ (Kearse <i>et al.</i> , 2012)	Oligo design and calculation, <i>in silico</i> cloning, analysis of sequencing results
Gen5 2.09.2	BioTek Instruments, Bad Friedrichshall	Microplate reading, analysis and documentation
Image Lab (Beta 2) 3.0.1	Bio-Rad Laboratories, München	Gel imaging and documentation
Microsoft Office 2010	Microsoft, Redmond, USA	Data processing
MiKTeX 2.9.6643	Christian Schenk	Thesis writing
ND-1000 3.8.1	Thermo Fisher Scientific, Bonn	Nucleic acid concentration/purity
Origin 7 SR2	OriginLab, Northhampton, USA	ITC analysis and documentation
PrimeView 5.31	GE Healthcare Bio-Sciences, Uppsala, SE	ÄKTA chromatography analysis and documentation
VPViewer2000 1.4.15	MicroCal, Northhampton, USA	ITC operation

Table 6.15: Software and Websites.

---

Name	Provider/Reference	Purpose
<a href="http://www.ncbi.nlm.nih.gov/pubmed">http://www.ncbi.nlm.nih.gov/pubmed</a>	National Institutes of Health, Bethesda, USA	Literature
<a href="http://www.rcsb.org">http://www.rcsb.org</a>	Research Collaboratory for Structural Bioinformatics (Berman <i>et al.</i> , 2000)	Protein structures
<a href="http://subtiwiki.uni-goettingen.de/">http://subtiwiki.uni-goettingen.de/</a>	General Microbiology, University of Göttingen (Zhu and Stülke, 2018)	<i>B. subtilis</i> database
<a href="http://www.tcdb.org/">http://www.tcdb.org/</a>	Saier Lab. Group, La Jolla, California, USA (Saier <i>et al.</i> , 2016)	Transporter classification database

---



## *Curriculum vitae*

### **Martin Weiß**

Date of birth: 24<sup>th</sup> June 1990

Place of birth: Erlangen

Nationality: German

### **Education**

- 01/2016 – present      ***Doctor rerum naturalium***  
Within the GGNB program “Microbiology and Biochemistry”  
Georg-August-University Göttingen
- 10/2013 – 09/2015      **Master of Science**  
Cellular and Molecular Biology  
Friedrich-Alexander-University Erlangen-Nürnberg
- 10/2010 – 09/2013      **Bachelor of Science**  
Biology  
Friedrich-Alexander-University Erlangen-Nürnberg
- 08/2000 – 06/2009      **Higher Education Entrance Qualification**  
Albert-Schweitzer-Gymnasium, Erlangen